The Antarctic ice sheet and environmental change:
a three-dimensional modelling study

Der antarktische Eisschild und globale Umweltveränderungen:
Eine dreidimensionale Modellstudie

Philippe Huybrechts

The Antarctic ice sheet and environmental change: a three-dimensional modelling study

Der antarktische Eisschild und globale Umweltveränderungen: Eine dreidimensionale Modellstudie

Philippe Huybrechts

Geografisch Instituut
Vrije Universiteit Brussel
Pleinlaan, 2
B-1050 Brussel
Belgium

und

Alfred-Wegener-Institut für Polar- und Meeresforschung
Postfach 120161
Columbusstraße
W-2850 Bremerhaven
Bundesrepublik Deutschland

CONTENTS

TABLE OF CONTENTS

TABLE OF CONTENTS

TABLE OF CONTENTS

FOREWORD

Antarctica is a fascinating continent. Ever since it was first sighted in the early 19th century, it has caught the imagination of adventurous discoverers and scientists alike. Also I did not escape to its attraction. I have really enjoyed my introduction to glaciology, above all owing to the people I have met and worked with during my travels. Many people have contributed to the completion of this thesis. Some of them I would like to thank in particular. First of all, Hans Oerlemans, who introduced me to the field of ice sheet modelling at the Rijksuniversiteit Utrecht and whose knowledge of ice and climate dynamics provided on many an occasion a good starting-point for lengthy and absorbing talks. These always took place in a friendly atmosphere. I am grateful for the confidence he offered me and the effort he took to comment on my model results when they became available.

Many thanks are also due to Hugo Decleir, the promotor of this thesis at the Vrije Universiteit Brussel, for his support and valuable advice to place my results in a wider context. I appreciate the freedom he has given me to carry out my research independently and am grateful for the possibility I had to participate in international meetings whenever there was a need for it. But above all, I thank him, and the Japanese host expedition (JARE 31), for the opportunity I was offered to visit that part of Antarctica Hugo knows so well, namely the Sør Rondane Mountains in Dronning Maud Land. My first encounter with the 'real thing' certainly was an instructive experience.

I am also deeply indebted to the Alfred Wegener Institut für Polar- und Meeresforschung, Bremerhaven, and to the head of the geophysics department, Heinz Miller, for the - it seemed unlimited - access I was granted to their CRAY-2 computing facilities at the University of Stuttgart. Without these facilities, this research would simply not have been possible. In total, I stayed more than one year in Bremerhaven and was able to work in a pleasant and stimulating environment. I thank my collegues of the glaciology section for their hospitality: Jürgen Determann, Hans Oerter and my room-mate Sepp Kipfstuhl for their interest, and Anne Letreguilly and Niels Reeh for the fruitful cooperation which resulted.

Acknowledgements are furthermore due to David Drewry and Paul Cooper, at that time associated with the Scott Polar Research Institute, Cambridge, for providing their data set on accumulation rate and surface temperature; to W.F. Budd and his co-workers at the University of Melbourne for communicating a

digitized version of basic SPRI-maps; to Hans Pfeiffenberger and Jens Schlüter of the AWI-Rechnergruppe for logistic support in dealing with yet another graphics device and computer link; to Tony Payne at the University of Edinburgh for proof-reading and commenting on the manuscript; to Jan Van Mieghem at the Geografisch Instituut of the VUB for drafting many of the figures; and to all those that expressed interest in my work.

Last but not least, I thank Monik for sharing and enduring the hardships of a scientist's life, which turned out to include almost more time abroad than at home.

Brussel, March 15th 1991   Philippe Huybrechts

KURZFASSUNG

Diese Arbeit befaßt sich mit den Reaktionen des antarktischen Eisschildes auf veränderte Umweltbedingungen, sowohl für die längere paleoklimatische Zeitskala (10^4-10^5 a), als auch für die kürzere, mit dem künftigen Treibhauseffekt in Verbindung stehenden Zeitskala (10^2 a). Die Reaktionen des antarktischen Inlandeises sind von großem Interesse, weil Änderungen seiner Mächtigkeit und Ausdehnung eine wichtige Rolle spielen für globale atmospherische und ozeanographische Prozesse. Diese Änderungen sind auch entscheidend verantwortlich für weltweite Meeresspiegeländerungen. In deren Zusammenhang wird oft ein schneller Zusammenbruch der Westantarktis, eines marinen Eisschildes, in Erwägung gezogen.

Der erste Teil gibt eine qualitative Beschreibung der Rolle des Eisschildes für die globale Umwelt und diskutiert mögliche gegenseitige Einflüsse. Außerdem wird ein Überblick über die glaziale Geschichte des Inlandeises gegeben und anhand von verfügbaren Feldmessungen dessen Ausdehnung während des letzten Glazials rekonstruiert.

Darauffolgend wird der antarktische Eisschild einschließlich der Schelfeise mit einem hochauflösenden dreidimensionalen Fließmodell untersucht. Das Modell berücksichtigt die Dynamik der Aufsetzlinie, basales Gleiten sowie isostatische Reaktionen des Untergrundes. Eisfluß und Temperaturfeld sind gekoppelt, so daß spezifizierte Umweltbedingungen die Geometrie des Eisschildes kontrollieren. Meeresspiegelschwankungen sowie Änderungen der Massenbilanz und Oberflächentemperatur treiben das Modell an.

Die Simulation des heutigen Eisschildes zeigt zunächst, daß das Modell realistische Ergebnisse liefert. Anschließend erfolgt eine Reihe klimatischer Experimente, in denen das Modell benutzt wird, das Inlandeis während des letzten Glazial-Interglazial-Zyklusses zu untersuchen. Das umfaßt eine Sensitivitätsstudie bezüglich veränderter Umweltbedingungen und eine zeitabhängige Simulation des letzten glazialen Zyklus. In Übereinstimmung mit glazial-geologischen Ergebnissen treten die deutlichsten Änderungen im Bereich der Westantarktis auf. Diese Fluktuationen werden im Wesentlichen von eustatischen Meeresspiegeländerungen kontrolliert, wohingegen typische Glazial-Interglazial Variationen von Temperatur und Niederschlägen zu einer gegenseitigen Balance tendieren.

Auf den kürzeren Zeitskalen der Treibhauserwärmung sind Änderungen der Massenbilanz bestimmend. Die Modellrechnungen zeigen, daß sehr

wahrscheinlich das antarktische Inlandeis wächst, solange die Temperaturerhöhung unter 5°C liegt, da Schmelzen am Rande des Eisschildes von höheren Niederschlägen auf dem Plateau kompensiert wird. Die Hypothese eines schnellen, katastrophalen Zusammenbruches des westantarktischen Eisschildes wird durch die in dieser Arbeit präsentierten Ergebnisse nicht gestützt.

ABSTRACT

This thesis addresses the response of the Antarctic ice sheet to changes in environmental conditions, both on the longer palaeoclimatic time scale (10^4-10^5 y) as on the shorter time scale (10^2 y) associated with future greenhouse warming. The Antarctic ice sheet is of large interest because changes in its elevation and extent have an important role in modulating global atmospheric and oceanographic processes, and because these fluctuations contribute significantly to world-wide sea levels. The possibility of a surge of the marine-based West Antarctic ice sheet is often mentioned as an important aspect.

In a first part a qualitative description is given of the role of the ice sheet in the global environmental system and the possible modes of interaction are discussed. An overview is also presented of the ice sheet's glacial history and of available field evidence of ice sheet expansion during the last glacial cycle. Subsequently, the Antarctic ice sheet is investigated using a high-resolution 3-D flow model covering the entire ice domain. This model incorporates a coupled ice shelf, grounding-line dynamics, basal sliding and isostatic bed adjustment. It has a full coupling between thermal field and ice flow and the ice sheet geometry is freely generated in response to specified environmental conditions. The model is driven by changes in sea level, surface temperature and mass balance.

A simulation of the present ice sheet reveals that the model is able to yield realistic results. A series of climatic experiments are then performed, in which the model is used to examine the ice sheet during the last glacial-interglacial cycle. This involves a sensitivity study with respect to changing environmental conditions and a time-dependent simulation of the last glacial cycle. In line with glacial-geological evidence, the most pronounced changes occur in the West Antarctic ice sheet configuration. These fluctuations are essentially controlled by variations in eustatic sea level, whereas typical glacial-interglacial changes in temperature and ice deposition rates tend to balance one another.

On the shorter greenhouse warming time scale, the model's response is determined by changes in the mass balance. It is found that as long as the temperature rise is below 5°C, the Antarctic ice sheet will probably grow, because melting at the ice sheet edge can still be offset by higher deposition rates on the plateau. The hypothesis of a catastrophic collapse of the West

Antarctic ice sheet is not supported by the model results presented in this thesis.

1. INTRODUCTION

The Antarctic ice sheet is one of the most prominent physical features on our planet. It is generally believed that its roots date back to Eocene and Oligocene times, a geological period in the Tertiary during which Australia and South America drifted northwards from Antarctica. The separation resulted in a strong circumpolar circulation in the ocean and triggered a gradual glacierization of the entire continent. Since then, this configuration of a huge ice-loaded continent, fringed by the Southern Ocean, has formed a relatively stable system (as compared to the northern hemisphere ice sheets) and has been instrumental in the creation of the Late Cenozoic global climates.

However, the concept of a so-called 'permanent' Antarctic ice sheet can be seriously questioned today. In recent decades, a growing body of observational evidence has become available, pointing to important variations in its configuration, especially during the Pleistocene glacial cycles. Glacial and marine geologists have spent many years in the field trying to reconstruct the ice sheet's former extent by examining morainic deposits left by the expanded ice cover and sequences of glacial-marine sediments in the surrounding seas. Although controversies still remain, this research has led to the view of a highly variable West Antarctic ice sheet, which may on several occasions have extended all the way to the edge of the continental shelf. According to these reconstructions, the larger East Antarctic ice sheet emerges as a comparably more passive feature, but this is not to say that its variations would be less important for the global environment. This is because of the huge amounts of ice involved, which mean that even relatively small fluctuations can have a major impact on, for instance, global changes in sea level.

11

INTRODUCTION

In addition to these observations, there has been growing concern about the future response of the Antarctic ice sheet to the anticipated greenhouse warming of the earth's atmosphere. Since the industrial revolution, mankind has met energy demands by burning fossil fuels at an ever increasing rate. As a consequence, atmospheric carbon dioxide concentrations have been steadily rising. Since CO_2 plays an important role in trapping long-wave radiation emitted by the earth's surface, the planet may be on the verge of an unprecedented change in climate. Although one cannot yet state that the greenhouse warming effect has been detected from meteorological records in a truly convincing way, there seems to be a growing concensus among climatologists that the global-mean temperature will be 2 to 4°C above the pre-industrial level somewhere during the second half of the next century. This has led to speculations concerning the effect on the cryosphere, and hence, on sea level. If such a warming were to take place and initiate the melting of polar ice sheets, the consequences could be disastrous for low-lying coastal areas. For instance, a 1% change in Antarctic ice volume would result in a change in the world-wide sea-level stand of some 70 cm. In particular the West Antarctic ice sheet has drawn a lot of attention. According to some workers, this ice cap may be inherently unstable, in such a way that a small change in environmental conditions could lead to the complete disintegration of the inland ice. In a worst-case scenario, the sudden collapse of the West Antarctic ice sheet could even lead to a 6 meter sea-level rise in as little as a few centuries time.

Because of the interaction of the ice cap with the atmosphere and the oceans and because it stores more than 70% of the earth's fresh water resources, it is thus fundamental to better understand the ice sheet's basic behaviour. A correct understanding of the ice sheet's past behaviour is also a necessary precursor to investigating its possible response to future climatic trends. Another good reason to study the Antarctic ice sheet stems from the fact that it is a good analogy for parts of the former midlatitude ice sheets, that once covered large sectors of Eurasia and North America during the ice ages.

With regard to palaeoclimatic conditions during the Pleistocene, it is of crucial importance to determine the history and extent of the ice sheet's fluctuations and to find out how they are related to changes in environmental conditions. This knowledge is useful in four areas. First, it has been widely speculated

12

INTRODUCTION

that eustatic sea-level changes were the primary cause of Antarctic ice-volume changes, but other factors such as changes in mass balance and ice temperature may also be of major importance. Second, reconstructions of past ice sheet configurations form part of the global boundary conditions that are a basis for atmospheric modelling studies of the ice ages. Third, a detailed knowledge of the ice thickness distribution in space and time is needed to interpret climatic information from ice cores, for instance in order to correct for local changes in surface elevation. Fourth, it is important to assess the sea-level changes these ice sheet fluctuations produced. Antarctic ice volume changes influence the loading distribution of the earths's mantle and hence, constrain interpretations of sea level stands recorded over the globe. This is of relevance to the northern hemisphere ice sheet history.

Recent developments in supercomputer technology have made it possible to address these questions by means of numerical modelling of ice flow. In addition to technical progress, advances have also been made regarding the observational data required by such a model. In the last few years, more and better field data on the present configuration of the ice sheet and on important boundary conditions determining ice flow have been compiled and mapped. At the same time, important new developments have taken place in the field of geochemistry and palaeoclimatic research. Stable isotope studies on the Vostok ice core, for instance, have provided detailed information on variations in such crucial parameters as temperature and accumulation rate during the last glacial-interglacial cycle. Although considerable gaps still exist in our knowledge, notably in the area of data coverage and in certain aspects of ice dynamics, it seems that sufficient material is available now to make large-scale modelling both feasible and necessary.

One of numerical modelling's primary benefits is that it can help to disentangle the complex interaction of environmental factors controlling the behaviour of the ice sheet, and reveal the magnitude and time scales of the associated responses. To accomplish this task, sensitivity experiments of the type 'all other things being equal' are set up and the model is run a number of times using different values for certain environmental factors in each experiment. Results of the different runs can then be compared to determine what effects given changes in environmental variables have on the ice thickness

distribution. In this way, the model can demonstrate which combinations of these variables are crucial and which can be disregarded.

Once this has been done, the model can be driven by 'known' variations in a set of relevant environmental parameters to predict the past behaviour of the ice sheet which can then be tested against empirical field evidence. If the model is able to simulate past ice sheet behaviour in reasonable agreement with geomorphological field evidence, in time as well as in space, it then has sufficient credibility to be used in predictions of future ice sheet changes, such as those associated with global warming and ice sheet decay. One cannot expect models to perfectly replicate all details of the glacial history. This is because the model contains many simplifications and ambiguities still exist in the interpretation of the field data. However, model results can also be used to point to those pieces of field evidence needed to test the model effectively and to the best locations where to find such evidence. In addition, model results may help glacial geologists by providing the physical arguments needed to resolve some of the controversies raised by their geomorphological data.

The few Antarctic ice sheet models developed so far either treat the ice as an isothermal body or include the coupling between ice temperature and flow, but do in that case not allow for changes in the lateral extent. None of these models takes into account ice shelf flow. Such a model is needed, however, because the ultimate ice configurations depend heavily on the mutual interactions. In this thesis, the Antarctic ice sheet is investigated using a newly developed numerical model. In the model, both grounded ice and ice shelves are treated simultaneously on a fine mesh, by solving the full set of thermomechanical equations for ice flow in three dimensions. There is free interaction between the flow in grounded and floating ice, so that the entire geometry is internally generated in response to specified environmental conditions. In addition, more efficient numerical techniques have been employed that allow for a finer grid and more accurate solutions in the basal shear layers.

From this study, I hope to better understand how the ice sheet behaves in the global climate system, in past as well as future environments. Although one of my aims is to make a tentative projection of the Antarctic component to future sea level changes, the reader will notice that much of this thesis is actually

INTRODUCTION

devoted to the last glacial cycle. This both helps to validate the model and is also an extremely intriguing problem in its own right. Chapter 2 introduces basic features of the Antarctic geophysical system and discusses the various modes of interaction with the global climate. Current thoughts on the continent's glacial history and past reconstructions based on field data are described in chapter 3. In chapter 4 the numerical model and the methods used to specify environmental conditions in different climates are presented. Results of the numerical experiments, involving various sensitivity tests and a simulation of the last glacial cycle then follow in chapters 5 through 7. Chapter 8 deals with the response to future greenhouse warming. The most important findings that have come out of the numerical computer simulations are summarized at the end of each chapter. Consequences for the overall behaviour of the Antarctic ice sheet are then discussed in the final conclusions.

2. THE ANTARCTIC ICE SHEET IN THE GLOBAL CLIMATE SYSTEM

Before embarking on a description of the ice sheet model and the various climatic experiments performed, it is of use to first place the Antarctic ice sheet in its broader geophysical and glacial geological context. With relevance to subsequent chapters, this chapter starts by elucidating basic features of the ice sheet's geographical, glaciological and climatological setting. The description then widens to a discussion of the different possible modes of interaction with the global environmental system.

2.1. CONFIGURATION AND FLOW

2.1.1. Bedrock

The Antarctic continent, about twice as large as Australia, is a high and almost zonally-symmetric polar-centred land mass. It is almost completely covered by ice. Less than 3% of the rock surface is exposed, mainly in the Antarctic Peninsula and in a coastal belt around East Antarctica that includes the Transantarctic Mountains and several other fringing mountain ranges. Apart from these nunataks, other non-glaciated areas consist of the so-called dry valleys, mainly in Victoria Land, and several small and isolated bare rock surfaces along the coast that are commonly known as oases. See fig. 2.1 for a comprehensive map of the ice sheet and a reference to the most important geographic names mentioned in the text.

Geologically, Antarctica can be broadly divided in two distinct provinces, separated by the Transantarctic Mountains that extend across the entire continent. The first region comprises the larger part of the continent and faces
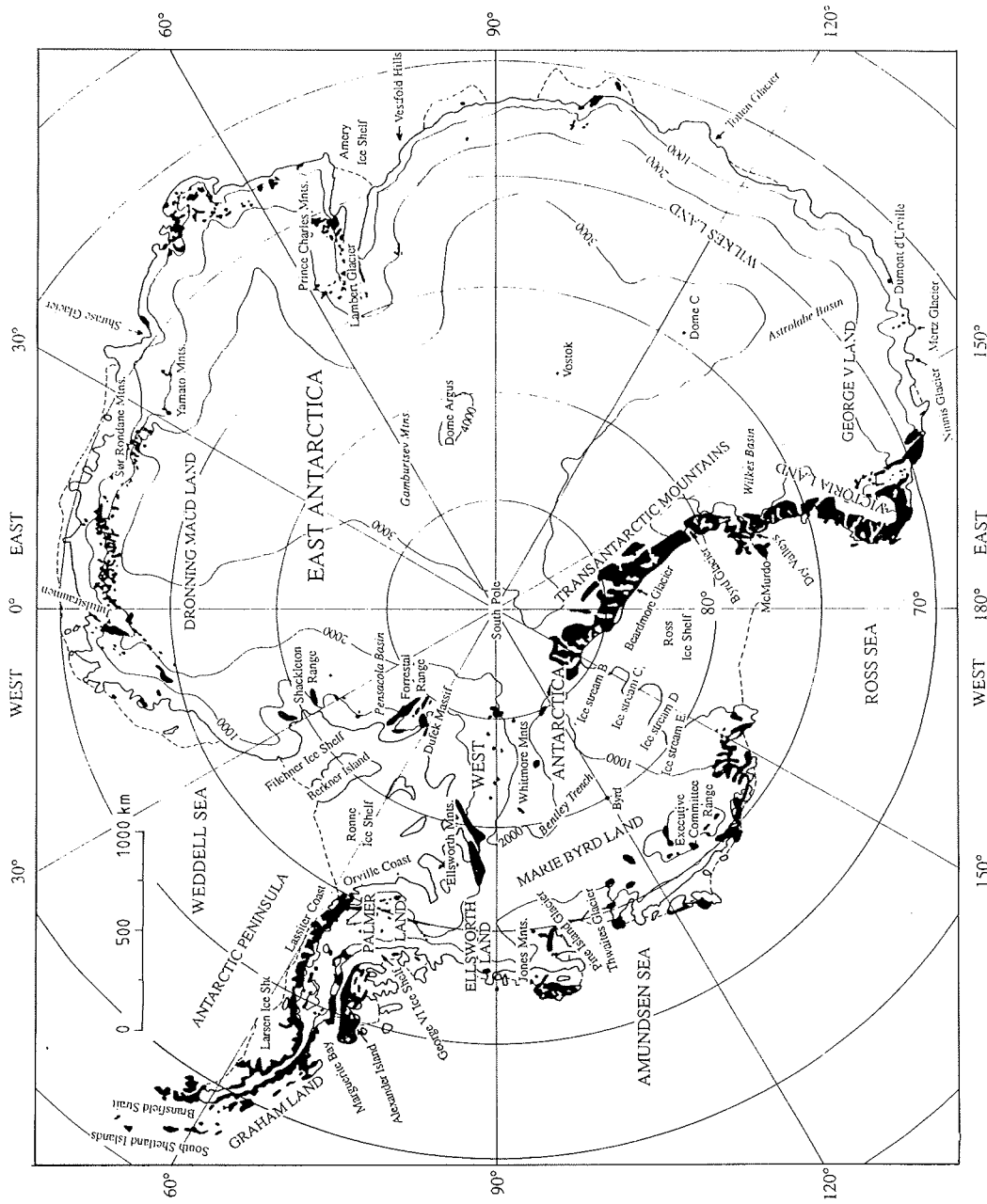
fig. 2.1: Index map of Antarctica showing the main geographic features referred to in this thesis. Black regions denote rock outcrops. Ice shelf edges are stippled. Italic script denotes subglacial features. Names are from Drewry (1983)

mainly upon the Atlantic and Indian Oceans. Since most of this region lies in the area of east longitudes, it is known as East Antarctica. West Antarctica, facing mainly upon the Pacific Ocean, makes up for the smaller part of the continent and lies in the western hemisphere. East Antarctica is a typical continental shield predominantly of Precambrian age. It consists of a foundation of igneous and metamorphic rocks overlain by a sequence of younger, flat-lying sedimentary and volcanic rocks (Craddock, 1982). Gneisses and granites are the most abundant rock types exposed in nunataks and mountain ranges. West Antarctica is composed of generally younger rocks that are widely deformed and metamorphosed. Sedimentary and volcanic sequences of Paleozoic and Mesozoic age are widely distributed, and some of these rocks are strongly folded. The age and nature of the basement rocks are poorly known, but Precambrian rocks have not yet been discovered (Craddock, 1982). In Marie Byrd Land, the rock surface changes in character from very rough inland to becoming smooth in the region bordering the Ross ice shelf. This region is believed to be part of a large sedimentary basin extending northwestwards beneath the Ross ice shelf towards the Ross Sea (Rose, 1982). Volcanism which began in middle Tertiary time has continued into recent times in much of coastal West Antarctica.

A major feature of the Antarctic crustal structure is the abundance of rift zones, the majority of which underlie the vast bedrock depressions (Grikurov, 1982; Kadmina et al., 1983). These structural features are particularly numerous in West Antarctica and in subglacial parts of Wilkes and Victoria Land. A linear chain of graben-like crustal depressions can also be traced across East Antarctica from the central Transantarctic Mountains through the subglacial Gamburtsev Mountains towards the Lambert Glacier and the Amery ice shelf. It is believed that these features are, at least to some extent, related to the presence of the ice sheet, which intensifies destructive tectonic processes. From a glaciological point of view, they are important because they cause channeling of the ice flow, in particular at the ice sheet margin.

Although at present a substantial part of the subglacial bed of East Antarctica lies beneath contemporary sea level, this would not be the case if the ice were to be removed (fig. 2.2). Apart from some marine incursions in Wilkes Land and George V Land, subsequent isostatic rebound would cause the land to rise almost completely above sea level. By contrast, a large part of West

18
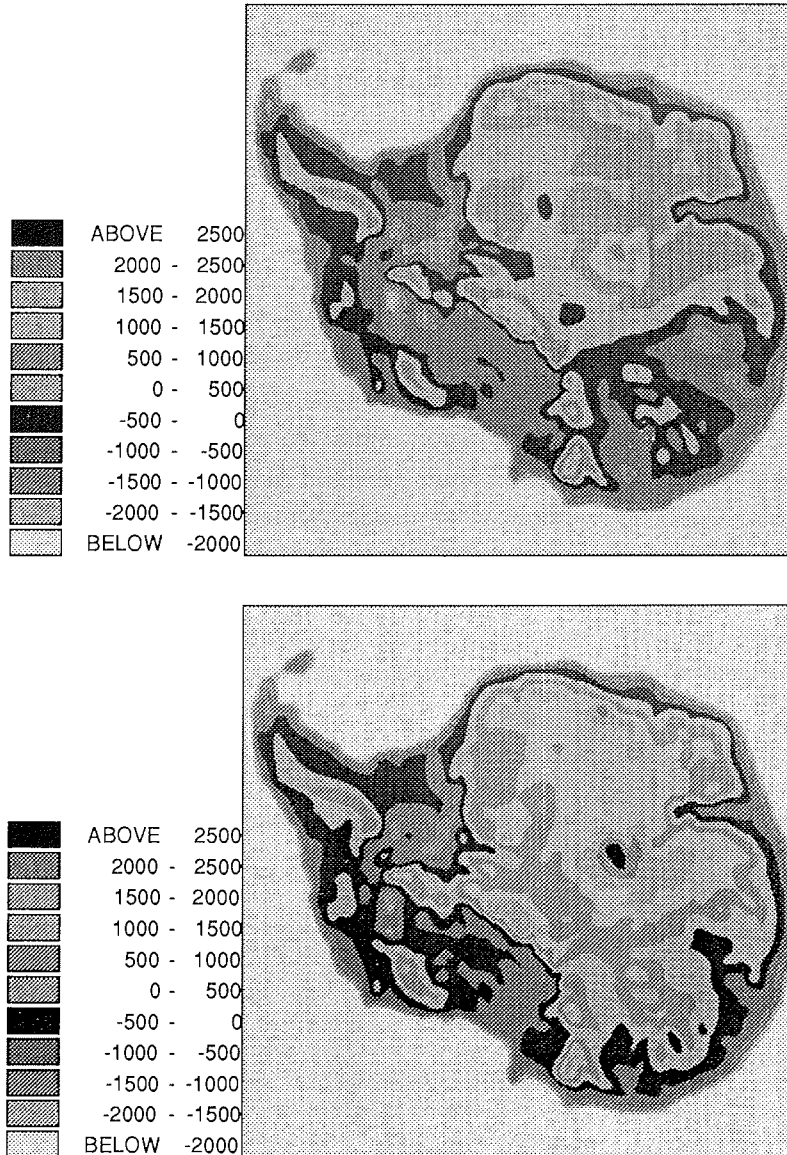
fig. 2.2: Plots of the current bedrock topography (above) and the rock surface that would result after removal of the present ice load and subsequent isostatic rebound (below). The raised bedrock surface has been calculated assuming isostatic equilibrium under present-day conditions with a method described further in 4.6. Contoured values shown [in meters] have undergone smoothing. Data have been digitized from the Drewry map folio series, sheet 3 (1983).

Antarctica consists of a bed that lies far below sea level, even in case of complete removal of the ice mass. In that event, only a few isolated island groups would rise above the ocean surface, but in some places the ocean depth would still be as much as 1000 meter or more.

2.1.2. Area and volume

The ice sheet overlying the continent is formed of three unequal parts. These are the large East Antarctic ice sheet; the smaller West Antarctic ice sheet with flanking, floating ice shelves in the Ross and Weddell Seas; and the Antarctic Peninsula. Together, they comprise an area of almost 14 million km^2, see table 2.1. Drewry et al. (1982) report a total ice volume of 30.11 million km^3, which is almost 25% greater than previous estimates cited in the Soviet literature. Curiously enough, when digitizing their base maps (published in Drewry, 1983), that are used as input in our modelling study as described later, we obtain a value for grounded ice volume of only 24.10 million km^3 as compared to the Drewry-figure of 29.53 million km^3. The source of this substantial discrepancy is unclear and was also noted in Radok et al. (1989).

region	area [10^{12} m^2]	% ice free	mean ice thickness [m]	volume [10^{15} m^3]
East Antarctica	10.354	1.9	2565	26.039
West Antarctica	1.974	2.8	1700	3.262
Antarctic Peninsula	0.522	14.3	510	0.227
Ross ice shelf	0.536	---	430	0.230
Ronne-Filchner ice shelf	0.532	---	660	0.352
Total	13.918	2.4	2160	30.110

table 2.1: Morphometric features of the Antarctic ice sheet, after Drewry et al. (1982).

By far most of the ice (over 85%) is contained in the East Antarctic ice sheet (table 2.1). Here, the largest measured ice thickness (by radio echo sounding) is 4776 m in the Astrolabe Subglacial Basin some 400 km inland from Dumont d'Urville. Thicknesses less than 1500 m are commonly observed above the

subglacial Gamburtsev Mountains in central East Antarctica (Drewry, 1983). The mean ice thickness value quoted in Drewry et al. (1982) is 2565 m, but our calculations give a figure closer to 2100 m. Mean ice thicknesses in West and East Antarctica have nearly the same order of magnitude, but the surface of West Antarctica is much lower. Perhaps also due to a denser grid of radio echo-sounding flight-tracks, the West Antarctic bedrock topography is more rugged and here the deepest point yet recorded on the Antarctic continent is located. This is the Bentley Subglacial Trench at an elevation of -2555 m. Assuming a surface ratio of roughly 1: 28.5 with respect to the oceans, melting of the East Antarctic ice sheet would raise world-wide sea levels by about 60 m. The corresponding figure for West Antarctica is only 6 m, not only because the ice sheet is smaller but also because much of it is at present displacing ocean water.

2.1.3. East Antarctic ice sheet

The surface of the predominantly continental East Antarctic ice sheet is rather smooth and constitutes a vast, relatively flat dome with a maximum elevation of just over 4000 m at Dome Argus. Ice flow towards the coast results mainly from internal deformation, where surface slopes and ice thicknesses produce sufficient gravitational forces to drive the ice outwards against frictional drag at the ice sheet base. Motion caused by sliding over the bed is believed to be relatively unimportant. Towards the margin, ice flow is impeded at several places by the substantial barriers of mountain ranges. The Transantarctic Mountains and the mountains in Dronning Maud Land (among which are the Sør Rondane Mountains) are the most important. It is here that the ice flow is concentrated into a small number of outlet glaciers. In between these glaciers, the ice sheet is often characterized by local domes and ridges.

The outlet glaciers resemble the valley glaciers of nonpolar mountain regions in their morphology, but differ from them in their huge dimensions and high ice discharge rates. They often flow through valleys originally formed by tectonic faults, of which the horst-and-graben structure in the lower part of Lambert Glacier is the most prominent one. It has also the largest glacier in Antarctica. In most of the outlet glaciers, there is a change in the mode of flow, away from internal creep towards a significant component of basal sliding. This is illustrated by the fact that surface slopes are usually too small to generate the

stresses needed to produce the observed velocities. The lower reaches of these glaciers have a surface profile which commonly exhibits an inflection point, coastward of which the profile is concave up rather than convex up. The driving stresses, which cause the ice to deform, usually peak in outlet glaciers somewhere within 100 km or so of the coast (Cooper et al., 1982). Typical ice velocities in East Antarctica are just a few meters per year over the vast interior plateau, but reach values of between 500 and 1000 m/y in the major active outlet glaciers (Budd and Smith, 1985).

2.1.4. West Antarctic ice sheet

The overall surface configuration of the West Antarctic ice sheet is more complicated. It basically consists of three domes centred over Ellsworth Land, the Executive Committee Range and the Whitmore Mountains. Nowhere does the surface rise above 2400 m. A prominent feature is the Vinson Massif in the Ellsworth Mountains, which protrudes above the ice to an altitude of 5140 m, thereby constituting the highest point in Antarctica. Much of the West Antarctic ice sheet rests on the seabed instead of on a continent and it is therefore called a marine ice sheet. A consequence is that the ice sheet is surrounded by floating ice shelves. The boundary between grounded ice and floating ice is called the grounding line. This junction has received much attention because of the idea that the grounding line in West Antarctica may be inherently unstable or at least strongly susceptible to movement, so that a small change may ultimately lead to the complete elimination of the inland ice. We will come back to this point later.

By far the largest part of West Antarctic ice is drained towards the Ross and Ronne-Filchner ice shelves, although a significant fraction also enters the Amundsen Sea through the Pine Island and Thwaites Glacier systems. This drainage largely takes place through ice streams, that persist some distance into the ice shelf. By definition, ice streams differ from outlet glaciers in that they are bordered by relatively stagnant ice, probably frozen to the bed, and not by rock walls. There are however many fast-flowing parts of the inland ice sheet that are more difficult to classify, such as Rutford ice stream which debouches into the Ronne ice shelf (Bentley, 1987). Good examples of pure ice streams are the ice streams B, C, D and E that feed into the Ross ice shelf. These 'Ross ice streams' are distinct in character in more than one sense and

have received much attention over the last two decades, in particular with respect to the problem of the stability of the West Antarctic ice sheet. They are characterized by very flat surface elevation profiles, low and smooth beds, and very low driving stresses that increase continually inland to the heads of the ice streams (Cooper et al., 1982). The lateral boundaries of these ice streams are sharply delineated by large and regular crevasses that indicate zones of very strong shear.

In contrast to the outlet glaciers in East Antarctica and even the other ice streams in West Antarctica, the Ross ice streams only occupy shallow depressions in relatively flat sedimentary terrain, and in some instances the ice stream boundary does not even coincide with the edge of the subglacial depression. Drewry (1983) suggests that the absence of deep subglacial troughs is an indication of their relative youthfulness, or possibly, their transient nature. Evidence for the latter may be the remarkable fact that ice stream C has become inactive. This apparently happened about 250 years ago, as estimated from the depth of burial of surface crevasses (Shabtaie and Bentley, 1987). Stephenson and Bindschadler (1988) report a deceleration of ice stream B by as much as 20% over the last decade. Thomas et al. (1988) speculate that the neighbouring ice streams B and C may be in an oscillatory mode, where rapid flow in one of the ice streams coincides with stagnation of the other, and vice versa.

Because of the low driving stresses in these ice streams, much, if not all, of the differential flow between the ice surface and the bedrock must be caused either by basal sliding or by a deforming subglacial till layer. The latter is indicated by seismic reflection measurements on ice stream B (Alley et al., 1986; Blankenship et al., 1986). This is confirmed by recent physical evidence obtained in boreholes drilled to the bottom in the same ice stream (Engelhardt et al. 1990). These brought to light that the ice stream indeed overlies a water-saturated till layer of at least 2 m thick, in which shear deformation takes place. Flow velocities in these ice streams are of the order of 500 m/y, compared to about 5 m/y in the adjacent ice sheet (Whillans et al., 1987)

23

2.1.5. Ice shelves

Most of the ice discharged towards the coast enters ice shelves, that float in equilibrium with the ocean water (fig. 2.3). Except along the northern coast of Ellesmere Island and locally in northeastern Greenland, ice shelves are not developed in any other glaciated area on earth. In total, ice shelves and floating ice tongues/outlet glaciers make up 57 % of the Antarctic coast line. They end in a vertical cliff generally some 30 m above sea level. Ice walls occupy 38 % and rock outcrops only 5 % of the remaining coastline (Drewry et al., 1982). The two largest ice shelves alone, the Ronne-Filchner and Ross, account for about half of the total ice discharge (Thomas, 1979a). They not only drain the largest part of the West Antarctic ice sheet, but a substantial fraction of the East Antarctic ice sheet as well.
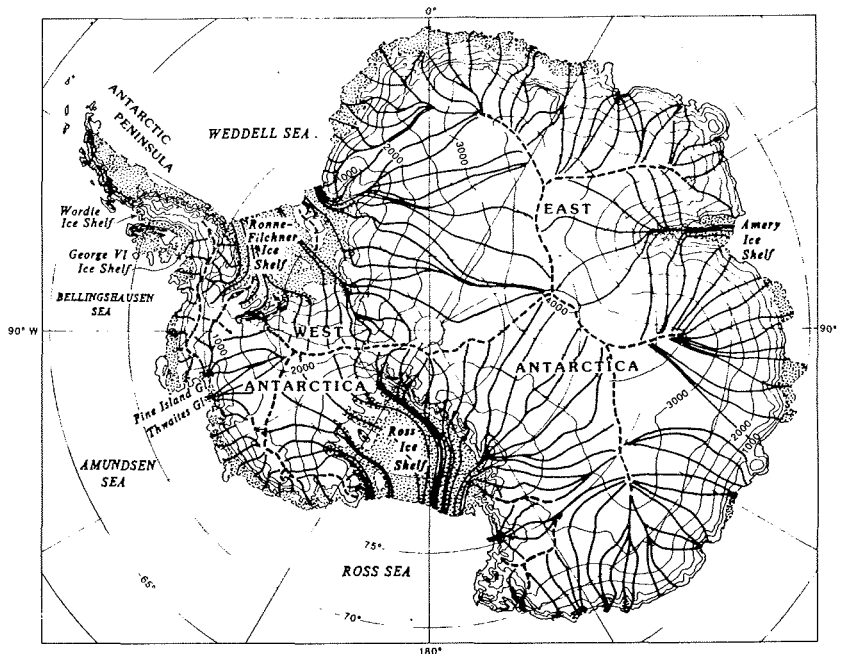
fig. 2.3: Surface topography (in m) and major flow lines (heavy lines) in Antarctica. Major ice divides that separate the different drainage systems, are shown by dashed lines. Ice shelves are stippled. From Drewry (1983).
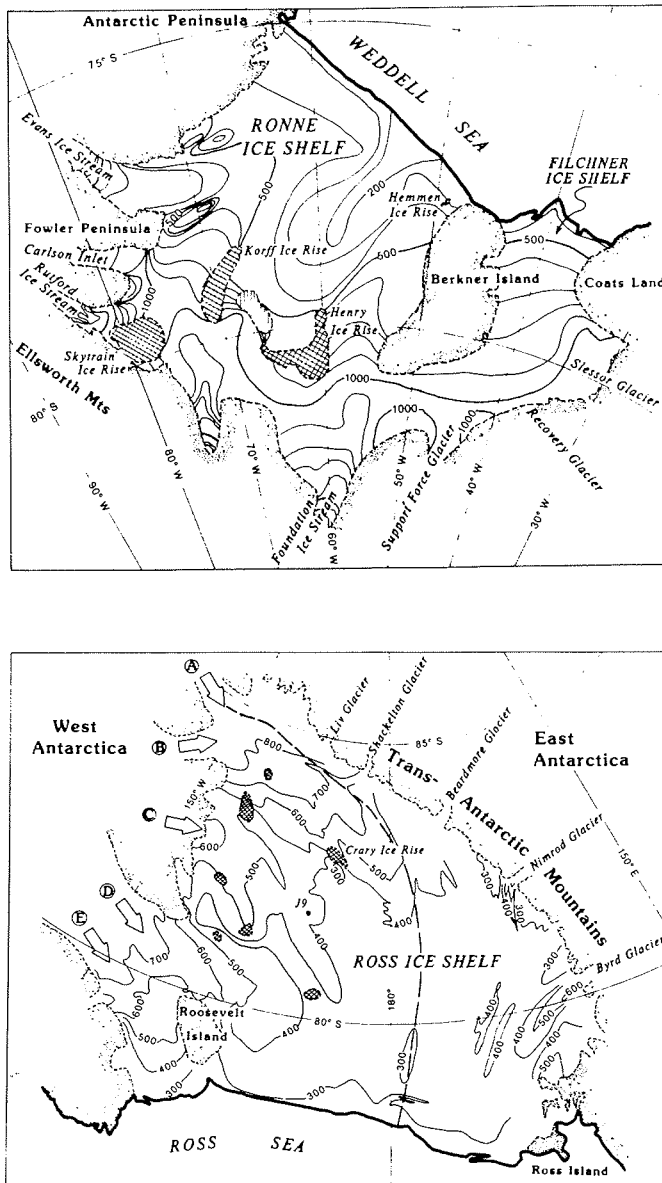
fig. 2.4: Maps of the Ronne-Filchner (above) and Ross ice shelf (below), showing thickness contours and major ice streams. Grounded ice and major islands are stippled and ice rises cross-hatched. From: DOE-report (1985): Glaciers, ice sheets and sea level: effect of a CO_2-induced climatic change.

From an ice-dynamical point of view, ice shelves effectively rest on a frictionless base and spread under their own weight as the ice moves outward to the sea. Restraining forces are provided by the sea water pressure at the ice front, by ice rises and by lateral shear along the valley-walls of the embayments, in which they are usually formed. At their inland margins, ice thicknesses of over 1000 m have been recorded (Drewry, 1983). The value at the ice shelf front is typically 250 m. This is a consequence of the rheological properties of ice. Flow velocities are an order of magnitude larger than in the grounded ice sheet, and attain values of over 1000 m/y at the seaward margin (Budd et al., 1982; Robin et al., 1983; Thomas et al., 1984). Basal melting rates have not been measured directly, but are believed to be of the order of 0.5 - 1 m/y within a few hundred kilometers of the front and near to the outlets of the major ice streams (Thomas, 1979a). Elsewhere, basal accretion may occur.

Fig. 2.4 shows thickness maps of the two largest ice shelves. Of these, the Ross ice shelf is larger by area, but the Ronne-Filchner ice shelf is the larger by volume, because of its greater thickness (table 2.1). These greater thicknesses occur because of the flow constraint imposed by large ice rises distributed across the ice shelf, which inhibit large-scale creep-thinning and cause the ice to thicken upstream. A striking feature of the central Ronne ice shelf is the zone of thin ice stretching nearly 300 km from the ice front. Robin et al. (1983) related this feature to the upstream restraint caused by the Korff and Henry ice rises, and the locally grounded ice in between ('Doake ice rumples'), which deflect ice to either side. Later borehole evidence, however, brought to light that the total ice thickness here is much greater than those mapped in fig. 2.4. The shallow radio-echo sounding reflections did not indicate thin ice, but came from an internal horizon formed by basal accretion of saline ice (Engelhardt and Determann, 1987).

2.1.6. Antarctic Peninsula

The Antarctic Peninsula, constituting the third part of the ice sheet, comprises an area of complex glacierization with several small merging ice caps, ice shelves, extensive mountainous terrain, outlet glaciers and ice-covered off-shore islands. Its more alpine type of glaciation is to a large extent dynamically uncoupled from the rest of the Antarctic ice sheet, although there

is a small contribution to the mass balance of the Ronne ice shelf at its western margin. It is also situated in the warmest part of the continent.

2.2. CLIMATE OF THE ANTARCTIC

The study of Antarctic glaciation is closely related to a knowledge of the climatic conditions prevailing in that part of the world. Characteristics of the present climate have been well described in Schwerdtfeger (1970, 1984). The main points are briefly introduced below.

2.2.1. Temperature regime

The present Antarctic climate is characterized by low air temperatures and little precipitation. The region is also an important heat sink of the earth-atmosphere system. This is because of the high snow albedo (around 0.85), the long polar night and the high emissivity, brought about by clear and dry atmospheric conditions, which limits the amount of counterradiation. The surface loses almost continually more energy than it receives, except during the short summer (the months of december and january), when the radiation budget is slightly positive. This loss of heat by radiation is compensated by the advection of warmer air from over the ocean, followed by the transport of sensible heat by vertical eddy motions and by particles of falling snow to the cold snow surface (Schwerdtfeger, 1984). Minor contributions in the surface energy budget are provided by heat conduction in the upper snow surface (upwards in winter, downwards in summer) and latent heat exchanges (hoarfrost formation and sublimation).

A conspicious feature of the Antarctic temperature regime is the strong inversion observed above the continent, in particular during the winter, which is caused by the intense radiative cooling over the interior region. The mean annual strength of the inversion is up to 20°C, and appears to be well correlated with surface temperature (Jouzel and Merlivat, 1984). Above the boundary layer, one usually observes a rather thick isothermal layer some 500 - 1500 m deep, in which relatively warm and moist maritime air is advected from lower latitudes (Schwerdtfeger, 1984). Fig. 2.5 shows the mean annual surface temperature distribution over the ice sheet. Above the 1500 m-

fig. 2.5: Isotherms of mean annual surface temperature in °C ($\approx$ temperature at 10 m depth). After Robin (1983).
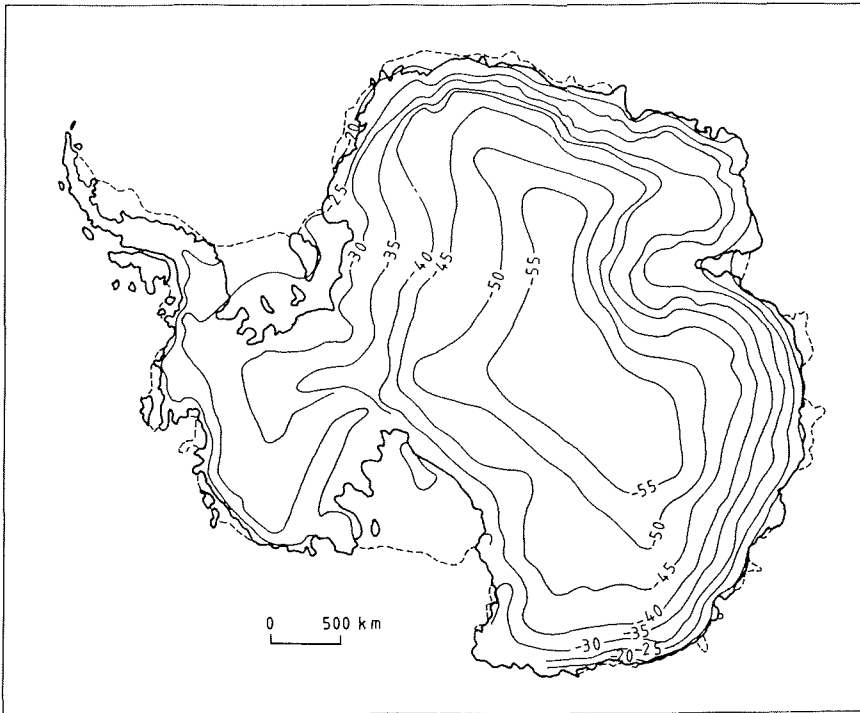
contour in East Antarctica, the surface lapse rate appears to be super-adiabatic. A mean value of $14.2°C$ / km was obtained from a linear multiple regression study on all available data (Fortuin and Oerlemans, 1990). This feature can also be explained by the strong radiative heat loss from the surface, which is very effective at these low temperatures and the associated low moisture content of the atmosphere. In addition, the emissivity of the atmosphere is further enhanced by about the square root of atmospheric pressure.

2.2.2. General circulation and surface winds

The general air circulation is dominated by a circumpolar vortex centered over the continent, with generally westerly flows in the middle and uppertroposphere. These westerlies reach their maximum north of a

circumpolar trough of all-year-round low sea level pressure located near the polar circle. The strength of these westerlies, with mean wind speeds exceeding those observed in other parts of the world, is related to the strong meridional temperature gradient in the southern hemisphere and the unbroken circumpolar Southern Ocean. In the boundary layer over the ice sheet, on the other hand, the flow of air is to large extent uncoupled from the free atmosphere and easterly winds dominate. This is mainly because of the boundary layer's pronounced static stability, which makes possible the strong effect of the terrain on the surface winds (Schwerdtfeger, 1984).

Over the ice sheet one usually distinguishes between inversion winds and katabatic winds. The former develop in response to the strong radiational cooling over the plateau and are characterized by a great constancy of direction and velocity. There is an approximate equilibrium between the sloped-inversion pressure gradient force, the Coriolis acceleration and friction. They blow downslope crossing the contour lines at an angle approximately 45° to the left of the fall line. The prevailing surface wind direction and speed are so closely related to the direction and steepness of the terrain and to the strength of the inversion, that the two former values can be well estimated if the latter are known with some precision (Parish and Bromwich, 1987).

On the steeper marginal slopes near the escarpment in East Antarctica, the wind takes on characteristics of purely gravity-driven flow and a transition to a katabatic wind regime takes place. Schwerdtfeger (1984) distinguishes katabatic winds from inversion winds by making use of the Rossby Number, i.e. a dimensionless quantity which gives the ratio between inertial forces and the Coriolis force. Rossby numbers Ro > 1 imply that inertial forces dominate on the Coriolis force and define pure katabatic flow; Ro < 1 classify the inversion winds. In contrast to the inversion winds, the frequency and intensity of katabatic winds, but not their direction, show extremely large variations and violent katabatic storms alternate with periods of weak winds or even calms. Apart from a few regions of strong confluence, persistent katabatic flow is exceptional, as this requires a continuous convergence of cold air currents fed by a drainage area of sufficient size and duration.

2.2.3. Accumulation regime

The characteristics of the lower atmospheric temperature regime and the associated circulation patterns as sketched above also help to explain the precipitation regime over the ice sheet. Because the moisture-carrying capacity of air diminishes strongly as its temperature decreases, the most important factor determining accumulation rates in Antarctica is air temperature. As a matter of a fact, over the vast interior of the continent, precipitation rates are so low (of the order of a few centimeters ice depth per year) that the plateau area can be classified as a true desert.

The precipitation mechanism over the East Antarctic plateau is of a peculiar nature. The predominantly convex surface geometry causes a slight divergence in the prevailing wind pattern, resulting in a slow and steady sinking motion in the boundary layer (subsidence). In this way the overlying relatively warm and moist air masses, that are often already in a state of supersaturation with respect to ice, are entrained within the inversion layer. This leads to an almost continuous process of clear-sky ice crystal precipitation and also some surface deposition of hoarfrost and rime. It is believed that this type of no-cloud precipitation forms the major contribution to the accumulation above some 3000 m altitude (Schwerdtfeger, 1984).

In the more marginal parts of the ice sheet, on the other hand, the accumulation regime is more closely linked to the synoptic situation and the intensity of cyclonic activity and snowfall rates are higher. Here, frequent incursions of moist maritime air above the inversion layer together with orographic lifting often produce intense upslope precipitation, even when the flow in the boundary layer is directed towards the coast. Precipitation is most abundant on the northwest side of the Antarctic Peninsula, when winds from the northwest quadrant lead to prolonged intervals of heavy snowfall on the windward side of islands and mountain ranges. The Antarctic Peninsula also constitutes a marked climatic divide, the Weddell side being some 4-6°C cooler and also much drier. The latter area is dominated by extensive sea ice.

Accumulation is not a matter of snowfall only. When surface winds become sufficiently strong, the wind stress causes snow particles to disengage from the surface and, consequently, snow is displaced in the general direction of

ANTARCTICA IN THE CLIMATE SYSTEM

the wind. Over the plateau, there can be little doubt that the winds are rather inefficient agents of downslope transport of drifting snow. If true katabatic storms were frequent phenomena in the interior, the ice cap would probably not persist and, moreover, may not have built up to its present size in the first place. Possible losses through evaporation and gains by sublimation are believed to be small and it can be assumed that in the interior accumulation virtually equals precipitation.

In the escarpment region wind velocities are higher and there may be a significant loss in the form of drifting snow as considerable amounts are probably blown into the Southern Ocean. A good example is the Lambert Basin close to the grounding line, where high rates of deflation and sublimation result in a very low surface mass balance and even areas of net ablation (McIntyre, 1985). As pointed out by Takahashi et al. (1988), the
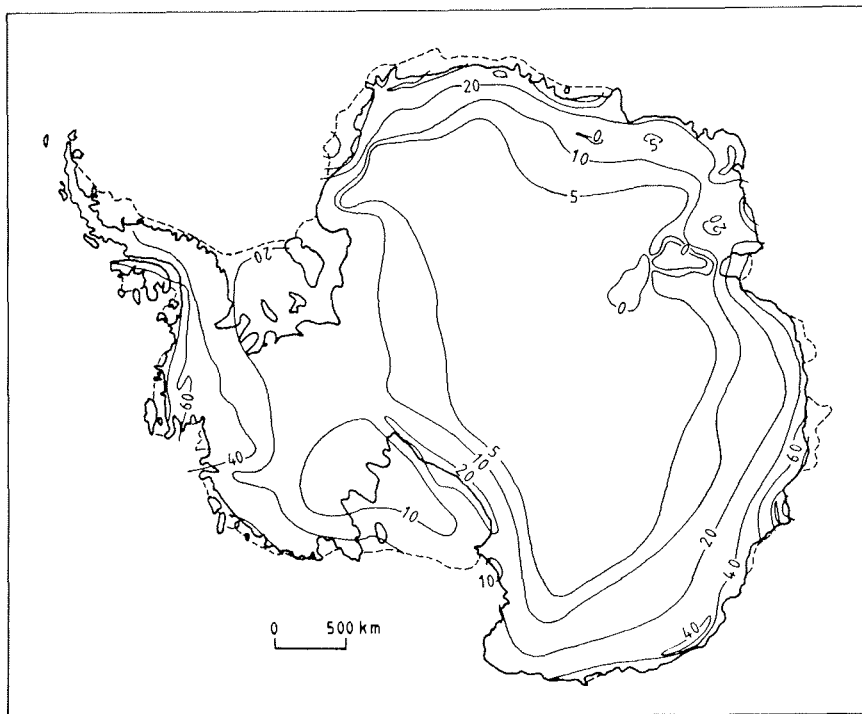
fig. 2.6: Surface mass balance rates in cm water equivalent per year. After Giovinetto and Bentley (1985).

presence of bare ice fields, such as those in the Lambert Basin and in eastern Dronning Maud Land, is well correlated with the horizontal divergence of a convex surface topography, which leads to a net mass export of drifting snow. Once a blue ice field has been formed, sublimation may be further enhanced by lower albedo and possibly, higher wind speeds over the smooth terrain. Nevertheless, it appears that the mass loss caused by blowing snow, although locally important, is only a small fraction of the total ice discharge from glaciers and ice shelves (Schwerdtfeger, 1970). Under present-day climatic conditions, runoff from the ice sheet is insignificant, although some surface melting during summer may occur in the Antarctic Peninsula and around the perimeter of East Antarctica.

A recent compilation of all available surface accumulation measurements, as presented in Giovinetto and Bentley (1985), is shown in fig. 2.6. As pointed out by these authors, the conspiciously low rate of surface mass balance inland of the Ross ice shelf is not caused by ablation, but by low accumulation rates. This feature can be explained by the low surface altitudes close to the grounding line, which lie below the lifting condensation level of advected air. In other words, it is probably a continentality effect, that is not obscured by the orographic effects which occur along the escarpment.

2.3. INTERACTION WITH THE ENVIRONMENT: BASIC MECHANISMS

The Antarctic ice sheet and its surroundings influence the climate on earth in a variety of ways and, in turn, changes in the global environment will lead to fluctuations of the ice cover. Here, we will first discuss how the ice sheet and its changes may affect global climate.

2.3.1. Impact of the ice sheet on climate

There can be little doubt of the strong impact of the ice sheet on the climate of the southern hemisphere and even on that of the globe as a whole. One can distinguish four main effects. The first is particularly evident in the high southern hemisphere equator-to-pole temperature gradient that drives more intense atmospheric and oceanic circulations than those observed in the

north. Second, the prevailing winds blowing off the ice sheet result in an equatorward advection of cold air, thereby significantly influencing the sea-ice extent and sea-surface temperatures. Third, melting of ice bergs, which account for over 99% of the total mass loss of the ice sheet, keep the surrounding waters close to freezing. Fourth, there is the climatic effect resulting from the formation of deep Antarctic bottom water, which owes its high density to salt rejection both during the formation of sea-ice and the process of accretion under ice shelves. The cold saline watermasses formed in this way compose most of the deep water of the world oceans and play a fundamental role in its circulation pattern.

The presence of the ice sheet affects the global energy budget in two main ways. First, to melt it would require an amount of energy equal to 7.6×10^{24} J. Although this may seem an enormous amount of heat - it is more than twice the amount of solar energy absorbed by the entire earth-atmosphere system in a year - it also corresponds to the energy needed to warm the oceans by little more than 1 degree (Oerlemans and Van der Veen, 1984). Hence, from an energetic point of view, changes in the ice sheet can easily be accomodated in the global budget. Although melting of large amounts of ice will certainly affect local conditions, increased advection of heat by atmospheric motion and oceanic currents will tend to counterbalance the local loss of energy. It can be calculated that complete melting of the ice sheet in 5000 years would disturb the global energy balance by around 0.1 Wm^{-2}. Compared to the mean solar absorption of 238 Wm^{-2}, this is indeed a negligible amount.

Second and more important is the impact of the ice sheet on the global radiation budget, since the amount of solar energy absorbed by the planet depends on the planetary albedo. The onset of Antarctic glaciation and the associated occurrence of an area of high surface albedo has probably been a major factor in cooling the global climate on a geological time scale. The magnitude of this effect can be crudely estimated by considering the zero-dimensional energy balance equation. For the earth as a whole, a balance should exist on the long time-scales between the absorption of incoming shortwave solar radiation and the emission of longwave radiation back to space:

$$Q(1 - \alpha) = I = a + bT \qquad (2.1)$$

where Q is the incoming solar radiation (340 Wm^{-2}), α (≈ 0.30) the mean planetary albedo, and a (207 Wm^{-2}) and b (2.04 $Wm^{-2}{}^{\circ}C^{-1}$) parameters that are found from zonal climatology (e.g. North and Coakley, 1979). I is outgoing infrared radiation. From eq. 2.1, it can be seen that for present conditions the mean planetary surface temperature should be around 15°C. The radiation budget S is given by the difference between incoming and outgoing radiation:

$$S = Q(1 - \alpha) - a - bT \qquad (2.2)$$

It can be estimated that removing the highly reflective ice sheet and sea-ice covers and replacing them by a surface with an albedo typical of mid-latitudes would raise solar absorption by 3%, which is equivalent to a perturbation of the radiation budget of $\delta S = 10$ Wm^{-2}. Considering linear perturbations in (2.2) and introducing the albedo-temperature feedback by the sensitivity parameter $\beta = \delta \alpha / \delta T$ (β negative), then leads to (Oerlemans and Van der Veen, 1984):

$$\delta T = \frac{\delta S}{b + \beta Q} \qquad (2.3)$$

The value of β can be derived from detailed studies with climate models, in which ice-age climates are compared with present conditions; it should be in the range -0.002 to -0.003 $^{\circ}C^{-1}$ (e.g. Lian and Cess, 1977). It follows that the mean surface temperature of an ice-free earth would be some 7 - 10°C higher than today, depending on the strength of the albedo- temperature feedback. Without this feedback, the direct effect would be some 5°C. Likewise, all other things being equal, melting of the Antarctic ice sheet in 5000 years ($\delta S = -0.1$ Wm^{-2}) would lower global temperature by only about 0.1 °C.

At shorter time scales, on the other hand, the Antarctic continent is relatively inert and passive with regard to its interaction with the atmosphere during climatic change. This is because the snow surface changes little in albedo and the ice sheet needs a long time to respond (of the order of thousands of years or more). By contrast, the Antarctic sea-ice region can change rapidly

and sensitively and is potentially important because of the effects of albedo, ocean mixing, and the heat exchange between ocean and atmosphere (Bentley, 1984). The latter effect arises because the sea-ice acts as an insulating blanket. The ocean mixing is induced by density and salinity variations in surface waters during the processes of melting and freezing. At present, the annual sea-ice cycle almost doubles the area of high surface albedo during late winter and early spring and is furthermore characterized by a high inter-annual variability. In this respect, significant correlations have been found between these inter-annual sea-ice variations and a number of meteorological variables such as temperature, pressure, wind speed, cyclogenesis and storm tracks, although cause and effect have not yet been clarified (Budd, 1982). This is because a number of important feedback mechanisms exist. For instance, low air temperatures resulting from the high albedo of the sea ice cover and the blanketing of the oceanic heat flux will lead to an increased sea-ice extent, and consequently, a further lowering of the temperature. However, the potential role of the albedo-temperature feedback in climatic change is flawed because the planetary albedo in the Southern Ocean is already high all-year round, due to the large cloud cover.

From the above description, it is clear that the interaction between Antarctic ice-sheet changes and the global climate is complicated and involves many inter-dependent processes. However, additional insight can be gained from numerical model studies. Broccoli and Manabe (1987) investigated the climatic influence of Antarctic ice sheet expansion during the Last Glacial Maximum using an atmospheric general circulation model coupled to a static mixed-layer ocean and a parameterization for sea-ice. They found that such a situation would have lowered the average southern hemisphere temperature by only 0.2°C. If their model correctly simulates real-world ice-age conditions, this means that the thermal effect of an enlarged Antarctic ice-sheet heat sink can be eliminated as a significant cause of southern hemisphere ice-age climates. Nevertheless, ice-core records and mountain snowlines indicate that ice-age climates in both hemispheres were roughly synchronous and of similar severity (Broecker and Denton, 1989). How then did the southern hemisphere cooling come about? It seems that the thermal impact of northern hemisphere ice sheets is also unlikely to have caused southern hemisphere climatic fluctuations. According to another study by Manabe and Broccoli (1985), expansion of continental ice is able to produce much of the observed

35

cooling in the northern hemisphere, but the loss of heat due to reflection was almost entirely compensated by a reduction in the upward terrestrial radiation from that hemisphere. As a result, little change in the inter-hemispheric transport of heat by the atmosphere occurred, leaving southern hemisphere temperatures virtually unchanged.

This apparently suggests the existence of other fast mechanisms able to transform northern hemisphere ice-sheet fluctuations into world-wide temperature changes. Part of the answer probably lies in the deep oceans, and more specifically on the role of the cross-equatorial heat flux and the effect of high-latitude deep convection on the atmospheric CO_2 concentration (Broecker, 1984; Broecker et al, 1985; Broecker and Denton, 1989). A key area appears to be the North Atlantic Ocean. There is evidence that the production rate of North Atlantic Deep Water (NADW) is very sensitive to changes of fresh-water input by the northern hemisphere ice sheets. Input of meltwater creates a lid of low-density surface water that may stop the formation of NADW and thus cease ventilation of the deep ocean. Consequently, the polar front is pushed far to the south and the oceanic circulation jumps to a state involving less meridional heat transport. Similarly, there are also indications that the formation of NADW may vary strongly with the salt content of advected waters, in this way linking the sinking motion to evaporation patterns in the more southerly parts of the North Atlantic Ocean. The resulting changes in the interaction between water mass mixing and biological cycles may then have altered the nutrient content of polar waters and the residence time of marine organisms, and hence, also the atmospheric CO_2 content. It is most likely that decreased levels of atmospheric carbon dioxide provided the major influence on southern hemisphere temperatures (Broccoli and Manabe, 1987).

2.3.2. Ice sheet response modes to changes in environmental conditions

Variations in the ice sheet are in turn driven by changes in climatological and environmental conditions in a number of ways. Concentrating on the longer Pleistocene time scales, when climate was generally colder than today and melting can be disregarded as a significant factor, there are three principal ways by which the global environment acts upon the ice sheet. These are

fluctuations in air temperature, accumulation rate and sea level stand. Here, we will first deal with stable interactions, as opposed to the possibility of more rapid unstable ice sheet behaviour, in particular in a warming climate, which is discussed in the next section.

In a classic paper, Hollin (1962) postulated the idea that glacial-interglacial expansions and contractions of the ice sheet might be largely controlled by world-wide sea level changes, rather than by climatic changes. During times of extensive glaciation in the northern hemisphere, the lowering of eustatic sea-level would lower the Antarctic grounding line and displace it northwards, allowing the ice sheet to expand onto the present continental shelf. This view has also been expressed elsewhere (e.g. Thomas and Bentley, 1978; Stuiver et al., 1981; Denton et al, 1989a), but still awaits thorough experimental verification. If proven correct, it would fit the concept of the globally interlocked ice sheet system of Denton et al. (1986), where sea level changes provide the direct mechanism linking the Antarctic ice sheet to the northern glacial cycle.

In discussing this hypothesis, however, a distinction should be made between the terrestrial East Antarctic ice sheet and the marine West Antarctic ice sheet. The reason for making this distinction is directly related to the subglacial bed topography. In West Antarctica, the bedrock between the grounding line and the edge of the continental platform is generally rather flat and this makes the position of the grounding line indeed very susceptible to changes in relative sea depth. A change in eustatic sea level, for example, will cause an immediate shift of the grounding line in order to preserve hydrostatic equilibrium.

However, it is important to realize that grounding-line migration may also occur because of local changes in ice thickness. This is illustrated by the fact that in its effect on grounding lines and pinning points, a 100 m thickening of the ice is equivalent to that of a 90 m lowering in sea level. For instance, lower air temperatures would probably lead to lower accumulation rates, so that the ice will tend to thin. However, after some time the effective ice temperature will also start to decrease, and the resulting lower creep rates should lead to increasing ice thickness. Ocean temperature and water circulation are also important in determining ice shelf behaviour. Changes in the melting or freezing rates at the bottom of an ice shelf could thus compete with variations

in snow accumulation at the surface. In addition, changes in the size of the ice shelf will lead to modifications in the stress field and this may in turn feed back on ice thickness at the grounding line. For instance, the formation of ice rises and pinning points will dam the ice flow and may create a positive feedback by thickening the ice at the grounding line during grounding-line advance (Thomas, 1979b).

The East Antarctic ice sheet, on the other hand, at present occupies almost the entire available land-base. Its outer limit or grounding line (in areas bounded by ice shelf) is in many places close to the steep continental slope, leaving little room for major seaward changes in its extent. For the ice sheet to recede from the continental platform, temperatures would have to *rise* by perhaps 10°C or more, in order to produce an ablation zone of sufficient width. This is because there is at present no snowline above sea level, which would divide an interior zone of net mass gain from a peripheral ablation zone. This implies that during the ice ages overall volume changes should essentially arise from local variations in ice thickness. For instance, lower rates of snow deposition associated with lower air temperatures will result in a lower surface level. However, equally important in cold ice masses will be the concomitant effects of changes in the thermal regime, especially in the lower layers and at the ice sheet base: as its temperature falls, ice deforms less easily and strain rates decrease, which should ultimately lead to a thickening. Also decreased amounts of basal water production may result in lower sliding velocities at the bed through decreased bed separation and basal water pressure. Again, this leads to a thickening.

It is instructive to illustrate how the combined effects of changes in surface temperature and accumulation rate may influence the steady state geometry of an idealized East Antarctic flowline, in which changes in flowline length are not considered. Fig. 2.7 shows results from such a two-dimensional experiment, in which the model ice sheet is submitted to combinations of typical glacial-interglacial changes in background air temperature and accumulation rate, i.e. a temperature lowering of 10°C and a halving of the snowfall rate. These schematic calculations take into account the fully coupled stress and temperature fields as well as isostatic adjustment, but not basal sliding. It is interesting to see that, although a cooler ice sheet is thicker and lower accumulation leads to a thinning as could be expected, there is only

ANTARCTICA IN THE CLIMATE SYSTEM
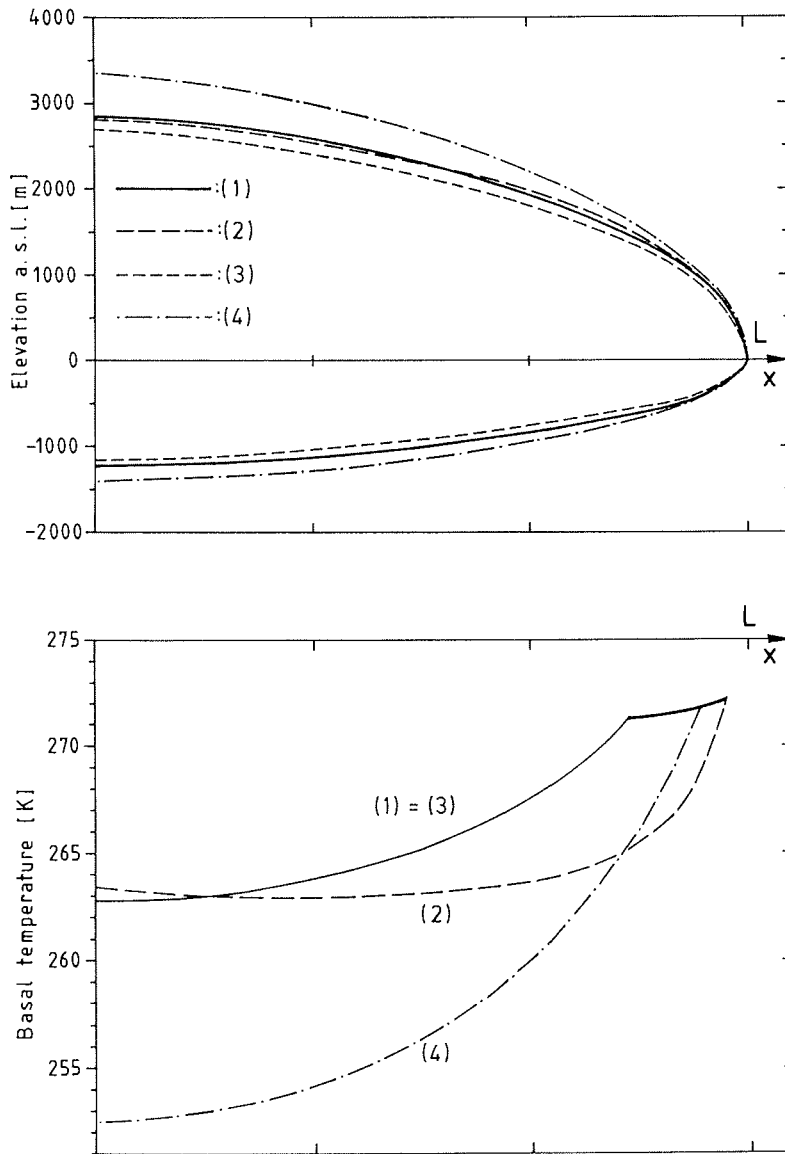
fig. 2.7: Steady state effects of glacial-interglacial changes in atmospheric conditions on the geometry of an idealized East Antarctic flowline (upper panel). The lower graph shows the corresponding basal temperature distribututions; a thick line refers to pressure melting. (1): present interglacial reference state; (2): 50% accumulation rate and 10°C surface temperature lowering; (3): 50% accumulation rate and fixed englacial temperature distribution; (4): 10°C surface temperature lowering and fixed accumulation distribution with respect to the reference run. From Huybrechts (1987).

little difference in the ice thickness distribution when both conditions now act together (as is the case in real world). This is an important result and also implies that changes in the ice sheet cannot be studied without taking into account thermomechanical coupling. In addition, the response time scales arising both from thermomechanical coupling (Huybrechts and Oerlemans, 1988) and grounding-line migration (Alley and Whillans, 1984) introduce transient effects, which may significantly modify the outcome during a glacial cycle. We will come back to this later in the full three-dimensional calculations reported in chapters 5 through 7.

So, from the above qualitative description, it is clear that the ultimate response of the ice sheet to changes in environmental conditions is a complicated matter. In particular, migration of the grounding line may be very difficult to predict. In fact, the complex nature of the various feedback mechanisms and the strong dependence on topography mean that only physical modelling of the complete ice sheet - grounding line - ice shelf system can yield an improved understanding of the interplay between environment and ice sheet volume.

2.4. INSTABILITY MECHANISMS

The preceding analysis dealt with stable behaviour, in the sense that the response for a relatively small change in boundary conditions is approximately linear and reversible. However, in the last two decades several instability mechanisms have been suggested that might cause catastrophic disintegration of appreciable parts of the Antarctic ice sheet in a comparably short time. The first of these concerns the West Antarctic ice sheet.

2.4.1. West Antarctic ice sheet grounding line instability

The marine nature of the West Antarctic ice sheet leads many glaciologists to believe that it may be inherently unstable and may respond drastically and irreversibly to a warming climate (Hughes, 1975; Mercer, 1978a; Thomas and Bentley, 1978; Thomas, 1979b; Thomas et al., 1979; Bentley, 1984; Lingle, 1984, 1985; and many others). This view is based on the idea that the large ice shelves surrounding West Antarctica control its stability and that a
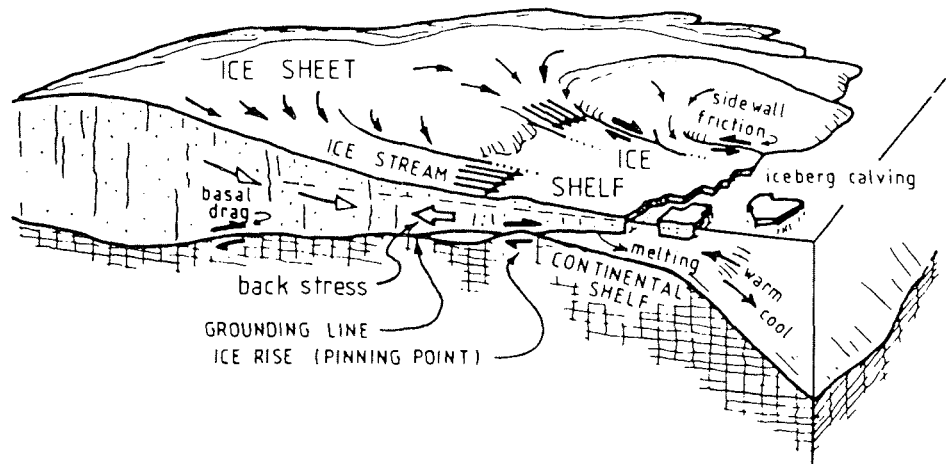
fig. 2.8: Sketch of a marine ice sheet, showing processes that control the flow of ice from the inland parts to the sea. From DOE-report (1985).

grounding-line tends to be unstable if the sea-depth is greater than a critical depth and the sea-floor slopes down towards the ice sheet interior. Through non-linear positive feedbacks, a small perturbation in boundary conditions (e.g. a rising sea level, a thinning ice shelf or lagged isostatic depression of the sea bed) may result in a run-away process in which the initial small displacement of the grounding line is amplified until the marine ice sheet completely collapses (Thomas, 1979b).

To understand this hypothesis, consider a situation in which the ice sheet is bounded by a freely floating ice shelf or where calving takes place near the grounding line. The rate of advance or retreat of the grounding line is then determined by the local ice surface and bedrock slopes, the local mass-balance and the rate of change of sea-depth through time, either by changes in sea-level or isostatic adjustments (Thomas and Bentley, 1978). If the bedrock in the vicinity of the ice sheet - ice shelf junction slopes down away from the ice sheet, then migration of the grounding line will be limited: the steeper the slope of the bed, the smaller the grounding line migration will be. Conversely, when the bedrock depth increases inland from the grounding line, as is typically the case in West Antarctica, a retreating grounding line will progressively encounter deeper water. This leads to a greater ice thickness at the grounding line, and since the creep-thinning rate depends on the fourth

power of ice thickness (Weertman, 1957), ice discharge at the grounding line will also increase. This is a positive feedback and will result in downdraw of the ice sheet and a further retreat of the grounding line. Under these conditions, the ice sheet will completely collapse unless there is a sufficiently high bedrock sill on which the grounding line can achieve equilibrium (Thomas, 1979b).

The major mechanism for stabilizing a marine ice sheet, however, involves the interaction of a marine ice sheet with a bounded or partially grounded ice shelf. Most ice shelves surrounding West Antarctica have formed in embayments and are locally pinned on ice rises. Hence, a compressive stress, stemming both from shear along lateral margins and drag from pinning points, is exerted on the ice streams debouching into the ice shelf. This back-stress leads to a decrease in the ice-shelf thinning rate and thereby has a damming effect on ice-stream discharge. In this way, the restraining force of the surrounding ice shelf ('its buttressing effect') may be strong enough to keep an otherwise unstable marine ice sheet in place (Thomas et al, 1979).

So, according to the arguments put forward above, it appears that the existence of the West Antarctic ice sheet depends upon the existence of its fringing ice shelves. In view of the anticipated CO_2-induced climatic warming, this led Mercer (1978a) to believe that the West Antarctic may at present be at the verge of a catastrophic collapse, in which the major part of the ice sheet could disintegrate in as little as 100 years time. This would lead to a world-wide sea level rise of 5 m. The effect of such a warming would be to weaken the ice shelves through increased calving and bottom melting, eventually resulting in their complete breakup. The ensuing reduction in back-stress would then strongly diminish their buttressing effect, and thus eliminate what could be a critical stabilizing factor. The possibility of a major deglaciation of the West Antarctic ice sheet is supported by the 6 meter higher than present sea level during the Sangamon interglacial some 120000 years ago, when temperatures were believed to be several degrees higher than today.

Later work, however, indicates that a sudden collapse on such a short time scale is unlikely to happen. For example, Thomas et al (1979) believe that disintegration would probably last longer because of a negative feedback: thinning of an ice shelf reduces its buttressing effect so that flow from the ice

sheet increases and partly compensates for the thinning. Thus, fast thinning and eventual breakup of the ice shelves may not be so imminent. Also, a climatic warming would probably not have a significant effect on the upper surfaces of most Antarctic ice shelves for some time to come, because their mean temperature (now less than -20°C) would still remain far below freezing and any summer melting would simply refreeze as it percolated downwards into the underlying snow layers (Bentley, 1984). This leaves basal melting as the only potential threat. However, at present little is known about how melting and freezing rates beneath ice shelves would be affected by changes in ocean temperature and circulation, or how fast the oceans would react in the first place. Although ice shelves are in principle very vulnerable to increased thinning rates, because that would lift them from their pinning points, additional feedback-loops may be involved. For instance, selective removal of the warmest and thus softest ice from the ice column would decrease the depth-averaged ice temperature and thus stiffen the remaining ice, thereby decreasing ice-shelf strain-rates (MacAyeal and Thomas, 1986).

Also, how effective the proposed mechanism of grounding-line instability is, still remains subject of considerable debate (e.g. Van der Veen, 1986; Muszynski and Birchfield, 1987). The crucial question in model studies appears to be how to couple the inland ice, whose motion is believed to be largely controlled by sliding, hence by basal shear stresses, to the ice shelf, whose motion is controlled by ice shelf spreading, hence by longitudinal stresses. All models except Van der Veen's have explicitly or implicitly assumed that ice movement at the grounding line is controlled solely by ice shelf spreading, but that the movement of the ice stream immediately inland is controlled by basal shear stresses. These models, which are all based on a study by Thomas (1977), yield an unstable retreat when the ice shelf is removed, continuing to the complete elimination of the inland ice. Hence, the disaster scenario of Mercer (1978a) is qualitatively confirmed: the West Antarctic ice sheet would not survive a major thinning or removal of its large, buttressing ice shelves.

However, Van der Veen (1986) strongly objects to these studies, mainly because the ice sheet/ice shelf feedback is taken into account at one point only and a discontinuity is introduced at the grounding line when calculating creep thinning rates and ice velocities. This would make these models

weakest at the grounding line, which happens to be the focal point. When introducing a stress transition zone into the ice stream and calculating ice velocities explicitly along a complete flowline, Van der Veen (1985) found that the position of the grounding line was only moderately influenced by changes in ice-shelf backpressure, and furthermore that an ice shelf is not needed to stop grounding-line retreat. These results suggest that a marine ice sheet might be more stable than hitherto assumed. But even if this were not the case, the general feeling seems to be that it would still take a long time for the ice shelves to weaken enough for the ice flow from the inland ice sheet to significantly increase. We will come back to this later in the greenhouse warming experiments discussed in chapter 8.

2.4.2. Large-scale surging

Recourse to marine ice sheets is not necessarily required for rapid change. It is well-known that some glaciers exhibit surge-type behaviour in which two alternating flow regimes are apparent. One is the slow flow of ice down-glacier, the other, a sudden rapid ice-mass discharge (surge). During a surge, which lasts a relatively short time (months to a few years), ice velocities may increase by two orders of magnitude and the glacier then settles down to a new steady state with a much smaller volume and 'normal' velocities. After a period of recovery, during which the glacier grows again to the pre-surge state, a new surge occurs, and so forth. An adequate explanation for glacier surging does not exist, but available theories relate the transient behaviour to varying thermal conditions at the base (in particular water lubrication), cf. Paterson (1981).

It has been suggested that large ice sheets may also surge. Wilson (1964) has put forward the hypothesis that the Antarctic ice sheet would surge periodically, thereby initiating an ice age by creating a huge ice shelf in the Southern Ocean. The resulting increase in reflected solar radiation would then lead to the temperature drop needed to initiate the ice sheets on the northern hemisphere continents. Conversely, during the recovery of the ice sheet, when ice discharge slows down, the ice shelf would not be sustained any longer, and its eventual breakup would drive the Earth out of the ice age. Although the proposed theory of ice ages can be dismissed as being unlikely in view of the arguments put forward in § 2.3.1, the idea that the Antarctic ice

sheet may exhibit surging behaviour has subsequently received considerable attention (e.g. Hollin, 1972; Flohn, 1974, Oerlemans and Van der Veen, 1984). Hollin (1980) reviews evidence for a short-lived (1000 years) jump in global sea-level, possibly amounting to 16 m, that occurred towards the end of the Last Interglacial. Together with evidence for a cooling, this would point to a major East Antarctic ice surge at 95000 BP. However, one of the critical points seems to be the interpretation of the higher sea-level stands, and in the light of calculations with geophysical models of the upper mantle, some inferences remain speculative (Watts, 1982; Peltier, 1985; Officer et al., 1988).

The possibility of surging has also been the subject of some model studies. With a 'frictional lubrication model', Budd and McInnes (1979) found that surging of certain sectors of East Antarctica is physically reasonable. Their flowline model is based on the assumption that changes in frictional heating are the major source for variations in basal temperature. When the ice-mass discharge exceeds a critical value, a lubricating water film is formed, and as a consequence, basal sliding sets in and velocities increase further. A surge is then transmitted through the ice sheet by longitudinal stress gradients. Depending on the size of the sector involved, the time between surges was found to range from 10000 to 25000 years. However, their 'thermodynamics' were very simple and it is doubtful whether this model, originally developed for glaciers, can really be applied to large continental ice masses. Nevertheless, self-sustained oscillations were also found by Oerlemans and Van der Veen (1984) when employing a two-dimensional model of the Antarctic ice sheet. Their model contains a simplified calculation of the basal ice temperature as well as the feedback between ice flow and basal water. Also here, for certain values of the model parameters, ice thickness over East Antarctica varied periodically with a time interval of typically a few thousand years. This was caused by the accumulation of basal water under the thicker parts. West Antarctica, on the other hand, remained close to a steady state with extensive melting and high sliding velocities. So, according to these studies it appears that surges are a possibility in East Antarctica, although much also seems to depend on how sliding is parameterized in terms of basal water and on how effective melt water is removed. As far as West Antarctica is concerned, this ice sheet appears to be already in the 'fast mode' (i.e. basal melting and high ice velocities) and the occurrence of surges seems unlikely (Oerlemans and Van der Veen, 1984).

2.4.3. Creep instability

Another mechanism that may bring continental ice sheets into the surging mode is creep instability. This mechanism acts entirely independent from sliding instability and is a consequence of the temperature dependence of the deformation properties of ice. As ice temperature increases, ice deformation rates will also increase. In this way, a small increase in deformation rate, by increasing the strain heating and thus the ice temperature, will result in a further increase in deformation rate. This is a positive feedback mechanism with regard to sudden global climatic changes, and under suitable conditions, a runaway temperature increase may result.

The potential importance of creep instability in destabilizing the East Antarctic ice sheet has been stressed by several authors (Clarke et al., 1977; Schubert and Yuen, 1982; Yuen et al., 1986; Saari et al., 1987). In the study by Clarke et al. (1977), it was demonstrated that the feedback between temperature and ice flow can lead to bifurcation. Under specific conditions, multiple steady states occur: either the ice sheet is thick and cold with low velocities, or it is thin and warm with high velocities, implying that the ice sheet can switch suddenly from the slow mode to the fast mode if external conditions change. They also carried out an analysis of linear stability, revealing that typical e-folding times for the runaway increase are in the 10^3 to 10^4 years range for large ice sheets. The study by Schubert and Yuen (1982) elaborates further on this problem. Their scenario calls on climatically enhanced accumulation to increase the thickness of the East Antarctic ice sheet above a critical value for the onset of an explosive shear heating instability. This would cause massive melting at the base and initiate a surge. In Yuen et al. (1986) conditions for the onset of this explosion were investigated. For certain values of ice rheological parameters, they found that a sudden increase in ice-sheet thickness by 1-2 km could lead to melting of the basal shear layer in only thousands of years.

However, as became clear in Huybrechts and Oerlemans (1988), the major objection against these analyses is that they are 'local': horizontal temperature advection and driving stress (ice sheet geometry) are not allowed to react to the changing temperature and velocity fields. These processes would tend to spread out temperature perturbations. It appeared that the development of a creep instability in the aforementioned studies was

46

essentially due to a basic shortcoming in model formulation, namely the neglect of horizontal heat advection, so that a basic damping mechanism was excluded.

3. GLACIAL HISTORY

Over the past two decades, a chronology of Antarctic glaciation has begun to be developed. Geomorphological and geological research carried out both on the Antarctic continent and in the surrounding ocean have started to provide a record of the former ice sheet evolution and extent, even though the interpretation of part of the field data is still a matter of speculation and controversy. This chapter presents a broad overview with special attention to what is known of the Last Glacial Maximum. This will also provide a benchmark against which to compare later model output. In the text that follows, however, we will first start with a presentation of evidence and current ideas bearing on the question of the ice sheet's inception during the Cenozoic, i.e. after about 65 million years ago (My).

3.1. INCEPTION AND GROWTH

3.1.1. The environmental record

The origin and evolution of the Antarctic ice sheet have been discussed by Denton et al. (1971), Drewry (1975,1978), Kennett (1977), Mercer (1978b), Kvasov and Verbitsky (1981), Ocean Drilling Program Leg 113 (1987), Ocean Drilling Program Leg 119 (1988), Webb (1990), and others. Direct evidence (glacial erosion, ice contact deposits and glacial marine sedimentation) and indirect evidence (sea-level changes and oxygen isotope ratios in biogenic sediments) indicative of glaciation are currently interpreted by most workers as pointing to at least some Antarctic ice after about 40 My. However, clear consensus has yet to be reached and alternative views on the timing of Antarctic glacial initiation exist. For instance, Frakes and Francis (1988)

interpret mudstone strata in central Australia as evidence for ice-rafting, implying some glaciation during the Cretaceous and early Cenozoic.

Rich fossil floras and vertebrate faunas in Tertiary stratigraphic sections indicate that temperate, ice-free and largely frost-free conditions existed over at least coastal Antarctica and the Antarctic Peninsula during the early part of the Cenozoic (65-50 My). Axelrod (1984) reviews evidence for early Tertiary Antarctic forests, describing them as broad-leaved evergreens adapted to ocean-influenced climates characterized by high rainfall well distributed through the year. Such forests are comparable to the present-day vegetation of coastal southeast Australia and northern New Zealand. A similar comparison is also made in Creber and Chaloner (1985), who note high-latitude Antarctic forests in the early Tertiary that were flourishing and highly productive. They assert that these forests could have coexisted with regions of glacial ice and have grown with the low solar radiation input and dark winter of that latitude, without the need to invoke changes in the earth's axis of rotation. Important information on the development of Antarctic glaciation is also due to the success of the Deep Sea Drilling Project (DSDP). DSDP Leg 113 (Ocean Drilling Program Leg 113, 1987), coring in the Weddell Sea, found evidence for warm and humid conditions prior to the beginning of the Oligocene at 38 My. Pollens present in Eocene sediments indicate the presence of temperate beech forests with an undergrowth of ferns in the northern Antarctic Peninsula. In addition, oxygen isotope analysis of biogenic calcium carbonate in DSDP sequences indicate warm Subantarctic surface and bottom water temperatures up to 45 My in the middle Eocene (Kennett, 1977).

A first major climatic threshold appears to have been crossed about 38 My near the Eocene-Oligocene boundary. Oxygen isotope changes in benthonic foraminifera from DSDP sites in the Subantarctic and the Tropical Pacific regions indicate that bottom temperatures decreased abruptly by approximately 5°C to near present-day levels (Kennett, 1977). This temperature drop would have occurred within 10^5 years, and is considered to represent the time when large-scale freezing conditions developed at sea-level around Antarctica, forming the first significant sea-ice. The earliest physical evidence for Antarctic glaciation found so far also dates from this period. Ocean Drilling Program Leg 119 (1988) reports lodgement tills in

GLACIAL HISTORY

Prydz Bay near the mouth of Lambert Glacier, indicating that a large glacier complex was grounded there during the earliest Oligocene (35 My) and possibly even during the mid to late Eocene (about 42.5 My).

Earlier, ice-rafted quartz grains with surface textures diagnostic of glaciation were reported to occur in Eocene sediments of the Southern Ocean (Margolis and Kennett, 1971), but this piece of evidence has subsequently been the subject of criticism in the literature. According to Drewry (1978), oceanic circulation and environmental conditions at that time could not have permitted ice berg drifting over the distances required to explain their occurrence. Alternatively, the 'glacial' fractures and markings may have originated from non-glacial high-energy processes such as turbidity currents and sub-aerial sedimentation (Drewry, 1975). It seems that the first unequivocal identification of ice-rafted debris in Antarctic marine sequences is late Oligocene in age ($\approx$ 25 My), as retrieved in near-continental sections in the Ross Sea sector. These glaciomarine sediments have been discussed by, amongst others, Drewry (1978) and Frakes (1978) and indicate the time when glaciers reached sea-level (again?) and considerable ice-berg calving took place. In addition, DSDP Leg 113 (1987) found a switch from carbonate to mainly siliceous microfossils off East Antarctica, which, along with ice-rafted detritus, also points to cooler Oligocene conditions and at least some ice. Evidence of smectite clays off West Antarctica, on the other hand, suggest that warm and ice-free conditions persisted in that part of Antarctica. In summary, it is still not entirely clear whether the Oligocene ice was relatively local (mountain glaciers and small high-altitude ice fields) or more wide-spread (as possibly called for by DSDP Leg 119 results), but oxygen-isotope evidence suggests that during this period no major ice cap had yet developed on Antarctica (Kennett, 1977).

A second important climatic change, both globally and over Antarctica, appears to have taken place during the mid Miocene ($\approx$15 My). Based on isotopic data, Kennett (1977) dates the formation of a major East Antarctic ice sheet between 14 and 11 My, with the ice cap remaining a semi-permanent feature exhibiting some changes in volume since then. This event was associated with an increase in the equator-to-pole temperature gradient, a rapid northward displacement of the Antarctic Convergence zone and a marked drop in global sea level. The West Antarctic ice sheet probably formed

50

later (10-5 My). The formation of a major Ross ice shelf between 10 and 8.5 My is suggested by the initial occurrence of dropstones and a major increase in sand size ice-rafted debris in a DSDP site off the coast of Victoria Land (Savage and Ciesielski, 1983). The first unequivocal evidence for a West Antarctic ice sheet of considerable extent is then provided by a marked stratigraphic break during the latest Miocene in Ross Sea sedimentary sequences (Drewry, 1978).

From Antarctica itself, direct evidence for the age and origin of continental glaciation is rare, probably because most of the critical data are now buried below the ice. Datable glacial erosion events are few and have been
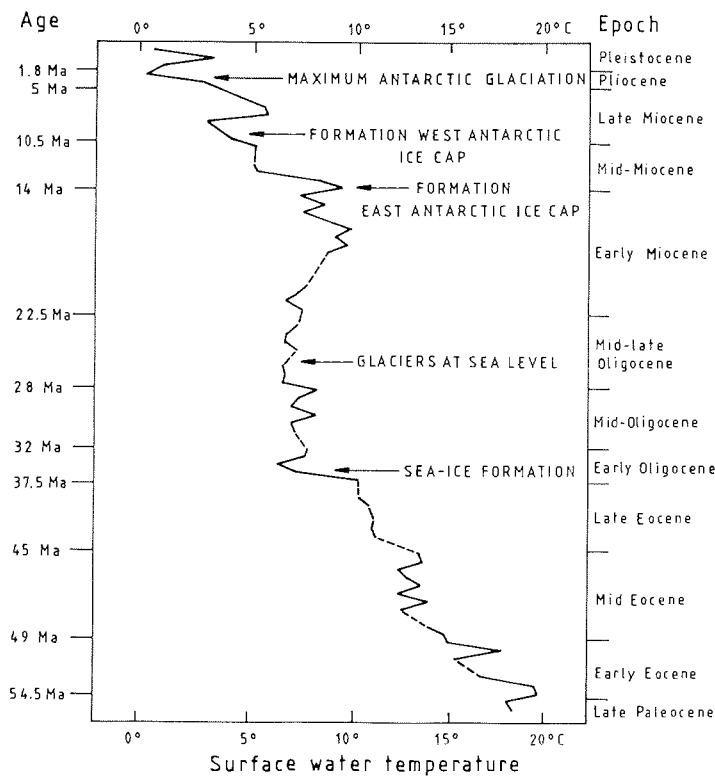
fig. 3.1: Sequence of Antarctic glacial events in the Cenozoic and ocean temperatures as derived from oxygen isotope ratios in planktonic foraminifera at Subantarctic DSDP sites. After Kennett (1977). Epoch boundary ages are after Berggren, as quoted in Frakes (1978).

reviewed in early papers by Denton et al. (1971) and Drewry (1975). The oldest definite evidence comes from tillites and striated pavements underlying volcanic rocks in the Jones Mountains, West Antarctica. These have been dated by K/Ar methods as between 7 and 10 My old. However, it is not clear whether these relate to local intramontane glaciation or originate from a full-grown West Antarctic ice sheet at that time. The same ambiguity also applies to older evidence for subglacially erupted volcanic rocks (hyaloclastites) found in Marie Byrd Land. Some hyaloclastites are believed to be as old as 26 My (LeMasurier and Rex, 1983), although it has also been suggested that the oldest rocks may have formed under water rather than beneath glacier ice (Frakes, 1978). Direct evidence for widespread glaciation in East Antarctica is much younger, even though glaciological considerations seem to demand that this ice sheet formed first (see below). In the Ross Sea region, valley incision into the Taylor and Wright Valleys is indicative of spill-over from a full-bodied East Antarctic ice sheet. Minimum dates for this glacial excavation, as obtained from lava flows in critical stratigraphic locations, are placed at 4 My. Since only minimum dates are known, it is clear that the question of the onset of large-scale glaciation cannot be answered from terrestrial evidence, nor can this evidence be used to settle the question of the relative timing of glacial initiation in East and West Antarctica.

Finally, recent findings in the Transantarctic Mountains could point to major fluctuations of the East Antarctic ice sheet in times pre-dating the Pliocene (Webb et al., 1983; Harwood, 1983; McKelvey et al., 1984). These findings relate to the Sirius Formation, a glacigenic sediment that is believed to have been deposited by an overriding ice sheet during the Pliocene. The recovery of reworked marine microfossils of late Miocene, late Oligocene and Eocene age from the Sirius Formation suggests periods of open marine sedimentation in low-lying parts of the East Antarctic craton (Pensacola and Wilkes basins), interchanged with intervals during which these basins were ice filled. This would challenge the view of a semi-permanent East Antarctic ice cap and point to one or more phases of deglaciation. However, at present these ideas appear to be rather speculative. It could for instance be that the cessation of marine sedimentation was due to regression associated with falling sea levels or continental uplift. Nor is it clear which mechanism could lead to episodic destruction of the East Antarctic ice sheet.

A summary of the Antarctic glacial history based on the oceanic temperature record is shown in fig. 3.1.

3.1.2. Causes of Antarctic glaciation

The onset of Antarctic glaciation during the Cenozoic is closely related to the much wider problem of the transition from a largely ice-free earth to a glaciated one. This is because the formation of the Antarctic ice sheet probably provided the starting point for the chain of climatic feedbacks that ultimately resulted in the Quaternary ice ages of the northern hemisphere. A clear answer to the causes for Antarctic glaciation cannot be given yet, but the fundamental role played by plate tectonics is a well established fact (Denton et al., 1971; Kennett et al., 1972; Kennett, 1977; Kvasov and Verbitsky, 1981; Weller et al., 1987; Webb, 1990; and others).

Apart from the late Cenozoic glacial period in which we live today, major shifts in the earth's climate and widespread continental glaciation are known to have occurred earlier during the Permo-Carboniferous some 300 million years ago and during the Ordovician (450 My), e.g. Hunt (1984). A recurrent theme in most hypotheses of glacial initiation is that land at high latitudes is a necessary pre-condition. Palaeomagnetic evidence shows that Antarctica has been in a polar position from at least the mid-Cretaceous to the present time (Kennett, 1977 and references quoted therein). However, as described previously, the initial glaciation did not commence until much later in the mid-Cenozoic, demonstrating that a near-polar position is not sufficient for glacial development. Instead, it is widely assumed that continental glaciation developed as the present-day Southern Ocean circulation system came into existence after obstructing land-masses moved aside.

Rifting and sea-floor spreading, which isolated Antarctica from Australia and South America, began about 55 My (Kennett et al., 1972) and a basically unrestricted circum-Antarctic current seems to have been established by 30 My (Kennett, 1977), see fig. 3.2. The last phase in this continental drift was the deepening of Drake Passage, separating the southern tip of South America from the Antarctic Peninsula. This removed the final barrier to a complete deep circumpolar circulation and is believed to have taken place by 23 My at the latest (Kennett, 1977). The strong zonal characteristics of the resulting

atmospheric and oceanic circulations then isolated Antarctica from the warm subtropical gyres and initiated the climatic cooling.

Nevertheless, despite continental isolation and the existence of freezing conditions from about 38 My (onset of sea-ice formation at the Eocene-Oligocene boundary), the development of a major ice cap appears to have
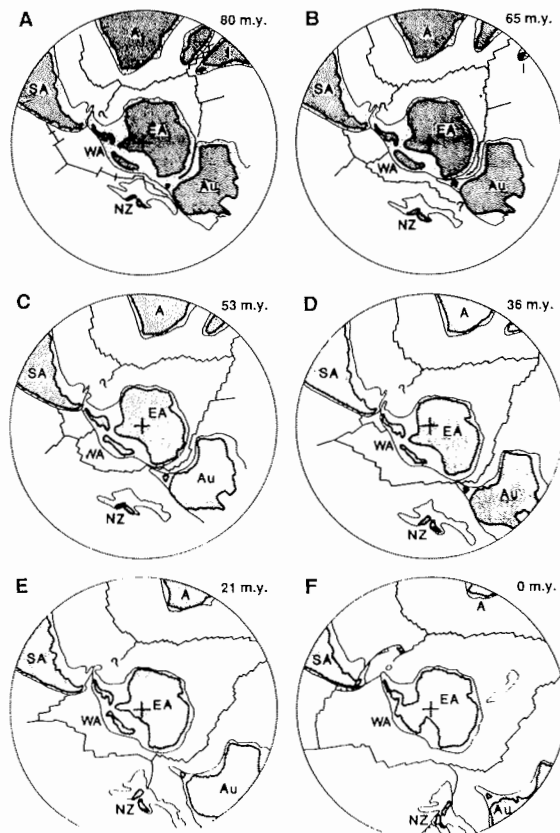
fig. 3.2: Evolution of the Southern Ocean from late Cretaceous time to the present showing the growing physical isolation of the Antarctic continent. Light stipple indicates continental shelves, heavy stipple continents. Lines in oceanic regions represent mid-ocean ridge spreading centers. SA, South America; A, Africa; I; India; Au, Australia; NZ, New Zealand; EA, East Antarctica; WA, West Antarctica. From Weller et al. (1987).

been delayed for at least another 10 - 15 My until mid-Miocene times. Reasons for this apparent paradox are not entirely clear and an adequate explanation is still lacking. Part of the answer may be related to continental uplift and mountain formation. In this respect, Smith and Drewry (1984) summarize geological data which indicates that the Transantarctic Mountains have risen by at least 4 km since the beginning of the Cenozoic. Ice sheet growth may then have been retarded until these mountains were high enough to support a local ice cap of sufficient size. Alternatively, atmospheric carbon dioxide levels rather than tectonic events may have been the crucial control on the earth's climatic history (Hunt, 1984), although it is hard to see how the existence of sea-ice can be reconciled with the absence of snow accumulation on land, even if the ground was relatively low. Another explanation could be that very dry conditions prevailed during the Oligocene and early Miocene. It is probably not a coincidence that the development of the ice cap occurred at a time of warmer global climates, because increased precipitation would have resulted from slightly warmer Antarctic surface waters (Kennett, 1977).

An interesting modelling study on this problem was recently conducted by Oglesby (1989). With an atmospheric general circulation model, he investigated the possible climatic effects of closing the Drake Passage (representing an increased meridional heat transport by the ocean) and lowering the elevation of Antarctica to only 200 m. From this study, it appeared that under all circumstances, even with greatly increased atmospheric carbon dioxide, conditions would still have been favorable for the maintenance of an Antarctic ice sheet. Thus, far-below-zero surface temperatures exist throughout most of the year and a positive surface mass-balance still prevails, certainly in more central areas. These results indicate the difficulties involved in explaining frost- and ice-free conditions in polar latitudes, even with different continental figurations. This dynamical problem was also noted by Hunt (1984). If these models simulate climate conditions correctly, this may indicate that, after all, the Antarctic ice sheet is older than the 15 My widely accepted. Otherwise only a fundamental change in the operation of the climatic system can account for the various conflicting pieces of evidence.

3.1.3. Models for ice sheet growth

Irrespective of the cause and timing of glacial inception, several glaciological models have been proposed for the sequence of events that ultimately resulted in a large ice sheet, both over East and West Antarctica. Denton et al. (1971) and Kvasov and Verbitsky (1981) hypothesize that the East Antarctic ice cap originated on the high bedrock plateau of the Gamburtsev Mountains. They invoke a mechanism similar to the 'instantaneous glacierization' and the 'highland origin-windward growth' hypotheses used for explaining the growth of the Laurentide and Fennoscandinavian ice sheets, but without a similar time constraint (the northern hemisphere ice sheets grew to maximum extent in roughly 50000 years). Precipitation-bearing storms would have penetrated far inland over the less elevated terrain of Dronning Maud Land and Wilkes Land, much like the cyclonic storms that circle Antarctica today. The appearance of an area of high albedo and its influence on local climate would then have triggered a feedback effect which led to further glacier growth covering the entire continent.

In an alternative model, Drewry (1975) considers that the Transantarctic Mountains provide a more likely growth center because of their coastal position, which makes them more likely to have large amounts of snowfall. Furthermore, airborne radio-echo-soundings appear to indicate a large network of inland-oriented sub-glacial valleys in the Transantarctic Mountains. Such features are far less numerous and well-defined in parts of the Gamburtsev Mountains. Drewry also quotes one source contending that the Gamburtsev Mountains represent a neotectonic reactivation of the basement resulting from ice loading of the crust, implying that they were not elevated prior to glaciation. So, in the Drewry-model, expanded mountain glaciers at the Ross Sea side would have calved into deep water, whereas ice flowing down the inland flank of the Transantarctic Mountains would have coalesced into large piedmont complexes. Ice moving further inland would then have eventually merged with glaciers from other highland ice caps, though developed after those in the Transantarctic Mountains, to form the East Antarctic ice sheet.

The preglacial topography of West Antarctica strongly suggests that the West Antarctic ice sheet probably matured later than its eastern counterpart,

because formation of the former necessarily requires an early ice shelf phase (Denton et al., 1971; Drewry, 1975, 1978; Lindstrom, 1988). Unlike the conditions required for glacial inception in East Antarctica, sea-level temperatures in West Antarctica would first have to be low enough to permit the local ice caps on the major island groups to reach sea level and form floating ice shelves. Further cooling would then allow the ice shelves to spread out between the islands and East Antarctica, which offered them the necessary protection and lateral constraints. Eventually, climatic conditions would have to be cold enough for the ice shelves to thicken, ground and merge with the local ice caps to form a large West Antarctic ice sheet. The pre-existing East Antarctic ice sheet could then have provided additional mass inflow through the valleys of the Transantarctic Mountains.

Based on these glaciological considerations, it seems that the East Antarctic ice sheet has most likely pre-dated the West Antarctic ice sheet. This widely held view is however challenged by Hughes (1982), who postulates that the West Antarctic ice sheet may actually have created the East Antarctic ice sheet, with a mechanism analogous to the marine ice transgression hypothesis proposed for northern hemisphere glaciation (Denton and Hughes, 1981). According to Hughes, the conditions required for such a mechanism could have occurred during the Oligocene, when post-Eocene continental drift led to heavy snowfall over the West Antarctic island archipelago, but prevented a contemporaneous infusion of warm ocean water. By a combination of basal freezing and surface snow accumulation, this would have created a broad marine ice dome, while dry and cold continental climates over East Antarctica prevented the simultaneous development of an extensive ice cover there. Such an event would not be detectable from oxygen isotope records because the marine ice dome would largely exist of frozen sea-water. This ice would never be much colder than -1.8°C and would not deplete the oceanic ^{16}O content, unlike terrestrial ice domes formed from snow-fall (Hughes, 1982). Eventually, a massive advance of West Antarctic marine ice into East Antarctica would have merged with spreading centers of terrestrial ice to create the East Antarctic ice sheet during middle Miocene times. However, the evidence and theoretical considerations described above make such a sequence of events hard to believe, and Hughes' view may be qualified equally 'outrageous' as the Arctic ice sheet proposed in Denton and Hughes (1981).

3.2. FLUCTUATIONS OF THE ICE SHEET SINCE THE PLIOCENE

The growth of the Antarctic ice sheet to a continental size is largely believed to have taken place in the late Miocene, but variations have taken place since and some of them have been large. Evidence for post-Miocene fluctuations is essentially restricted to scattered ice-free areas near the coast (mountain ranges and nunataks); to marine sediments in the Ross and Weddell basins; and, for the most recent fluctuations, to oxygen isotope ratios in ice cores. A unique area for the reconstruction of the glacial history is the Dry Valleys region (Taylor and Wright Valleys) near McMurdo Sound in Victoria Land. This presently ice-free area contains traces of ice advances moving both westward from a grounded Ross ice shelf (reflecting variations of the West Antarctic ice sheet) and eastward from the East Antarctic polar plateau. These ice-filling periods appear furthermore to have alternated with episodes of marine invasions and lacustrine sedimentation in a fjord environment. In addition, local alpine glaciers on the valley flanks to the north and south have varied considerably in extent. Important information on these changing environments was obtained from sediment cores during the Dry Valley Drilling Project (DVDP; e.g. Brady, 1982).

3.2.1. The 'Queen Maud' maximum

On the basis of mainly terrestrial evidence, there seems to be a general concensus that the Antarctic ice sheet reached its maximum extent sometime during the early Pliocene. This maximum was larger than any state recorded since. Depending on the area examined, this major ice expansion is usually referred to as the Queen Maud (Mayewski and Goldthwait, 1985), Taylor V (Denton et al., 1971) or Ross Sea 5 Glaciation (Hughes, 1973). However, the correlation between glacial events in different regions is often unclear and equivocal.

Traces left by this maximum ice sheet are relatively widespread and have been found on nunataks all over the continent. The most productive area is the Transantarctic Mountains, and more specifically the Queen Maud Mountains and the Dry Valley region (for their location, see fig. 3.3). Probably the most important findings relate to the Sirius Formation in the Queen Maud Mountains. This fossiliferous glacial till is found at elevations above 2000 m

GLACIAL HISTORY
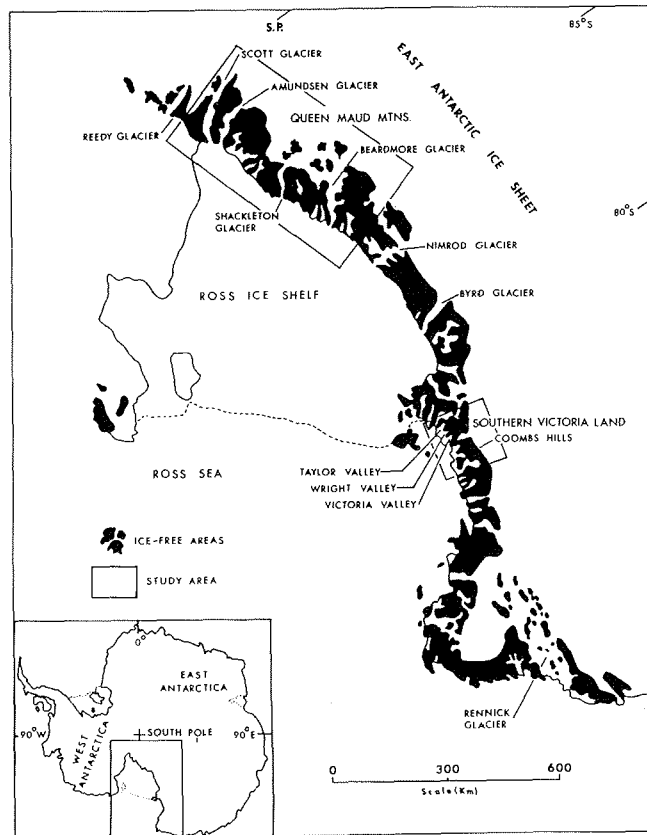
fig. 3.3: Map of the Transantarctic Mountains showing the most important locations for evidence of post-Miocene fluctuations. From Mayewski and Goldthwait (1985).

and caps the highest peaks in the range (up to 4115 m on Mount Mackellar; Prentice et al., 1986). It overlies a rock surface with fresh striations in many places and thus indicates massive overriding of the Transantarctic Mountains by a wet-based ice sheet. Mayewski and Goldthwait (1985) date the Queen Maud Glaciation (to which the Sirius Formation has been coupled) as older than 4.2 My, but the presence of certain Pliocene diatom flora in the Sirius Formation would imply a maximum age of 3 My (Harwood, 1983; Webb et al., 1983, 1986). However, these conflicting dates may just reflect different substages of the same glacial phase (Mayewski and Goldthwait, 1985).

GLACIAL HISTORY

Evidence for the complete inundation of the Transantarctic Mountains sometime between 2 and 3.38 My is also reported by Denton et al. (1983) in the Dry Valleys region. The minimum ice thickness needed to account for the observed subglacial features would indicate that the highest mountains were buried by 500 meters of ice, which corresponds to a local thickening of 2 to 3 km. However, part of the implied increase in surface elevation may be apparent rather than real, because neotectonic activity could have raised the Transantarctic Mountains after deposition of the glacial tills. Compelling evidence and time control is lacking, but Katz (1982) contends that post-Jurassic synclinal warping and uplift of the Transantarctic Mountains (the so-called Victoria Orogeny) also continued further into Plio-Pleistocene times. In view of this, Denton et al. (1983) consider 300 m a realistic estimate for tectonic uplift over the last 3 My. This value is to be expected if uplift was at the inferred long-term average rate of 90-100 m My^{-1} for the last 50 My (Fitzgerald et al, 1987; Stern and ten Brink, 1989).

Within this period of maximum glaciation, the ice probably extended to the far edge of the continental shelf, so that the Weddell and Ross basins were completely covered by grounded ice (e.g. Hughes, 1973; Anderson et al., 1982). In the Antarctic Peninsula area, Yoshida (1985) reviews evidence for a phase of maximum Pliocene glaciation during which ice crossed the shallow Bransfield Strait and completely covered the South Shetland Islands. It is likely that this phase also corresponds to the Queen Maud glaciation. Further evidence for higher glacier stands, possibly correlated to the Queen Maud stage even though dates cannot be given, have been retrieved from nunataks in such East Antarctic locations as the central Sør Rondane Mountains (surface ice level 300 - 350 m higher than present, Hirakawa et al., 1988), the Dufek Massif and Forrestal Range (+ 400 m; Boyer, 1979), and the Yamato Mountains (+ 1000 m; Yoshida, 1985). However, also here complications are introduced by the possibility that tectonic uplift and/or glacial erosion took place after the glaciations. With respect to the latter process, much depends on basal temperature conditions (whether the ice is frozen to the bedrock or basal sliding occurs) and the speed of the ice flow. As an upper-bound case, Wellman and Tingey (1981) describe data for the Prince Charles Mountains region, where active erosion below the Lambert outlet glacier is believed to have lowered bedrock surfaces by as much as 50 m My^{-1}. Moreover, glacial erosion itself could be a cause for uplift because of the mechanism of isostatic

compensation (Wellman and Tingey, 1981; Oerlemans, 1984), implying the need for some caution when interpreting older moraine positions in terms of ice thickness and surface elevation.

From a glaciological point of view, complete burial of the Transantarctic Mountains must have led to a fundamentally different flow pattern as the East Antarctic ice sheet was forced to traverse the 3000- 4500 meters high ridge-line. Striations in rock surfaces underlying the superficial glacial tills all indicate ice flow in diagonal to perpendicular directions across major valleys (Denton et al., 1983; Prentice et al., 1986). Together with extensive grounding in the Ross and Weddell Seas, this suggests unification of the East and West Antarctic ice sheets to form a radially symmetric ice cap, possibly centred near the South Pole. On the basis of simple parabolic profiling, Mayewski and Goldthwait (1985) calculated that such an ice cap would have contained 60% more ice than at present. This would have had the effect of lowering sea level by at least 37 m below today's value.

A similar 'giant-ice' scenario was also proposed in Denton et al. (1983), but contrasting views exist. For instance, Webb et al. (1986) propose a 'dwarf-ice' hypothesis on the assumption that the Sirius Formation remnants were lifted by approximately 2000 m since their deposition. This would obviously have made the Transantarctic Mountains threshold less elevated, so that a thinner East Antarctic ice sheet would be required, leading to a less dramatic degree of overriding and a reduced expansion of ice across the Ross Sea. Although the proposed 2000 meters of uplift looks unreasonably high, recent lithospheric calculations seem to suggest a much higher degree of up-flexing in central parts of the Transantarctic mountains (Stern and ten Brink, 1989). In addition, Webb (1990) reports the presence of a young fault dislocation in the Beardmore glacier area.

3.2.2. Further Plio-Pleistocene history

Since the early Pliocene maximum, available evidence suggests that the Antarctic ice sheet has undergone at least 4 more major glaciations, defined as expansions strong enough to cause significant grounding of the Ross and Ronne-Filchner ice shelves (Denton et al., 1971; Hughes, 1973). In the latter somewhat dated paper, the following sequence of events was described. After

GLACIAL HISTORY

Ross Sea 5 Glaciation, rapid retreat occurred in the Ross Sea sector and by 3.7 My the ice sheet had retreated sufficiently to permit an invasion of marine waters into Wright Valley (as documented in the environmental record, cf. Prentice et al., 1985). A similar retreat also occurred in the Weddell Sea, beginning at 3.3 My and ending perhaps some 2.4 My. The ice shelf in the Ross Sea re-grounded and by 2 My the grounding line seems to have advanced to near the continental shelf edge. Until as late as 0.82 My, the ice sheet remained grounded near the edge of the continental shelf in Marie Byrd Land. In the Weddell Sea, this glaciation began 2.4 My and ended 0.3 My. Subsequently, the ice thinned considerably and by 0.7 My the northern Ross Sea was covered with a large floating ice shelf. Further thinning occurred by 0.5 My, when ice sheet elevations in the Marie Byrd Land area were comparable to present elevations. According to the chronology given in Hughes (1973), this pattern of retreat and advance was repeated at least 3 more times, the last clearly identifiable glaciation being from 145000 to 107000 years BP.

According to Denton et al. (1971), at least 5 advances were recorded in the Taylor and Wright Valleys during the same time interval, with each glaciation being successively less extensive than the previous one. The implied local glacial history is likely to be incomplete, however, since any glacial advance whose extent is less than a later one would not be identifiable. In this review paper, all 5 advances were interpreted in terms of fluctuations of the East Antarctic ice sheet, which is believed to have spilled into these valleys during glaciations. Advances were labelled Taylor I to V. In their chronology, Taylor I is probably the current, for the present surface now occupies its maximum level in a very long time. More recent evidence from DVDP cores (Hendy et al., 1979; Brady, 1982) still seems to support the general sequence of events as inferred by Denton et al. (1971) on the basis of surface geological surveys.

A somewhat similar Plio-Pleistocene chronology was proposed in Mayewski and Goldthwait (1985). Dissecting drainage channnels both in the Sirius Formation and in tills at slightly lower elevations indicate a major ice regression during the Gallup Interglacial, dated by correlation to similar glacial events as between 4.2 and 2.7 My. The ice cover at this time may have been similar to or less than the present Antarctic ice sheet. A renewed thickening in the Queen Maud Mountains then caused the Scott Glaciation between 2.7 and 2.1 My. The

GLACIAL HISTORY

Age	Denton et al. (1971) Dry Valleys	Hughes (1973) Ross ice shelf	Mayewski and Goldthwait (1985) Queen Maud Mountains
0 My	Taylor I		Amundsen Glaciation (<9 ky)
		Ross Sea 1 (0.145-0.107 My)	
		Ross Sea 2 (0.205-0.165 My)	
	Taylor II		
		Ross Sea 3 (0.255-0.235 My)	
1 My	Taylor III (<1.6 My)		Shackleton Gl.(1.6-0.049 My)
		Ross Sea 4 (2.4-0.7 My)	
2 My			
	Taylor IV (2.7-2.1 My)		Scott Glaciation (2.7-2.1 My)
3 My			
			Gallup Interglacial (4.2-2.7 My)
4 My			
	Taylor V (>3.7 My)	Ross Sea 5 (7.0-3.5 My)	Queen Maud Glac. (>4.2 My)
5 My			

fig. 3.4: Correlation and chronology of glacial events in the Dry Valley region, Ross Sea and Queen Maud Mountains. After authors as indicated.

assumed grounding line in the area of the present Ross ice shelf (obtained by parabolic profiling) would have extended up to 150 km seaward of the present grounding line off the coast of Queen Maud Land and up to 60 km from the coast of southern Victoria Land. Other complexes of lateral moraines mark the surface of the Shackleton Glaciation (0.049 -1.6 My) in the Queen Maud Mountains and have been found up to several hundred meters above the present glacier surface. Lateral moraines overlying and flanking today's surfaces would then relate to the Amundsen Glaciation (younger than 9490

years BP), coinciding morphologically with the present configuration of the Antarctic ice sheet.

A correlation of the post-Miocene glacial history in these regions based on the above studies is shortly summarized in fig. 3.4. The picture that emerges is no doubt incomplete and also somewhat confusing. Many questions still remain. First of all, the figure suggests that the Antarctic ice sheet was more lively during the last few hundred years or so, but this need not necessarily be the case. Later glaciations tend to destroy the evidence of preceding ones, so that there may have been substantially more glaciations than presented here. For instance, if the bulk of the ice cap, and the West Antarctic ice sheet in particular, expands and contracts in phase with cycles of northern hemisphere glaciation, then the Late Quaternary Antarctic history should primarily consist of multiple advances and retreats with a period of roughly 100000 years. Continuous oxygen isotope profiles in the deep oceans show a sequence of 8 cold and 9 warm phases during the last 700000 years (e.g. Berggren et al., 1980). The dates given by Hughes (1973) do not quite reflect this.

Another important problem raised in the literature is related to the interpretation of the various moraine complexes in the Transantarctic Mountains. In this respect, Stuiver et al. (1981) strongly criticize Mayewski's interpretations. They state that the increased surface elevation of the glaciers after the Scott Glaciation was not caused by increased volume of the East Antarctic ice sheet, but by increased volume of the West Antarctic ice sheet and grounding of the Ross ice shelf. This view seems to be the more convincing now (e.g. Yoshida, 1985).

In addition to these uncertainties, it has also been suggested that the pattern of glaciation exhibited by glaciers in Victoria Land (including Taylor Glacier) does not correspond to the variations of the East Antarctic ice sheet as a whole. Drewry (1980) argues that the ice in Victoria Land originates from a local dome, which is subject to different glacio-climatic controls than those affecting the bulk of the ice sheet. Unlike more complex behaviour elsewhere, such a local dome would essentially respond to changes in precipitation amounts. Since this precipitation comes primarily from air advected over the Ross Sea, regulated by such factors as seasonal ice cover and degree of open water, advances of Taylor Glacier would only occur during the warmer

interglacials, when on the other hand rising sea levels would trigger inland retreat and thinning of the overall ice cap. Conversely, episodes of global sea level depression associated with northern hemisphere ice build-up would cause expansion of ice across the continental shelf and lead to thickening of the bulk of the Antarctic ice sheet. However, reduced precipitation rates would at the same time lead to the recession of the Victoria Land glaciers. As a consequence of such a bimodal or dual response to sea level and accumulation, Drewry (1980) concludes that the Ross Sea and Taylor glaciations were essentially out-of-phase with each other, and that the latter cannot be interpreted in terms of major East Antarctic glaciations. By analogy, a similar note of caution should also apply to the Mayewski chronology.

3.3. THE LAST GLACIAL CYCLE

The history of peripheral advance and retreat during the last glacial cycle is of special interest because this provides the type of empirical data needed to test the glaciological model. Unfortunately, a full consensus has not been reached and different reconstructions have been proposed.

3.3.1. The Last Interglacial

From oxygen isotope ratio's of deep sea sediments and ice cores in various areas of the world, it has been confidently established that the last ice age started some 120000 years ago (e.g. Shackleton, 1987). The build-up of ice was essentially confined to the continents of the northern hemisphere, but research on the East Antarctic Vostok ice core has clearly revealed that the associated climatic cooling was of a world-wide nature and was roughly in phase in both hemispheres (Lorius et al., 1985; Jouzel et al., 1987). However, the oceanic record also indicates that during the last 700000 years, only during the Last Interglacial (i.e. the Sangamon/Eem period preceding the Wisconsin glaciation between around 135000 and 120000 years BP) there was less water locked up in ice sheets than at present, and this by an amount equivalent to 4-6 m of sea level (Harmon et al., 1981). This feature has often been interpreted as indirect evidence for the absence of the West Antarctic ice sheet at that time, particularly in view of the assumed vulnerability of its ice

shelf system and the fact that temperatures were several degrees higher than today (e.g. Mercer, 1979; cf. § 2.4.1).

However, compelling evidence for a major collapse is not available and alternative explanations for the isotope data have been proposed. Apart from West Antarctica, also the Greenland ice sheet contains the requisite amount of ice, and some workers believe that deglaciation of the latter must have been responsible for the inferred higher sea level stand. This is also the opinion expressed in Koerner (1989). According to a fresh interpretation of the Camp Century and Dye-3 ice cores of Greenland, certain basal features could be indicative of a partial or even complete meltdown during the Last Interglacial. This view seems to be to some extent corroborated by recent modelling work. Calculations with a 3-D model for the Greenland ice sheet, quite similar to the one described in this thesis, suggest that the Greenland ice sheet might have been smaller during the Eem, with a corresponding rise of sea level by 2-3 m (Huybrechts et al., 1990; Letreguilly et al., 1990, in press). Such a situation removes the necessity of having to invoke a collapse of the entire West Antarctic ice sheet. In this respect, it is interesting to note that recent evidence in the Weddell Sea for the cessation of turbidite deposition already since the Pliocene also suggests a more stable West Antarctic ice sheet than often assumed (Ocean Drilling Program Leg 113, 1987).

According to Hollin (1980), evidence for a sea-level rise of possibly 16 m during isotope stage 5c would point to a major surge of the East Antarctic ice sheet at 95000 years BP, but this inference has been the subject of considerable debate. A critical point is the effect of vertical bedrock movement on the interpretation of the higher sea level stands (Mörner, 1980; Watts, 1982). Also is it not quite clear which mechanism could be responsible for partial destruction of the East Antarctic ice sheet (cf.§ 2.4.2 and § 2.4.3).

3.3.2. The Last Glacial Maximum

Despite the uncertainties just described, there are good reasons to believe that the Last Interglacial was followed by a substantial expansion of the Antarctic ice sheet. This culminated in the Last Glacial Maximum (LGM) sometime between 20000 and 15000 years BP (e.g. Denton and Hughes, 1981). Before then, correlation with glacier fluctuations in the Southern Andes

suggests that a minor maximum might have taken place around 70000 years BP (Mercer, 1978b).

Information about the climate of the Antarctic during the LGM has been obtained from the deep ice cores of Vostok, Dome C and Byrd (Jouzel et al., 1989; Lorius et al., 1990). These records indicate a cold phase around 60000 years BP prior to the LGM at 18000 years BP. The full amplitude of surface temperature change across a glacial-interglacial cycle appears to have been 8-10°C, and the full-glacial accumulation rate is interpreted to be about half of the Holocene value. A strong increase of the dust concentration in the ice would point to a more intense atmospheric circulation and an increased aridity in the southern hemisphere during the height of the LGM.

3.3.2.1. CLIMAP reconstruction

Evidence for the global status of ice sheets during the LGM were thoroughly collated and interpreted during the CLIMAP project in the late 1970's. As part of this program, Stuiver et al. (1981) proposed a numerical reconstruction for the Antarctic ice cap. Their reconstruction was based on available geological data from ice-free areas in mountains adjacent to, and projecting through, the former, expanded ice sheet. Most of the evidence originated from the Transantarctic Mountains, and ice sheet fluctuations in other areas were subsequently derived by analogy or on the basis of certain theoretical considerations (in essence following Hollin, 1962). The resulting pieces of information served as input in a plastic ice-flow model to calculate former elevations and flowline profiles. The outcome of this exercise is displayed in fig. 3.5. According to their tentative reconstruction, grounded ice expanded close to the edge of the continental shelves in the Ross and Weddell Seas. In East Antarctica, the expansion of the marine margin could only have occurred over quite short distances (typically 75 to 90 km depending on bedrock slope), leading to a relatively minor interior thickening.

Despite the meticulous work done by the CLIMAP group, other interpretations of the field data have been made. Much of the discussion turns around the recognition and identification of stranded moraines adjacent to outlet glaciers in the Transantarctic Mountains, and the resulting consequences for grounding in the Ross Sea. According to the interpretation of Stuiver et al.
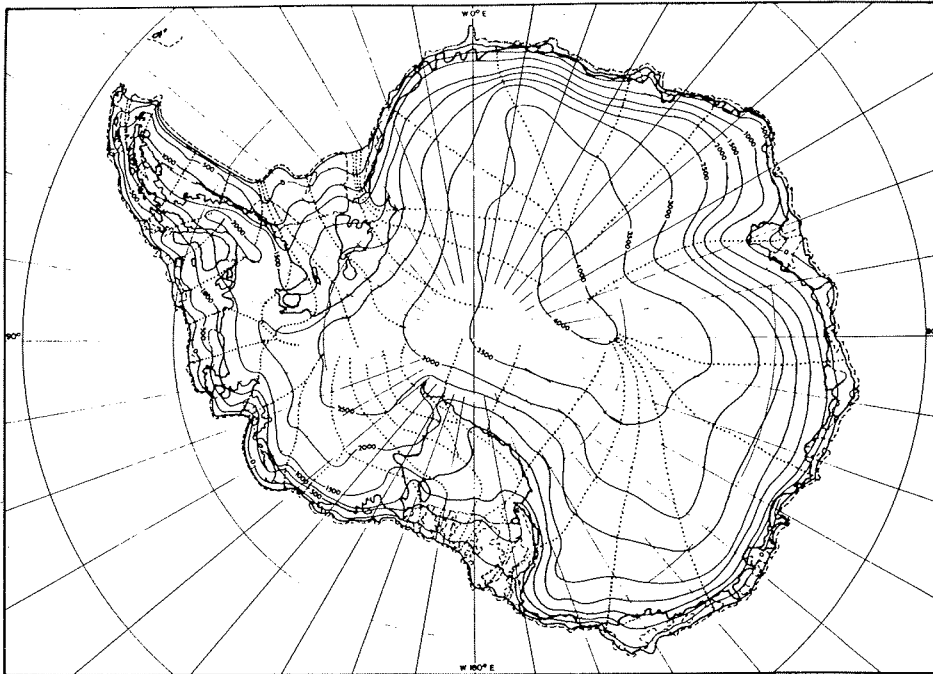
fig. 3.5: Numerical reconstruction of the late Wisconsin Antarctic ice sheet based on geological data. From Stuiver et al. as published in Denton and Hughes (1981).

(1981), lateral moraines which are high above current ice surfaces at the glacier foot, merge and approach the surface of the present day East Antarctic ice sheet towards the glacier head. Hence, the thickening recorded by these moraines gradually increases downstream, indicating that a grounded Ross ice sheet, rather than a thicker East Antarctic ice sheet, was responsible for the higher glacier stands. That grounded Ross ice pushed westwards into these valleys is further substantiated by evidence for inland-oriented lobes of ground moraine (the so-called Ross Sea drift) and dammed glacial lakes in the ice-free Taylor and Ferrar valleys. Stuiver et al. (1981) estimated that the depth of grounded ice in McMurdo Sound attained a maximum of 1325 m.

In contrast to the above moraine interpretation, Mayewski and Goldthwait (1985) postulate that synchronous moraine complexes of Shackleton age are parallel to the current surfaces of outlet glaciers along their entire length. This implies a thickening of the East Antarctic ice sheet and only a minor northward

migration of the grounding line. On the basis of simple parabolic profiling, they calculated a grounding line position 130 km seaward of the present coast of the Queen Maud Mountains and up to 35 km seaward of southern Victoria Land.

However, in subsequent work it appears that the interpretation given by Stuiver et al. (1981) is probably the more correct (Denton et al., 1989a; Bockheim et al., 1989). Even so, Drewry (1979) argues that the CLIMAP maximum ice sheet reconstruction represents only one possible and probably extreme case. He proposed an alternative working hypothesis, in which he kept an expanded ice shelf regime over the major part of the Ross Sea throughout most of the last glaciation. This follows from bathymetric and glaciological considerations, since a sea-level depression of 120-130 m sustained over more than 10000 years (an exceptional situation) would be needed for the ice shelf to fully ground in the Ross Sea. Limited support for the Drewry-hypothesis is provided by marine sedimentary studies below the Ross ice shelf (Kellogg and Kellogg, 1981), but the most convincing evidence for a minimum West Antarctic ice sheet comes from the glaciology of the Byrd ice core. According to Whillans (1976), the surface elevation near Byrd station shows only small changes over the last 30000 years, if it is assumed that no flowline migration took place. Moreover, analysis of the air content in the Byrd core indicates that the West Antarctic ice sheet was actually thinner during the last part of the recent ice age, and that a 200-250 m thickening occurred only after the end of the last glaciation (Raynaud and Whillans, 1982, who attribute this to increased accumulation rates). These results clearly do not favour the Stuiver et al. (1981) reconstruction which requires a thickening of some 1700 m at Byrd Station during the Wisconsin maximum.

3.3.2.2. data acquired since CLIMAP

Since the theoretical CLIMAP reconstruction, based in many places on little data, more geomorphological and glacial geological observations have become available. Some pieces of new field evidence agree well with the CLIMAP reconstruction, but others imply that some amendments are necessary.

GLACIAL HISTORY

With respect to the Weddell Sea region, there appears to be little doubt that the late Wisconsin ice sheet extended to the edge of the continental shelf. Elverhøi (1981) describes dated sedimentological data which clearly suggest grounding of the Ronne-Filchner ice shelf down to a water depth of 500 m. Further support for widespread grounding is provided by the presence of fresh striations and erratics on nunataks. These have been found at elevations up to 500 m above the current ice surfaces along the Orville Coast (Carrara, 1981) and the Lassitter Coast (Waitt, 1983). Both areas lie on the east side of the southern Antarctic Peninsula, respectively adjacent to the Ronne ice shelf and the Weddell Sea. Similar evidence for a thickening of 1000 to 2000 m has been reported at the head of the Ronne-Filchner ice shelf, based on trimline elevations in the Heritage Range, Ellsworth Mountains (Rutford et al, 1980). According to the latter study, the surface of the 'Whitmore dome' of the West Antarctic ice sheet rose by 300 - 500 m, but remained at the same location throughout the Wisconsin.

Also in the Antarctic Peninsula area, Clapperton and Sugden (1982) postulate a late Wisconsin maximum ice cover in broad agreement with CLIMAP, although their geomorphologic observations did not support ice flowing from the Peninsula axis across Alexander Island to the edge of the continental shelf in the west. Rather, they believe that separate ice domes were centred over both Alexander Island and Palmer Land, with the ice converging into George VI Sound prior to flowing northwards. Grounded ice probably expanded to the continental shelf break elsewhere in the Pacific sector as well. This is indicated by the presence of basal tills in such critical locations as Marguerite Bay along the Antarctic Peninsula (Kennedy and Anderson, 1989) and Pine Island Bay in the Amundsen Sea (Kellogg and Kellogg, 1987b). In the latter area, grounded ice filled the entire bay for distances of up to 400 km from the present ice sheet margin, although Kellogg and Kellogg emphasize that dating control was not firm.

Further support for the theoretical CLIMAP reconstruction comes from additional, though still sparse, evidence for Wisconsin margin positions in East Antarctica. Adamson and Pickard (1983) review data (mainly glacial striations) for a late Wisconsin advance of the ice sheet across the Vestfold Hills region, an oasis near the Australian research station of Davis. The striations clearly indicate recent (25000-10000 years BP) overriding in a

direction pointing radially outwards. Also submarine terminal moraines seaward of the Ninnis and Mertz outlet tongues are in good agreement with the Stuiver et al. reconstruction (Domack et al., 1989). Here, the ice sheet expanded over a distance of 150 km to a position where the water depth is some 400 m below contemporary sea level.

In contrast, it appears that the controversy which centred around the history of the marine ice sheet in the Ross Sea is still not resolved. The available data are still open to a considerable degree of interpretation and at best only constrain a maximum and minimum reconstruction. The problem is that dated evidence on the seafloor is still lacking. The ice sheet margin therefore has to be estimated from the altitude of side moraines in the Transantarctic Mountains. Detailed descriptions of late Wisconsin drift sheets have recently been made for Beardmore glacier (Denton et al., 1989a) and Hatherton/ Darwin glacier (Bockheim et al., 1989). In accordance with the CLIMAP interpretation, they both show late Wisconsin longitudinal profiles that are close to the current surface near the plateau, but rise far above the Ross Sea ice shelf near the glacier mouth. A typical value for the late glacial surface elevation near the present grounding line is 1300-1400 m.

On the basis of these new ice surface profiles, Denton et al. (1989b) have presented new reconstructions for a minimum and maximum extent of grounded ice in the Ross Embayment. They are shown in fig. 3.6. They both depict grounded ice along the entire inner Ross Embayment together with little change (compared to the present) of the inland plateau surface adjacent to the Transantarctic Mountains. The major difference between the two reconstructions lies in the areal extent of grounded ice in the outer Ross Embayment and was due to different glaciological assumptions. The minimum reconstruction was based on the assumption that West Antarctic ice streams persisted at the last glacial maximum, hence the surface morphology of the ice flowing from West Antarctica did not change significantly. The maximum reconstruction assumes that ice streams did not exist during the late Wisconsin glaciation (Denton et al., 1989b). Compared to the CLIMAP reconstruction (fig. 3.5), both new reconstructions share a considerably less extensive and thinner grounded ice cover. However, neither of the reconstructions in fig. 3.6 are based on ice flow models or make use of seafloor sediments, because they lack numerical chronology.
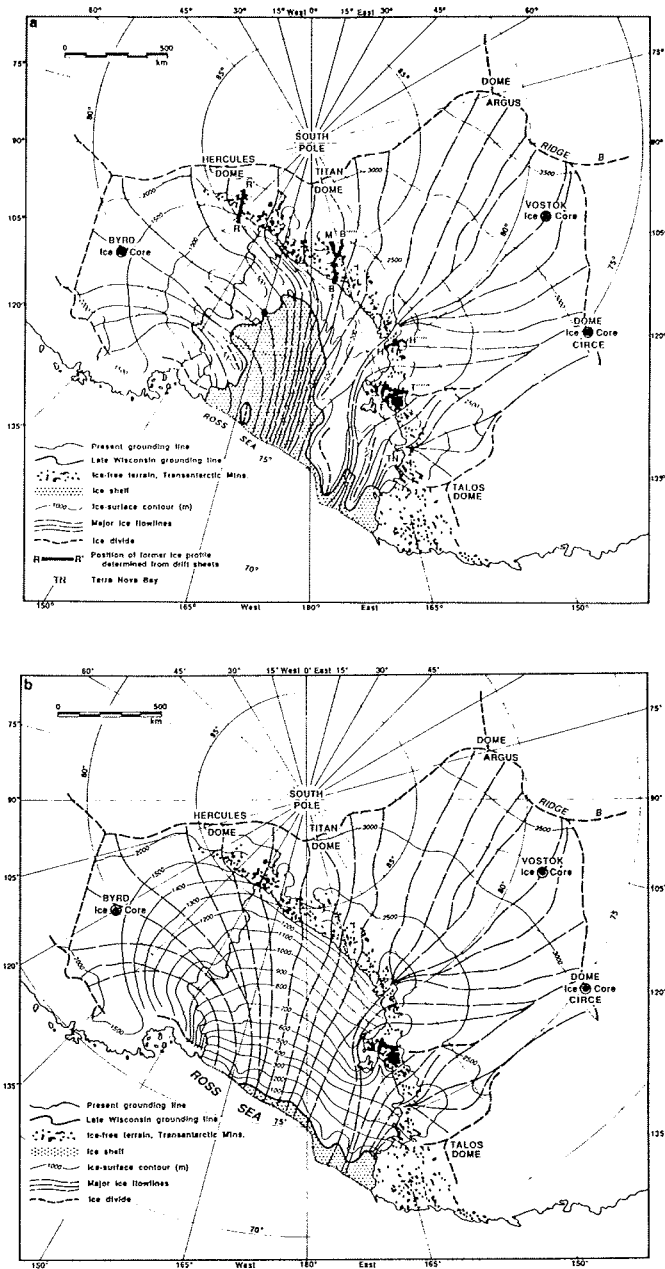
fig. 3.6: Minimum (a) and maximum (b) reconstructions of grounded Wisconsin ice in the Ross Embayment based on the glacial geology of the Transantarctic Mountains. The position of the ice shelf front in both diagrams is arbitrary. From Denton et al. (1989b).

Figure 3.7 shows another sketch (not a numerical reconstruction) of the entire Antarctic ice sheet during the Wisconsin maximum, also by the Maine geology group (Denton et al., 1986). It takes into account some of the more recent geological data just mentioned and, where available, data on total-gas content from deep ice cores. The latter parameter is closely related to the temperature and atmospheric pressure at the time of pore-closure, and hence, is indicative of changes in ice-surface elevation. Noteworthy differences between fig. 3.7 and the older CLIMAP reconstruction include a lower ice-sheet surface in West Antarctica, which features several divides with domes and saddles. Peripheral domes in the Ross and Weddell Seas are common. Also ice-surface elevations in interior East Antarctica are little different from those of today. This is assumed to be a direct consequence of lower accumulation rates. The position of the ice sheet margin, however, is almost similar to the CLIMAP reconstruction.
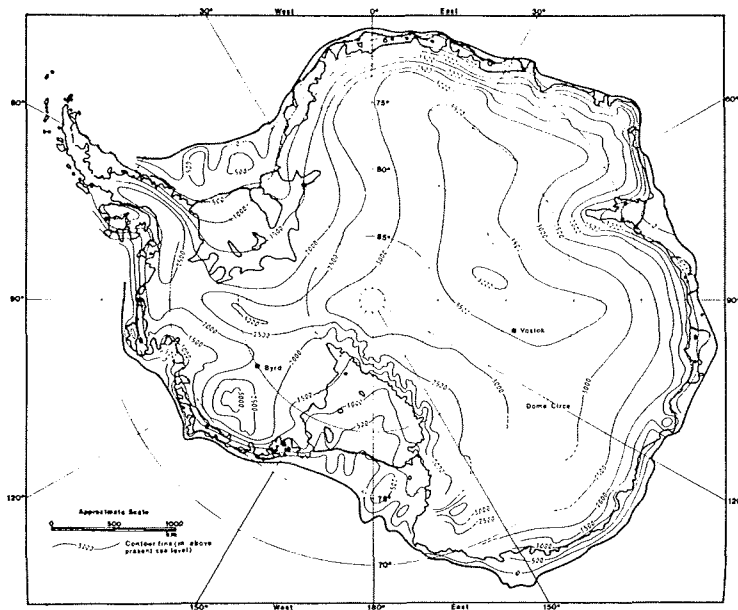
fig. 3.7: Sketch of the entire Antarctic ice sheet during the LGM taking into account more recent glaciological and geological data. The outer heavy line shows the tentative reconstruction of the grounding line. From Denton et al. (1986), who stress that this figure is only a working sketch and not a numerical reconstruction.

Finally, in addition to the expansion of grounded ice, mention should be made of the ice extent in the Southern Ocean. From lithological changes, sedimentation rate changes and distribution of ice-rafted detritus in Antarctic deep-sea sediments, Cooke and Hays (1982) predict that the winter sea-ice cover during the late Wisconsin was probably about double of today's, with a surface area of 40×10^6 km^2 and extending to 46°S in the southern Atlantic Ocean. Summer sea ice 18000 years ago was probably similar to today's winter coverage. Denton et al. (1986) proposed that the Antarctic ice sheet was bounded by an extensive ice shelf in dynamic equilibrium with the grounded portions of the ice sheet. They believe that the ice shelf merged imperceptibly with the permanent pack ice and possibly extended as far as 800 km beyond the continental shelf limit. Similarly, Johnson and Andrews (1986) argue that during the late Wisconsin the Antarctic continent was entirely encircled by a vast ice shelf. According to their reconstruction, this ice shelf may have extended to 55°S.

To summarize then, it seems that available geomorphological and glacial geological data suggest a late Wisconsin ice sheet which was grounded at the edge of the continental shelf. Such an ice sheet would have shown only minimal surface elevation changes over the vast East Antarctic polar plateau and have been completely surrounded by an enormous ice shelf. Only in the Ross basin does the evidence not permit to reconstruct a maximum ice sheet with sufficient confidence. Here, the reconstructed late glacial extent varies from a position close to the continental break to several ice lobes with low surface slopes covering only the inner Embayment.

3.3.3. Holocene retreat

According to Stuiver et al. (1981) and Denton et al. (1989b), thick ice plugged the mouth of Taylor Valley from as early as 23800 years BP to 12500 ^{14}C-years BP. The Holocene retreat of grounded ice, which was underway by 13040 ^{14}C-years BP, caused massive lowering of the ice surface after 12330 ^{14}C-years BP and was completed by 6600- 6020 years BP. The data of Denton et al. (1989b) suggest that grounded Ross Sea ice still occupied McMurdo Sound until as late as 8340 years BP. By 6600 ^{14}C-years BP marine waters penetrated into McMurdo Sound. Similar dates are also found elsewhere along the Transantarctic Mountains. Bockheim et al. (1989),

working in the Hatherton Glacier area, report the retreat of the grounding line to near its current position by 6020- 5740 ^{14}C-years BP. Lateral moraines indicate that the retreat of grounded ice from the Ross Embayment was accompanied by little change of East Antarctic plateau levels inland of the Transantarctic Mountains.

In Marie Byrd Land, the Holocene retreat of the grounding line of the Ross ice shelf did not leave geological evidence on an exposed coast, but these grounding line histories have been the subject of model studies (Thomas and Bentley, 1978; Clark and Lingle, 1979, Lingle and Clark, 1985). Assuming that West Antarctic ice grounded to the edge of the continental shelf at 18000 years BP, these studies indicate that retreat began soon after sea level started to rise (≈15000 years BP). Initially, the retreat was rather slow, but recession accelerated after 13000 years BP, and by about 5000 years BP, the ice-sheet grounding line established a new equilibrium position close to its current location. Thereafter, the grounding-line may have advanced because continuing viscous uplift of the bed caused relative sea depth to decrease. According to the study by Lingle and Clark (1985), such a reversal occurred after 3000 years BP. By contrast, Peltier (1988) believes that the retreat of West Antarctic ice substantially lagged the retreat of northern hemisphere ice. On the basis of a detailed analysis of a large number of southern hemisphere relative sea level data, he comes to the conclusion that the time of onset of Antarctic glaciation must have coincided with the time of most rapid disintegration on the northern hemisphere, which is near 11000 years BP. A time lag of 7000 years (relative to 18000 years BP) was needed to reconcile misfits between the observations and theoretical models of relative sea level and the upper mantle.

Radiocarbon datings of submarine sediments elsewhere indicate that the timing and speed of grounding-line retreat probably varied between different portions of the Antarctic ice sheet. Evidence investigated by Domack et al. (1989) suggests a mid-Holocene retreat in the region of the George VI coast in East Antarctica, that occurred between 9000 and 2500 years BP. Kellogg and Kellogg (1987a, 1987b) contend that retreat in the Amundsen Bay area occurred until as recently as 3000 years BP or less. According to these authors, a recent episode of ice-shelf retreat in the Pine Island Bay probably took place within the last century. In another part of East Antarctica, retreat in

the Vestfold Hills commenced about 8000 years BP, and was completed by 3000 years, when glacier fronts neared their current positions. Here, moraine ridges some 1- 2 ky old were interpreted in terms of a small Neoglacial advance (Adamson and Pickard, 1983).

From ice-core data, Robin (1983) suggests that the warmest climate in Antarctica occurred between 11000 and 10000 years BP, which is more than 3000 years before the postglacial Climatic Optimum ($\approx$6500 years BP) in the northern hemisphere. According to Mercer (1978b), the Hypsithermal (period of maximum Holocene warmth) in the southern hemisphere peaked ca. 9400 years ago. George VI ice shelf, which is in a marginal environment for its survival, apparently disappeared around 8000 years ago, when the Sound was ice-free (Sugden and Clapperton, 1980). The ice shelf probably reformed after 6500 years BP.

3.3.4. Present evolution

Hughes (1973, 1975) has suggested that the West Antarctic ice sheet, because of its assumed unstable nature, may already be disintegrating. However, a growing preponderance of field evidence indicates that the part of the West Antarctic ice sheet that flows into the Ross ice shelf is probably nearly in steady state or gaining mass slightly. A calculation based on the continuity equation indicated that the southeastern corner of the Ross ice shelf is growing thicker by almost 1 m/y, which would imply an advance of the grounding line by nearly 1 km/y (Thomas, 1976; Thomas and Bentley, 1978). Further evidence for such behaviour comes from geophysical observations. Isostatic gravity anomalies show a clear trend of negative values in the western part of the Ross ice shelf, which is consistent with incomplete rebound from crustal loading by the former Ross ice sheet (Bentley et al., 1982). Interpretation of these anomalies suggests that a sea floor uplift of the order of 100 m is still to be expected near the present grounding line (Greishar and Bentley, 1980). According to this study, the equilibrium grounding line should eventually reach a position running roughly from Roosevelt Island to Beardmore Glacier, i.e. halfway down the present Ross ice shelf. This tendency for grounding-line advance is also supported by modelling studies (Clark and Lingle, 1979; Lingle and Clark, 1985). Local mass balance studies

in the central part of the ice sheet near Byrd station, on the other hand, show a slow thinning of some 30 mm/y (Whillans, 1977).

Although these pieces of evidence seem to suggest a positive mass balance for the entire Ross basin, individual catchment areas may behave differently. Shabtaie et al. (1988) report negative mass balances for ice streams A and B and a strongly positive mass balance for the inactive ice stream C. Whillans and Bindschadler (1988) have calculated that the mass deficit of ice stream B corresponds to a mean thinning rate of 0.06 ± 0.04 m/y. However, as noted by Thomas et al. (1988), if these ice streams oscillate, it becomes extremely difficult to determine their long-term trends and a comparison of ice discharge with total accumulation may only give a snapshot of their changing behaviour.

Estimates of present evolution and mass balance have also been made for some other major drainage systems of the West Antarctic ice sheet. With respect to the Amundsen Sea sector, the Pine Island and Thwaites Glacier system has been regarded as an area where catastrophic flow may now be occurring, because these ice streams calve into an open embayment and are unimpeded by a buttressing ice shelf (Hughes, 1981). Mass budget calculations in this area imply a large excess of mass input over mass output (Lindstrom and Hughes, 1984). This result has been interpreted as evidence that Pine Island Glacier may be in the process of drawing down its drainage basin, by enlarging its catchment area at the expense of neighbouring areas. However, such an inference is very speculative, even though Kellogg and Kellogg (1987a) also report a recent episode of ice-shelf retreat in Pine Island Bay, which is possibly continuing today.

In the Antarctic Peninsula area, scattered glaciological data reviewed by Doake (1982) yield an inconclusive answer as to whether the ice is presently thickening or thinning. However, there is some indication that the higher central parts near the ice divide may be thinning slightly, and that these changes in ice thickness increase towards the margin and become positive (thickening). In the Weddell Sea drainage basin, there is no definite evidence for important changes in mass balance (Doake, 1985). In East Antarctica, thinning of the ice sheet at an average rate of between 0.5 and 1 m/y is believed to occur on Mizuho Plateau upstream of the Shirase outlet glacier (Naruse, 1979). According to an analysis of total gas content from shallow ice

cores, this thinning phenomenon may represent a long-term trend (Kameda et al., 1990). The ice level on Mizuho Plateau may have been lowered by 350 m over the last 2000 years.

In summary, it is still not known whether the total mass of the Antarctic ice sheet is increasing, decreasing, or unchanging. In a global study, Budd and Smith (1985) have compared all available data on surface mass balance with ice velocities. They find that the total influx of ice (2088 x 10^{12} kg/y) is about 11% larger than the outflow (1879 x 10^{12} kg/y). However, data are still poor and subsequent estimates of the total accumulation show large variations. Giovinetto and Bentley (1985) estimate the accumulation over the grounded part of the ice sheet to be only 1468 x 10^{12} kg/y. With the discharge number of Budd and Smith, this then implies a negative net balance of -411 x 10^{12} kg/y. But also the inference of ice mass discharge from a limited number of surface velocity measurements involves many uncertainties. Outflow velocities vary dramatically from point to point, so that lateral extrapolation and interpolation around the coast is likely to introduce large errors. In a review of these studies, Warrick and Oerlemans (1990) conclude that a 20% imbalance of mass turnover can at present not be detected in a definite way. This corresponds to a mean change in ice thickness of 37 mm/ y.

4. THE ICE SHEET MODEL

4.1. STATEMENT OF THE PROBLEM

The aim of this work is to develop a numerical ice flow model for Antarctica, that can be used to investigate the role of its ice sheet as an interactive component within the global climate system. Before doing so, however, one should first be clear about what type of model one has in mind. A basic requirement is that the model has to be able to respond realistically to fluctuations in environmental conditions, such as eustatic sea level, accumulation rate and air temperature, by changes in the three-dimensional ice sheet geometry. In addition, the model should also be able to produce relevant boundary conditions and a number of 'derived physical characteristics' (such as velocity fields and thermal parameters at the ice-rock interface), to facilitate both amendment and validation, as to open the way to wider applications. The model becomes credible if this is done with the minimum of built-in constraints and the maximum number of internal degrees of freedom. So, in order to achieve this goal, a successful model has to include, in some way or another, all of the ice sheet's subsystems and physical mechanisms which have an effect on the spatial and temporal distribution of ice thickness, which is the main variable of interest feeding back into the climate system.

In view of this, a number of important physical mechanisms have to be distinguished. First , as discussed previously in § 2.3.2., in polar ice sheets ice flow and its thermodynamics are strongly related. Temperature determines to a large extent the viscosity of ice so that for a 10 °C temperature change, strain rates, for a given stress, may change by up to an order of magnitude. Since ice flow is also a means of heat transfer through the advective and frictional terms, this implies that the equations governing ice-flow mechanics

have to be solved simultaneously with the thermodynamic equation. Doing this in three-dimensions and in a fully time-dependent fashion then has the additional advantage that such a model could also be used to help dating ice cores, even in transient situations.

A second series of mechanisms, to be included in an Antarctic ice sheet model, is related to the problem of grounding line migration. Since the outer ice sheet boundary is generally located on bedrock below sea level, where the ice starts to float, it follows that the position of the grounding line, and hence, the extent of the ice sheet, results from the local interplay between ice thickness and water depth. Changes in its position therefore follow from a number of competing mechanisms, and are difficult to predict a priori. Continuity requirements imply that changes in ice thickness arise from the combined effect of fluctuations in the mass balance, either due to surface accumulation or basal melting, and variations in the divergence of the ice-mass flux. These latter fluctuations in turn depend on the amount of ice advected from the grounded ice sheet and on creep thinning caused by the presence of an ice shelf. Further complications are added by changes in ice temperature and the associated change in flow properties.

Moreover, at the grounding line a fundamental transition takes place in the force balance. This transition is from areas where the pressure-gradient force is basically balanced by shearing (in grounded ice) to areas where longitudinal stresses (that cause ice shelf stretching) prevail. It follows that calculating the flow at the grounding line is not a straightforward matter and also depends on the dynamical stress regime in the ice shelf itself. Of particular importance is whether the ice is floating freely or is spreading subject to shearing along its sides and to backpressures exerted by ice rises and pinning points. So, in order to properly take into account all these mechanisms and some of the potential feedback-loops involved, the model should not only be able to cope with the flow across the grounding line, but also in the ice shelf. So far, such a model has not been developed. Bedrock response is also a feature that needs to be modelled. This is because, assuming no changes in eustatic sea level, variations in water depth are caused by isostatic adjustments of the earth's mantle in response to changing ice loading.

THE ICE SHEET MODEL

In the Antarctic, an important part of the grounded ice is discharged through smaller-scale and relatively fast-flowing features such as outlet glaciers and ice streams (cf. § 2.1). Since the outlet glaciers are often channeled in deep bedrock troughs, this means that the resolution of the model should be high enough to capture the essential characteristics of the topography, particularly at the margin. Ice velocities depend on ice thickness to the fourth power, and a correct representation of the topography is therefore likely to produce the desired increases in mass fluxes. Incorporation of the ice streams, especially those debouching in the Ross ice shelf, on the other hand, may present somewhat more serious difficulties. Their locations are only weakly controlled by the bedrock structure, and some of the ice streams may even be transient features. However, one of the things that has become clear in recent years is the importance of basal sliding, because this enables the ice streams to form. Another pre-condition for ice stream formation may be the occurrence of unconsolidated sub-glacial sediments, which act as a lubricant (MacAyeal, 1989). Unfortunately, modelling the basal velocity boundary condition is a complicated matter and at this stage it seems fair to state that a detailed physical representation of ice streams in large scale models is still beyond reach. For instance, an attempt to model ice streams explicitly along flow lines may only shift the problem to determining their location in a changing ice sheet geometry.

In theory, it is well possible to calculate the size of an ice sheet, the distribution of stress, temperature and velocity in it, and how these quantities change with time for a prescribed variation in boundary conditions. The basic equations one needs to solve are conservation equations for mass (the 'continuity equation') and temperature, supplemented with stress-equilibrium equations and a constitutive relation for ice, relating the strain rate components (which are linear functions of the velocity gradients) to some form of the stress components. In practice, however, a number of simplifying assumptions, either based on physical reasoning or observational evidence, need to be set to make the solution more feasible, but even then the mathematical problem is far too complicated to be solved analytically. This means that numerical methods have to be used and we have to call for help from the computer. In this connection, a final and decisive requirement for the model has to be that the numerical scheme is able to yield stable solutions (this is by no means

self-evident!), while being at the same time fast enough to enable a long time integration with a sufficiently high resolution.

The Antarctic ice sheet model developed in this thesis represents an effort to address some of the problems mentioned above. It is described in detail in § 4.3 to § 4.9. Before doing so, however, a brief survey is presented of previous modelling studies of cold ice masses and of the Antarctic ice cap in particular.

4.2. PREVIOUS MODELLING STUDIES

4.2.1. Thermodynamic models

Historically, the first papers on the temperature distribution in ice sheets did not deal with the interaction of velocity and temperature, but were attempts to give a theoretical explanation for observed temperature profiles (e.g. Robin, 1955; Weertman, 1968; Philberth and Federer, 1971). In these calculations simple one-dimensional (vertical) steady-state models were involved. Due to the neglect of horizontal advection these models could only be applied in regions close to the ice divide. The moving-column model, based on a vertical model, but taking into account in a crude way the effect of horizontal advection, has subsequently been used to investigate two-dimensional (vertical plane) temperature distributions, see for example Budd et al. (1971), where this model is used extensively under steady state conditions to assess the "Derived characteristics of the Antarctic ice sheet". In this model, horizontal advection enters the calculations in an indirect way through changes in surface temperature as an initially vertical column travels downwards along a flowline. Critical to its applicability is the vertical shear in the horizontal velocity because the assumption that the column remains vertical is not realistic far from an ice divide. Nevertheless, when ice motion is almost entirely by basal sliding, or when all velocity shear is concentrated in the lower layers, the moving-column model appears to work well.

4.2.2. Dynamic ice flow models

A more recent development concerns the modelling of ice flow for the isothermal case, in which ice deformation is assumed in first approximation to

depend on the stress field alone. One of the first glacier-flow modelling studies was carried out for a simple dynamical system in three dimensions by Rasmussen and Campbell (1973), where the ice was treated as a Newtonian viscous material (i.e. with n = 1 in the flow law). Later, Budd and Jenssen (1975) developed a two-dimensional model which also includes longitudinal strain-rate differences in the force balance and deduces the flow velocity at any point along a flowline. The three-dimensional model (although vertically integrated, so some would call it two-dimensional) of Mahaffy (1976) assumed internal deformation by shear strain and was developed as a numerical computer program to find the heights of an arbitrary ice sheet on a rectangular grid. Provided the ice cap is on relatively flat ground and basal sliding is not the dominant flow mechanism, this model can be considered as the first really time-dependent model to calculate the shape of an ice sheet and was applied to Barnes ice cap. This type of model has become known as a 'continuity model' and has proved to be a very useful tool in the study of the growth and decay of (isothermal) glaciers and ice masses. It has been used extensively, for instance by Oerlemans (1980, 1981a, 1982a, 1982b, etc...) in a number of climatic and glaciological studies in one and two-dimensional space.

4.2.3. Thermomechanic models

However, in polar ice sheets the flow is also to a large extent a temperature-dependent problem. To date, the most ambitious model is that of Jenssen (1977). It is a three-dimensional model incorporating the mutual interaction between ice flow and its thermodynamics. The approach taken to the flow problem is quite similar to that of Mahaffy (1976). Jenssen introduced a scaled vertical coordinate, transformed the relevant continuity and thermodynamic equations (prognostic equations for ice thickness and temperature) and tried to solve the system numerically. In applying the scheme to the Greenland ice sheet, however, numerical instabilities occurred, forcing the calculations to be interrupted after 1000 years of integration. This was attributed to the use of a coarse grid (200 x 100 km and 10 layers in the vertical) and to an unsophisticated approach to modelling the ice boundary. Nevertheless, this model appears to be the first that dealt with the ice flow-temperature coupling in a truly dynamic fashion.

THE ICE SHEET MODEL

In the last few years, more advances have been made in the formulation and analysis of thermo-mechanically coupled ice sheets, showing the effect of changing temperature fields on the geometry of the ice sheet. For instance, Hutter et al. (1986), Hindmarsh and Hutter (1988), Hindmarsh et al. (1989) and Dahl-Jensen (1989) have presented numerical solutions for the steady state two (vertical plane) dimensional case based on a treatment given by Morland (1984). However, in the Hutter papers it appears that numerical problems are still encountered, reducing the applicability of their solutions to cases where the basal sliding velocity component is far larger than the movement caused by internal deformation.

4.2.4. Antarctic models

The first dynamic model for the Antarctic ice sheet was published by Oerlemans (1982a) in a study of the response of the Antarctic ice sheet to a climatic warming. It is a vertically integrated model, where the ice is deforming as an isothermal material by Glen's flow law, and has a horizontal grid spacing of 100 km. Changes in the horizontal domain are modelled using a geometric construction. The ice at the grounding line is first redistributed over neighbouring gridpoints according to a prescribed snout steepness (derived from plastic flow theory), before a flotation criterion is applied. This allowed the edge to move from one gridpoint to another. Although it is not completely clear whether this scheme for grounding line migration was retained, a later version also included ice shelves and the response of the bedrock to a varying ice load (Oerlemans, 1982b). In this model, ice shelves were modelled using a diagnostic procedure, giving ice thickness as a function of both distance to the grounded ice sheet and ice thickness at the grounding line. It is based on the observation that ice shelves are mainly formed in large embayments and that apparently the degree of enclosure by grounded ice plays an important role. Using this model, Oerlemans was able to grow the Antarctic ice sheet in about 30000 years. Although the resemblance to the present ice sheet was not too bad, the model could not simulate the Ronne-Filchner ice shelf and also overpredicted grounded ice cover in the vicinity of the Antarctic Peninsula. When sea level was lowered by 100 m, the model responded by a large increase in the volume of the West Antarctic ice sheet. However, it failed to let the ice sheet retreat again to its present position when sea level was raised. To unground the ice sheet in these areas, a sea level rise of at least 600 m

was required. It was suggested that this might be because basal sliding was not taken into account. Although the need was recognized to include thermodynamics and to deal with ice shelves and grounding line dynamics in a much more refined way, this model can nevertheless be considered as a first step towards the development of a complete model for the entire Antarctic ice sheet.

The model of Budd and Smith (1982) was developed along similar lines. It used a different flow law but still excluded a temperature calculation within the ice. They also used a 100 km resolution and approximated ice shelves in a crude way by prescribing a constant horizontal strain rate, derived from freely floating ice shelves. Although the inclusion of creep thinning can certainly be regarded as an improvement, this approach is still unable to deal with more complex ice shelf geometries because the associated stress and strain rate conditions are likely to be different. Also, they did not include any special treatment of the flow in the transition zone between grounded and floating ice. A considerable number of sensitivity experiments were performed with this model, but the overall model performance appeared to be heavily constrained by the coarse numerical grid. Notably, when the ice sheet was run to equilibrium under present-day environmental conditions, its volume became far too large compared to the figure currently accepted (by more than 50%), and a sea level rise of 150 m was required to simulate the West Antarctic ice sheet more in accordance with its present geometry. The same model, but with an increased resolution, surfaced again recently (Payne et al., 1989), in a study on the growth and decay of the Antarctic Peninsula ice sheet during the last glacial-interglacial cycle.

The original idea of Jenssen (1977) was taken up again by Herterich (1988) in an attempt to construct a model to describe the evolution of the ice-age ice sheets during the Pleistocene. This model also operates on a 100 km grid, has a fixed vertical resolution of 285 m and was applied to the Antarctic ice sheet for testing. In this study, the ice sheet was assumed to be in a stationary state and a calculation was made of the amount of accumulation that would be needed to balance the horizontal divergence of the vertically integrated flow field. This procedure to test model performance is basically similar to comparing 'balance velocities' with 'dynamics velocities' in Budd-type models (e.g. Budd and Jenssen, 1989). Herterich suggested that the omission of

basal sliding might explain the mismatch between observed accumulation rates and the ones calculated for steady state.

In a later development of this model, the constraint of stationarity was partially lifted and an attempt was made by Böhmer and Herterich (1990) to incorporate variations in the extent of the grounded ice sheet. Based on the assumption that the transition zone between grounded and floating ice may be treated as a sub-grid scale process, they tried to parameterize its effect in terms of ice thicknesses defined on the coarse grid. To do this, the integral force balance was formulated along a closed loop in a vertical plane perpendicular to the grounding line. After some simplifications, the characteristics of the transition zone then entered the calculations formally through a 'friction coefficient (μ)', that could be interpreted as the surface slope at the last grounded ice sheet point. The position of the grounding line was then constructed geometrically by intersection of the line defined by μ and the surface of a hypothetical ice shelf, calculated with an empirical model of Oerlemans-type. By varying the value of μ, and thus prescribing the surface slope and the rate of outflow from the grounded ice sheet, they were able to produce a number of ice sheet geometries that may resemble possible states of the Antarctic ice sheet. Although their approach is interesting from a methodological point of view, a number of objections can be made. The critical point in their analysis is probably connected with the neglect of the longitudinal stress deviator at the grounding line. This assumption may not be justified, but could not be avoided mainly because longitudinal stresses cannot be calculated from their ice-shelf model. Apart from an interpretation problem (what do variations in μ stand for ?), prescribing the geometry of the transition zone, rather than to let it be determined by the appropriate physics, also leads to a violation of the principle of conservation of mass. As a result, and for a constant present-day value of $\mu = 0.05$, their model is insensitive to changes in environmental conditions (as well as internal adjustments); in order to produce a forward migration of the grounding line by 1 gridpoint (100 km), ice thickness would have to increase by nearly 5 km. Alternatively, to produce the same effect with a sea level drop of 100 m, one would have to assume an extremely large bedrock slope. These are unrealistic requirements, and one could question the applicability of such an approach to study grounding-line dynamics.
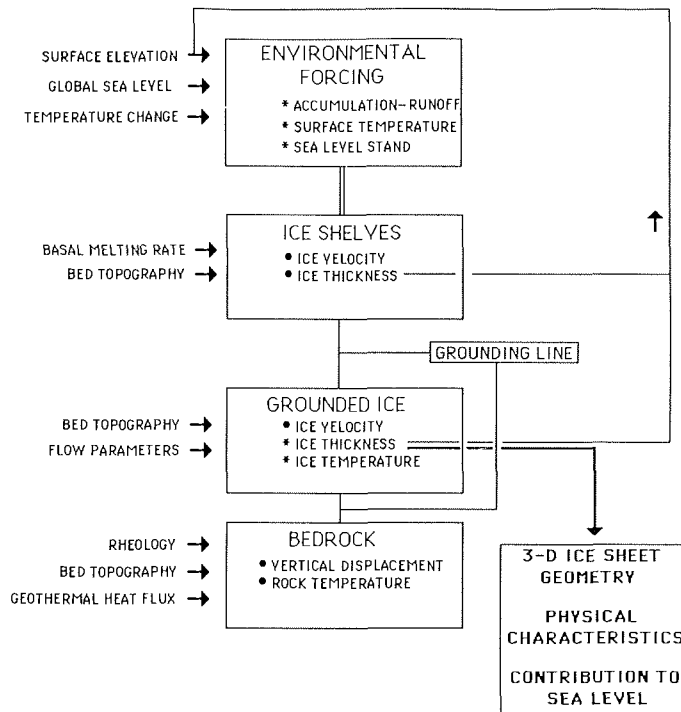
86

4.3. STRUCTURE OF THE HUYBRECHTS MODEL

The Huybrechts model represents another step towards a more complete and detailed model of the Antarctic ice sheet. It is time-dependent and computes the full set of coupled thermomechanical equations for ice flow in three dimensions (with the only restriction that the horizontal velocity vector cannot change direction with depth), as well as the geographical distribution of ice mass. The primary difference between this model and those used in earlier studies, however, is a rigorous treatment of the flow, not only in the ice sheet, but also across the grounding line and in the ice shelf, so that the position of the grounding line can be traced during the calculations by means of a flotation criterion. This is done by allowing for different velocity solutions in grounded and floating ice and by defining a stress transition zone in between at the grounding line. The basic idea here is to incorporate in each subdomain all relevant stresses in the stress equilibrium equations and in the flow law, from which the ice velocities are calculated. This means that there is free interaction between ice sheet and ice shelf and thus that the position of the grounding line is entirely *internally generated.*

The model also includes basal sliding, which is restricted to regions that are at the pressure melting point. It considers the response of the underlying bedrock to changing ice load, taking into account both the rigidity of the lithosphere and the viscosity of the asthenosphere, and including a temperature calculation. Fig.4.1 shows the structure of the model.

Also more efficient numerical techniques have been used, that allow for a finer mesh. The finite difference scheme is based upon the Alternating-Direction-Implicit method, and, in order to avoid boundary problems in the thermodynamic calculations, the vertical coordinate is scaled to local ice thickness. The horizontal grid point distance is 40 km. There are 10 layers in the vertical, which have closer spacing towards the bedrock surface where the shear concentrates. There are also 5 grid points in the bed for the temperature calculations. In total, this leads to a domain of somewhat more than 300000 gridpoints. In this setup, the model requires a supercomputer and all numerical integrations discussed in this thesis have been performed on a CRAY-2. In order to preserve numerical stability, time steps can be taken up to

THE ICE SHEET MODEL

```
                        ┌──────────────────────────────────────┐
                        │                                      │
SURFACE ELEVATION ─→  ┌─────────────────────┐                 │
                      │  ENVIRONMENTAL      │                  │
GLOBAL SEA LEVEL  ─→  │     FORCING         │                  │
                      │                     │                  │
TEMPERATURE CHANGE ─→ │  * ACCUMULATION-RUNOFF                 │
                      │  * SURFACE TEMPERATURE                 │
                      │  * SEA LEVEL STAND  │                  │
                      └─────────────────────┘                  │
                                                               │
                      ┌─────────────────────┐            ↑    │
BASAL MELTING RATE ─→ │  ICE SHELVES        │                 │
                      │  • ICE VELOCITY     │                 │
BED TOPOGRAPHY ─→     │  • ICE THICKNESS ───┼─────────────────┤
                      └─────────────────────┘                 │
                               ┌─────[GROUNDING LINE]─┐        │
                      ┌─────────────────────┐                 │
                      │  GROUNDED ICE       │                 │
BED TOPOGRAPHY ─→     │  • ICE VELOCITY     │                 │
                      │  * ICE THICKNESS ═══╪══             │
FLOW PARAMETERS ─→    │  * ICE TEMPERATURE  │                 │
                      └─────────────────────┘          ↓
                      ┌─────────────────────┐     ┌──────────────────┐
RHEOLOGY ─→           │  BEDROCK            │     │  3-D ICE SHEET   │
                      │  • VERTICAL DISPLACEMENT   │  GEOMETRY        │
BED TOPOGRAPHY ─→     │  • ROCK TEMPERATURE │     │                  │
                      └─────────────────────┘     │  PHYSICAL        │
GEOTHERMAL HEAT FLUX ─→                           │  CHARACTERISTICS │
                                                  │                  │
                                                  │  CONTRIBUTION TO │
                                                  │    SEA LEVEL     │
                                                  └──────────────────┘
```

fig.4.1: Structure of the Huybrechts model. Inputs are given at the left-hand side. Prescribed environmental variables drive the model, which has ice shelves, grounded ice and bed adjustment as major components. The position of the grounding line is not prescribed, but internally generated. The model essentially outputs the time-dependent three-dimensional ice sheet geometry and the coupled temperature and velocity fields.

40 years. The model then needs about 18 min. CPU-time for a 10000 year integration.

Part of the model builds on a 2-D precursor, which had a fixed domain and was used to study thermomechanical response patterns with changing climate of the East Antarctic ice sheet (Huybrechts, 1987; Huybrechts and Oerlemans, 1988). A detailed discussion on the complete numerical scheme used to solve the thermomechanical equations for grounded ice was given in Huybrechts (1986). The text of sections § 4.4. to § 4.7, on the various model formulations and the numerical techniques involved, is to a large extent based on these publications. Those readers not interested in the more technical aspects of the

model, however, may skip it and continue with § 4.8 (data sets and model forcing). A list of used symbols (constants and variables) is included at the end of the chapter (§ 4.9).

4.4. FORMULATION OF THE ICE FLOW

Defining a right-handed Cartesian coordinate system x,y,z, with the x-y plane parallel to the geoid and the z-axis pointing vertically upwards (z = 0 at sea level), the basic equation to be solved in the model is a continuity equation for ice thickness H:

$$\frac{\partial H}{\partial t} = -\nabla \cdot (\vec{v}H) + M \tag{4.1}$$

where $\vec{v}$ is the depth-averaged horizontal velocity vector, M the mass balance, t time (in y) and the ∇- operator is understood to be two-dimensional (in the x-y plane). Basically, the solution of (4.1) follows from reformulating the velocity
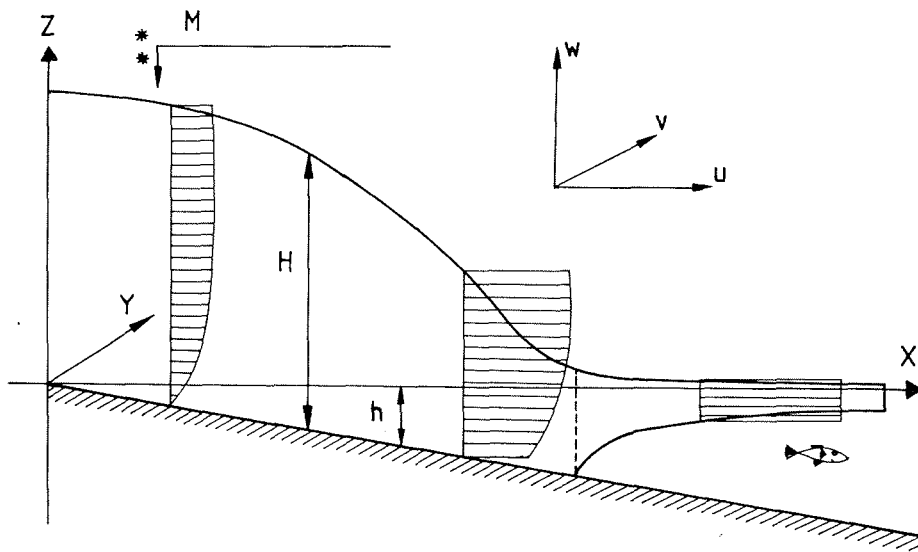

fig.4.2: Model geometry. For explanation of variables, see text.

field in terms of the ice sheet geometry (ice thickness and surface gradient), so that only one unknown remains. The resulting equation is then a partial differential equation of parabolic type, but nonlinear, and has to be solved by numerical methods. The model geometry is shown in fig. 4.2.

4.4.1. General force balance and flow law

In order to arrive at equations describing the velocity distribution, we start with the mechanical equations expressing balance between body forces (gravity in this case) and surface forces (stresses) acting on an element of ice. Since accelerations in an ice sheet can be neglected, Newton's second law for a continuum can be expressed as (Paterson, 1981):

$$\frac{\partial \tau_{xx}}{\partial x} + \frac{\partial \tau_{xy}}{\partial y} + \frac{\partial \tau_{xz}}{\partial z} = 0 \qquad (4.2)$$

$$\frac{\partial \tau_{yx}}{\partial x} + \frac{\partial \tau_{yy}}{\partial y} + \frac{\partial \tau_{yz}}{\partial z} = 0 \qquad (4.3)$$

$$\frac{\partial \tau_{zx}}{\partial x} + \frac{\partial \tau_{zy}}{\partial y} + \frac{\partial \tau_{zz}}{\partial z} = \rho g \qquad (4.4)$$

Here, τ_{ij} are the stress tensor components [Nm^{-2}], with subscripts $i \neq j$ denoting the shear stresses, $i=j$ the normal stresses, g the acceleration of gravity [9.81 ms^{-2}], and ρ ice density [910 kgm^{-3}], assumed to be constant.

A second equation follows from the material properties of ice and is provided by an expression relating deformation to stress. The flow law governing the creep of polycrystalline ice is assumed to be of Glen-type with exponent n = 3 and can be written as (Paterson, 1981):

$$\dot{\varepsilon}_{ij} = A(T^*) \, \tau_*^2 \, \tau'_{ij}$$

$$\text{and} \quad \tau_*^2 = \tau_{xx}'^2 + \tau_{yy}'^2 + \tau_{xx}' \tau_{yy}' + \tau_{xz}^2 + \tau_{yz}^2 + \tau_{xy}^2 \qquad (4.5)$$

In this expression, $\dot{\varepsilon}_{ij}$ are the strain rate components related to velocity gradients by definition ($\dot{\varepsilon}_{ij} = [\partial u_i/\partial x_j + \partial u_j/\partial x_i]/2$), τ'_{ij} the stress deviators

(defined as the full stress minus the hydrostatic component: $\tau'_{ii} = \tau_{ii} - (\tau_{xx} + \tau_{yy} + \tau_{zz})/3$) , τ_* the effective stress defined in terms of all the stress deviator components so that it is independent of the coordinate system (where τ'_{zz} has been eliminated employing the incompressibility condition: $\tau'_{xx}+\tau'_{yy}+\tau'_{zz}=0$) and $A(T^*)$ is a temperature dependent flow law parameter [$Pa^{-3}y^{-1}$].

The values of the flow law parameters n and A probably introduce the main uncertainty in the model, because their values are not exactly known. For a discussion, see e.g. Journal of Glaciology, 1978, no. 85 on the physics and chemistry of ice; Paterson, 1981, chap. 3. In this study, we will follow the recommendations of Paterson and adopt a mean value of n = 3. A depends on such factors as ice temperature, crystal size and orientation, impurity content, the presence of interstitial meltwater and possibly other factors (Budd and Jacka, 1989). Here only the temperature dependence of A will be taken into account. This approximation is needed because sound quantitative information on how variations in other ice properties affect flow is lacking.

Laboratory experiments suggest an Arrhenius relationship:

$$A(T^*) = m \cdot a \exp\left\{ \frac{-Q}{RT^*} \right\} \tag{4.6}$$

where a is specified below, R is the gas constant [8.314 $Jmol^{-1}K^{-1}$], Q the activation energy for creep, and T^* absolute temperature corrected for the dependence of the melting point on pressure ($T^* = T + 8.7 \times 10^{-4}$ (H + h - z), with T measured in K). m is an enhancement factor. With the following values for a and Q:

$T^* < 263.15\ K$	$a = 1.14 \times 10^{-5}\ Pa^{-3} y^{-1}$	$Q = 60\ kJmol^{-1}$
$T^* \geq 263.15\ K$	$a = 5.47 \times 10^{10}\ Pa^{-3} y^{-1}$	$Q = 139\ kJmol^{-1}$ (4.7)

$A(T^*)$ lies within the bounds put forward by Paterson and Budd (1982). The higher value of Q for $T^* \geq -10$ °C appears to be connected with enhanced creep due to the presence of liquid water at grain boundaries. Figure 4.3 shows the adopted temperature dependence of the flow law coefficient. The
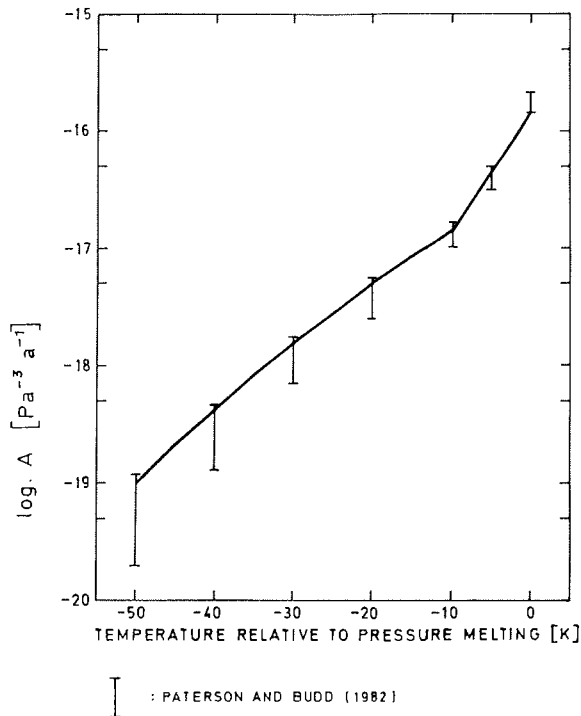
fig 4.3: Temperature dependence of the flow law coefficient A as used in the model.

enhancement factor m (controlling the ice sheet's height-to-width ratio) serves a 'tuning' purpose. In this way, the softening effects caused by impurity content and crystal fabric can be implicitly included. As mentioned by Paterson and Budd (1982) these factors may alter A by up to an order of magnitude. In the model runs discussed in this thesis, its value is set at 5 for grounded ice and 1 for the ice shelf.

In ice, the vertical normal stress can generally be taken to equal the weight of the overlying ice ($\tau_{zz}(z) = -\rho g(H+h-z)$, with h bed elevation), allowing us to rewrite the stress equilibrium equations in a more convenient form for the analysis below. This is equivalent to the assumption that horizontal gradients in the vertical shear stresses are small compared to ρg in (4.4). After substituting for stress deviators and rearranging the terms, this gives:

$$\frac{\partial \tau_{xz}}{\partial z} = \rho g \frac{\partial (H + h)}{\partial x} - 2 \frac{\partial \tau'_{xx}}{\partial x} - \frac{\partial \tau'_{yy}}{\partial x} - \frac{\partial \tau_{xy}}{\partial y} \qquad (4.8)$$

$$\frac{\partial \tau_{yz}}{\partial z} = \rho g \frac{\partial (H + h)}{\partial y} - 2 \frac{\partial \tau'_{yy}}{\partial y} - \frac{\partial \tau'_{xx}}{\partial y} - \frac{\partial \tau_{xy}}{\partial x} \qquad (4.9)$$

These equations are in principle valid over the whole ice sheet domain, but are further simplified below by setting appropriate assumptions for the three separate flow regimes considered, namely grounded ice, floating ice and a transition zone in between at the grounding zone.

4.4.2. Grounded ice

4.4.2.1. ice deformation

In the case of grounded ice, variations in the longitudinal directions are small in comparison to variations in the vertical (small geometric aspect ratio). Thus, simplifications can be made according to the 'shallow ice approximation' (for a more rigorous definition, see Hutter, 1983). This implies that the longitudinal strain-rate components are negligible compared to the shear strain-rate components, in effect stating that the normal stress tensor is isotropic and hydrostatic equilibrium prevails everywhere ($\tau_{xx} = \tau_{yy} = \tau_{zz}$ or $\tau'_{xx} = \tau'_{yy} = \tau'_{zz} = 0$). Although this assumption breaks down at the margin (large gradients and therefore substantial non-zero longitudinal stress deviators) and at the centre (longitudinal strain-rates prevailing), the inclusion of longitudinal stress deviators does not alter significantly the profile of ice sheets larger than about 30 km (Weertman,1961). Neglecting longitudinal strain-rates limits the use of the model to cases where basal sliding is relatively unimportant. It also requires slopes to be smoothed over a distance an order of magnitude greater than ice thickness to circumvent problems associated with small scale bedrock irregularities (Budd, 1970). However, this condition will generally be met when resolving the equations on a computational grid with typical spacings in the 20 - 100 km range. In summary, the above assumption has shown general applicability in large-scale ice sheet modelling (e.g. Mahaffy,1976; Oerlemans,1981a).

With the further remark that the grounded ice sheet does not experience shear at its sides ($\tau_{xy} = 0$), the stress balance is now between the horizontal shear stresses τ_{xz} and τ_{yz} and surface-slope induced pressure gradients. Resulting expressions for the shear stress distribution then follow after integrating (4.8), (4.9) from the surface (which can support no shear) to a height z:

$$\tau_{xz}(z) = \tau_{xz}'(z) = -\rho g(H + h - z)\frac{\partial(H + h)}{\partial x} \qquad (4.10)$$

$$\tau_{yz}(z) = \tau_{yz}'(z) = -\rho g(H + h - z)\frac{\partial(H + h)}{\partial y} \qquad (4.11)$$

Expressions for the velocity components are derived by invoking the flow law. Using the above assumptions, (4.5) reduces to its two-component form as:

$$\dot{\varepsilon}_{xz} = \frac{1}{2}\left[\frac{\partial u}{\partial z} + \frac{\partial w}{\partial x}\right] = A(T^*)\,\tau_*^2\,\tau_{xz}' \qquad (4.12)$$

$$\dot{\varepsilon}_{yz} = \frac{1}{2}\left[\frac{\partial v}{\partial z} + \frac{\partial w}{\partial y}\right] = A(T^*)\,\tau_*^2\,\tau_{yz}' \qquad (4.13)$$

$$\tau_* = \left[\tau_{xz}^2 + \tau_{yz}^2\right]^{\frac{1}{2}} \qquad (4.14)$$

where u,v,w are the x,y,z components of the three-dimensional velocity vector $\vec{V}$ [my^{-1}].

Integrating (4.12), (4.13) with respect to z and assuming that $\partial w/\partial x \ll \partial u/\partial z$; $\partial w/\partial y \ll \partial v/\partial z$ then yields an expression for the horizontal velocity vector $\vec{v}$:

$$\vec{v}(z) - \vec{v}(h) = -2(\rho g)^3\left[\nabla (H+h).\nabla (H+h)\right]\nabla (H+h)\int_h^z A(T^*)(H+h-z)^3\,dz \qquad (4.15)$$

$\vec{v}(h)$, the two-dimensional basal-sliding velocity enters here as a boundary condition; $\vec{v}(z) - \vec{v}(h)$ expresses the deformational part of the horizontal velocity. Since $A(T^*)$ depends on temperature (and therefore on position)

equation (4.15) now has to be evaluated numerically, given the temperature distribution.

4.4.2.2. basal sliding

When the temperature of the basal layers reach the melting point, bottom water is formed and basal sliding may occur. Views on how this should be modelled, however, differ widely. Numerous theories have been proposed that predict sliding velocities from various geometric aspects of glaciers and ice sheets, but for obvious reasons these theories are all hampered by the scarcity of direct observations (Paterson, 1981, chapter 7). It seems fair to state that at present a general theory is not yet available. Nevertheless, theoretical considerations and laboratory studies suggest that basal sliding depends on the shear stress at the bed raised to some power; on bed roughness; and on the 'effective normal load', which generates a frictional force resisting the sliding motion (Budd et al., 1979). Since sliding only occurs if meltwater is present, the weight of the overlying ice column (normal load) is then partially compensated by an upward buoyancy force due to the pressure of the basal water. This causes the normal pressure to be less effective (e.g. Lliboutry, 1968; Weertman, 1972). A generalized sliding law should therefore be of the form:

$$\vec{v}_b = A_s \frac{\vec{\tau}_b^{\,p}}{Z^q} \tag{4.16}$$

where A_s is a constant that is inversely proportional to the bed roughness, τ_b is basal shear stress, Z the reduced normal load and p, q are numbers to be determined.

Bindschadler (1983) compared different sliding laws with observations on West Antarctic ice streams and concluded that a Weertman-type sliding law (Weertman, 1964), corrected for the effect of subglacial water pressure, seems to be preferable. We follow this analysis and use $q=1$ and $p=3$. In the model, sliding is restricted to regions that are at the pressure melting point. The sliding velocity is given by:

$$\vec{v}(h) = -A_s \, (\rho g H)^3 \left[\nabla(H+h) \cdot \nabla(H+h) \right] \nabla(H+h) / Z^* \tag{4.17}$$

where $A_s = 1.8 \times 10^{-10} \, N^{-3} yr^{-1} m^8$ and Z^* is the height above buoyancy:

$$Z^* = H + \rho_w \, (h - H_{sl}) / \rho \tag{4.18}$$

Here ρ_w is water density [1028 kgm^{-3}] and H_{sl} sea level stand with respect to present conditions. This empirical relation expresses the view that pressurized subglacial water ('connected to the sea') reduces basal friction when the grounding line is approached, leading to high sliding velocities. In this way, a smooth transition to ice shelf flow is assured. Although eq. 4.18 is strictly only valid for bedrock areas below sea level, it is also used on higher ground. This does not present a serious problem because Z^* then becomes very large.

4.4.2.3. complete velocity field

A second integration from the base to the surface then yields the mean horizontal ice mass flux:

$$\vec{v}H = \int_{h}^{H+h} \vec{v}(z) \, dz \tag{4.19}$$

where vertical motion, which occurs as a result of accumulation and vertical strain, is calculated from the incompressibility condition:

$$\frac{\partial u}{\partial x} + \frac{\partial v}{\partial y} + \frac{\partial w}{\partial z} = 0 \tag{4.20}$$

yielding immediately:

$$w(z) - w(H+h) = -\int_{H+h}^{z} \nabla \cdot \vec{v}(z) \, dz \tag{4.21}$$

The kinematic boundary condition at the upper surface is given by:

$$w(H+h) = \partial(H+h)/\partial t + \vec{v}(H+h) \cdot \nabla(H+h) - M \qquad (4.22)$$

and M is positive in the case of accumulation. Equations (4.15) and (4.21) now fully describe the three-dimensional velocity field $\vec{V}$, with the only limitation that $\vec{v}$ is not allowed to change direction with depth, its direction being solely determined by the local surface slope. It is important to note that the velocity in the ice sheet is a local variable and is completely defined by the local geometry (surface slope and ice thickness).

4.4.3. Ice shelf

Ice shelves are in hydrostatic equilibrium with the ocean water and thus the flotation criterion applies:

$$H + h = \left[1 - \rho_i / \rho_w \right] H \qquad (4.23)$$

In contrast with the stress equilibrium conditions in grounded ice, the stress balance is now between the pressure gradient force arising from the surface slope, opposed by longitudinal gradients in normal deviatoric stresses (that cause ice shelf stretching) and by lateral shearing induced by side-walls and ice rises (Thomas, 1973). The base of the ice shelf experiences negligible friction, so there is no shearing in horizontal planes ($\tau_{xz} = \tau_{yz} = 0$) and strain rates and velocities are independent of depth. This would be perfectly true if the surface were horizontal, but is a good approximation because ice shelves have very small surface slopes.
With these simplifications in mind, the stress equilibrium in ice shelves can be restated as (from eqs. 4.8-4.9):

$$2\frac{\partial \tau'_{xx}}{\partial x} + \frac{\partial \tau'_{yy}}{\partial x} + \frac{\partial \tau_{xy}}{\partial y} = \rho g \frac{\partial(H+h)}{\partial x} \qquad (4.24)$$

$$2\frac{\partial \tau'_{yy}}{\partial y} + \frac{\partial \tau'_{xx}}{\partial y} + \frac{\partial \tau_{xy}}{\partial x} = \rho g \frac{\partial(H+h)}{\partial y} \qquad (4.25)$$

Equations describing the velocity distribution follow after introducing the flow law (eq. 4.5) and making use of the constitutive relation in its second-order invariant form:

$$\dot{\varepsilon} = A(T^*)\, \tau_*^3 \tag{4.26}$$

so that τ'_{ij} in (4.5) can be written as:

$$\tau'_{ij} = \dot{\varepsilon}_{ij}\, A(T^*)^{-\frac{1}{3}} \cdot \varepsilon^{-\frac{2}{3}} \tag{4.27}$$

After substituting (4.27) together with expressions relating strain rates to velocity gradients (cf. eq. 4.5) in eqs. 4.24- 4.25 and some algebraic manipulation, details of which are omitted for the sake of brevity, the following expressions result (for a more rigorous derivation, the interested reader is referred to Herterich (1987), where a similar 2-D vertical plane derivation is performed):

$$2\frac{\partial}{\partial x}\left[\, f\frac{\partial u}{\partial x}\,\right] + \frac{\partial}{\partial x}\left[\, f\frac{\partial v}{\partial y}\,\right] + \frac{1}{2}\frac{\partial}{\partial y}\, f\left[\, \frac{\partial u}{\partial y}+\frac{\partial v}{\partial x}\,\right] = \rho g A(T^*)^{\frac{1}{3}}\, \frac{\partial(H+h)}{\partial x} \quad \text{(a)}$$

$$2\frac{\partial}{\partial y}\left[\, f\frac{\partial v}{\partial y}\,\right] + \frac{\partial}{\partial y}\left[\, f\frac{\partial u}{\partial x}\,\right] + \frac{1}{2}\frac{\partial}{\partial x}\, f\left[\, \frac{\partial u}{\partial y}+\frac{\partial v}{\partial x}\,\right] = \rho g A(T^*)^{\frac{1}{3}}\, \frac{\partial(H+h)}{\partial y} \quad \text{(b)}$$

$$\text{with } f = \left[\, \left(\frac{\partial u}{\partial x}\right)^2 + \left(\frac{\partial v}{\partial y}\right)^2 + \left(\frac{\partial u}{\partial x}\right)\left(\frac{\partial v}{\partial y}\right) + \left[\frac{1}{2}\left(\frac{\partial u}{\partial y}+\frac{\partial v}{\partial x}\right)\right]^2\,\right]^{\frac{-1}{3}} \tag{4.28}$$

Equations 4.28 (a-b) are a set of second-order partial differential equations of elliptic type, but nonlinear, and can be solved by point relaxation (for more details see further under numerical methods). The non-linearity of the flow law is introduced by the f-term = $\dot{\varepsilon}^{-2/3}$ (f = 1 for a linear rheology). These equations can in principle cope with the most complex ice shelf geometries, because the

only simplification is the absence of shearing in horizontal planes. The only restrictions in their use are connected with the resolution of the numerical grid and the assessment of an 'effective' temperature for the ice stiffness parameter. Also, using mean ice density instead of the observed variation of density with depth may result in an overestimate of the effective stress by a factor of 2 (Paterson, 1981 and references quoted therein). However, it is believed that these effects are crudely incorporated by the use of the tuning parameter m in the flow law (cf. eq. 4.6).

4.4.3.1. boundary conditions

In reality, a thinning ice shelf will break off at its seaward margin once a critical minimum thickness is reached (usually around 250 m). In the model, however, calving physics are not considered explicitly, and the ice shelf is actually made to extend all the way to the edge of the numerical grid. Testing indicates that this does not present a serious problem. Model runs, in which the ice shelf was 'cut off' closer to the coast (but still outside the main embayments) did not have appreciably different ice thickness distributions or grounding line positions (which is of final interest).

Boundary conditions at the seaward margin are then applied for unconfined, freely floating and uniformly spreading (complete stress and strain-rate symmetry in the x- and y-directions) ice shelves. This is equivalent to setting $\tau'_{xx} = \tau'_{yy}$; $\tau_{xx} = \tau_{yy}$; and $\tau_{xy} = 0$. Velocity components then follow from the flow law (eq. 4.5):

$$\dot{\varepsilon}_{xx} = \frac{\partial u}{\partial x} = 3 A(T^*) \tau'^{3}_{xx} \tag{4.29}$$

$$\dot{\varepsilon}_{yy} = \frac{\partial v}{\partial y} = 3 A(T^*) \tau'^{3}_{yy} \tag{4.30}$$

$$\dot{\varepsilon}_{xy} = \frac{\partial u}{\partial y} + \frac{\partial v}{\partial x} = 0 \tag{4.31}$$

where an expression for the deviatoric stresses can be found from the condition that the net total force on the ice shelf front must be balanced by the horizontal force exerted by the sea water:

$$\int_{h}^{H+h} \tau_{xx}\, dz = \int_{h}^{0} \rho_w gz\, dz \qquad (4.32)$$

From hydrostatic equilibrium (eq. 4.23), an expression for the stress deviator $(\tau'_{xx} = [\tau_{xx} - \tau_{zz}]/3)$ and $\tau_{zz} = -\rho g(H+h-z)$, this yields:

$$\tau'_{xx} = \tau'_{yy} = \rho g H\, (1 - \rho/\rho_w)/6 \qquad (4.33)$$

At the grounding zone, boundary conditions are not velocity gradients, but follow from the vertically integrated velocity components.

4.4.4. Stress transition zone at the grounding line

In view of the basically different nature of the stress balance in grounded and floating ice, there must be a stress transition zone located somewhere in between near the grounding line. Here, a change should take place from shear-dominated flow to a situation where longitudinal stresses prevail, so that all stress components could be potentially important. As discussed before, the thickness at the grounding line results from a subtle balance between a whole number of competing mechanisms and feedback-loops, even so that by excluding one stress component almost any result can be obtained. Modelling the transition zone is thus a delicate matter and requires careful consideration of the various terms in the force balance. Of interest in this respect are studies by Van der Veen (1985, 1987) and Herterich (1987), who addressed the flow at the grounding line in a 2-D (vertical plane) approach. In order to deal with the ice sheet - ice shelf interaction at the grounding line in a proper way, Van der Veen (1987) advocated to include the longitudinal deviatoric stress in the effective stress term of the flow law. The present 3-D approach incorporates this fundamental idea.

Two assumptions are made as follows. First, it is taken for granted that the width of the stress transition zone is smaller than typical gridsizes in large scale numerical models. The validity of this assumption appears to be corroborated by the two-dimensional studies of Herterich (1987) and Van der

THE ICE SHEET MODEL

Veen (1987), although the length of the zone over which longitudinal stresses are important may be larger where basal sliding is the dominant flow mechanism. Consequently, the grounding zone in the model has a width of one gridcell and includes all grounded grid points that border the floating ice region. The second simplification assumes that deviatoric stress *gradients* can be neglected as a contribution to the shear stresses in the stress equilibrium (eqs. 4.8-4.9). This may represent a somewhat more dubious approximation, in particular in fast-flowing outlet glaciers and ice streams, where longitudinal stretching may support part of the weight (e.g. McMeeking and Johnson, 1985). In spite of this, however, one could simply argue that this is probably the only option, because to do otherwise would imply complicated and time-consuming stress integrations along the x- and y-axes respectively. On the other hand, in Van der Veen (1987), this assumption did not appear to be crucial to the model outcome and as far as the ice sheet profile was concerned, the only thing that really mattered was the longitudinal deviatoric stress (and much less its gradient) at the grounding line only. A scale analysis of eqs. 4.8-4.9 for typical grid spacings in numerical models seems to support this. Moreover, in a recent detailed calculation of the stress distribution near the grounding zone of Byrd Glacier (an outlet of the East Antarctic ice sheet), Whillans et al.(1989) found a close correlation between the driving stress and basal drag. These points seem to indicate that, as far as large-scale numerical models are concerned, the ice sheet approximation may still be valid, so that the shear stresses follow from the usual equations (4.10-4.11). Other assumptions in Van der Veen's analysis are also used here, such as replacing the deviatoric stresses by their vertical mean, because information on their vertical profile is lacking.

In view of this, the vertically integrated mass flux at the grounding line (that is of final interest) can also be found by integrating expressions for the shear strain rates $\dot{\epsilon}_{xz}$ and $\dot{\epsilon}_{yz}$ twice along the vertical, however incorporating all stress components in the effective stress term of the flow law:

$$\vec{v}H = -2(\rho g)^3 \left[\nabla (H+h).\nabla (H+h) \right] \nabla (H+h) \int\limits_{h}^{H+h} \int\limits_{h}^{z} A(T^*) (H+h-z)^3 \, dz \, dz' \qquad (4.34)$$

$$- 2 \rho g \left[\overline{\tau'^2_{xx}} + \overline{\tau'^2_{yy}} + \overline{\tau'_{xx} \tau'_{yy}} + \overline{\tau'^2_{xy}} \right] \nabla (H+h) \int\limits_{h}^{H+h} \int\limits_{h}^{z} A(T^*) (H+h-z) \, dz \, dz' + \vec{v}(h) H$$

where $\overline{\tau'_{xx}}, \overline{\tau'_{yy}}, \overline{\tau'_{xy}}$ in the transition zone cannot be specified directly, but have to be obtained by invoking the constitutive relation (4.5). The procedure relies on the fact that the stress field can be calculated from the flow law, given the ice sheet geometry, strain rates and the rate factor. Integrating expressions for $\dot{\varepsilon}_{xx}, \dot{\varepsilon}_{yy}, \dot{\varepsilon}_{xy}$ along the vertical and dividing by ice thickness to obtain vertical mean values then formally yields:

$$\frac{1}{H} \int\limits_{h}^{H+h} \dot{\varepsilon}_{ij} \, dz = \frac{1}{H} \int\limits_{h}^{H+h} \left[A(T^*) . (\tau'^2_{xx} + \tau'^2_{yy} + \tau'_{xx}\tau'_{yy} + \tau'^2_{xy} + \tau^2_{xz} + \tau^2_{yz}). \tau'_{ij} \right] dz$$

$$\text{for } \dot{\varepsilon}_{xx}, \dot{\varepsilon}_{yy}, \dot{\varepsilon}_{xy} \qquad (4.35)$$

After making use of Leibnitz' rule to change the order of integration and some algebraic manipulations (details of which are omitted here in order to save space), this leads to the following set of coupled equations:

$$A(T^*) \overline{\tau'_{xx}} \left[\overline{\tau'^2_{xx}} + \overline{\tau'^2_{yy}} + \overline{\tau'_{xx} \tau'_{yy}} + \overline{\tau'^2_{xy}} + \frac{H^2}{3} (\rho g)^2 \left[\nabla(H+h) . \nabla(H+h) \right] \right]$$

$$- \frac{\partial \bar{u}}{\partial x} - \frac{1}{H} \left[\bar{u} \frac{\partial H}{\partial x} - u(H+h) \frac{\partial (H+h)}{\partial x} + u(h) \frac{\partial h}{\partial x} \right] = 0 \qquad (4.36)$$

$$A(T^*) \overline{\tau'_{yy}} \left[\overline{\tau'^2_{xx}} + \overline{\tau'^2_{yy}} + \overline{\tau'_{xx} \tau'_{yy}} + \overline{\tau'^2_{xy}} + \frac{H^2}{3} (\rho g)^2 \left[\nabla(H+h) . \nabla(H+h) \right] \right]$$

$$- \frac{\partial \bar{v}}{\partial y} - \frac{1}{H} \left[\bar{v} \frac{\partial H}{\partial y} - v(H+h) \frac{\partial (H+h)}{\partial y} + v(h) \frac{\partial h}{\partial y} \right] = 0 \qquad (4.37)$$

102

$$2\,A(T^*)\,\overline{\tau'_{xy}}\left[\overline{\tau'^2_{xx}}+\overline{\tau'^2_{yy}}+\overline{\tau'_{xx}\,\tau'_{yy}}+\overline{\tau'^2_{xy}}+\frac{H^2}{3}\,(\rho g)^2\Big[\,\nabla(H+h)\,.\,\nabla(H+h)\,\Big]\right]\;-\frac{\partial\overline{u}}{\partial y}-\frac{\partial\overline{v}}{\partial x}$$

$$(4.38)$$

$$-\frac{1}{H}\left[\overline{u}\frac{-\partial H}{\partial y}-u(H+h)\frac{\partial(H+h)}{\partial y}+u(h)\frac{\partial h}{\partial y}\right]-\frac{1}{H}\left[\overline{v}\frac{-\partial H}{\partial x}-v(H+h)\frac{\partial(H+h)}{\partial x}+v(h)\frac{\partial h}{\partial x}\right]=0$$

Since τ'_{xz}, τ'_{yz} follow from eqs. 4.10-4.11 and all strain rates and gradients can be calculated from the velocities and ice thicknesses that result on the grid, this represents a non-linear system of three equations in the three unknowns ($\overline{\tau'_{xx}}$, $\overline{\tau'_{yy}}$, $\overline{\tau'_{xy}}$) that can be solved by an iterative method (see further under § 4.7.3.3).

The main effect of treating the transition zone in this way is that the ice is apparently softened there (the depth-averaged deviatoric longitudinal stresses may be up to 3 times larger than the shear stresses), so that lower shear stresses are needed to produce the same ice mass flux. Also, this treatment fully couples ice shelf flow to the inland flow regime. This is because longitudinal stresses reflect the dynamic state of the ice shelf as well. The deformational velocity at the grounding line (and indirectly also the basal sliding velocity through changes in the ice sheet geometry) is therefore able to react to changes in ice shelf geometry. For instance, restraining forces in the ice shelf which inhibit free spreading will reduce the velocity at the grounding line, whereafter the flux divergence decreases, in turn leading to thicker ice and smaller surface slopes. Of course, the shear stresses may react to this and increase, causing a thinning, and so forth..... The important thing is that this approach is able to represent a number of potentially effective feedback mechanisms in the flow. The adopted coupling scheme seems to work well, because it allows the grounding line to move in both directions. As such, this certainly represents an improvement over previous Antarctic models.

4.5. HEAT TRANSFER

To close the set of equations specifying ice deformation, the temperature distribution needs to be known simultaneously in order to adjust the ice

stiffness parameter. This is necessary, since $A(T^*)$ changes by three orders of magnitude for the temperature range encountered in polar ice sheets (-50°C - 0°C; Paterson, 1981). In the model, ice temperature is calculated in the grounded ice sheet, but prescribed in the ice shelf. Some of the model runs, in particular the time-dependent ones, also consider heat conduction in the bedrock below.

4.5.1. Ice temperature

Taking the fixed coordinate system of fig. 4.2, the temperature distribution within the ice sheet is calculated from the general thermodynamic equation governing the transfer of heat in a continuum. It reads:

$$\frac{\partial T}{\partial t} = \frac{k_i}{\rho c_p} \nabla^2 T - \vec{V} . \nabla T + \frac{\Phi}{\rho c_p} \tag{4.39}$$

Here T is absolute ice temperature [K], t time [y], k_i thermal conductivity [$Jm^{-1}K^{-1}y^{-1}$], ρ ice density [910 kgm^{-3}], c_p specific heat capacity [$Jkg^{-1}K^{-1}$], V three-dimensional ice velocity [my^{-1}] and Φ internal frictional heating [$Jm^{-3}y^{-1}$] caused by deformation. In this equation, heat transfer is considered to result from vertical diffusion (first term), three-dimensional advection (second term) and deformational heating. Simplifications made in (4.39) include the use of constant density and the omission of melting and refreezing processes in the variable density firn layer (which is of minor importance on the scales considered). Furthermore, horizontal conduction in an ice sheet can be disregarded as temperature gradients in the horizontal directions are usually small compared to the vertical gradient, thus $\nabla^2 T$ can safely be replaced by $\partial^2 T/\partial z^2$.

The calculations also include the temperature dependence of the thermal parameters of ice. The effect is not negligible since c_p and k_i may change by up to 30% for temperatures ranging between 0°C and -50°C. The following relations were adopted:

104

$$c_p = 2115.3 + 7.79293 \, (T - 273.15) \qquad \text{(Pounder, 1965)}$$

$$k_i = 3.101 \times 10^8 \exp(-0.0057 \, T) \qquad \text{(Ritz, 1987)} \qquad (4.40)$$

The internal heating rate per unit volume can be expressed as:

$$\Phi = \sum_{ij} \dot{\epsilon}_{ij} \, \tau_{ij} \qquad (4.41)$$

Assuming that the deformational heating from longitudinal strain-rates is small compared to that from horizontal shear strain-rates (which is certainly true near the base where heating is largest), leads to:

$$\Phi = 2 \, \dot{\epsilon}_{xz} \tau_{xz} + 2 \, \dot{\epsilon}_{yz} \tau_{yz} = -\rho g (H + h - z) \frac{\partial \vec{v}}{\partial z} \cdot \nabla (H + h) \qquad (4.42)$$

according to (4.10), (4.11) and the assumptions made in (4.12), (4.13).

4.5.2. Boundary conditions

Boundary conditions are chosen as follows. At the surface, temperature is set equal to the mean annual air-temperature at that altitude and location. This is justified because over the Antarctic ice sheet screen temperatures are generally within 1°C of the firn temperature at 10 m depth, where the annual cycle fades out (Loewe, 1970). At the base, the ice sheet gains heat from both sliding friction and the geothermal heat flux. These contributions can most easily be incorporated in the basal temperature gradient:

$$\left\{ \frac{\partial T}{\partial z} \right\}_b = \gamma_g + \frac{\vec{\tau}_b \cdot \vec{v}(h)}{k_i} \qquad (4.43)$$

where γ_g [Km^{-1}] is the geothermal heat entering the ice expressed as a temperature gradient, $\vec{\tau}_b$ two-dimensional basal shear stress and $\vec{v}(h)$ basal sliding velocity. The geothermal heating can take two forms, depending on whether or not heat conduction is considered in the rock below:

$$\gamma_g = \frac{G}{k_i} \qquad\qquad \text{no bedrock heat conduction}$$

$$\gamma_g = \frac{k_r}{k_i} \left\{ \frac{\partial T}{\partial z} \right\}_r \qquad \text{with bedrock heat conduction} \qquad (4.44)$$

A value of -54.6 mW/m^2 or -1.72 x 10^6 Jm^{-2}y^{-1} is taken for the geothermal heat flux G (Sclater et al., 1980). This corresponds to 1.30 HFU (Heat Flow Units), which is a typical value for old Precambrian shields. As for the thermal conductivity of rock k_r, a value of 1.041 x 10^8 Jm^{-1}K^{-1}y^{-1} is adopted, which is a mean value for a number of rocks listed in Turcotte and Schubert (1982).

Phase changes at the base are incorporated in the model by keeping the basal temperature at the pressure melting point whenever it is reached and using the surplus energy for melting. This may eventually lead to the formation of a temperate ice layer between z = h and z = z_{melt}. The basal melt rate S [my^{-1}] can be calculated as follows:

$$S = \frac{k_i}{\rho L} \left[\left\{ \frac{\partial T}{\partial z} \right\}_c - \left\{ \frac{\partial T}{\partial z} \right\}_b \right] + \frac{1}{\rho L} \int_h^{z_{melt}} \Phi \, dz \qquad (4.45)$$

where $(\partial T/\partial z)_c$ is the basal temperature gradient after correction for pressure melting, $(\partial T/\partial z)_b$ the basal temperature gradient as given in (4.42) and L the specific latent heat of fusion [3.35 x 10^5 Jkg^{-1}]. The pressure melting point is given (e.g. Paterson, 1981, p.193) by:

$$T_{pmp} = T_0 - \beta(H + h - z) \qquad (4.46)$$

with T_0 = 273.15 K, the triple-point of water, H ice thickness and β = 8.7 x 10^{-4} Km^{-1} of ice. When the melting point is reached, the melt rate beneath the Antarctic ice sheet is typically of the order of a few mm/y, but may reach values of several cm/y in the fast flowing outlet glaciers. The present model does not make use of the melt rate, but S might be a useful quantity when a relation is added that governs melt water flow. Such a process can be

important, for instance in the development of an advanced theory for basal sliding.

In the ice shelf, the effects of basal melting and/or basal accretion and of spatially varying density and ice stiffness were ignored. Instead, a steady state linear vertical temperature distribution was assumed, with a surface temperature of -18 °C (representing present day ice shelf conditions and allowed to vary with climatic change) and a fixed basal temperature of -2 °C. The flow parameter is then taken to represent mean ice shelf temperature conditions. This implies that the thermal inertia of the ice shelves is ignored. However, the assumption of stationarity seems safe to make because the associated response time scale is small compared to the one for land ice (of the order of 10^2 years as compared to 10^3-10^4 years).

4.5.3. Rock temperature

Since the thermal conductivity of rock is of a comparable magnitude to that of ice, any time-dependent model experiment should take into account the thermal inertia of the bed. As pointed out by Ritz (1987), this effect may damp the basal temperature response by up to 50% for climatic oscillations operating on the longer time scales. In the bed, only heat transfer by vertical diffusion needs to be taken into account :

$$\frac{\partial T_r}{\partial t} = \frac{k_r}{\rho_r c_r} \frac{\partial^2 T_r}{\partial z^2} \qquad (4.47)$$

where T_r is rock temperature [K], ρ_r rock density [3300 kgm^{-3}], c_r specific heat capacity [1000 Jkg^{-1}K^{-1}] and k_r was specified above. The lower boundary condition is given by the geothermal heat flux entering through the base of the rock column. At the upper rock surface, boundary conditions follow from the basal ice temperature and by considering flux continuity at the ice-rock interface:

T_r (upper) $=$ T_i (basal) and

$$\left\{ \frac{\partial T}{\partial z} \right\}_r = \frac{k_i}{k_r} \gamma_g \qquad \text{at the upper surface}$$

$$\left\{ \frac{\partial T}{\partial z} \right\}_r = \frac{G}{k_r} \qquad \text{at the lower surface} \qquad (4.48)$$

where the indices r and i refer to rock and ice respectively. In the model, a rock slab of 2000 m thickness is considered, which appears to be sufficient to describe the essential features of the physical process.

Including the bedrock thermal inertia has the effect that the basal temperature gradient in the ice also depends on the temperature evolution in the rock. In effect, adding such a 'thermal buffer' gives rise to a negative feedback :
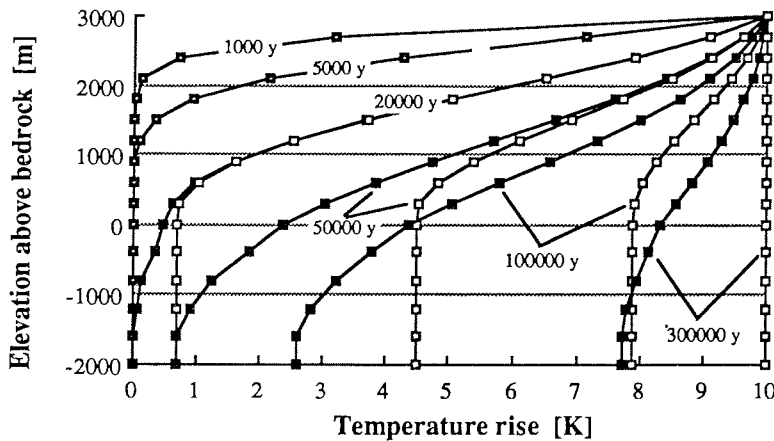

fig.4.4: Demonstration of the effect of heat conduction in the rock on the englacial temperature distribution. A sudden temperature increase of 10 K is applied at time zero at the upper ice surface. Vertical heat diffusion and advection are considered in an ice slab of 3000 m thick that overlies a rock slab of 2000 m thickness. The upper velocity boundary condition is -5 cm/y, linearly decreasing downwards. The graph shows the temperature rise throughout the complete ice-rock column after the indicated time has elapsed. The right curve of each pair (open squares) corresponds to an experiment where heat conduction in the bed is not considered.

whenever a warm wave is conducted into the bed, temperature gradients will decrease in the rock, in turn decreasing the amount of geothermal heat flowing through the ice-rock interface, thereby counteracting the original warm wave. The effect on the englacial temperature distribution is illustrated in more detail in fig. 4.4.

4.6. ISOSTATIC BED ADJUSTMENT

The Antarctic ice sheet is in some places over 4500 m thick, with a mean value of around 2000 m. A considerable pressure is therefore exerted on the underlying bedrock, which bends downwards to restore the equilibrium of forces. The model includes a time-dependent calculation of bedrock depression because the relaxation time for isostatic adjustment is of comparable magnitude to the reaction time of the ice sheet to changing environmental conditions. This is particularly important for changes in the position of the grounding line, which are the result of a subtle interplay between variations in ice thickness and water depth, so that delayed isostatic displacements may provide an additional cause for grounding-line migration.

In our approach, bed adjustments are calculated with a two-layer earth deformation model that consists of a viscous fluid asthenosphere enclosed by a uniform, thin and elastic lithospheric plate, which is in floating equilibrium with the underlying substratum of the asthenosphere. The elastic properties of the rigid lithosphere determine the deflection, which gives the ultimate shape of the bedrock depression. The *rate* of bedrock adjustment, on the other hand, is governed by the rate of outflow in the asthenosphere and thus by its viscous properties.

Appropriate values for asthenospheric thickness and viscosity are not very well known, but data from observations of glacial rebound in Scandinavia and North America provide an estimate for an asthenospheric diffusion constant (Walcott, 1973). The time-dependent response of the underlying substratum may therefore be modelled by a diffusion equation for bedrock elevation h (e.g. Oerlemans and Van der Veen, 1984, chap.7), yielding:

$$\frac{\partial h}{\partial t} = D_a \nabla^2 (h - h_0 + w')$$ (4.49)

where $D_a = 0.5 \times 10^8$ m²y⁻¹ is the asthenospheric diffusivity, h_0 the undisturbed bed topography in the absence of loading and w' the deflection, taken positive downwards. Using equation (4.49) implies that the characteristic time scale for bedrock sinking depends on the size of the load. With a typical length scale (L) of 1000 km this leads to a relaxation time for bedrock adjustment of the order $T = L^2/D_a = 20000$ years.

The rigidity or flexural stiffness of the crust causes the effect of a point load to be spread out beyond the boundary of the load itself. The lithosphere will not only bend downward under the load, but deflect upward in more remote areas, thereby creating a weak forebulge. These rheological properties of the lithosphere give rise to deviations from *local* isostatic equilibrium, that become especially marked near the ice sheet edge, where grounding line migration takes place (order of magnitude: 30 m). Thus, the rigidity of the lithosphere must be taken into account. The thin plate equation for flexural deformation may be written in its two-dimensional form as (Brotchie and Silvester,1969; Turcotte and Schubert,1982):

$$D_r \nabla^4 w' = q - \rho_m g w'$$ (4.50)

$$q = \rho_i g H \qquad \text{if} \quad -\rho_i / \rho_w H + H_{sl} \le h$$

$$q = \rho_w g (H_{sl} - h) \qquad \text{if} \quad -\rho_i / \rho_w H + H_{sl} > h$$

where D_r is lithospheric flexural rigidity and ρ_m mantle rock density [3300 kgm⁻³]. The right-hand side gives the applied load q minus the upward buoyancy force arising when the lithospere bends downwards into the asthenosphere; the left-hand side represents the bending resistance opposing lithospheric flexure. D_r is proportional to the elastic thickness of the plate raised to the third power. If the rigidity of the plate is low (implying that its thickness is small), then buoyancy forces dominate and compensation for the load is local. If D_r is large then the bending resistance term becomes dominant and the compensation is more regional in character. D_r is taken as 10^{25} Nm for the

entire Antarctic bedrock (cf. Drewry, 1983, sheet 6). This corresponds to a lithospheric thickness of 115 km.

Bending of a rigid plate is a linear process, so that the total isostatic displacement in one point on a numerical grid can be obtained by superimposition of contributions from neighbouring gridpoints. The solution for (4.50) reads (Brotchie and Silvester, 1969):

$$w'_{ij}(x) = \frac{q \; \Delta x \, \Delta y \, L_r^2}{2 \, \pi \, D_r} \; \text{kei}(x)$$

$$x = \frac{r}{L_r} \qquad L_r = \left[\frac{D_r}{\rho_m \, g} \right]^{1/4} \qquad\qquad (4.51)$$

where $w'_{ij}(x)$ is the deflection in an element ij caused by a central point load q at normalized distance x from the centre of loading, r the distance to the centre of loading [m], L_r the so-called 'radius of relative stiffness', which depends on the elastic properties of the lithosphere [= 132573 m], $\Delta x = \Delta y = 40$ km the gridpoint spacing and kei (x) are Kelvin functions of zero order. Tables of this function can be found e.g. in Abramowitz and Stegun (1970).

Dividing both sides of (4.51) by the load q means that the right hand side now contains constants that can be conveniently tabulated in a matrix as a function of distance x. The deformation coefficients obtained define a bell-shaped function and are shown graphically in fig. 4.5. They represent the contribution of each gridpoint to the total deflection. In order to calculate lateral deflections caused by a central point load, a square with sides equal to 800 km was used, comprising a 21 x 21 = 441 element matrix; all the deformation coefficients together add up to 1. Downward deflections can be seen to extend over a distance of four times the radius of relative stiffness (approx. 530 km) from the centre of loading at i = j = 11. Beyond this distance, a weak forebulge results. The actual total downward displacement in any point is then found by calculating the respective deflections for all 440 surrounding gridpoints, multiplied by the appropriate deformation coefficient. The resulting isostatic depression is then the sum of the contributions from all 441 elements.
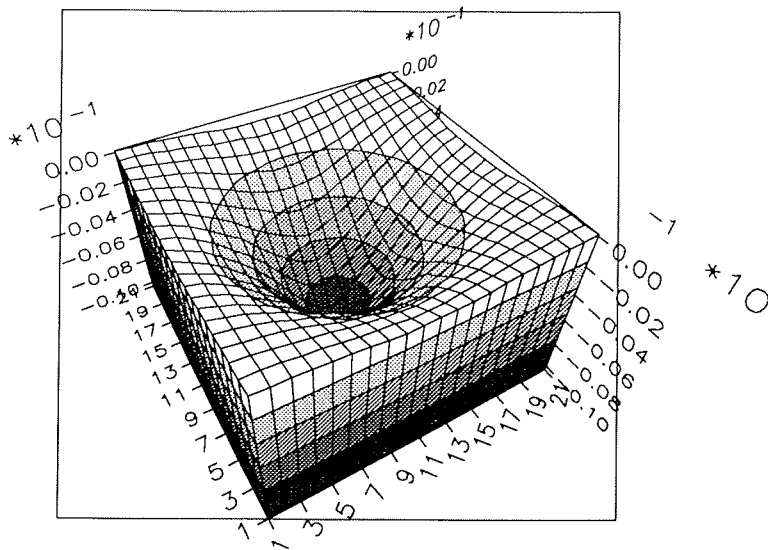
fig. 4.5: Pictorial representation of the crustal deflection caused by a central point load in (11,11). The central depression extends to a lateral distance of about 530 km. One side unit equals 40 km. In the model, deformation coefficients are multiplied by the central point load to obtain lateral isostatic displacements.

Glaciostatic depression by present ice load [m]
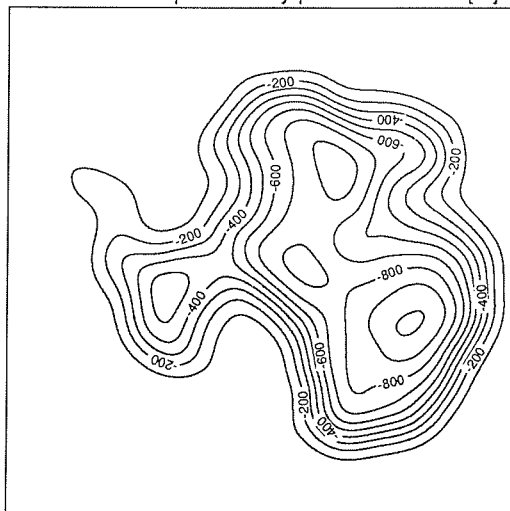
fig. 4.6: Isostatic uplift that would result from complete removal of the current ice load and subsequent isostatic rebound.

Fig. 4.6 shows the crustal downwarping caused by the present Antarctic ice load as calculated with this model. It also represents the uplift that would result if the current ice load were to be removed and full isostatic recovery were to take place. The effect turns out to be a very smooth imprint of the local ice loading distribution. Isostatic adjustments caused by changing sea level and/or ocean water merely displacing submarine ice are automatically incorporated in the calculations, because (4.50) takes into account the loading caused by both ice and water.

In a recent paper, Stern and ten Brink (1989) have criticized the model of lithospheric flexure used here, which assumes a continuous, constant rigidity plate. They propose that both East and West Antarctica are separate plates with free edges at their common boundary (the Transantarctic Mountains). This results in a somewhat different pattern of induced flexure when subjected to an ice cap load. In particular, lithospheric displacements in the Transantarctic Mountains are in their model smaller (they are up to 500 m in our approach). Stern and ten Brink agree on the D_r value for East Antarctica, but estimate the flexural rigidity for the Ross Embayment to be more than two orders of magnitudes less at 4×10^{22} Nm (corresponding to a lithospheric elastic thickness of only 19 km). Using this alternative model would make isostatic adjustments more local in West Antarctica.

In retrospect, it appears that also the diffusion approach for athenospheric viscous flow (eq. 4.49) may not be the most appropriate way to model the transient upper mantle response (G. Deblonde, personal communication). In particular, the implied response time scale may be too long and the resulting transient forebulge may not be entirely realistic. This is inferred from comparison of modelled postglacial rebound with observed relative sea-level data (e.g. Peltier, 1985, 1988). It is not clear whether these improvements would influence the fundamental outcome of the ice sheet model, however.

4.7. NUMERICAL METHODS

Solving the various model equations using a computer requires discretization onto a numerical grid. This means that continuous derivatives have to be approximated by finite functions, which can then be solved by algebraic

methods. The main procedures adopted are outlined below. Lengthy derivations are however avoided, and where possible, reference is made to the relevant papers.

4.7.1. Numerical grid

The model calculations are performed on a square grid that is laid out over a polar stereographic projection with standard parallel at 71°S. The grid is centred at the pole and comprises a 141 x 141 gridpoint matrix. Small distortions in distance arising from the sphericity of the earth have been ignored. The following transformation formulas are used to transfer data from stereographic maps and other sources (point measurements for instance) onto the grid (Snyder, 1982):

$$x = 2R_e k_0 \tan\left[\frac{\pi}{4} + \frac{\phi}{2}\right] \sin\lambda$$

$$y = 2R_e k_0 \tan\left[\frac{\pi}{4} + \frac{\phi}{2}\right] \cos\lambda \qquad (4.52)$$

$$\phi = \arcsin\left[-\cos c\right]$$

$$\lambda = \arctan\left[\frac{x}{y}\right]$$

$$c = 2\arctan\left[\frac{\sqrt{x^2 + y^2}}{2R_e k_0}\right] \qquad (4.53)$$

$$i = \frac{x}{\Delta x} + 71 \qquad\qquad j = \frac{y}{\Delta y} + 71 \qquad (4.54)$$

where R_e [6371.221 km] is the radius of a sphere which has the same volume as the International Ellipsoid, k_0 [0.9728] a scale factor and $\Delta x = \Delta y$ are the horizontal mesh sizes. i,j are the coordinates of the numerical grid. Latitude ϕ is taken negative in the southern hemisphere and longitude λ increases clockwise. Fig. 4.7 shows the grid boundaries and values for the various coordinate systems involved.
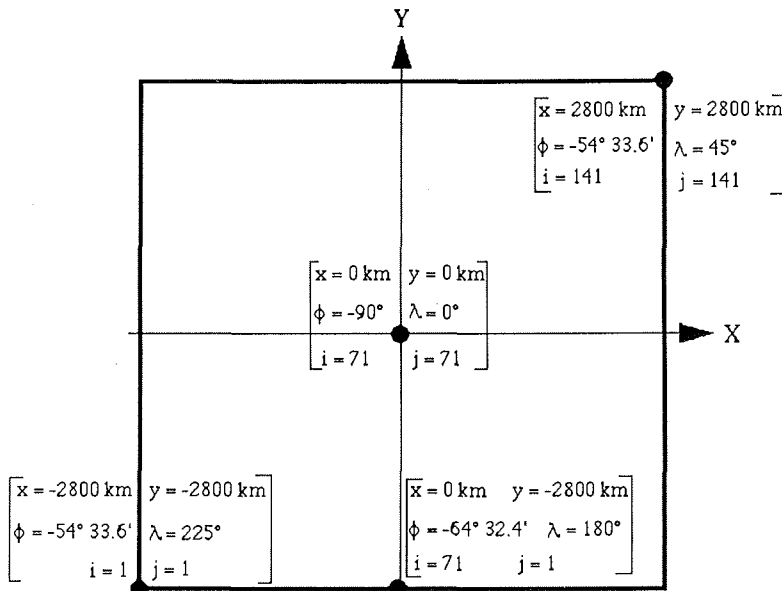
fig.4.7: Model domain and coordinates of its boundaries

Ideally, the horizontal grid point distance should be of the order of ten ice thicknesses, because local irregularities tend to smooth out over this distance and the model assumptions break down for smaller grid sizes. This resolution is especially needed at the margin, where the ice is chanelled in outlet glaciers and/or ice streams with a lateral spatial scale often less than 50 km. However, such a mesh would contrast strongly with typical scales of variation in the interior of the ice sheet and also with the density of measurements in these remote areas. One solution could be a multigrid approach, where a finer mesh is used wherever necessary, but this was not attempted because of the anticipated difficulties in coding. Ultimately the resolution largely depends on the available machine. Memory requirements are not the problem here, but CPU time: halving the grid size will in general lead to an increase of the calculation time by a factor of 16, because 4 times more gridpoints need to be evaluated and the maximum time step for numerical stability reduces to one fourth! In the model, a horizontal resolution of 40 km was taken, regarded as a fair compromise between the physical problem and the potential of the CRAY-2 computer. This grid is shown in fig. 4.8.
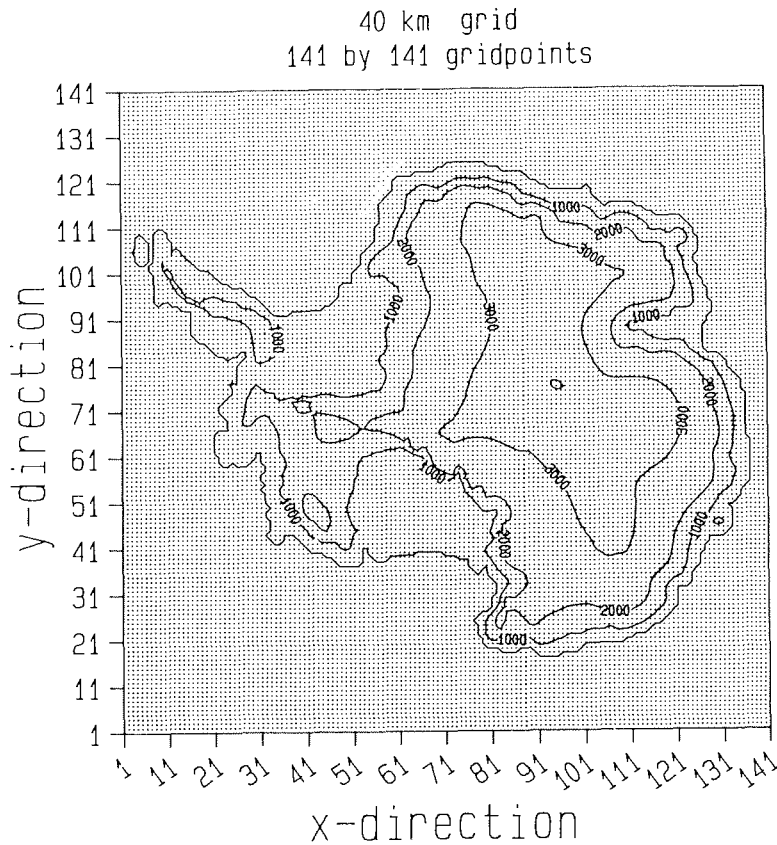
fig.4.8: Numerical grid on which the calculations are performed. The model domain is covered by 141 x 141 = 19881 gridpoints. Every point in turn represents a vertical, which is subdivided into 10 layers. Contour lines are surface elevation; the lowest contour represents the ice shelf edge.

Integrating the thermodynamic equation on a fixed vertical grid is rather inconvenient, as the upper and lower ice boundaries will generally not coincide with grid-points. Instead of decreasing the grid-size (implying larger computing times) or devising some or other interpolation scheme, these problems are readily overcome by introducing a new vertical coordinate ζ, scaled to local ice thickness. This approach was originally proposed by Jenssen (1977) in analogy to the σ-coordinate system of numerical weather forecasting. The stretched dimensionless vertical coordinate is defined by:

$$\zeta = \frac{H + h - z}{H} \qquad (4.55)$$

such that $\zeta = 0$ at the upper surface and $\zeta = 1$ at the base of the ice sheet for all values of x,y and t. The derivative of a variable f in the (x,y,z,t)-system (subscript z denotes a derivative in the x,y,z-system; ζ stands for the new x,y,ζ-system) is then transformed (e.g. Haltiner, 1971, p.194) as:

$$\frac{\partial f}{\partial r}\bigg|_z = \frac{\partial f}{\partial r}\bigg|_\zeta + \frac{\partial f}{\partial \zeta}\frac{\partial \zeta}{\partial r} \qquad r = x,y,t \qquad (4.56)$$

$$\frac{\partial f}{\partial z}\bigg|_z = \frac{\partial \zeta}{\partial z}\frac{\partial f}{\partial \zeta} \qquad (4.57)$$

leading to:

$$\frac{\partial f}{\partial r}\bigg|_z = \frac{\partial f}{\partial r}\bigg|_\zeta + \frac{1}{H}\frac{\partial f}{\partial \zeta}\left[\frac{\partial(H+h)}{\partial r} - \zeta\frac{\partial H}{\partial r}\right] \qquad r = x,y,t \qquad (4.58)$$

$$\frac{\partial f}{\partial z} = \frac{1}{H}\frac{\partial f}{\partial \zeta} \qquad (4.59)$$

$$\frac{\partial^2 f}{\partial z^2} = \frac{1}{H^2}\frac{\partial^2 f}{\partial \zeta^2} \qquad (4.60)$$

and for the integral transformation:

$$\int_h^z f(z)\,dz = -H\int_1^\zeta f(\zeta)\,d\zeta \qquad (4.61)$$

The resulting equations in this non-orthogonal system will not be shown here, but more details on the relevant transformations can be found in Huybrechts (1986) and Huybrechts and Oerlemans (1988). In this approach, velocity and temperature fields are computed at levels of constant ζ (the layer interfaces). The model's vertical domain was subdivided into ten layers concentrated

117
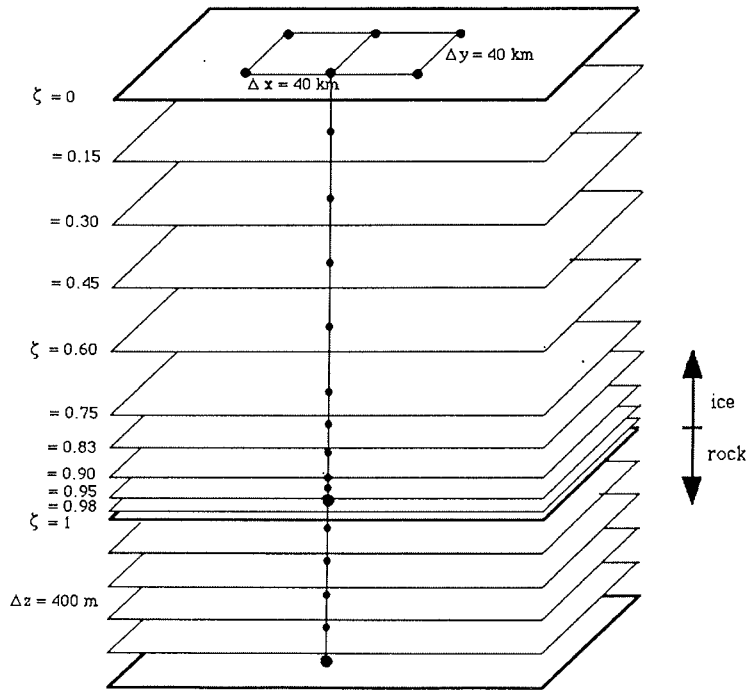
fig.4.9: Representation of the vertical grid

towards the base (where the variation in velocity is largest), with an uppermost layer thickness of $\Delta\zeta=0.15$ and a lowermost grid spacing of $\Delta\zeta=0.02$. This proved to be sufficient to capture the essential characteristics of the model variables. In the bedrock only 5 layers were considered, which are equally spaced at 400 m. This geometry is illustrated in figure 4.9.

4.7.2. Solution of the continuity equation: ADI scheme

The continuity equation can be rewritten as:

$$\frac{\partial H}{\partial t} = -\nabla . \vec{F} + M \tag{4.62}$$

where $\vec{F} = \vec{v}H$ is the horizontal ice mass flux. It depends on ice thickness to the fifth power and surface gradient to the third power because of the non-linearity of the flow law.

Although there is at present in glaciology a surge of interest in finite element modelling techniques as well (e.g. Hooke et al., 1979; Nixon et al., 1985; Hodge, 1985; MacAyeal and Thomas, 1986; Fastook and Chapman, 1989), we opt for a finite difference approach. This is mainly because the finite-element method does not seem to be suited for the type of studies envisaged here. Apart from being far more complicated in coding the finite element method appears to be unable to deal with changing boundaries (Hutter, 1983; Lliboutry, 1987), because the elements have to be redefined every time the model domain changes its dimensions. Also, it does not seem to be as efficient in terms of computer time, especially when one wants to integrate a 3-D model for Antarctica, say, 100000 years forward in time.

Having replaced the derivatives by finite-differences, the resulting equations are usually quite readily solved using an explicit integration scheme. However, such a scheme has the important drawback that in order to preserve stability, time steps necessarily have to be small. On the other hand, a fully implicit scheme would be highly unpractical as it requires the solution of a set of nonlinear equations in two space dimensions at the advanced time level. Alternatively, the Alternating-Direction-Implicit (ADI) method can be used. This is a two-step method involving the solution of sets of equations along lines parallel to the x- and y-axes at the first and second step respectively. It is not unconditionally stable, because of the nonlinearity of the flow law and coupling through the source terms. However, this scheme allows time steps to be chosen which are an order of magnitude larger than an explicit approach, and this without a noticeable loss of accuracy (steady state solutions corresponding up to 5 figures). With the present resolution of 40 km, the maximum stable time step is 40 years. The resulting tridiagonal systems are easily solved by some form of Gaussian elimination.

The ADI-scheme is constructed with the Peaceman-Rachford formula (Mitchell and Griffiths, 1980, p.60), employing a staggered grid in space, so that mean mass fluxes are calculated in between grid points. Smoothing in this way keeps the integration stable. Considering a rectangular domain in x,y space,

where i,j denotes the index numbers of a grid point with Nx, Ny the total number along the respective axes, this scheme reads:

$$H_{i,j,t+1/2} + \frac{\Delta t}{2\Delta x} \cdot \left[F_{i+1/2,j,t+1/2} - F_{i-1/2,j,t+1/2}\right] =$$

$$H_{i,j,t} - \frac{\Delta t}{2\Delta y} \cdot \left[F_{i,j+1/2,t} - F_{i,j-1/2,t}\right] + \frac{\Delta t}{2} \cdot \left[M_{i,j,t}\right]$$

$$i = 2, Nx - 1 \quad \text{for} \quad j = 2, Ny - 1 \quad\quad (4.63)$$

fig.4.10: Grid used to perform the first x-ADI step along rows of constant j. Thick lines refer to the implicit direction

with similar sets of equations along rows of constant i for the second step:

$$H_{i,j,t+1} + \frac{\Delta t}{2\Delta y} \cdot \left[F_{i,j+1/2,t+1} - F_{i,j-1/2,t+1}\right] =$$

$$H_{i,j,t+1/2} - \frac{\Delta t}{2\Delta x} \cdot \left[F_{i+1/2,j,t+1/2} - F_{i-1/2,j,t+1/2}\right] + \frac{\Delta t}{2} \cdot \left[M_{i,j,t+1/2}\right]$$

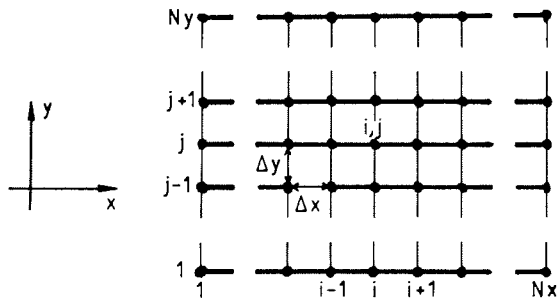$$j = 2, Ny - 1 \quad \text{for} \quad i = 2, Nx - 1 \quad\quad (4.64)$$
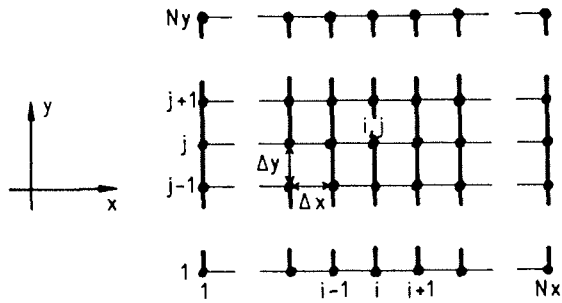
fig.4.11: Grid used to perform the second y-ADI step along rows of constant i. Thick lines refer to the implicit direction

where mass fluxes F (that are a function of ice thickness H) are evaluated formally as shown in fig. 4.12.

Formally rearranging the terms in (4.63) then leads to a tridiagonal set of equations for row j of the type:

$$-\alpha_{i,j,t} H_{i-1,j,t+1/2} + \beta_{i,j,t} H_{i,j,t+1/2} - \gamma_{i,j,t} H_{i+1,j,t+1/2} = \delta_{i,j,t} \qquad i = 2, Nx-1 \qquad (4.65)$$

fig.4.12: Representation of the staggered grid used to calculate mass fluxes in between grid points

121

where the boundary conditions at the ice shelf edge $H_{1,j}$; $H_{Nx,j}$ are zero ice thickness gradient.

With the additional conditions (that are fulfilled) that:

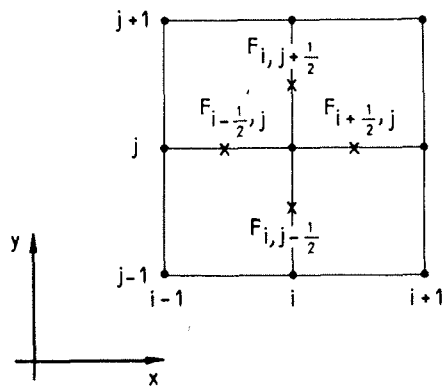$$\alpha_{i,j,t} \; , \; \beta_{i,j,t} \; , \; \gamma_{i,j,t} \; > \; 0 \quad \text{and} \quad \beta_{i,j,t} \; \geq \; \alpha_{i,j,t} \; + \; \gamma_{i,j,t} \qquad (4.66)$$

a highly efficient method is available for solving the tridiagonal system (Mitchell and Griffiths, 1980, p.32):

$$w_{2,j,t} = \frac{\gamma_{2,j,t}}{\beta_{2,j,t}} \qquad\qquad g_{2,j,t} = \frac{\delta_{2,j,t} + \alpha_{2,j,t} H_{1,j}}{\beta_{2,j,t}}$$

$$w_{i,j,t} = \frac{\gamma_{i,j,t}}{\beta_{i,j,t} - \alpha_{i,j,t} w_{i-1,j,t}} \qquad\qquad g_{i,j,t} = \frac{\delta_{i,j,t} + \alpha_{i,j,t} g_{i-1,j,t}}{\beta_{i,j,t} - \alpha_{i,j,t} w_{i-1,j,t}}$$

$$i = 3 \, , \, Nx - 1 \qquad\qquad (4.67)$$

The new ice-thicknesses at the intermediate time step are then found from backsubstitution:

$$H_{Nx-1,j,t+1/2} \; = \; w_{Nx-1,j,t} H_{Nx,j} \; + \; g_{Nx-1,j,t}$$

$$H_{i,j,t+1/2} \qquad = \; w_{i,j,t} H_{i+1,j,t+1/2} \; + \; g_{i,j,t} \qquad\qquad i = Nx-2, \, 2 \qquad (4.68)$$

and condition $H_{i,j,t+1/2} \; \geq \; 0$

This procedure involving the solution of Ny - 2 tridiagonal sets of Nx equations with Nx - 2 unknowns along rows of constant j is then repeated along rows of constant i to complete the integration forward in time. Temperature and bedrock elevation are updated every half time step. All the ADI-coefficients are time dependent and thus need continuous re-evaluation.

4.7.3. Determination of the ice mass fluxes

4.7.3.1. ice sheet

The calculation of the mass fluxes in the grounded ice sheet is made easier by rewriting the continuity equation as a diffusion equation for ice thickness H. The flux divergence term $-\nabla.\vec{F} = -\nabla.(\vec{v}H)$ in (4.62) then becomes $-\nabla.D\nabla(H+h)$. Here, D is a nonlinear diffusion coefficient depending strongly on ice thickness and surface slope, given by the scalar component of (4.19), i.e.:

$$D = -2(\rho g)^3 \left[\nabla(H+h) . \nabla(H+h) \right] \int_h^{H+h} \int_h^z A(T^*) (H+h-z)^3 \, dz \, dz' + \frac{\vec{v}(h) H}{\nabla(H+h)} \qquad (4.69)$$

where in the layer approach the "vertically integrated" diffusion coefficient D now contains a deformational part evaluated at layers of constant ζ (D^l) and a contribution from basal sliding (D^s):

$$D = H \int_0^1 D^l(\zeta) \, d\zeta + D^s \qquad (4.70)$$

As defined here D is a negative quantity.

The mass fluxes, to be substituted in (4.63), are now obtained by considering a mean diffusivity, that is however evaluated at the old time step. This is necessary in order to avoid the complication of having to solve a set of nonlinear equations at the advanced time step. This leads to:

$$F_{i+1/2,j,t+1/2} = \left[\frac{H_{i+1,j,t+1/2} + h_{i+1,j,t} - H_{i,j,t+1/2} - h_{i,j,t}}{\Delta x} \right] . \left[\frac{D_{i,j,t} + D_{i+1,j,t}}{2} \right] \qquad (4.71)$$

and analogues for $F_{i-1/2,j,t+1/2}$; $F_{i,j+1/2,t}$; $F_{i,j-1/2,t}$; and in (4.64):

$$F_{i,j+1/2,t+1} = \left[\frac{H_{i,j+1,t+1} + h_{i,j+1,t+1/2} - H_{i,j,t+1} - h_{i,j,t+1/2}}{\Delta y} \right]$$

$$\cdot \left[\frac{D_{i,j,t+1/2} + D_{i,j+1,t+1/2}}{2} \right] \tag{4.72}$$

and analogues. The mean diffusivity defined in between grid points is needed to keep the integration stable. The time dependent elements of δ and the coefficient matrix α,β,γ for the respective ADI steps are then constructed after some algebraic manipulations (Huybrechts, 1986). Finally, once the diffusivities D^l in (4.70) have been evaluated, it becomes an easy matter to determine the three-dimensional velocity components on the layer nodes, that are needed in the thermodynamic calculations.

4.7.3.2. ice shelf: point relaxation scheme

The coupled system of equations 4.28 (a,b) which describe the velocity distribution in the ice shelf are most easily solved by point relaxation (e.g. Smith, 1969). To do this, finite differences are introduced and the equations rewritten formally as:

$$a_{i,j} u_{i,j} + c_{i,j} = 0$$

$$b_{i,j} v_{i,j} + c'_{i,j} = 0 \tag{4.73}$$

where $u_{i,j}$, $v_{i,j}$ are the x and y velocity components in an ice shelf gridpoint i,j and $a_{i,j}$, $b_{i,j}$, $c_{i,j}$ and $c'_{i,j}$ are functions of the other variables:

$$u^2_{i,j} = u^1_{i,j} - \frac{1}{a_{i,j}} R^{u1}_{i,j}$$

$$v^2_{i,j} = v^1_{i,j} - \frac{1}{b_{i,j}} R^{v1}_{i,j} \tag{4.76}$$

will then tend to make residuals during the next step $R^{u2}_{i,j}$, $R^{v2}_{i,j}$ locally zero. An iterative method is necessary because the new solution $u^2_{i,j}$, $v^2_{i,j}$ will also change functional values in the eight surrounding grid points needed to calculate all the derivatives. It is applied until the maximum error on the grid is below a certain level, in this case 1m/y. In general, convergence is rather slow (initially requiring up to a few thousand iterations, starting from $u_{i,j} = v_{i,j} = 0$), but once an equilibrium solution was obtained, only a few iterations proved to be necessary.

The mass fluxes are then defined as:

$$F_{i+1/2,j,t+1/2} = \left[\frac{H_{i+1,j,t+1/2} + H_{i,j,t+1/2}}{2} \right] \cdot \left[\frac{u_{i+1,j,t} + u_{i,j,t}}{2} \right] \tag{4.77}$$

and analogues, from which coefficients for the solution of the tridiagonal systems can be readily obtained.

Small-amplitude grid-point to grid-point oscillations appearing in the simulated ice shelf thicknesses during the integration were eliminated by applying a spatial smoothing operator. This smoothing was accomplished by setting the value of H at each interior ice shelf grid point equal to the average of the ice thickness in a 9 grid-point square, where the eight surrounding grid points had a weight of 5% of that of the central grid point.

4.7.3.3. grounding zone

The equations for the stress components at the grounding line (4.36)- (4.38) represent a non-linear system of three equations in the three unknowns ($\overline{\tau'_{xx}}$, $\overline{\tau'_{yy}}$, $\overline{\tau'_{xy}}$), that may be represented formally by $f_i(x=\overline{\tau'_{xx}}, y=\overline{\tau'_{yy}}, z=\overline{\tau'_{xy}})$:

$$a_{i,j} = -\frac{4\,f_{i,j}}{\Delta x^2} - \frac{f_{i,j}}{\Delta y^2}$$

$$c_{i,j} = \frac{2\,f_{i,j}}{\Delta x^2}\cdot\left[u_{i+1,j} + u_{i-1,j}\right] + \frac{f_{i,j}}{2\Delta y^2}\cdot\left[u_{i,j+1} + u_{i,j-1}\right] +$$

$$\frac{3\,f_{i,j}}{8\Delta x\Delta y}\cdot\left[v_{i+1,j+1} + v_{i-1,j-1} - v_{i+1,j-1} - v_{i-1,j+1}\right] - \frac{\rho g A(T^*)^{\frac{1}{3}}}{2\Delta x}\cdot\left[1-\frac{\rho}{\rho_w}\right]\cdot\left[H_{i+1,j} - H_{i-1,j}\right]$$

$$\text{with } f_{i,j} = \left[\left[\frac{u_{i+1,j}-u_{i-1,j}}{2\Delta x}\right]^2 + \left[\frac{v_{i,j+1}-v_{i,j-1}}{2\Delta y}\right]^2 + \left[\frac{u_{i+1,j}-u_{i-1,j}}{2\Delta x}\right]\cdot\left[\frac{v_{i,j+1}-v_{i,j-1}}{2\Delta y}\right] + \frac{1}{4}\left[\frac{u_{i+1,j}-u_{i-1,j}}{2\Delta x} + \frac{v_{i,j+1}-v_{i,j-1}}{2\Delta y}\right]^2\right]^{\frac{-1}{3}} \quad (4.74)$$

and analogues for $b_{i,j}$ and $c'_{i,j}$. The horizontal gradients $\partial f/\partial x$ and $\partial f/\partial y$ in 4.28 are neglected. This is equivalent to the assumption that lateral variations of the effective strain rate are small compared to variations of the individual strain rates. This does not significantly influence the result and saves on the calculations (J. Determann, personal communication). The validity of this assumption is also confirmed by spreading data of Antarctic ice shelves interpreted by Doake and Wolff (1985).

The numerical solution then proceeds by introducing a guessed solution $u^1_{i,j}$, $v^1_{i,j}$ and determining local residuals $R^{u1}_{i,j}$, $R^{v1}_{i,j}$, given by:

$$R^{u1}_{i,j} = a_{i,j}\,u^1_{i,j} + c_{i,j}$$

$$R^{v1}_{i,j} = b_{i,j}\,v^1_{i,j} + c'_{i,j} \quad (4.75)$$

Updating the guessed solution by:

$$f_i(x,y,z) = 0 \qquad\qquad i = 1,2,3 \qquad\qquad (4.78)$$

Let $(x_{n+1}, y_{n+1}, z_{n+1}) = (x_n+\Delta x, y_n+\Delta y, z_n+\Delta z)$ be the exact solution so that f_i $(x_{n+1}, y_{n+1}, z_{n+1}) \equiv 0$, then this solution may be obtained iteratively by expanding each relation in a Taylor series and subsequently solving a linear system in the increments Δx, Δy, Δz:

$$\Delta x\frac{\partial f_i}{\partial x}(x_n,y_n,z_n) + \Delta y\frac{\partial f_i}{\partial y}(x_n,y_n,z_n) + \Delta z\frac{\partial f_i}{\partial z}(x_n,y_n,z_n) = - f_i(x_n, y_n, z_n)$$

$$i = 1,2,3 \qquad\qquad (4.79)$$

This is equivalent to a Newton-Raphson iteration. Only a few iterations are needed to obtain an acceptable solution. Mass fluxes are in this case constructed by checking whether the neighbouring gridpoint is grounded or floating and adopting the appropriate relations as presented before.

4.7.4. Thermodynamic equation

The critical time step for stability is set by the smallest grid spacing, which is along ζ. It seems therefore sensible to make the terms involving ζ-derivatives implicit, leading once more to a set of tridiagonal equations that have to be solved at every gridpoint. Even with time steps up to 500-1000 years, the calculations then appear to be fully stable. However, replacing the horizontal advective derivatives by central differences generated oscillations in the solution. This problem is usually circumvented in diffusion-convection equations with a high Peclet number (a constant proportional to the ratio of advective velocity and diffusivity) by introducing an artificial horizontal diffusion process.(e.g. Mitchell and Griffiths, 1980, p.224 ; Gladwell and Wait, 1979, chap. 11). We use an 'upwind' differencing scheme. Although this scheme introduces an artificial horizontal diffusivity equal to $v.\Delta r/2$, where v is the velocity and Δr the grid spacing, such an approach keeps the solution stable and influences results only marginally. In most cases the associated artificial heat transfer was an order of magnitude smaller than the horizontal heat advection. Temperature features organized on the limited scale of the model resolution (40 km) are however lost after several time steps.

127

The resulting tridiagonal set of $N\zeta$ equations in $N\zeta$ - 2 unknowns is most easily solved by Gaussian elimination. It formally reads:

$$- \alpha_{i,j,k,t} \, T_{i,j,k-1,t+1} + \beta_{i,j,k,t} \, T_{i,j,k,t+1} - \gamma_{i,j,k,t} \, T_{i,j,k+1,t+1} = \delta_{i,j,k,t}$$

$$k = 2 \, , \, N\zeta - 1 \tag{4.80}$$

For a definition of the ADI-coefficients in this case, the interested reader is once more referred to Huybrechts (1986). Finally, a similar procedure is adopted for the heat conduction equation in the rock.

4.7.5. Bedrock adjustment equation

For reasons of efficiency, accuracy and stability, an ADI scheme was chosen to compute the 2-D bedrock response as well. Since (4.49) is a linear parabolic differential equation, the corresponding equations are straightforward and will not be given here. In this case, the ADI-coefficients α, β, γ are independent of time and only need evaluation once. At the grid edge, boundary conditions follow from isostatic equilibrium.

4.8. DATA SETS AND MODEL FORCING

Model inputs are bed topography, surface temperature, mass balance, thermal parameters and an initial state (that may be a thin slab of ice of equal thickness). The external forcing is by both prescribing eustatic sea level stand and imposing a uniform background temperature change. The latter drives changes both in the accumulation and surface temperature distributions. The model then outputs the time-dependent three-dimensional ice sheet geometry and the fully coupled velocity and temperature fields, as well as a number of derived physical characteristics.

4.8.1. Geometric model input

Bedrock elevation, surface elevation and ice thickness data for the present ice sheet originate from a 20 km-digitization by the Australian group (Budd et al,

1984) of the Drewry (1983) map folio series. They have been interpolated onto the 40 km grid by selecting every second value in the original data set as a new, central grid point. The information of the 8 surrounding grid points in the 20 km data set was then incorporated in the 40 km grid with the following weights:

$$
\begin{bmatrix}
1/16 & 2/16 & 1/16 \\
2/16 & 4/16 & 2/16 \\
1/16 & 2/16 & 1/16
\end{bmatrix}
\tag{4.81}
$$

The data have been locally complemented beneath ice shelf areas with data from bathymetric charts (GEBCO, Canadian Hydrographic Service) and more recent sources (Herrod, 1986). Furthermore, it was necessary to re-digitize the surface elevation data at the grounding line and in the ice shelves in order to satisfy the adopted flotation criterion with constant ice density. Contoured representations of the resulting initial bed topography and ice thickness are shown in figs. 4.13-4.14. Undisturbed bedrock heights, needed in the bed adjustment calculations, have been reconstructed assuming present isostatic equilibrium. This may introduce an error, because uplift following the last glacial-interglacial transition some 15000 years ago is probably still in progress (Greishar and Bentley, 1980), but a sound alternative is not readily available.

4.8.2. Climatic model input

Climatic input is provided by the ice temperature at 10 meter depth and the mean-annual snow deposition rate. Both boundary conditions are reasonably well documented for the present climate (cf. § 2.2.1. and § 2.2.3), but since the purpose of the model is to investigate the ice sheet with respect to environmental change, it is also necessary to specify these external variables for other climates and ice sheet geometries. A general formulation would be desirable, in which these boundary conditions depend on relevant geometrical and physical parameters in an explicit way. Parameterizations in terms of such variables as elevation, surface slope, moisture content, and distance to ocean (continentality), have been made by Oerlemans (1982a,

Bed elevation [m]

ABOVE   1500
1000 -   1500
 500 -   1000
   0 -   500
-500 -   0
-1000 - -500
-1500 - -1000
BELOW   -1500
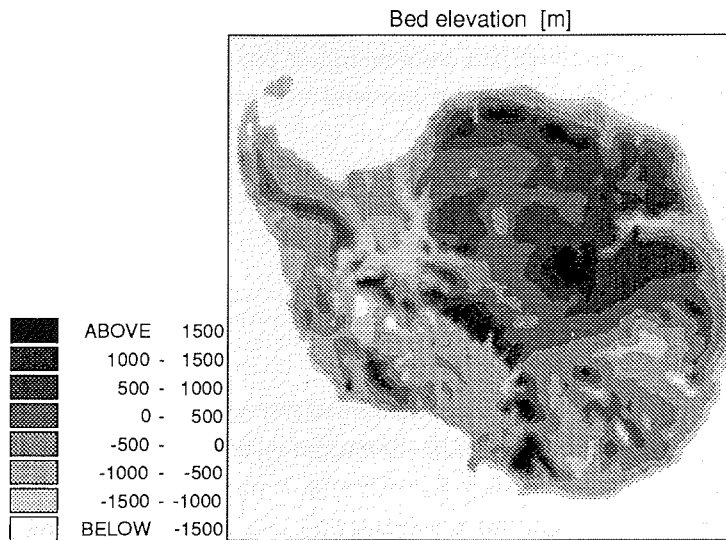
fig. 4.13: Present bedrock topography as digitized on the 40 km grid. Note the high resolution and the associated detail, in particular in the coastal mountain ranges. The subshelf topography in the Ronne-Filchner and Ross areas has been re-digitized using more recent data and deviates locally from the original SPRI maps.

Ice thickness [m]

ABOVE   3900
3000 -   3900
2100 -   3000
1200 -   2100
 300 -   1200
BELOW   300
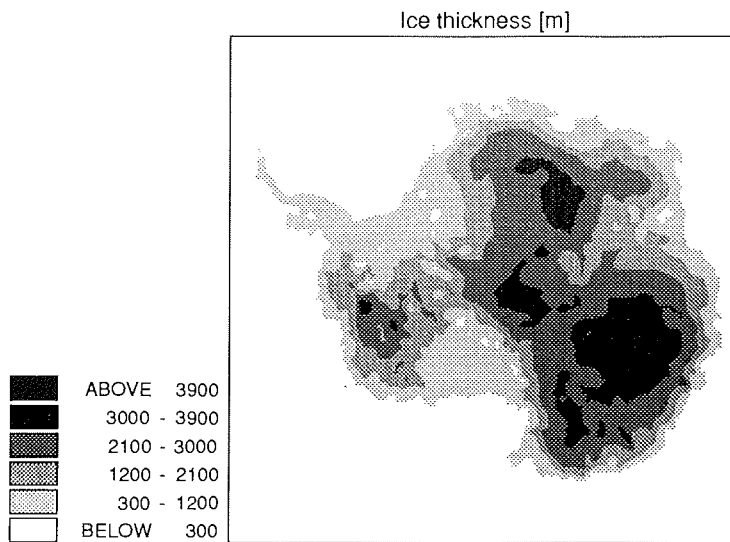
fig. 4.14: Present ice thickness distribution, used as initial condition in the calculations.

130

THE ICE SHEET MODEL

fig.4.15: Upper boundary condition for the temperature calculations. Values are in °C.

fig. 4.16: Accumulation rate data [in m/y ice equivalent] corresponding to the present topography. The above fields are perturbed in the experiments to include the effects of both different climates and ice sheet geometries. Data outside the stippled area are not shown, because they do not influence the model outcome.

1982b), Muszynski and Birchfield (1985) and Fortuin and Oerlemans (1990). However, it appears that in particular the distribution of accumulation is hard to parameterize. F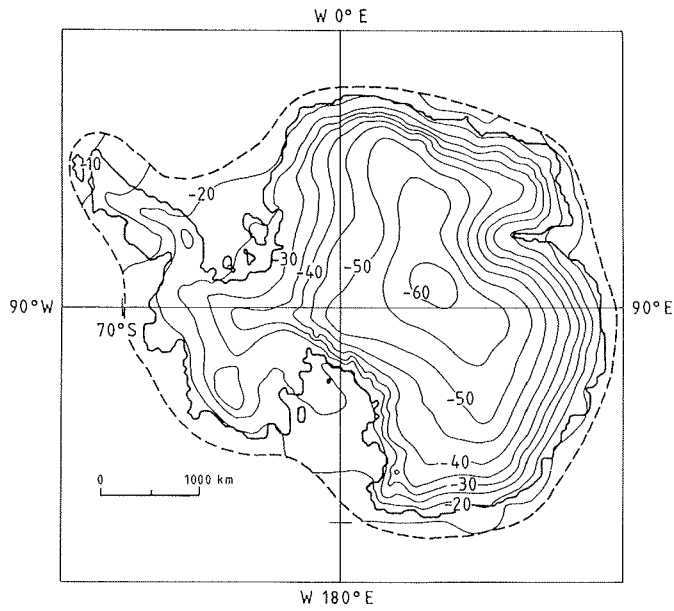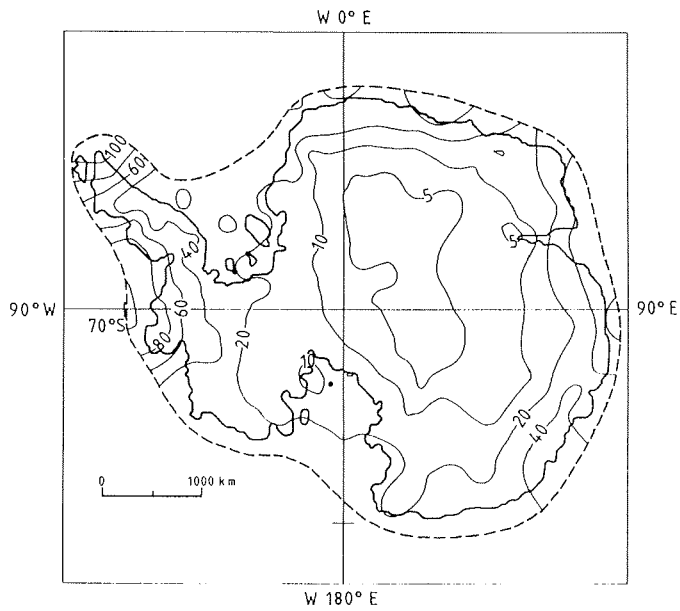or instance, with a multiple regression model applied to all available Antarctic accumulation data, Fortuin and Oerlemans (1990) could at best explain 39% of their variance. The corresponding value for the interior area (above 1500 m) was higher (71%), but other areas had a value as low as 17 %. This is caused by local meteorological conditions related to such factors as general air circulation and cyclonic activity, which are difficult to model. A better approach is to use the presently observed values and to perturb the resulting field by a prescribed change in a meteorological variable like temperature. In other words, a parameterization of *perturbations* rather than absolute values is probably the best one can do.

The basic climatic data sets needed for the 10m-ice temperature and surface accumulation rate were also constructed from data compiled at the Scott Polar Research Institute, Cambridge. Gridded values on the regular 40 km grid were obtained by a computer interpolation from the original point measurements (each data set contained approximately a thousand points). A quadratic interpolation technique was used, where data points were selected and weighted according to their distance relative to the central gridpoint in a circle of radius = 500 km. These data sets are presented in figs. 4.15-4.16. They differ slightly from the maps presented earlier in § 2.1. Apart from the fact that accumulation rates are expressed in different units (water equivalent versus ice depth), this merely reflects the degree of uncertainty in those areas where few measurements are available.

In the model, the gridded temperature data are perturbed in response to changes in background temperature (assumed uniform and synchronous over the ice sheet) and local changes in surface elevation. The latter was done using an atmospheric lapse rate of 5.1 °C/1000m below the 1500 m contour and 14.3 °C/1000m above the inland plateau (i.e. above 1500 m). These are the values suggested by the multiple regression study of Fortuin and Oerlemans (1990).

Changes in surface temperature also serve to calculate accumulation rates in different climates. As first noticed by Robin (1977), the precipitation rate over Antarctica appears to be strongly governed by the water vapour saturation

pressure above the surface inversion layer, with a relation similar to the Clausius-Clapeyron equation. Its physical significance is that it sets an upper limit to the amount of vapour available for precipitation. Based on the assumption that the observed spatial correlation between the precipitation rate and saturation vapour pressure can be applied to climatic change, this argument was employed to help dating the Vostok ice core (Lorius et al. 1985), and is also used here to perturb the basic accumulation distribution. This method of estimating past precipitation seems to be consistent with accumulation rates deduced from cosmogenic [10]Be (Yiou et al, 1985). Furthermore, after a careful reexamination of the Byrd, Dome C and Vostok ice core chronologies, Jouzel et al. (1989) concluded that the vapour pressure argument can probably be extended over most of the ice sheet.

It is assumed that the temperature of formation of precipitation T_f is close to the temperature prevailing at the top of the inversion layer. The following linear relation (r=0.99) between T_s (the surface temperature) and T_f is suggested by Jouzel and Merlivat (1984):

$$T_f [K] = 0.67 \, T_s [K] + 88.9 \tag{4.82}$$

If the accumulation rate is governed by the amount of water vapour in the air, it should be proportional to $\partial P / \partial T$, where P is the water-vapour pressure at the condensation temperature T. The accumulation rate for any perturbed climatic state is therefore obtained from the product of its reference (present) value, times the ratio of the derivatives of the saturation water vapour pressure over a plane surface of ice for the reference and perturbed states (Lorius et al., 1985). This gives:

$$\dot{M}[T_f(t)] = \dot{M}[T_f(present)] \cdot \exp\left\{ 22.47\left[\frac{T_0}{T_f(present)} - \frac{T_0}{T_f(t)} \right] \right\} \cdot \left\{ \frac{T_f(present)}{T_f(t)} \right\}^2$$

$$\tag{4.83}$$

$T_0 = 273.16$ K is the triple point of water. For surface temperatures prevailing over Antarctica, resulting accumulation rates are typically 50- 60 % of their Holocene values for a 10°C temperature decrease.

This approach implies that the precipitation pattern does not follow changes in either ice sheet geometry or different patterns of air circulation and their associated storm tracks. This may be questionnable, in particular at the ice sheet margin, however Fortuin and Oerlemans (1990) did not find significant correlations with such factors as distance to open water and surface slope (related to orographic effects). Moreover, as mentioned before, there are strong indications that, insofar *changes* are considered, the temperature of the inversion layer is the really relevant variable, also in past climates. This is attributed to relatively simple meteorological conditions over the Antarctic ice sheet (Jouzel et al., 1989).

Model runs involving the glacial cycle (chapters 5-7) do not consider ice ablation. Such a process may become important in warmer climates, however. The corresponding treatment of melting and runoff is described later in the relevant greenhouse warming chapter (§ 8.3.2).

4.8.3. Model forcing during the last glacial-interglacial cycle

As indicated above, the model is forced by prescribing only two parameters, namely changes in temperature and global sea level. Variations in each during the longer model integrations covering a complete glacial- interglacial cycle are briefly discussed below.

4.8.3.1. temperature

The temperature signal used to perturb the accumulation and 10m - temperature fields is taken from the deuterium record of the Vostok deep ice core, and dates back to 164000 years before present (Jouzel et al., 1987). It is displayed in fig. 4.17. This record covers all of the last glacial cycle and stretches back well into the ice age that preceded the last interglacial. However, the chronology (established with a two-dimensional flow model) may be somewhat uncertain in the lower part of the core. This is suggested by the fact that the Last Interglacial Period in the Vostok record is about twice as
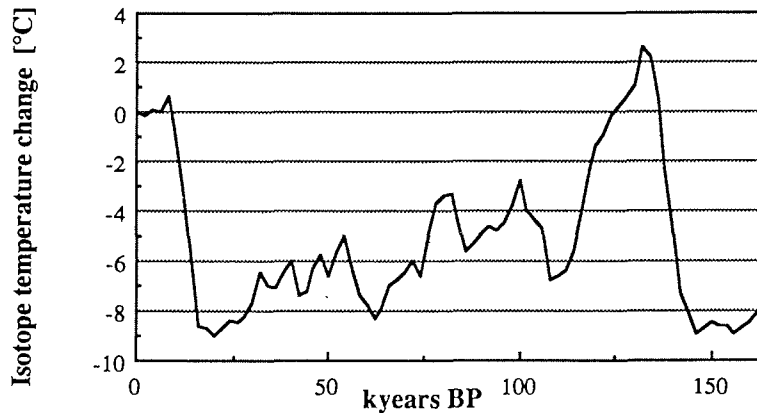
fig.4.17: Vostok isotope temperature signal, used to perturb the accumulation and surface temperature boundary conditions in model experiments involving the last glacial cycle. Data are from Jouzel et al. (1987)

long as the marine chronologies suggest, but a comparison with insolation curves, on the other hand, tends to support the Vostok dating (Jouzel et al. 1987).

Another potential problem in using the Vostok record is connected with the extraction of an independent temperature signal of climatic origin. This is because the deuterium content of the ice not only records changes in climate, but also temperature changes caused by general changes in ice thickness and in the motion of the ice from its origin. Experiments described in this thesis (chapter 7), suggest that altitude changes for Vostok station during the last glacial-interglacial cycle were of the order of 100-150 m. As these elevation changes appear to be in first approximation roughly in phase with the temperature forcing itself, this would amplify the amplitude of the estimated temperature variations by some 1-2°C (assuming a surface lapse rate of 0.015 °Cm^{-1}). This effect is however not taken into consideration, since the bias introduced is still an order of magnitude smaller than the main signal and falls within the range of uncertainty introduced by other factors (such as the background isotopic values in the ocean, laboratory accuracy and the various assumptions used to relate deuterium values to surface temperature).

4.8.3.2. sea level

An unequivocal forcing function for global sea level is more difficult to construct. Several sea level records over the last climatic cycle exist, but all have their deficiencies. In this respect, $\delta^{18}O$ values in deep ocean cores have long been considered a good proxy for continental ice volume and hence of the glacio-eustatic component of sea-level change. In a recent discussion on the matter, however, Shackleton (1987) argues that this simple interpretation is no longer tenable, because oxygen isotope values in benthonic foraminifera differ from the water value by an amount that is temperature dependent. Chappell and Shackleton (1986) made a detailed comparison between the best available oxygen isotope record from the deep Pacific and a sea level record derived from a sequence of raised marine terraces on the Huon Peninsula, New Guinea (see fig. 4.18 for a graphic representation of these records). They arrived at the conclusion that this temperature effect may partially explain the large discrepancy between these records and thus that the temperature of the deep ocean must have been an actively-varying component of the global climate system.
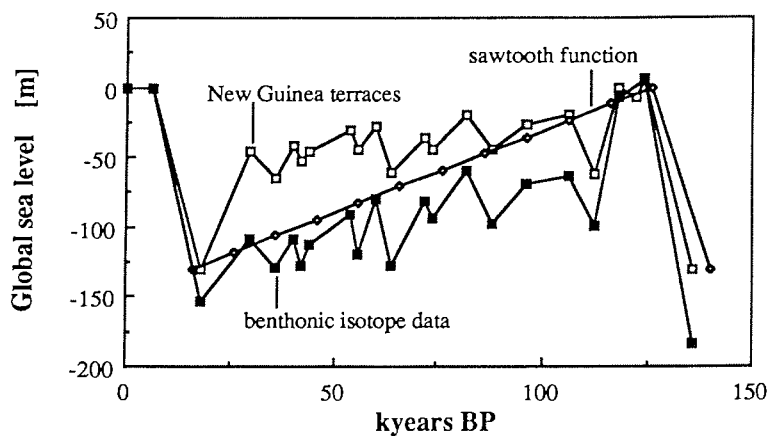

fig.4.18: Sea-level records for the last glacial-interglacial cycle. For reasons discussed in the text, the 'standard' model run described later in chapter 7 makes use of the sawtooth function, which is intermediate between the deep-sea level record and the New Guinea data. Data for the New Guinea terraces and benthonic $\delta^{18}O$ values are from Chappell and Shackleton (1986).

Another source of uncertainty in the $\delta^{18}O$ deep-sea record has been reviewed by Mix and Ruddiman (1984), who demonstrated that the average isotope composition of the former ice sheets must have varied with their size and extent. They showed how a growing ice sheet becomes progressively more isotopically light, as the snow deposited on its surface is formed in a gradually cooling environment, both due to rising elevations and a colder climate. As a result of ice transport, the isotopically heavier ice leaves the ice sheet first, and ocean oxygen isotope values become increasingly more positive, even when the ice sheets are already stabilized at their maximum extent. The latter transport mechanism is particularly effective in the Antarctic ice sheet. The total effect would even increase the difference between the sea level record implied by the deep sea data and that derived from the altitude of dated coral terraces.

In turn, the interpretation of the New Guinea record is complicated by tectonic crustal movements (Chappell and Shackleton, 1986). Variations also arise from isostatic adjustments to glacial/ interglacial changes of ice and ocean volumes, but the magnitude of these variations differs from one geophysical model to another. In particular, values adopted for mantle rheology play a crucial role (for a thorough discussion on this matter, see e.g. Mörner, 1980).

In summary, large differences exist between the various sea level reconstructions. This is also the reason why the more familiar 'saw-tooth' sea level function, piecewise linearly connecting the points (-140 ky BP, -130 m; -125 ky, 0m; -16 ky, -130 m; -6ky, 0 m; 0 ky, 0 m), is chosen as 'standard forcing' in the model experiments discussed later in chapter 7. All these curves are displayed together on fig. 4.18.

4.9. LIST OF SYMBOLS

4.9.1. Constants

a	Arrhenius constant	$[Pa^{-3}y^{-1}]$
A_s	sliding law parameter	$[1.8 \times 10^{-10} N^{-3} y^{-1} m^7]$
c_r	specific heat capacity of rock	$[1000\ Jkg^{-1}K^{-1}]$
D_a	asthenosphere diffusivity	$[0.5 \times 10^8\ m^2y^{-1}]$
D_r	lithospheric flexural rigidity	$[10^{25}\ Nm]$
g	acceleration of gravity	$[9.81 ms^{-2}]$
G	geothermal heat flux	$[-54.6\ mWm^{-2}]$
k_r	thermal conductivity of rock	$[1.04 \times 10^8 Jm^{-1}K^{-1}y^{-1}]$
k_0	stereographic map scale factor	[0.9728]
L	specific latent heat of fusion	$[3.35 \times 10^5\ Jkg^{-1}]$
L_r	radius of relative stiffness	[132573 m]
m	flow enhancement factor	[1-5]
n	Glen flow law exponent	[3]
Q	activation energy for creep	$[kJmol^{-1}]$
R	universal gas constant	$[8.314\ Jmol^{-1}K^{-1}]$
R_e	earth radius	[6371221 m]
T_0	triple point of water	[273.15 K]
β	constant for calculating pressure melting	$[8.7 \times 10^{-4}\ Km^{-1}]$
Δx	gridpoint spacing in x-direction	[40 km]
Δy	gridpoint spacing in y-direction	[40 km]
Δt	time step	[40 y]
π	pi	[3.1415926]
ρ, ρ_i	ice density	$[910\ kgm^{-3}]$
ρ_r, ρ_m	rock density	$[3300\ kgm^{-3}]$
ρ_w	ocean water density	$[1028\ kgm^{-3}]$

4.9.2. Variables

A	pre-exponential flow law parameter	$[Pa^{-3}y^{-1}]$
c_p	specific heat capacity of ice	$[Jkg^{-1}K^{-1}]$
D	ice diffusivity	$[m^2y^{-1}]$
D^l	layer ice diffusivity	$[my^{-1}]$
D^s	basal sliding diffusivity	$[m^2y^{-1}]$

F	ice mass fluxes	$[m^2 y^{-1}]$
M	surface mass balance	$[m/y]$
h	bed elevation above present sea level	$[m]$
h_0	undisturbed bed elevation	$[m]$
H	ice thickness	$[m]$
H_{sl}	sea level stand relative to present	$[m]$
k_i	thermal conductivity of ice	$[Jm^{-1}K^{-1}y^{-1}]$
q	applied lithospheric load	$[Pa]$
S	basal melt rate	$[m/y]$
t	time	$[y]$
T	ice temperature	$[K]$
T^*	ice temperature relative to pressure melting	$[K]$
T_f	temperature above surface inversion layer	$[K]$
T_{pmp}	pressure melting point	$[K]$
T_r	rock temperature	$[K]$
T_s	surface temperature	$[K]$
u	x-component of the velocity vector	$[m/y]$
v	y-component of the velocity vector	$[m/y]$
$\bar{v}$	depth-averaged horizontal velocity	$[m/y]$
$\vec{V}$	three-dimensional velocity vector	$[m/y]$
w	z-component of the velocity vector	$[m/y]$
w'	lithosphere deflection	$[m]$
Z^*	height above buoyancy	$[m]$
$\dot{\varepsilon}$	effective strain rate	$[y^{-1}]$
$\dot{\varepsilon}_{ij}$	strain rate components	$[y^{-1}]$
ϕ	geographical latitude	$[°]$
Φ	internal frictional heating	$[Jm^{-3}y^{-1}]$
γ_g	geothermal basal ice temperature gradient	$[Km^{-1}]$
λ	geographical longitude	$[°]$
τ_{ij}	stress tensor components	$[Nm^{-2}]$
τ'_{ij}	stress deviator components	$[Nm^{-2}]$
τ, τ^*	effective stress	$[Nm^{-2}]$
$\vec{\tau}_b$	basal shear stress	$[Nm^{-2}]$

5. BASIC SENSITIVITY EXPERIMENTS WITH FIXED GROUNDING LINE

5.1. EXPERIMENTAL SETUP

The aim of this first series of numerical experiments is to produce initial input for the forthcoming prognostic runs and to conduct a fundamental sensitivity study with respect to basic input parameters and some of the model formulations (in particular, basal sliding and the geothermal heat flux). In these experiments ice thickness is a free variable but the present ice sheet *extent* is fixed. The fact that changes in the grounded ice domain are not taken into account has three advantages.

First, in this way the flow and temperature fields can be initialized in a stepwise fashion. This reduces the risk that calculations immediately 'blow up' due to ill-conditioned model input, in case all degrees of freedom would be incorporated right from the start.

Second, comparing the stationary ice thickness distribution produced by the model with observations provides a good test of global model performance. In this way, continuity requirements are fulfilled and discrepancies may then either point to model deficiencies (formulation and/or data) or a 'real world' transient state. The procedure can be considered an alternative to more usual validation methods, in which either present-day ice thickness is used as a boundary condition and the diagnostic velocity field is compared with ice velocities required for a stationary state (the 'dynamics' versus 'balance' velocities approach, e.g. Budd and Jenssen, 1989), or the flux divergence of the diagnostic velocity field is compared with observed accumulation rates (Herterich, 1988). An advantage of the present approach is that it allows an equilibrium to be established between the input data and the model physics.

140

The ice sheet geometry is therefore at least able to remove those artefacts and discontinuities that arise solely by reading surface data from a map onto a grid. If it is realized that velocity is a locally-defined quantity which depends on ice thickness to the fourth power and surface gradient to the third power, these errors can certainly become important!

Third, since changes in ice thickness produced by grounding-line migration are not incorporated, this model setup makes it possible to isolate the role of thermomechanical effects (i.e. from the mutual interaction between ice temperature and flow) on the long-term evolution of the ice sheet. Such a study is relevant in the light of the long time-scales connected with these thermomechanical effects (e.g. Huybrechts and Oerlemans, 1988). In this respect, it is likely that the temperature distribution of the ice sheet is still out of balance with the present climate. The geographical distribution and magnitude of the present ice thickness imbalance can then be determined by carrying out a sufficiently long time integration, forced, for instance, by the Vostok temperature signal. This experiment is also discussed here.
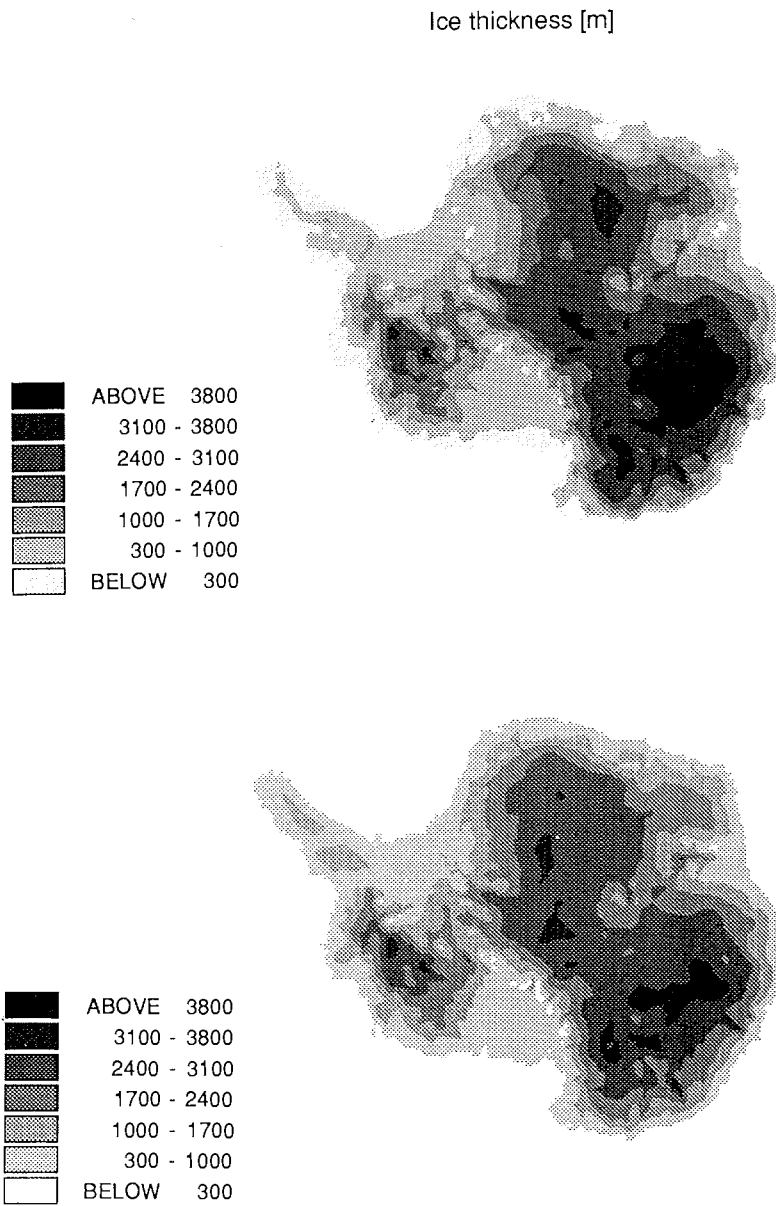
5.2. RESULTS

5.2.1. The present reference state

In order to investigate the points mentioned above, a reference state has to be defined. This is accomplished in two steps. First, the coupled velocity and temperature fields are run forward in time for 100000 years in a diagnostic way (thus keeping present ice thickness and grounding line position fixed) until an approximate steady solution is reached. Following this, the position of the grounding line is still prescribed but ice thickness is allowed to relax to steady state for another 100000 years.

This defines the reference run and a comparison between observed and modelled ice thicknesses is shown in fig. 5.1. In general, modelled ice thicknesses appear to be within 5-10% or so of reality, which is certainly acceptable. Nevertheless, somewhat larger deviations do occur in several places. However, this does not necessarily have to mean that the model is in error. Alternative explanations could be that bedrock data coverage is

Ice thickness [m]

ABOVE 3800
3100 - 3800
2400 - 3100
1700 - 2400
1000 - 1700
300 - 1000
BELOW 300

ABOVE 3800
3100 - 3800
2400 - 3100
1700 - 2400
1000 - 1700
300 - 1000
BELOW 300

fig.5.1: A comparison between observed ice thicknesses and those produced by the model
in the reference run. upper panel: observations; lower panel: model.

insufficient in these areas and/or the fact that the ice sheet is just not in steady state. In this respect, it is interesting to note that the model produces substantial thicker ice in the Pine Island and Thwaites Glacier catchment areas (approx. 100°W) in West Antarctica. This happens to be an area which is considered to be very sensitive to grounding line instability, because the ice streams flowing into Pine Island Bay are presently unimpeded by a buttressing ice shelf (cf. § 3.3.4.). Indeed, there is independent evidence that the Pine Island ice stream may at present be in the process of drawing its drainage basin down (Lindstrom and Hughes, 1984; Kellogg and Kellogg, 1987a). As a consequence, steady state ice thicknesses under 'normal conditions' are likely to be larger than the present day values. The model seems to confirm this.

The overprediction of ice cover in the Antarctic Peninsula, on the other hand, must be attributed to the poor quality of the bedrock data. The SPRI map actually shows blanks in these areas and a 'bad interpolation' is the prime cause for an inaccurate prediction of the grounding lines in the area of the Larsen and King George VI ice shelves and between Graham Land and the South Shetland Islands. Since the Peninsula ice sheet and its alpine-type glacier system are to a large extent dynamically uncoupled from the rest of West Antarctica, no further attempts have been made to improve this situation. Although less obvious, insufficient bedrock data coverage may also be the reason for the thicker ice produced by the model upstream the Shackleton Range in Dronning Maud Land (30-40°W, EAIS). In this area, bedrock elevation contours are based on only a few measurements (Drewry, 1983, sheet 3).

The associated (depth-averaged) velocity and basal temperature fields (relative to pressure melting) are displayed in figs. 5.2 - 5.3 and provide an additional check on overall model performance. As far as can be judged from available data, the velocity field looks reasonable, with very low velocities over central East Antarctica, typically around 200 m/y at the grounding line and up to 1500 m/y along central portions of the three major floating ice regions, namely the Ronne-Filchner, Amery and Ross ice shelves. These modelled ice shelf velocities are certainly of the right magnitude, although they tend to be somewhat higher than the observations: the Ronne and Filchner ice shelves flow at a maximum rate of ± 1500 m/y (Robin et al., 1983);

Velocity magnitude [m/y]

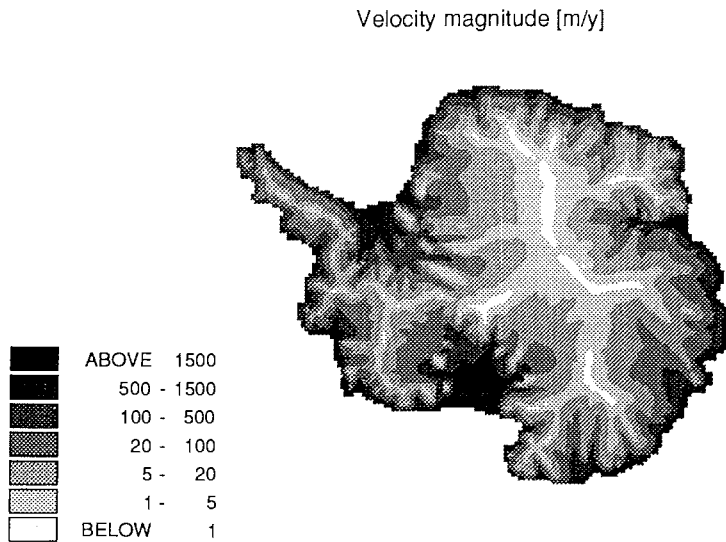|	
ABOVE	1500
500 -	1500
100 -	500
20 -	100
5 -	20
1 -	5
BELOW	1

fig.5.2: Calculated speed of ice flow. Shown are depth-averaged values. The corresponding surface velocities in the grounded ice sheet are 5-10 % larger, depending on the temperature conditions in the bottom layers and the amount of basal sliding.

Basal temperature relative to pmp [deg. C]

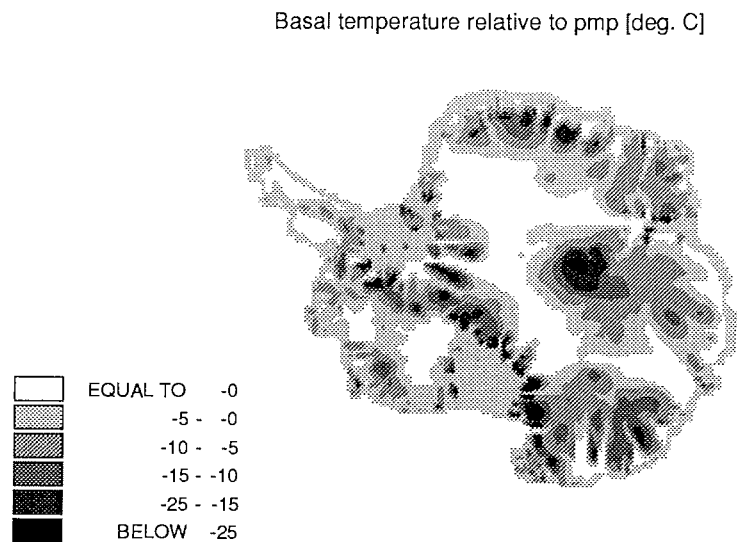|	
EQUAL TO	-0
-5 -	-0
-10 -	-5
-15 -	-10
-25 -	-15
BELOW	-25

fig.5.3: Bottom temperatures produced by the model. They have been corrected for the dependence of temperature on pressure. Yellow areas are areas where basal melting occurs.

the Ross ice shelf at ±1100 m/y (Thomas et al., 1984); and the Amery ice shelf at ±1300 m/y (Budd et al., 1982). This discrepancy may be due to the neglect of basal melting in the mass balance of the ice shelf. As a consequence, the model probably overpredicts the mass outflow and, since the thicknesses agree much better, this results in somewhat higher velocities.

Although ice streams and outlet glaciers (discharging an important fraction of the ice mass into the ice shelves and the ocean) are not explicitly included in the calculations, they are apparent in the results and are characterized by velocities of 500 m/y or more (fig.5.2). This is essentially a consequence of the fine grid used. Despite anticipated difficulties mentioned earlier (cf. § 4.1), also the major ice streams discharging into the Ronne- Filchner and Ross ice shelves can be clearly identified. This is an encouraging result and is largely because of basal sliding.

According to the model, bottom ice at pressure melting point is dominant over most of the Antarctic Peninsula and is widespread in West Antarctica. In East Antarctica, basal melting is confined to the thick interior regions (because of the insulating effect of ice) and the fast flowing regions at the margin (fig.5.3). This temperature field can be reconciled with independent evidence for the locations of temperate ice from radio-echo sounding, where sub-ice lakes in central areas have been found to obscure reflections (Oswald and Robin, 1973). The coolest basal layers are found above the Gamburtsev Mountains, where the ice is relatively thin (1500 - 2000m), and along the fringing mountain ranges, where both thin ice and cold ice advection from above play an important role.

The distribution of pressure melting as obtained here deviates from the calculation presented in Herterich (1988) with a similar model. Despite a lower value for the geothermal heat flux used in his study, Herterich's map shows basal melting to be substantially more widespread. This disagreement seems to be primarily the consequence of a different experimental setup. Herterich derived the vertical velocity component from the flux divergence of the horizontal flow field. However, since the shape of his ice sheet was fixed, the horizontal velocity field was not in internal equilibrium with the ice thickness distribution. This disequilibrium may indicate a real world imbalance (as assumed by Herterich) but it may also just reflect shortcomings in the

model physics. Uncertainties in the flow law parameters and in the ice thickness distribution may easily lead to changes in the diagnostic velocity field by up to an order of magnitude. His velocity components, which are needed for the advective terms in the heat equation, therefore do not necessarily correspond to a balanced stationary state. Also the use of a fixed vertical coordinate in the Herterich model may introduce numerical errors when values are interpolated to the actual upper and lower ice surfaces.

5.2.2. Effect of basal sliding

In the model, ice flow results from both internal deformation and basal sliding (cf. eqs. 4.17-18). Basal sliding may become important when the bottom ice is at the pressure melting point and a lubricating waterfilm is formed. Although general agreement on how to model bottom sliding has not yet been reached (see § 4.4.2.2 for a small discussion on the problem), basal sliding is nevertheless believed to play an important role in the dynamics of the marine-based West Antarctic ice sheet. This not only applies to the potential of basal sliding in enhancing any instability mechanism, but the occurrence of bottom sliding (whether it be at the ice-rock interface or by means of a thin and deformable till layer) has also been linked to the concave surface profile observed inland of the large ice shelves (Budd et al., 1984). The process of basal sliding may then account for the fact that, in the lower reaches of West Antarctic ice streams, the gravitational driving stress (that causes the ice to deform) is decreasing downstream, while ice velocities increase.

As discussed before in § 4.4.2.2, we adopted a Weertman-type sliding relation corrected for the effect of subglacial water pressure. Such a functional relationship was found by Bindschadler (1983) to give the best fit to observations on West Antarctic ice streams. With this law, sliding velocities in wet-based areas (expressed as a fraction of the total movement) are below 10 % in central East Antarctica, typically of the order of 20 - 40% in interior West Antarctica and well over 90 % where the grounding line is approached. So the expected increase in sliding velocities towards the margin is found.

The effect on the ice thickness distribution (and thus also on the surface profile) can then be investigated by performing a model experiment in which basal sliding is omitted and model output is compared with the reference
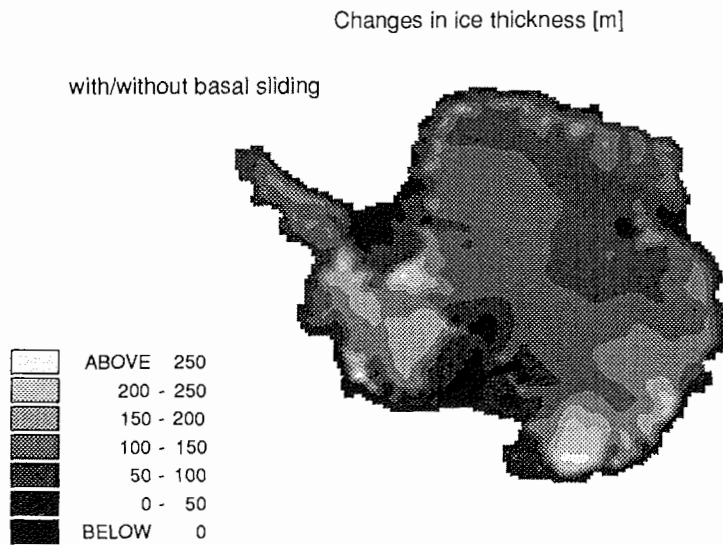
146

FIXED GROUNDING LINE EXPERIMENTS

Changes in ice thickness [m]

with/without basal sliding

ABOVE   250
200 - 250
150 - 200
100 - 150
 50 - 100
  0 - 50
BELOW   0

fig.5.4: Changes in ice thickness when the adopted sliding relation is omitted. Results are relative to the reference run.

Changes in ice thickness [m]

1.30/1.17 HFU

ABOVE   125
100 - 125
 75 - 100
 50 - 75
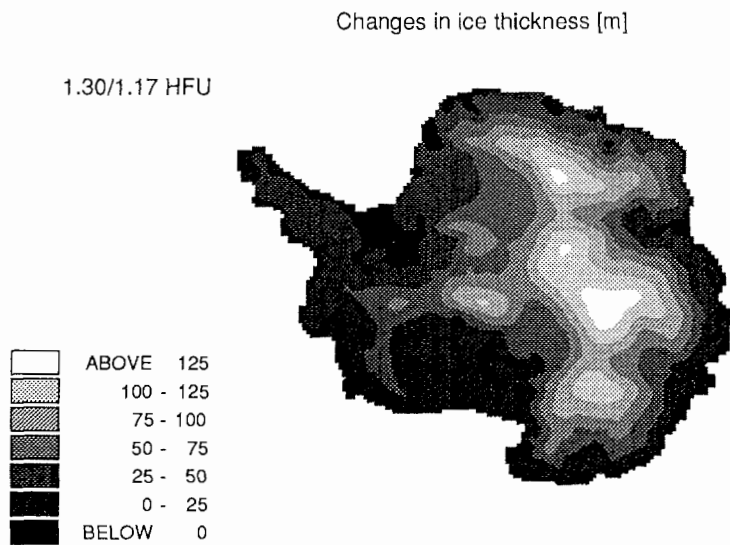 25 - 50
  0 - 25
BELOW   0

fig.5.5: Increase in ice thickness when the geothermal heat flux is reduced by 10%, all other things being equal. The pattern for an increase in the geothermal heat flux by 10% is similar, but of opposite sign.

state. The result is displayed in fig. 5.4. It shows an overall thickening of the ice sheet by up to a few hundred meters and the effect is indeed more pronounced towards the grounding line and in those areas where meltwater is produced (the effect is most apparent in West Antarctica and in the overdeepened outlet glaciers along the East Antarctic coast). Thus, excluding basal sliding does lead to somewhat steeper slopes at the margin, although the impact is not particularly significant. As a matter of a fact, a rather similar overall thickening could also have been obtained by lowering the enhancement factor in the flow law. In view of this, Van der Veen (1987) suggested that a Budd-type relation (Budd et al., 1984) might be preferable, in which sliding is inversely proportional to the square of the height above buoyancy and depends linearly on the basal shear stress. However, this option was rejected because it generated too high velocity gradients at the ice sheet margin and thereby oscillations in the solution.

5.2.3. Effect of geothermal heat flux

In the model experiments discussed in this thesis, we used a value for the geothermal heat flux of 1.30 HFU (1 Heat Flow Unit equals 42 mWm^{-2}). However, direct measurements of the heat flow at the ice-rock interface are not available and the exact value of the geothermal heat flux for Antarctica is unknown. In general, it depends on rock age and rock type and is strongly correlated with near-surface concentrations of radiative and heat producing isotopes. Its value is also likely to vary from place to place and it is probably not constant in time either. In spite of this, 1.3 HFU is thought to be a representative value for the Precambrian rocks which make up for most of the Antarctic continent (Sclater et al., 1980). An overall ±10% range of uncertainty is probably realistic. So, in order to investigate the effect of such changes on the temperature and ice thickness distribution, two sensitivity runs were carried out, one in which the geothermal heat flux G was raised by 10% (1.43 HFU), and one in which a value of 1.17 HFU was applied.

The resultant shifts in ice thickness for the -10% case are displayed in fig. 5.5. The corresponding sensitivity to an increase in G is not shown, but is of the same magnitude and of opposite sign. Consequences for the *steady state* pattern of basal melting areas are shown in fig 5.6, where a comparison is also made with the reference state. Clearly, increasing the basal heat input

148

leads to larger areas of pressure melting, while the reverse is apparently true when the heat input at the base is decreased. Although the value of G is certainly important for a diagnosis of the present state, some further experimentation also revealed that its value is not so critical to the *sensitivity* of the model, at least when changes in ice thickness are concerned. In other words, the model's response to a glacial-interglacial contrast does not seem to depend in a crucial way on how the present day temperature field is diagnosed.

5.2.4. Role of flow-temperature coupling

### 5.2.4.1. general effects

It must be emphasized that fluctuations of the Antarctic ice sheet cannot be studied without taking into account the mutual interaction between ice flow and ice temperature. This is mainly because changes in the surface climate not only alter the ice sheet's mass balance, but also its thermal regime, which affects the flow properties of the ice. A whole number of feedbacks are involved, and different modes of heat transfer operate on different time scales in different parts of the ice sheet. The ultimate outcome is generally a complicated matter and simple reasoning is inadequate to predict a priori what will happen to the ice sheet in a different climate. A thorough discussion on this matter has been given by Hindmarsh et al. (1989) and by Huybrechts and Oerlemans (1988). However, in order to aid the interpretation of the experimental results, it is useful to give a brief qualitative description of basic mechanisms involved.

To this purpose, consider a situation in which a temperature lowering of typical glacial-interglacial magnitude (say 10°C) is applied at the ice sheet's surface. A first consequence is that a cold wave will be slowly conducted downwards. This wave will at some stage reach the basal layers, where ice deformation is concentrated. Cooler ice deforms less readily, leading to decreased strain rates and a general thickening of the ice sheet. However, colder air carries less precipitable moisture, so a cooling of the surface climate in the Antarctic is also accompanied by lower accumulation rates. This has a number of additional consequences. First, the mass balance of the ice sheet decreases. This is a thinning effect and will counteract the thickening caused
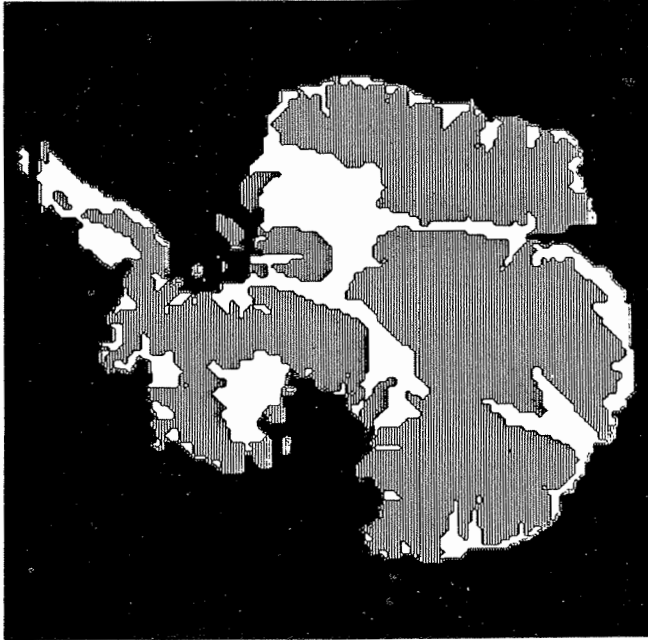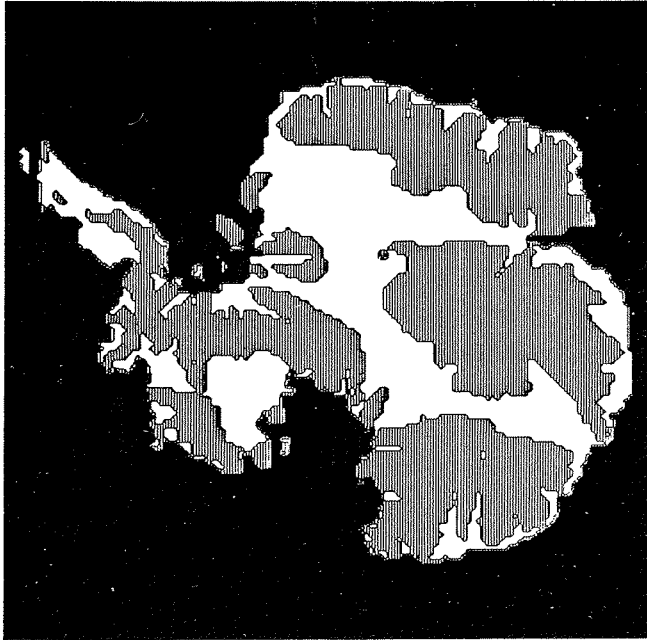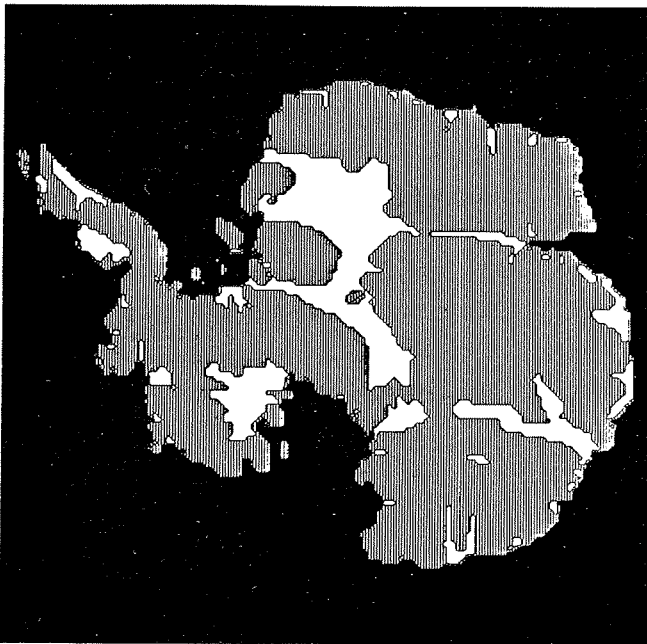
(a)
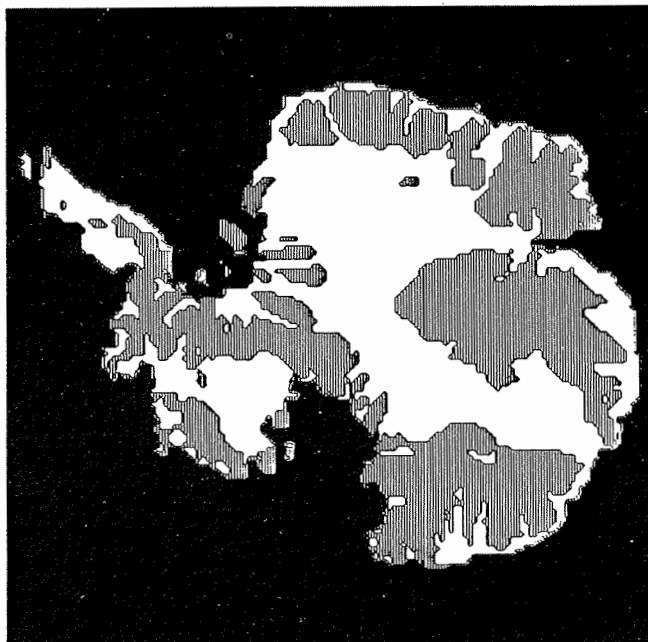
(b)

fig.5.6: Geographical distribution of pressure melting (white areas) as a function of the geothermal flux. (a): heat flux - 10%, 1.17 HFU; (b): heat flux + 10%, 1.43 HFU.

(c)

(d)

fig. 5.6 (continued): (c): reference state, 1.30 HFU; (d): the 'glacial state' (see § 5.2.4. for a definition) is added for comparison.

151

by the colder base. Second, less ice needs to be transported towards the ocean, so lower accumulation rates also imply lower velocities. A direct effect is that less heat will be generated by dissipation, especially at the margin, where friction is the main heat source. Additionally, advection of cold ice towards the basal layers becomes less effective, which should result in a warming.

All of these mechanisms ultimately cause a change in the thickness of the ice sheet and this will in turn feed back on the surface boundary conditions. A thickening of the ice sheet implies higher elevations and, consequently, lower surface temperatures. This is a positive feedback. A lowering of the surface because of lower deposition rates, on the other hand, leads to higher surface temperatures (=positive feedback), but it also implies higher accumulation rates, which is a negative feedback. Changes in ice thickness are also important for the vertical heat diffusion process. Thicker ice, for instance, enhances the insulating effect of the ice sheet and makes the evacuation of geothermal heat towards the surface more difficult. In view of all these (in part) counteracting effects, it is clear that numerical calculations are needed in order to find out what the ultimate response of the modelled ice sheet will be.

5.2.4.2. experimental results

Three sensitivity experiments were performed, in which lower surface temperatures and the associated lower accumulation rates were applied, either singly or in combination. Calculations were continued for 100000 years, so that approximately stationary conditions were achieved. As an illustration, figure 5.7 shows the resulting velocity and temperature profiles for a central location in East Antarctica. At this location, lowering accumulation to glacial levels alone (which are roughly 60% of presently observed values) appears to be a particularly effective way of bringing the base to the pressure melting point and inducing basal sliding (curve 3). The velocity curves at the left also demonstrate that ice deformation can in effect be considered as a basal process. About half of the velocity shear is confined to the lowermost 5% of the ice thickness. This follows from the non-linearity of the flow law and is enhanced because the warmest temperatures (implying the softest ice) occur at the bottom.
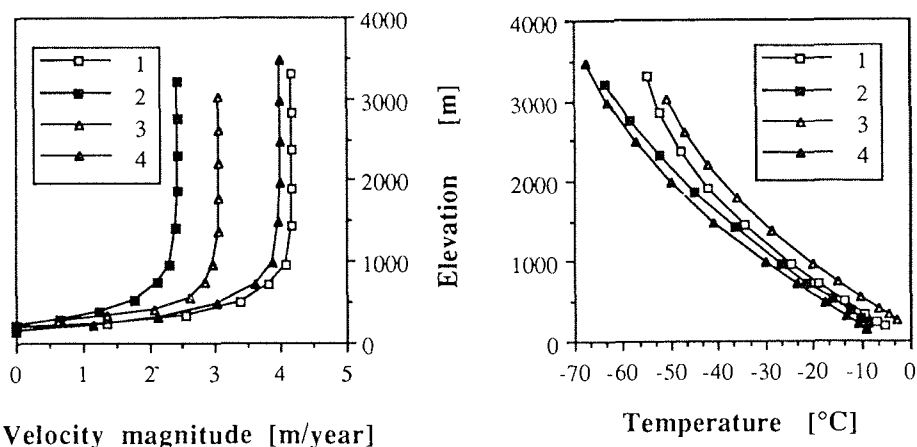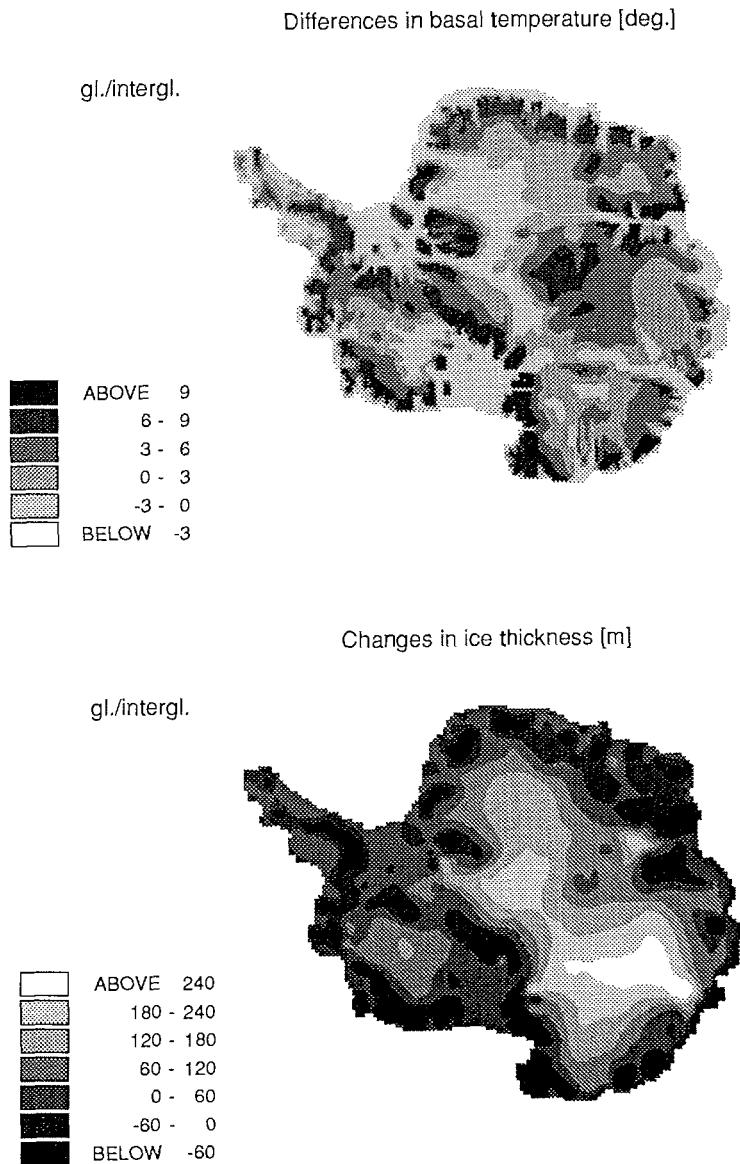
fig.5.7: Calculated steady state velocity and temperature profiles following glacial-interglacial contrasts in boundary conditions. (1): reference state; (2): -10 °C and glacial accumulation rate; (3): glacial accumulation rate; (4): -10 °C in background temperature. Corresponding curves are for gridpoint (100, 62), which is near Vostok, East Antarctica.

Modelled distributions of basal temperature and ice thickness in the experiments in which either surface temperature or accumulation rate are varied are not shown here, but results are shortly summarized in table 5.1 (§ 5.3). Typically, 'glacial' accumulation rates lead to decreased ice thicknesses by 10-15% and a slightly warmer base. Conversely, a background temperature lowering of 10°C implies an average thickening of 11.7% and a mean cooling at the base of some 5°C. The corresponding geographical distributions of steady state differences in these variables following a full glacial-interglacial contrast in temperature *and* accumulation rate, are displayed in fig. 5.8. The ultimate effect is a basal warming (relative to the glacial stage) which is most pronounced at the margin. Corresponding pressure melting distributions for these two model runs are shown in fig. 5.6 (c-d).

However, the combination of this warmer base together with higher accumulation rates leads to surprisingly small changes in ice thickness. Thus, typical glacial-interglacial changes in both temperature and accumulation rate have a largely counteracting effect on the ice sheet geometry. A small

153

FIXED GROUNDING LINE EXPERIMENTS

Differences in basal temperature [deg.]

gl./intergl.

	ABOVE	9
	6 -	9
	3 -	6
	0 -	3
	-3 -	0
	BELOW	-3

Changes in ice thickness [m]

gl./intergl.

	ABOVE	240
	180 -	240
	120 -	180
	60 -	120
	0 -	60
	-60 -	0
	BELOW	-60

fig.5.8: Geographical distribution of steady state shifts in ice thickness (above) and bottom temperature (below) in response to a glacial-interglacial change in surface boundary conditions. Values are relative to the glacial state, which is forced by a uniform 'background' temperature drop of 10 °C and where concomitant reduced accumulation rates are applied.

154

thickening is apparent both in the ice sheet interior and in those places that were wet-based in the glacial state (so that the base cannot warm any further). However, fig. 5.8 also shows a slight thinning in marginal areas because of the strong impact of basal warming. These complex response patterns once more demonstrate that changes in ice volume cannot be adequately investigated without taking into account thermomechanical coupling.

The experimental results described above relate to steady states. In the real world, however, it is unlikely that such a state would ever be reached, because the climatic input varies on a substantially shorter time scale than the thermomechanical coupling. This is demonstrated in fig. 5.9, in an experiment in which lower surface temperatures are applied at time zero and the temperature and velocity fields are relaxed forward in time. Although heat conduction is admittedly the slowest component within the system, the result clearly suggests that it may take up to 100000 years for a new stationary state to be reached. Furthermore, as demonstrated before in fig. 4.4., this time scale may even become longer in case heat conduction in the bedrock is incorporated as well.
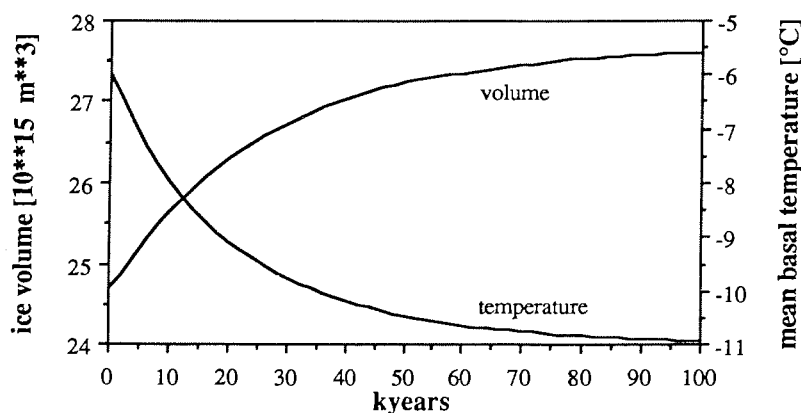

fig.5.9: Evolution of ice volume and mean basal temperature after a stepwise change in surface boundary conditions. This example is for a run in which temperature is lowered by 10°C, without the corresponding 'glacial' change in accumulation rates. It demonstrates the long response time scales involved.

5.2.5. Response to a complete glacial-interglacial cycle

In view of these long response time scales, finally a time-dependent experiment was conducted which involves the last glacial-interglacial cycle. The Vostok temperature signal was employed to drive changes in surface temperatures and accumulation rates. Results of a steady state run with $\Delta T = -5°C$ served as an initial condition and calculations started at 164 ky BP. This model setup should minimize the effect of the initial conditions on the results. Two experiments were carried out, one in which heat conduction in the bedrock was included (after 140 ky BP) and one in which this effect was omitted.

The corresponding evolution of mean basal temperature and ice volume are shown in fig. 5.10. They are compared to the associated glacial and interglacial stationary states which would occur if the climate was stable for a sufficiently long time. Clearly, the temperature response is strongly damped during a glacial cycle. Between the onset of the last deglaciation at 16 ky BP and present-day only a fraction of the expected temperature rise has been completed. Consequently, deep ice temperatures are still reacting to past changes in boundary conditions. Also the additional effect of including the thermal inertia of the bedrock is as expected. Together with changes in basal stress conditions induced by increased accumulation rates, this also influences the evolution of ice volume. In this case, there is an overshoot effect: the amplitude of the transient evolution of ice volume is larger than the amplitude of the associated steady states.

The results displayed in fig. 5.10 relate to a mean state for the entire ice sheet. However, it must be realized that the problem is really temporally *and* spatially dependent. Heat dissipation is a virtually instantaneous process, and is dominant in the marginal areas. Advection is important in the upper layers and typically operates on a time scale of 10^4 years. Heat diffusion is important for the thermal regime in the basal layers in more central areas. It is also the slowest component. Ice dynamics also introduce a time lag. This is because the ice sheet needs some time to react to changes in basal stress conditions, which are induced by fluctuations in the ice sheet geometry. Depending on the accumulation rate, these response times are in the range of 10^3 to 10^4 years. So different regions are probably reacting in a different way at a
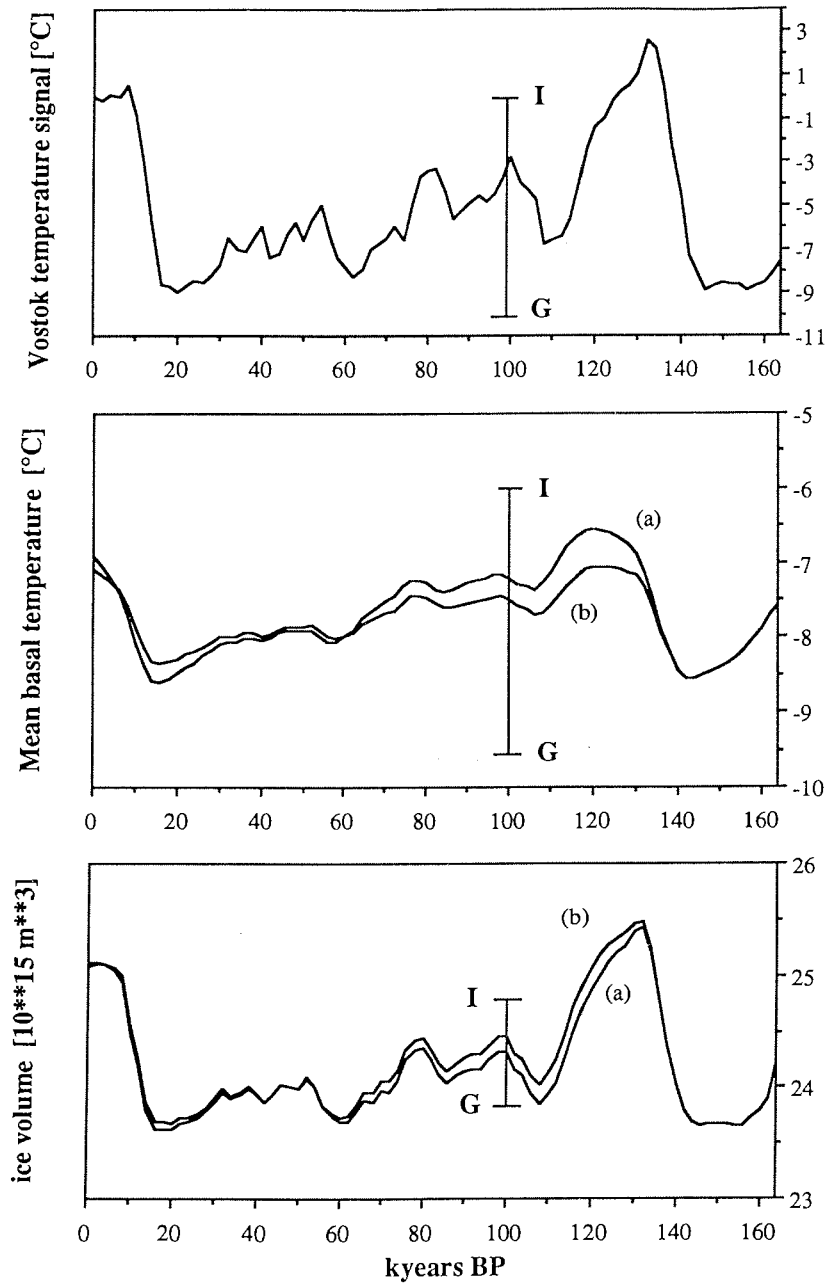
fig.5.10: Evolution of some large scale variables in a time-dependent experiment forced by the Vostok temperature signal (upper panel). Lower panel: grounded ice volume. Middle panel: mean basal temperature. Vertical bars refer to stationary states, G: glacial, I: interglacial. (a): no heat conduction in bedrock, (b): including heat conduction in bedrock.

Differences in basal temperature [deg.]

-16/0 ky BP

bed cond.

ABOVE   6
    4 - 6
    2 - 4
    0 - 2
   -2 - 0
BELOW -2
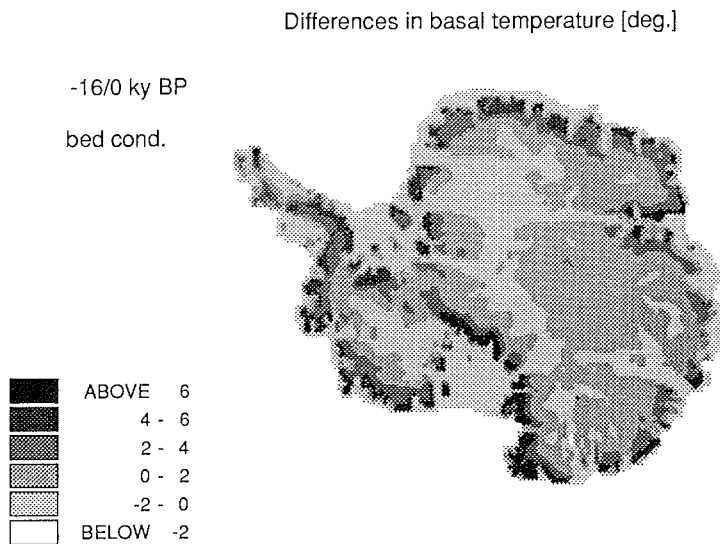
fig.5.11: Basal temperature rise between the onset of the last deglaciation at 16 ky BP and the present time. This plot is for the Vostok-experiment and includes heat conduction in the rock.

Differences in basal temperature [deg.]

0 ky / intergl.

bed cond.

ABOVE   4
    3 - 4
    2 - 3
    1 - 2
    0 - 1
   -1 - 0
BELOW -1
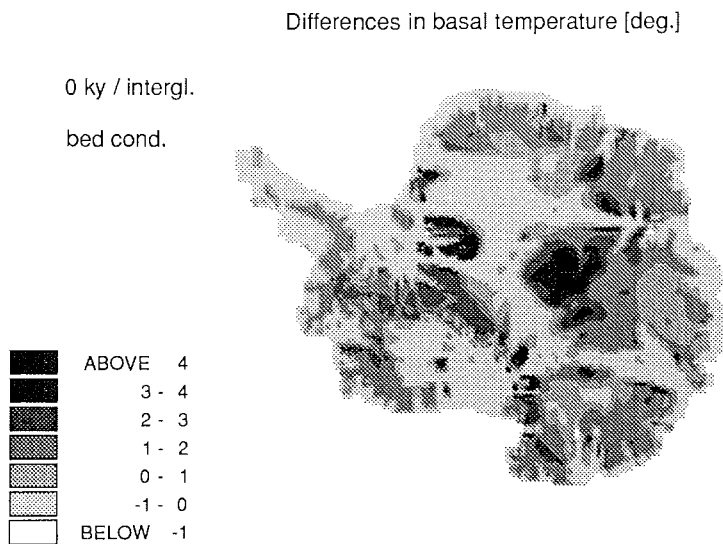
fig.5.12: Temperature rise needed in order to achieve steady conditions under present-day climatic conditions. Same experiment as in the figure above.

158

Local ice thickness imbalance [m/y]

ABOVE   0.009
0.006 - 0.009
0.003 - 0.006
0.000 - 0.003
-0.003 - 0.000
-0.006 - -0.003
BELOW   -0.006
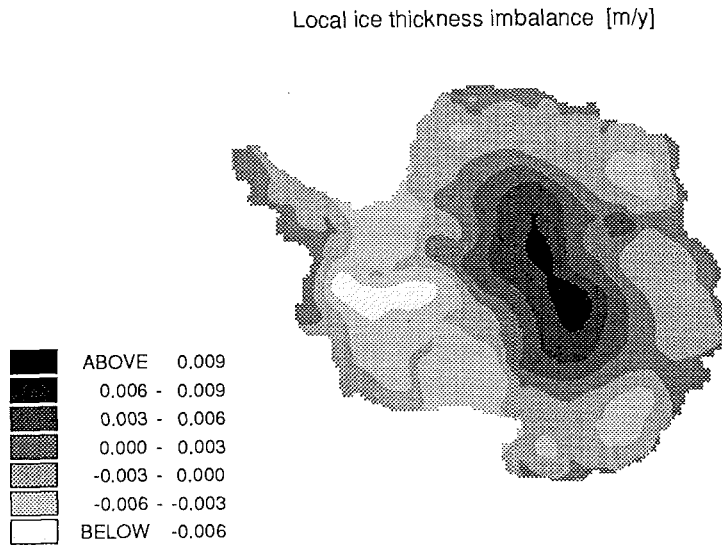
fig. 5.13: Geographical distribution of the present-day rate of ice thickness change following a complete glacial cycle. These rates are caused by flow-temperature coupling. The plot is for the Vostok-experiment at time = 0, and includes heat conduction in the rock. The pattern for the model experiment without bedrock heat conduction resembles this one to a large extent, but values tend to be slightly more negative.
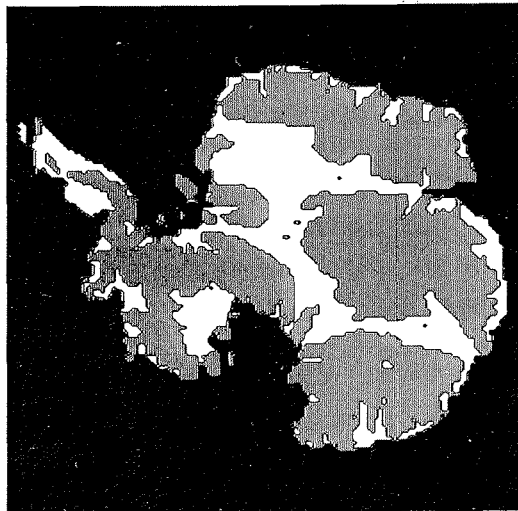
fig.5.14: Basal areas at pressure melting (in white) in the Vostok experiment at time zero. With the restriction that changes in ice sheet extent have not been considered, this is the distribution that should be compared with observed locations of subglacial lakes to constrain the value of the geothermal heat flux.

159

different time.

The resulting response patterns are given in figs. 5.11 and 5.12. They show the geographical distribution of shifts in the basal temperature field following the last glacial-interglacial transition. The temperature response is at present nearly completed at the margin but interior regions, in particular in the East Antarctic ice sheet, have not even started to react yet! Clearly, palaeotemperatures still exist beneath the Antarctic ice sheet and bottom temperatures may be out of balance with the present day climate by more than 5°C. This implies that the ice sheet will still be responding to its climatic history for a long time to come, irrespective of future climatic trends.

Fig. 5.13 shows the geographical distribution of the present-day ice thickness imbalance. The overall balance *due to thermomechanical effects* appears to be only slightly positive, corresponding to a mean increase in ice thickness of 1 mm/y. Nevertheless, some interesting spatial differences occur. The interior of the East Antarctic ice sheet appears to be still thickening at a rate of about 1 cm/y following increased accumulation rates some 16000 years ago. Since the warmer surface temperatures have not influenced basal layers yet, this situation is likely to go on for some time. The picture changes gradually towards the margin, however. Here, ice thicknesses and basal stresses have already adapted to the new mass balance field and since the base is still warming, a thinning trend becomes evident. These circumstances appear to be most pronounced in the West Antarctic ice sheet, where the area facing the Ronne-Filchner ice shelf is found to be thinning at a rate of over 1 cm/y. The experiment without heat conduction in the bedrock (not shown) yields the same basic pattern, but values tend to be less positive and more negative than those displayed in fig. 5.13.

5.3. SUMMARY

In this chapter, we have discussed results from a number of sensitivity experiments in which grounding line migration was excluded. This experimental setup allowed the role of thermomechanical effects on the ice sheet's evolution to be investigated in an isolated fashion. The main points

FIXED GROUNDING LINE EXPERIMENTS

Model experiment	Mean ice thickness [m]	Mean basal temperature [°C]
observations	1898	no data
reference state ('interglacial')	1946	-5.98
no basal sliding	2027	-5.57
1.17 HFU (-10%)	1988	-7.40
1.43 HFU (+10%)	1910	-4.86
-10°C	2174	-10.94
glacial accumulation rate	1692	-5.24
-10°C and glacial accumulation rate	1878	-9.60
Vostok temp. forcing, at present (*)	1975	-6.92
Vostok temp. forcing, at present (†)	1979	-7.10

table 5.1: Steady state ice thickness and mean basal temperature for the experiments discussed in this chapter. In order to obtain the grounded ice volume, values listed in column 2 have to be multiplied by 12.696×10^{12} m^2 (i.e. the constant ice sheet area). (*): no heat conduction in the bedrock; (†): including heat conduction in the bedrock.

that have come out of this study can be summarized as follows (see table 5.1 for an overview):

(i) the model appears to be able to model the free surface of the ice sheet rather well. It resolves major flow features, including the various ice streams and outlet glaciers. Areas in which the model produces somewhat larger discrepancies with respect to the measurements can probably be explained by deviations from steady state and/ or inadequacies in the bedrock data coverage.

(ii) the inclusion of a Weertman -type sliding law, corrected for the effect of subglacial water pressure, leads to more gentle surface slopes inland of the large ice shelves (as indicated by the observations). However, it is not not

found to alter the ice sheet profile in a really significant way. Consequently, modelled surface slopes in West Antarctica are still a little too high.

(iii) the sensitivity of the basal temperature field with respect to a ± 10% change in the geothermal heat flux is nearly of the same magnitude as a typical glacial-interglacial contrast. Nevertheless, once a fixed value for G is chosen, model sensitivity is not crucially affected by this choice.

(iv) decreasing surface temperature to glacial levels leads to a cooler base and to larger ice thicknesses, while the reverse is true when lower accumulation rates are applied. However, when both conditions are applied together there is little difference in the overall ice thickness distribution: glacial-interglacial changes in accumulation rate and surface temperature have roughly counteracting effects. In the *steady state*, their impact is of equal magnitude, but of opposite sign.

(v) palaeotemperatures still exist under the Antarctic ice sheet: there is very little change in the basal temperatures of interior regions between the onset of the last deglaciation 16000 years ago and the present time. Since climatic change did not cause rapid changes in the basal temperature field, this means that the reasoning with respect to the value of the geothermal flux may be reversed. A comparison of the calculated present-day temperature field with the observed distribution of subglacial lakes is likely to put important constraints on its value. The calculated distribution for a value of G = 1.3 HFU is shown in fig. 5.14.

(vi) the mutual coupling between ice flow and its thermodynamics causes ice sheet evolution to have a long time scale. Consequently, the ice sheet is still reacting to past changes in climatic boundary conditions. An experiment with the Vostok temperature and accumulation forcing yields the present imbalance of the ice sheet caused by these thermomechanical effects. It indicates that the overall balance is quasi-stationary to slightly positive. The spatial distribution suggests that East Antarctica is still thickening, whereas West Antarctica appears to be generally thinning. A typical rate for the local imbalance is 1cm/y and the thickening is slightly enhanced when heat conduction in the bedrock is included.

FIXED GROUNDING LINE EXPERIMENTS

It should be stressed, however, that all these results relate to experiments in which changes in the area of the ice sheet have not been taken into account. It is conceivable that the response of, in particular, the West Antarctic ice sheet may be entirely different in case also changes in the grounded domain come into play. This is discussed in subsequent chapters.

6. SENSITIVITY EXPERIMENTS ON THE GLACIAL-INTERGLACIAL CONTRAST

6.1. EXPERIMENTAL SETUP

Although the fixed-domain sensitivity experiments discussed in the previous chapter certainly give valuable insight into basic mechanisms at work, the real variable of interest in climatic studies are changes in ice sheet extent and the associated changes of ice volume. This certainly applies to the longer climatic time scales, when fluctuations of the Antarctic ice sheet have an important role in modulating global atmospheric and oceanographic processes, and contribute significantly to world-wide sea levels.

As described previously in § 2.3.2., on these longer time scales four main mechanisms can be identified by which the Antarctic ice sheet reacts to changes in the climate system. First, changes in surface boundary conditions which result in lower ice temperatures in the basal shear layers will reduce deformation rates, thereby leading to a thickening. Second, changes in ice deposition rates modify the local stress field through changes in mass balance and ice sheet geometry and affect the amount of ice that is discharged into the ice shelf. Third, lower global sea level stands, induced by the glacial cycle on the continents of the northern hemisphere, reduce the thickness necessary for grounding in regions where the bed is below sea level. Fourth, isostatic bed adjustments and fluctuations in ice shelf thickness, associated with different stress conditions and climatic forcing, have a similar effect on grounding.

These mechanisms raise a number of fundamental questions concerning the Antarctic ice sheet's basic behaviour, namely (i) what is the relative importance of changes in these environmental conditions; (ii) what are the response time scales connected with these changes; and (iii) what is the

spatial distribution of the resulting ice sheet fluctuations. In this chapter an attempt is made to answer these questions by means of *steady state* sensitivity experiments of the type 'all other things being equal'. Reconstructions of past Antarctic ice sheet configurations will then provide estimates of the associated contribution to world-wide sea level. Some of the results presented here have also been published in Huybrechts (1990b).

6.2. RESULTS

6.2.1. Interglacial 'steady state' reference run

Studying changes in ice sheet geometry requires a reference state, against which model output can be compared. Starting from the observed ice sheet and running the model forward in time with prescribed changes in environmental conditions is a less meaningful way to proceed, because it is unlikely that the input data are in full internal equilibrium with the model physics. The model ice sheet will certainly evolve from the present observed state, but it would be unclear why. Shortcomings in the description of ice mechanics, insufficient data, or the fact that the present ice sheet is just not in steady state could all play a role. As a consequence, it would be impossible afterwards to distinguish between the 'natural model evolution' and the 'real' ice sheet response. One way to circumvent this ambiguity is to define a steady state and relax the model to equilibrium. The resulting steady state interglacial run, although differing from the presently observed data in some detail, should then be used as reference in a climatic change experiment.

To do this, the reference state described in § 5.2.1 is taken, but the grounding line is allowed to migrate to a stationary state for another 100000 years. The result is shown in fig. 6.1, where a comparison is made with present day measurements. Apart from the deviations in ice thickness for reasons discussed previously in § 5.2.1 (in particular in the Antarctic Peninsula, and in the Pine Island and Thwaites Glacier catchment areas), the model now also shows a slight recession of the grounding line at the seaward edge of the most overdeepened outlet glaciers of the East Antarctic ice sheet (Totten, Ninnis and Mertz Glaciers). In West Antarctica, the model fails to resolve several narrow channels seperating ice covered islands from the mainland.
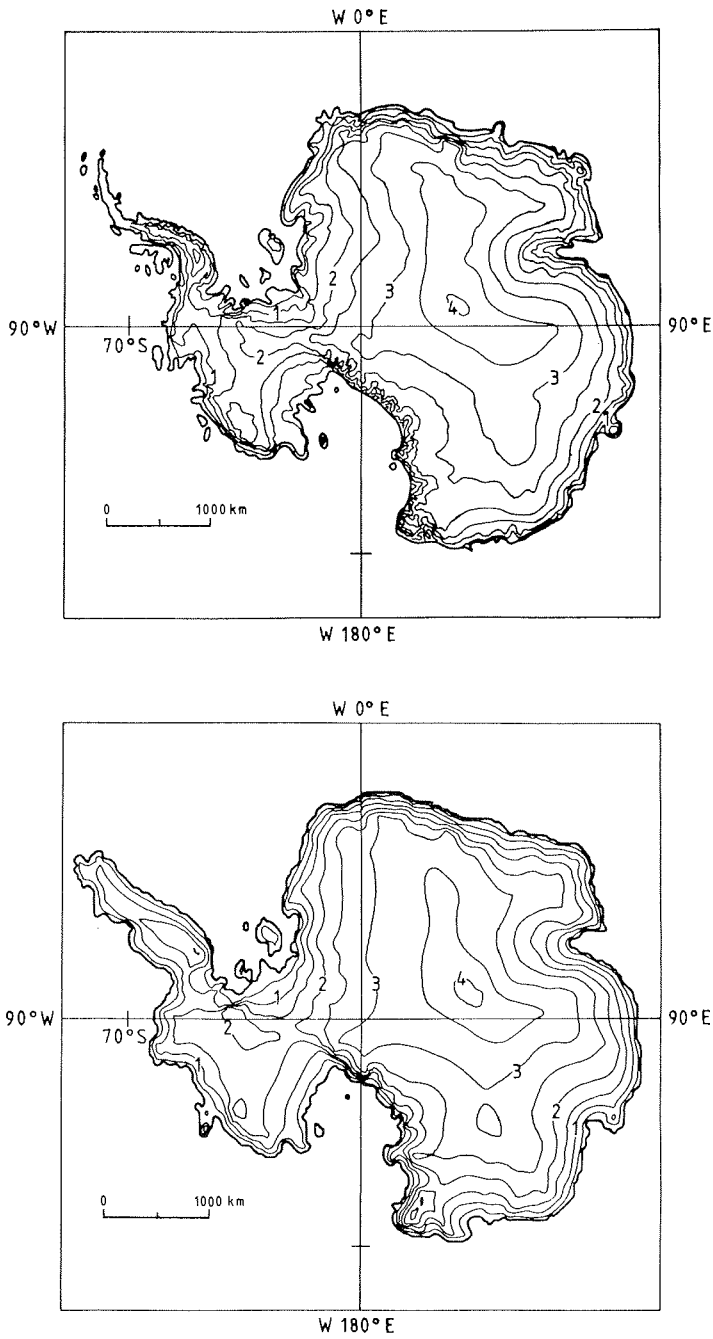
165

fig.6.1: A comparsion between surface elevations produced by the interglacial 'steady state' reference run and the observations. upper: observations; lower: model.

Also surface slopes inland of the Ross ice shelf tend to be somewhat larger than observed. However, considering the complexity of the model and the fact that the complete geometry is *internally generated*, the resulting configuration is certainly acceptable, and the model seems capable of reproducing the most important characteristics of the ice sheet. Notably in this respect is the successful simulation of the various ice domes and the semi-circular pattern of contour lines upstream some of the larger outlet glaciers, such as Byrd Glacier and Lambert Glacier. In the reference state, the ice sheet's volume is 25.02 million km^3 and its grounded area is 12.59 million km^2, compared to 24.10 million km^3 and 12.69 million km^2 for the observations, respectively.

6.2.2. Effect of changes in environmental conditions

In order to examine how environmental factors combine to produce the glacial extent, as documented in the geological record, the model has been submitted to shifts in accumulation rate, surface temperature and eustatic sea level of typical glacial-interglacial magnitude. These are a 10°C uniformly distributed temperature drop, the associated reduction in surface depositon rates (calculated relative to the saturation water vapour pressure of the air circulating above the surface inversion layer) and a eustatic sea level depression of 130 m. Another potentially important external forcing, namely melting beneath ice shelves, has been disregarded, simply because its present distribution is not known very well, let alone the potential effect of a modified sub-shelf circulation during glacial times. However, since the interest is in colder climates than today, it is unlikely that bottom melting played a major role.

Six experiments were considered, in which each of the above mentioned factors are involved, either singly or in combination. In these experiments, sudden stepwise changes in boundary conditions were applied and the model was run 100000 years forward in time, so that approximately steady conditions are achieved. Calculations started from the fixed-domain ice sheet geometry described in the previous chapter. Model runs combining 'full-glacial' conditions in temperature *and* accumulation rate had the fixed-domain glacial run as initial condition.
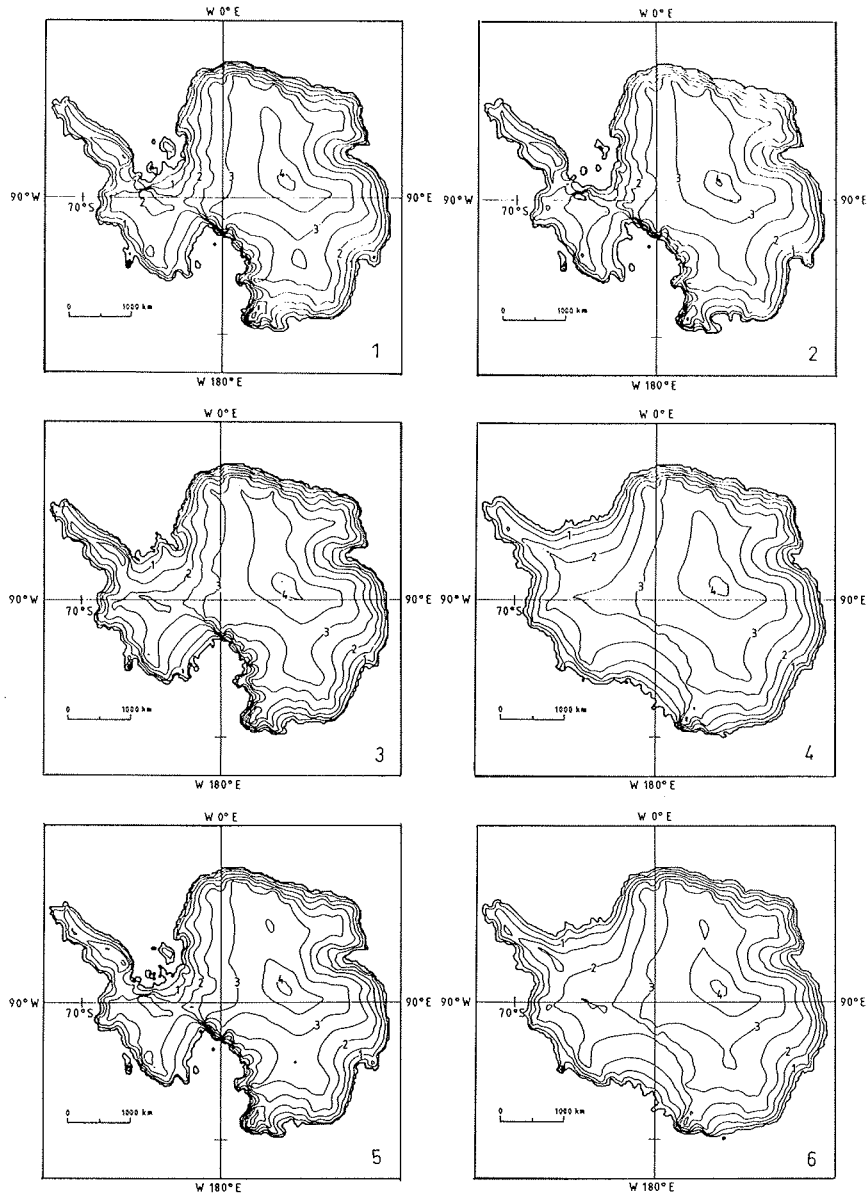
6.2.2.1. ice sheet geometries

The resulting geometries are displayed in fig. 6.2. Lowering accumulation rate to glacial levels (about 50-60 % of Holocene values) results in a thinning of grounded ice by several hundred meters. This effect is enhanced by grounding line retreat in the West Antarctic ice sheet. Although the grounding line enters progressively deeper water, it appears that a new equilibrium can still be established between ice thickness and water depth and there is no collapse. The opposite result is seen when lower surface temperatures are imposed, which eventually reduce deformation rates in basal layers. In this case, ice volume increases substantially over East Antarctica and an important part of the Ronne ice shelf runs aground on the shallow seabed, resulting in a significant advance of the grounding line. As these climatically-induced effects are of comparable magnitude, but of opposite sign, it is not surprising that the ice sheet geometry is almost unchanged, when both climatic conditions are now varied together. So, once more, glacial-interglacial changes in accumulation rate and ice temperature have largely counteracting effects on ice thickness. This is true not only in the grounded ice sheet (cf. chapter 5), but also for the ice shelf and at the grounding line.

It is also evident from figure 6.2 that by far the most decisive environmental factor is eustatic sea level: lowering sea level by only 130 m is sufficient to initiate complete grounding over the shallow continental shelf areas. The effect is particularly pronounced over the West Antarctic ice sheet, where the present Ross and Ronne-Filchner ice shelves completely disappear and grounded ice extends to the edge of the continental shelf. Although apparent in some places (in particular along major outlet systems in Wilkes Land), seaward changes in the East Antarctic ice sheet are rather limited. This is a direct consequence of the subglacial bed topography, which is relatively steep and slopes down towards the sea.

Imposing full glacial conditions reduces ice thickness somewhat, but the extent of the ice sheet appears to be primarily governed by fluctuations in sea level. Comparing this glacial state with the reference run demonstrates that surface elevations over the East Antarctic ice sheet do not change much. The thickening in its western counterpart is much more pronounced, because of important changes in the horizontal ice sheet domain. Apart from speculation

fig.6.2: Calculated ice sheet geometries in response to glacial-interglacial changes in environmental conditions. Elevation contours (in km) are 0.5 km apart, the lowest contour is the grounding line. (1) interglacial reference state. (2) glacial accumulation rate. (3) background temperature drop of 10°C. (4) sea level depression of 130 m. (5) combination of 2 and 3. (6) full glacial state, i.e. a combination of 2, 3 and 4. See text for more explanation of these boundary conditions.

169

that the ice sheet might have been somewhat smaller in the Ross Embayment, this picture seems to fit rather well with Antarctic reconstructions based on empirical field evidence (cf. chapter 3). It also suggests that the model is able to describe the relevant physics of the coupled ice sheet-ice shelf system in a fundamentally correct manner.

6.2.2.2. temperature distributions

The corresponding basal melting areas in these experiments are shown in fig. 6.3. These fields are important in the dynamics of the ice sheet, because they constrain areas where basal sliding can occur. The occurrence of melting also indicates that old ice is gradually lost at the base. This is of relevance to the establishment of a time scale for the bottom layers of deep ice cores. In general, the higher ground beneath the East Antarctic ice sheet is unaffected by basal melting. Melting becomes widespread when the ice sheet completely grounds under present climatic conditions and reduced sea level (panel 4). Besides thickening the ice, another particularly effective way of warming the base is to reduce accumulation rates (panel 2), so that less cold ice is advected downwards. It is also interesting to note that the ice sheet filling the Ross and Ronne-Filchner Embayments at maximum glaciation is always wet-based. This has consequences for the surface slopes in these areas, which are shown in fig. 6.2. to be flatter than those in continental-based East Antarctica.

How the different modes of heat transfer combine to yield the temperature field in a vertical cross-section through the ice sheet for the reference and the glacial states, is shown in figure 6.4. In the interglacial state, upper layers tend to be significantly more isothermal and the plot also shows a tongue of cold ice pointing towards the base. As a result, the vertical temperature profile exhibits an inversion in the more marginal parts of the ice sheet, which is due to cold ice advection from above. These effects become much less pronounced in the glacial state, when accumulation rates are lower. The modelled temperature profiles appear to be qualitatively in good agreement with theoretical predictions and are consistent with the sparse observations from deep drilling sites (Robin, 1983; Bolzan, 1985; Ritz, 1989).
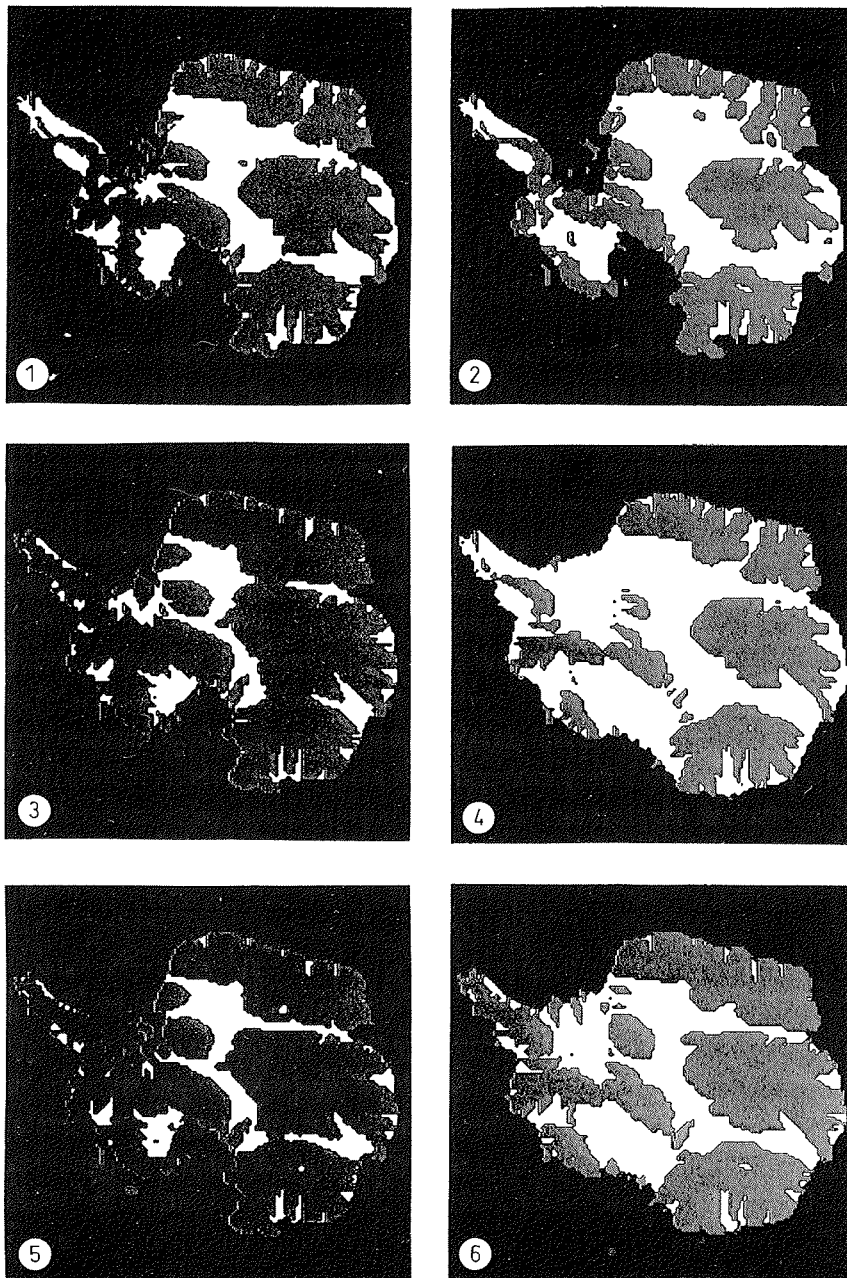
fig.6.3: Areas at pressure melting point (white) under different environmental conditions. (1) interglacial reference state. (2) glacial accumulation rate (50-60% of Holocene values). (3) background temperature drop of 10°C. (4) sea level depression of 130 m. (5) combination of 2 and 3. (6) glacial state, combination 2, 3 and 4.
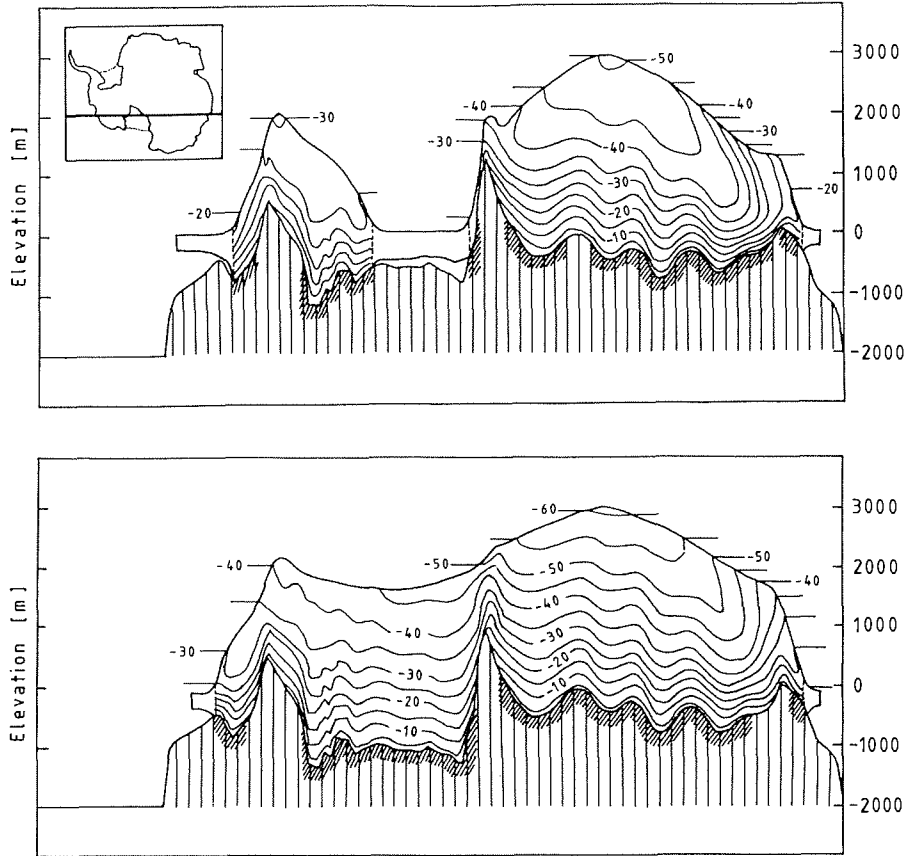
fig.6.4: Vertical cross-sections through the ice sheet showing the temperature distribution. The upper plot refers to the interglacial reference run, the lower is for glacial conditions. Basal melting is indicated by cross-hatched bars. The bold line in the inset gives the location of the cross-section (for j = 51).

6.2.2.3. response time scales

The experimental setup makes it possible to assess the associated response time scales . Fig. 6.5 summarizes the time evolution of some large-scale model variables in these sensitivity runs. Shown are the number of grounded grid-points (1 gridpoint represents an area of 16 x 10^8 m^2), ice volume, ice volume expressed in equivalent sealevel change and mean basal temperature. Looking at model run (6), which is the glacial state, it appears

fig. 6.5: Evolution of some large-scale variables in these model simulations. Numbers relate to the same experiments as in previous figures. (1) interglacial reference. (2) glacial accumulation rate (50-60% of Holocene values). (3) background temperature drop of 10°C. (4) sea level depression of 130 m. (5) combination of 2 and 3. (6) glacial state, combination of 2, 3 and 4.

173

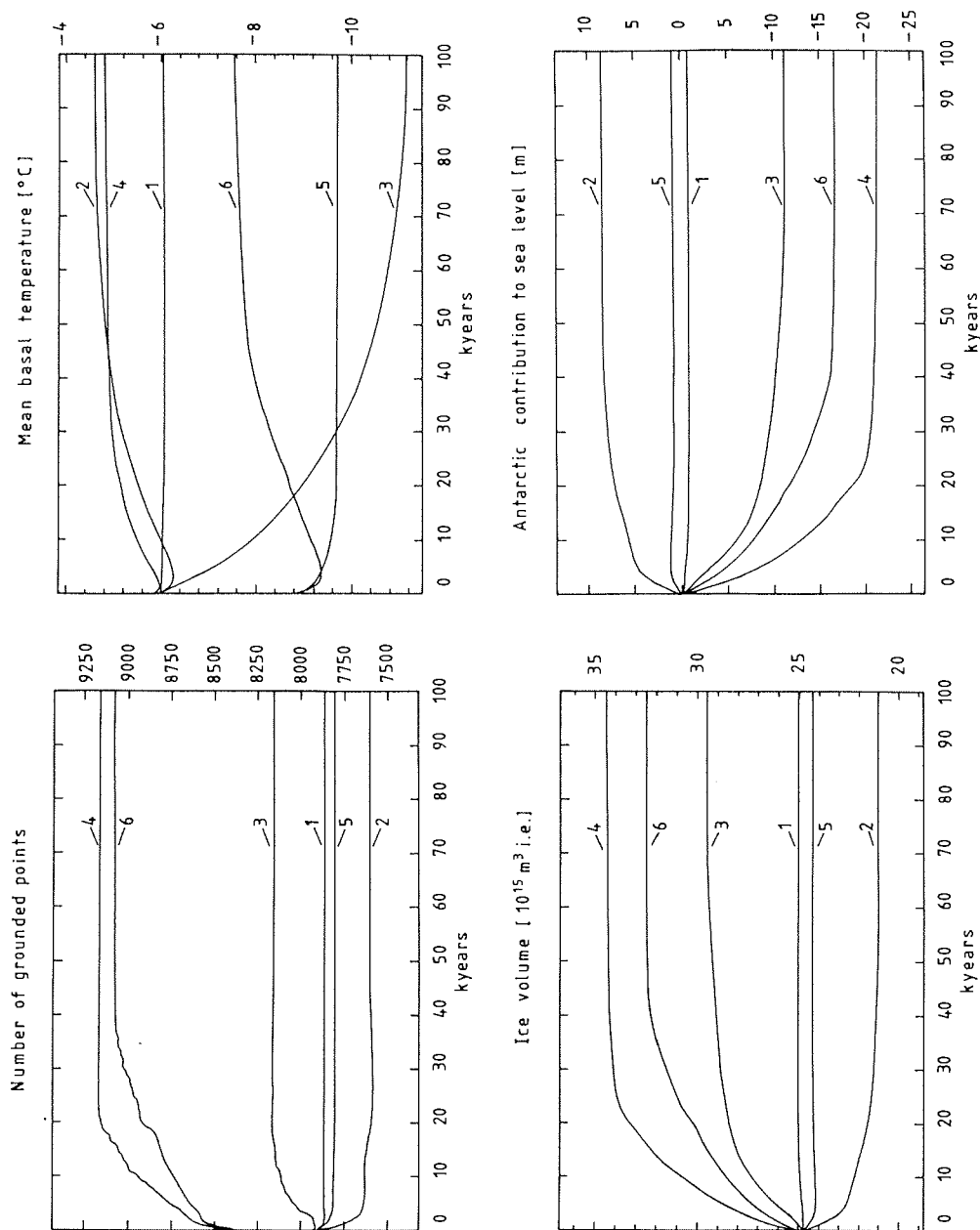that it may take up to 30-40000 years for the Ross and Ronne-Filchner ice shelves to become completely replaced by grounded ice. This is mainly a consequence of the low accumulation rates prevailing over the Antarctic ice sheet. This time lag should be considered as an upper bound, because accumulation rates were already at the glacial level at time zero. However, it is a good indication for the large inertia involved. In a real-world transition to a glacial state, environmental conditions change more gradually, and the time span separating the ice sheet extent at any stage from its equilibrium is therefore likely to be shorter.

The transient mechanism for grounding-line advance can be understood as follows. When the level of the water is lowered, the ice shelf grounds in those areas where the free water depth is insufficient to float the ice, leading to an immediate northward displacement of the grounding line. Following this, the newly formed grounded ice starts to thicken because the ice no longer rests on a frictionless base but on a rough bed. This thickening is by both local accumulation and inflow from upstream. Outflow is reduced until the necessary stresses are build up to drive the ice outwards. This is a positive feedback and results in a further advance of the grounding line. It stops when a new equilibrium is established between ice thickness and water depth. Changes in ice shelf spreading rates enter indirectly by partial control on the mass outflow at the grounding line. This process may take several ten thousands of years depending on the amount of accumulation, as just described.

Fig. 6.5 also provides some numbers on the final ice sheet geometries. According to the model, the 'glacial' ice sheet area has expanded by 17%, but the volume has increased from 25.0 to 32.4 x 10^6 km^3 of ice (i.e.+30%). This corresponds to an Antarctic contribution to global sea level lowering of some 16 m, assuming a value of 362 million km^2 for the surface of the world's oceans and including the effect of grounded ice that is merely displacing ocean water. Imposing a background temperature drop of 10°C (run 3) leads to an increase in ice volume of 4.2 x 10^6 km^3 (+16.9%), but the associated reduced accumulation rates (run 2) largely counteract this (-16.0%). When both conditions are applied together (run 5), ice volume diminishes by only 2.8%. Keeping the surface climate fixed, but imposing a sea level lowering of 130 meter (run 4) results in the largest ice volume. In this case, the

174

corresponding contribution to global sea level amounts to some 20 m (relative to the interglacial reference run).

6.2.3. Comparison with previous studies

It is of interest to make a comparison of these model simulations with results obtained in previous studies. Estimates of the Antarctic contribution to sea level lowering at maximum glaciation have been made earlier in numerical studies by Oerlemans (1982b) and Budd and Smith (1982). These ice flow models operated on a coarser 100 km grid and excluded thermodynamics and ice shelf flow. In common with the present result, both studies predicted a large increase in the volume of the West Antarctic ice sheet if sea level was lowered by 100-150 m. Ice volume increases *with respect to the observations* turned out to correspond to sea-level falls of between 27.5 m (Oerlemans, 1982b) and 33 m (Budd and Smith, 1982). However, these models were unable to simulate the Ronne-Filchner ice shelf in the reference state and strongly overpredicted the ice cover over the Antarctic Peninsula. As a result, calculated ice volumes for present-day conditions were already far in excess of the observations by 25-50%.

A similarly high estimate for the late Wisconsin contribution to global sea level was also reported by Nakada and Lambeck (1988). They believe that Holocene retreat of the Antarctic ice sheet could have added as much as 35 m to the world's oceans. This result was obtained in an indirect way, by subtracting the equivalent of the ice volume of fully-grown northern hemisphere ice sheets from the 130 m of total sea level change and matching the resulting melting histories with calculated and observed vertical movements of the Earth's mantle.

Although modelling approaches are fundamentally different, a further comparison can be made with the steady state reconstruction of the CLIMAP-group (Stuiver et al., 1981; cf. fig. 3.5). In their approach, ice sheet margins were not generated by the model, but 'known' locations of domes, flowlines and margins served as constraints to calculate former elevations and flowline profiles. This was done by employing plastic ice flow theory, where the yield stress for each point was calculated in a complicated way from such elements as basal thermal conditions (sliding/ no sliding) and transverse flowline

175

geometry. However, their reconstructed ice thicknesses were also substantially larger than those produced in our simulation (fig. 6.2), although the ice sheet extent agrees more closely. In particular over the West Antarctic ice sheet, the CLIMAP surface elevations are consistently higher by more than 500 m. The total ice volume during the LGM would in their reconstruction have increased to 37.1×10^6 km^3. This is equivalent to 24.7 m of sea-level fall, of which 16.3 m originates from West Antarctica and 8.4 m from East Antarctica. Using a rock-to-ice density ratio of 3 instead of their preferred value of 4 would result in even larger volumes, yielding corresponding figures of 29.2 m, 17.7 m and 11.5 m (Stuiver et al., 1981).

In contrast to these studies, we obtained a value of only 16 m. This can be explained by a more refined treatment of ice mechanics, especially in the basal layers, and the incorporation of thermo-mechanical coupling. Also the inclusion of lower accumulation rates during the LGM, as indicated by the Vostok ice core, represents a significant contribution to our result. These additional factors were not included in any of the studies discussed above.

6.3. SUMMARY

In this chapter, we discussed results from a number of steady state experiments with the complete model, in which all internal degrees of freedom were taken into account. This approach helped to disentangle the complex interaction of environmental controls (accumulation rate, ice temperature and sea level) on the behaviour of the ice sheet. The main points that arise of this study can be listed as:

(i) first, it appears that the model is able to account for the major characteristics of the ice sheet's flow pattern, including a correct simulation of the main ice divides, ice domes and major ice shelves. The calculated grounding line under present-day environmental conditions is generally close to its observed position. Somewhat larger deviations include a slight recession (order of magnitude: 100 km) along the most overdeepened outlet glaciers in East Antarctica and the incorporation of several small ice-covered off-shore islands into the main ice sheet in West Antarctica. These imperfections may

respectively be attributed to a possible overprediction of basal sliding and the coarse representation of deep bedrock channels.

(ii) in line with glacial-geological evidence, the most pronounced ice sheet fluctuations occur in the West Antarctic ice sheet. Most of the implied spreading of grounded ice across the shallow Ross and Weddell Seas during glacial periods can be attributed to lower global sea levels.

(iii) lower ice temperatures also lead to expanded ice cover and larger ice thicknesses, but the associated accumulation rate reduction largely counteracts this effect. In the full-glacial state, surface elevations over the East Antarctic plateau do not change much.

(iv) grounded ice in the Ross and Weddell Seas is always at the pressure melting point and basal sliding occurs. This results in smaller surface slopes compared to the East Antarctic ice sheet.

(v) according to our steady state reconstruction, the Antarctic ice sheet may contribute some 16 m (relative to the reference run) to global sea level lowering at maximum glaciation. This is substantially less than other figures put forward in previous studies. In particular, our ice thicknesses do not support the CLIMAP reconstruction of Stuiver et al. (1981), even though the ice sheet extent agrees better. This is because of the more sophisticated modelling, the incorporation of thermomechanical coupling and the inclusion of a more realistic climatic forcing.

(vi) the low accumulation rates prevailing over the ice sheet lead to long response time scales. The model needed up to 30000-40000 years to relax to ·a full-grown West Antarctic ice sheet after a sudden change in sea level was applied.

An implication of (vi) is that a steady state approach may not really be appropriate to reconstruct the ice sheet's history during a glacial cycle. In other words, since environmental conditions in the Antarctic have not been stable during the long times needed to reach equilibrium, it is unlikely that the ice sheet ever reached a stationary state. This would reduce the figure of 16 m at the Last Glacial Maximum obtained here even further. Consequently, the

177

problem should be envisaged as time-dependent and an attempt should be made to simulate the ice sheet during a complete glacial cycle. This is the subject of the next chapter.

7. MODELLING THE LAST GLACIAL-INTERGLACIAL CYCLE

7.1. EXPERIMENTAL SETUP

A direct consequence of the long response times found in the previous chapter is that the Antarctic ice sheet may never completely reach its 'maximum possible' glacial extent. This possibility is further explored in this chapter, where an attempt is made to model the last glacial-interglacial cycle. Apart from yielding a more detailed picture of the transient behaviour of the ice sheet as a whole, and thus of its contribution to global ice volume and sea levels during the last ice age, results of such an experiment may also be of wider interest.

First, information on dynamic changes of the ice sheet, in particular of such features as surface elevation and the general flow pattern, are important in the light of the interpretation of climatic information in ice cores (Byrd, Vostok, Dome C). Second, a detailed knowledge of the ice thickness distribution in space and time is one of the boundary conditions for models of other components of the climate system.

Third, modelling a full glacial-interglacial cycle is a good validation of the model: not only should the model be able to simulate a glacial buildup, but it should also reproduce a deglaciation. In other words, if the model can simulate past ice sheet behaviour in reasonable agreement with geomorphological field evidence, then it would have sufficient credibility to be used in predictions of future ice sheet changes, such as those associated with the expected greenhouse warming of the earth's atmosphere. Finally and more speculatively, such an experiment may yield information on the present

evolution of the ice sheet. Up to now, a model run of this type has not been performed.
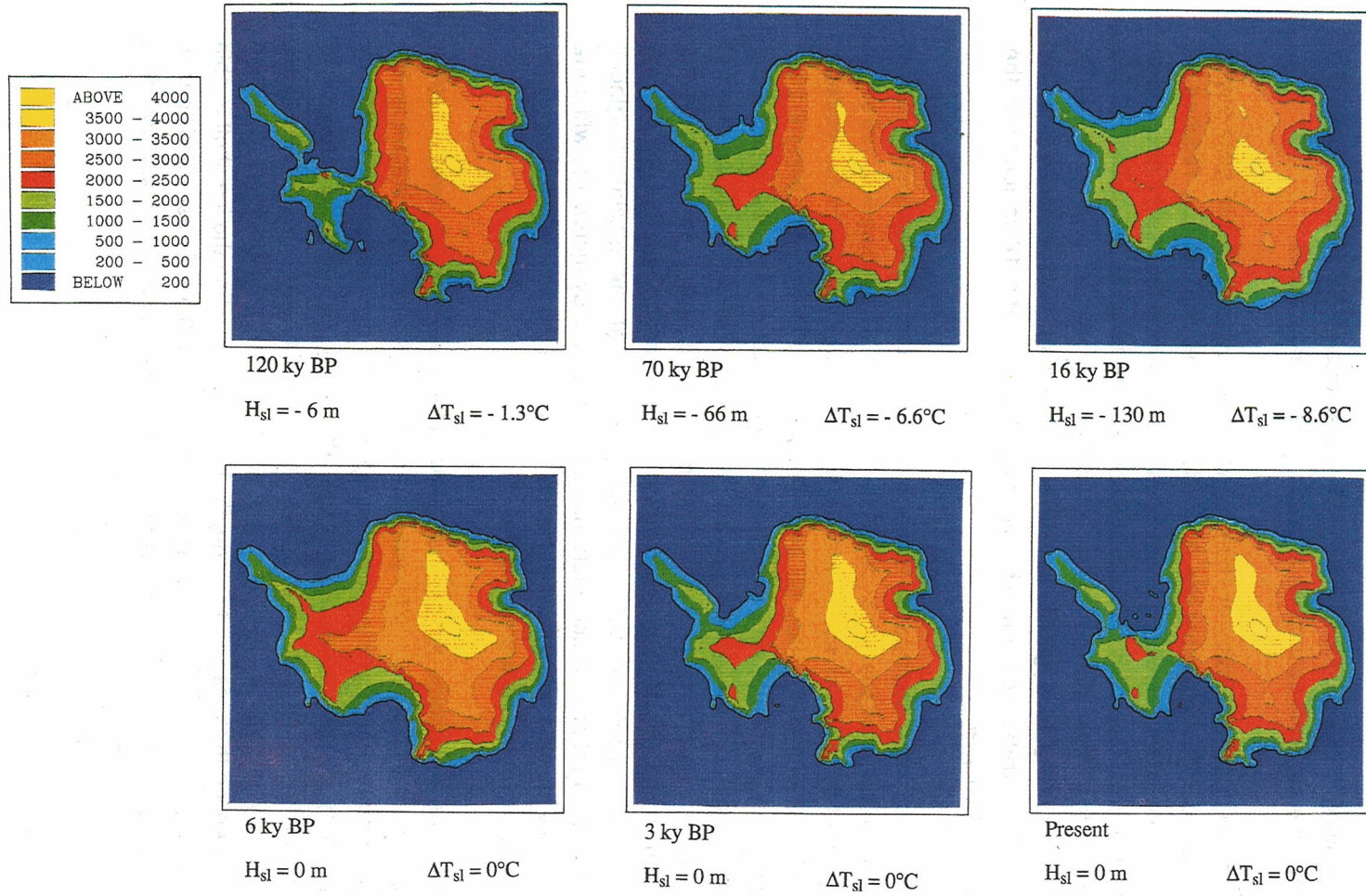
The model ice sheet has been run initially to a stationary state with a sea level depression of -130 m and a temperature perturbation of -5°C. Calculations start at 164000 years BP. Model forcing consists of the Vostok temperature signal, which perturbs the accumulation and surface temperature fields, and sea level, which is prescribed as a piecewise-linear sawtooth function. In order to assess the impact of this specific sea-level function, an additional experiment is conducted with a sea level record derived from coral terraces on New Guinea, and results are compared. These forcing functions were discussed in more detail in § 4.8.3. The main model results presented here have also been described in Huybrechts (1990a).

7.2. RESULTS

7.2.1. Ice sheet evolution

Figure 7.1 displays the Antarctic ice sheet at several stages during the last glacial cycle. The first picture is of the ice sheet during the Eem interglacial at 120 ky BP. Clearly, the ice sheet is significantly smaller than today, in particular in West Antarctica. However, as pointed out below, this model behaviour should not necessarily be interpreted as proof for a West Antarctic ice sheet collapse at that time, and is probably also caused by the specific startup conditions used.

During the subsequent glacial buildup (second picture), a moderate lowering of sea level by some 35-40 m is enough to initiate grounding in the Weddell Sea, and the ice shelf runs aground on a number of high sea-banks near the present ice shelf front. This obstructs the ice flow landinwards and results in a relatively rapid thickening, so that almost instantaneous grounding occurs over a large area. The situation in the Ross Sea, on the other hand, is quite different. Here, the free water depth below the ice shelf generally *increases* towards the sea and consequently, grounding is of a more gradual nature. Also the threshold for grounding appears to be larger and widespread

ABOVE	4000
3500	– 4000
3000	– 3500
2500	– 3000
2000	– 2500
1500	– 2000
1000	– 1500
500	– 1000
200	– 500
BELOW	200

120 ky BP

$H_{sl} = -6$ m $\Delta T_{sl} = -1.3°C$

70 ky BP

$H_{sl} = -66$ m $\Delta T_{sl} = -6.6°C$

16 ky BP

$H_{sl} = -130$ m $\Delta T_{sl} = -8.6°C$

6 ky BP

$H_{sl} = 0$ m $\Delta T_{sl} = 0°C$

3 ky BP

$H_{sl} = 0$ m $\Delta T_{sl} = 0°C$

Present

$H_{sl} = 0$ m $\Delta T_{sl} = 0°C$

fig.7.1: Stages in the modelled evolution of the Antarctic ice sheet during the last glacial-interglacial cycle . Hsl: world-wide sea level stand; ΔTsl: temperature change. Times as indicated; contours are in m above present sea-level.

grounding is only produced in the later stages of a glacial period, in particular when the sea level depression exceeds 100 m (third picture).

Comparing the simulation at 16 ky BP with the stationary 'glacial' geometry in fig. 6.2 demonstrates that the Antarctic ice sheet has not fully reached its maximum extent, especially in the Ross Sea. This was anticipated because of the long response time scale for grounding-line advance (§ 6.2.2.3). At this stage, the Antarctic ice sheet volume has grown to 31.0×10^6 km^3, corresponding to a global sea level lowering of 12.3 m relative to the interglacial reference run. This is even less than the 16 m found in the previous chapter.

The concomitant deglaciation of the Antarctic ice sheet is essentially a partial desintegration of the West Antarctic ice sheet. Grounding-line retreat is triggered by a rise of world-wide sea-level, but lags behind. In the model, it begins around 8000 years BP and is nearly completed by the present time. This delay may be related to increased accumulation rates, which during the early stages of the Holocene thicken the ice and offset the retreating effect of rising sea level. The time lag between the onset of the recession and the beginning of the climatic warming is also the reason why the ice volume reaches a maximum during the early stages of the glacial-interglacial transition: at that time accumulation rates have already increased, while the ice sheet domain has not yet started to shrink and the surface warming signal has not reached basal shear layers.

Once the thresholds for grounding-line retreat are passed, overall retreat appears to take around 6000 years to complete. An important feature is that this disintegration seems to develop its own dynamics: environmental boundary conditions do not change after 6 ky BP, and the process of grounding-line retreat, once it has been initiated, then becomes entirely internally controlled. It only stops when a new equilibrium is achieved between ice thickness and sea depth. This happens when the ice shelf is able to stabilize the ice sheet and prevent excessive outflow. Stress conditions in the ice shelves then keep the grounded portions in place, and consequently, there is no collapse.

Fig. 7.1 also shows that the ice sheet retreats earlier in the Ross Sea than in the Weddell Sea. Like the glacial buildup, this is caused by the existence of a eustatic threshold for grounding-line migration, which is larger for the Ross Sea. A crucial role is also played by the bed adjustment process: it allows the grounding line to retreat into depressed inland areas, but subsequent isostatic rebound slows the retreat down and eventually results in a small advance. It is interesting to note that during this evolution, ice rises in the Ronne-Filchner ice shelf (Korff Ice Rise and Berkner Island) never completely disappear. In the East Antarctic ice sheet, on the other hand, changes in ice thickness are less pronounced and reflect the combined effects of accumulation and temperature changes much like the fixed-domain studies discussed earlier, onto which a thinning wave caused by postglacial grounding line retreat is superimposed. The thresholds for grounding-line recession are also different for each outlet system. Retreat occurs first in the Totten Glacier area at about 9 ky BP and ends at 6 ky BP. In the Ninnis/Mertz glacier system, retreat starts at 5 ky BP and is finally completed only by 3 ky BP. When the model is run for another 50000 years into the future, it produces an ice sheet virtually identical to the present interglacial reference state.

The overall response of the ice sheet in this experiment is summarized in fig. 7.2. Displayed are the model forcing functions and the evolution of ice volume and the equivalent sea level changes. Clearly, the dominant forcing is eustatic sea level, and the response is modulated by fluctuations in accumulation rate and ice temperature. Changes in surface altitude are of considerable interest in the interpretation of information from deep ice cores. They are shown in the lower panel for two locations. Typical elevation changes at Vostok station (East Antarctic ice sheet) are generally within 150 m, whereas the modelled fluctuations at Byrd (West Antarctic ice sheet) are substantially larger. These values should not be taken too literally, in particular during the first 50000 years or so which are needed for the model to forget its initial conditions. However, they suggest that the climatic signal recovered at Vostok is probably not biased too much by level fluctuations. The situation for Byrd, on the other hand, is likely to be a lot more complicated because of important changes in the grounded ice domain.

GLACIAL CYCLE
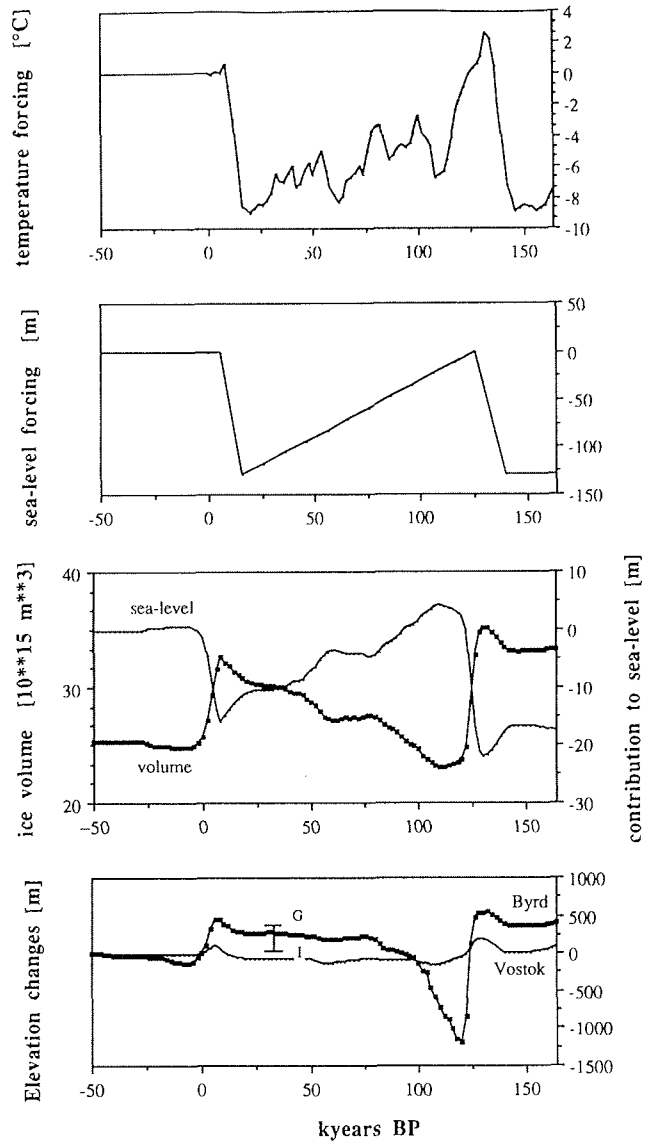
fig.7.2: Forcing (upper panels) and evolution of some large-scale model variables (lower panels) in the 'standard' model experiment on the last glacial cycle. The vertical bar in the lowest panel refers to the glacial (G) and interglacial (I) steady states at Byrd (80°S, 120°W). The corresponding bars for Vostok (78.5°S, 106.8°E) should be at -9 and -1m, respectively. They are not shown because they almost coincide, which is because of the counteracting effects of changes in accumulation rate and temperature, and to a lesser extent grounding-line movements. The conspicious 'low' during the Eem should not be taken too literally and may be a model artefact for reasons discussed in the text.
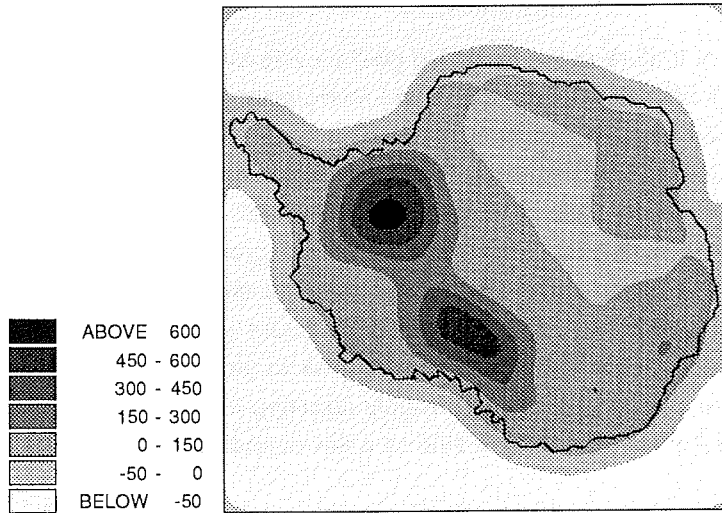
184

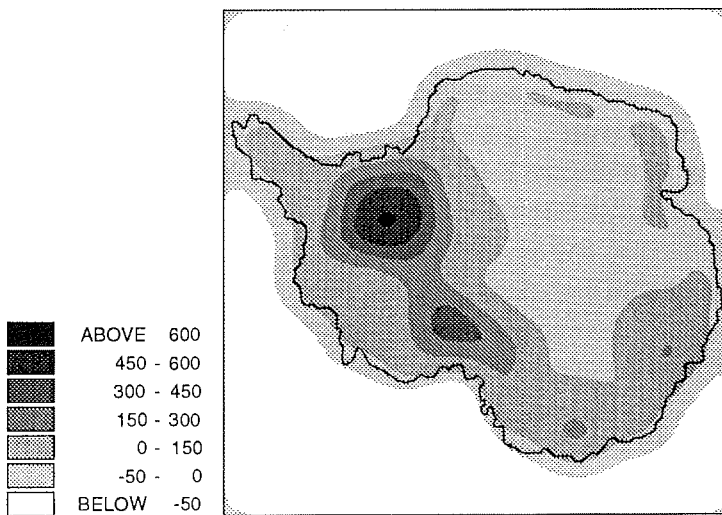## 7.2.2. The Antarctic ice sheet during the Last Interglacial

An apparent feature of the modelled glacial cycle is the remarkable low during and shortly after the Sangamon (Eem) interglacial, when the calculated West Antarctic ice sheet is substantially smaller than today. Although there is no complete collapse, this ice sheet geometry would contribute almost 4 meter to global sea level. This situation is of special interest because global temperatures during the Eem were several degrees higher than during the Holocene and because the state of the polar ice sheets then is often seen as an analogue of behaviour during possible future greenhouse warming. The effect of such higher temperatures would be to weaken the ice shelves and reduce their buttressing effect, possibly resulting in the collapse of the West Antarctic ice sheet in as short a time as a few centuries (cf.§ 2.4.1).

It should be stressed, however, that this mechanism of grounding line instability is not of relevance here, since the present experiment does not consider the possibility of disintegrating ice shelves that break up completely. Nor is basal melting beneath the ice shelves included. Instead, since environmental forcing during the last two deglaciations (i.e. between 140-125 ky and 16-6 ky BP) appears to be qualitatively quite similar, the modelled reaction seems to be primarily a consequence of the choice of initial conditions, in particular a fully depressed steady state 'glacial' bed at 140 ky BP. Together with specific bathymetric conditions beneath the West Antarctic ice sheet (bedrock sloping down towards the interior), these startup conditions allow the grounding line to retreat substantially more into inland areas during the Last Interglacial than during the Holocene. The effect is illustrated in more detail in fig.7.3, showing the bedrock depression relative to the interglacial reference run at the onset of the last deglaciation (16 ky BP, lower plot) and at the onset of the preceding deglaciation (140 ky BP, upper plot). Clearly, in central parts of the Ross Sea the bed is depressed more at 140 ky BP (by up to 150 meters) than at 16 ky BP. Although not leading to a catastrophic collapse, these results nevertheless suggest that a greater disintegration of the West Antarctic ice sheet is possible, as long as the bed is depressed deeply enough and/or sea-level is rising more rapidly than the land is being uplifted isostatically. In other words, these results suggest an alternative enhanced retreat mechanism, in which the interplay between sea level and crustal rebound during a glacial-interglacial transition are key elements, and

GLACIAL CYCLE

ABOVE 600
450 - 600
300 - 450
150 - 300
0 - 150
-50 - 0
BELOW -50

140 ky BP

ABOVE 600
450 - 600
300 - 450
150 - 300
0 - 150
-50 - 0
BELOW -50

16 ky BP

fig.7.3: Depression of the subglacial bed relative to the interglacial reference run [in meter, positive downwards]. upper: steady state 'glacial' situation at 140 ky BP; lower: situation at 16 ky BP.

which may be amplified under suitable conditions. In reality, however, the depression at 140 ky BP may not have been at equilibrium, and the glacial-interglacial transition may have been more like the situation at 16 ky BP.

7.2.3. Present-day imbalance of ice thickness and bed elevation

The experimental setup also allows us to estimate the magnitude of the present-day imbalance between ice thickness and bed elevation, although such an interpretation must be reserved because of the late deglaciation produced by the model. The bedrock rise needed before steady conditions are achieved is displayed in fig. 7.4. As can be seen from this plot, central areas in West Antarctica still have to recover between 200 and 250 m, before full isostatic equilibrium is established. It is also interesting to note that according to this calculation an uplift of the order of 100 to 200 m is still to be expected below the Ronne-Filchner ice shelf. This is substantially more than the presently observed free water depth in a large area below the shelf. In particular near the ice shelf front, the sea-bottom is often only 50 m below the ice. If retreat took place as recently as indicated by the model and if the bedrock model is correct, then this suggests that the present ice shelf may be a transient feature and could exhibit internally generated grounding, in the sense that a deglaciation automatically leads to renewed grounding because of delayed isostatic uplift. Different topographic conditions (the sea floor generally slopes down towards the sea) imply that such a mechanism is not likely to occur in the Ross ice shelf. Although on the basis of the results presented here, a substantial advance of the grounding line in the future is certainly conceivable.

Another implication of the imbalance shown in fig. 7.4 is that the assumption of a present-day steady state bed to calculate the undisturbed bed heights (w' in eq. 4.49) may not quite hold true. This ambiguity can however not be avoided because the ice sheet's past history and present-day uplift rates are not well known from observations. If both of these were known, they could be used to constrain models for bedrock adjustment. This would minimize uncertainties in the bedrock's rheology and the unloaded bedrock surface could then be calculated in an iterative way. Using results of ice sheet models (which also depend on isostasy!) to validate models of the upper mantle would in this respect just lead to a circular argument. However, it is not considered likely

187

Bed elevation: deviation from steady state [m]

0 ky BP

ABOVE 200
150 - 200
100 - 150
50 - 100
0 - 50
-50 - 0
BELOW -50
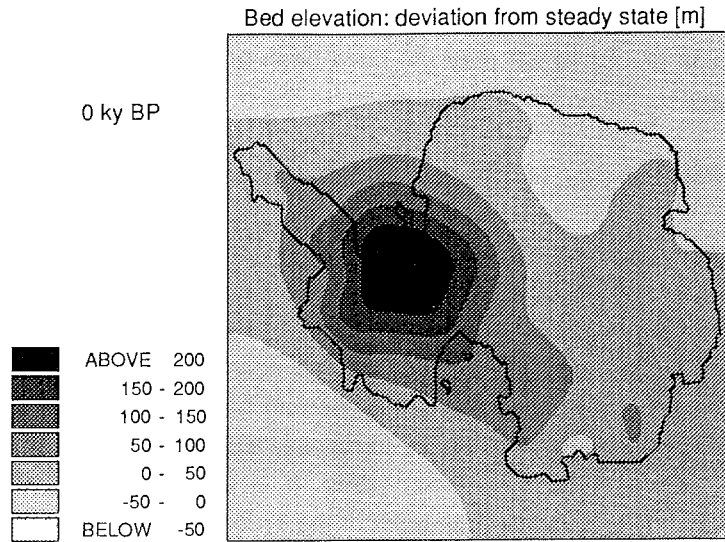
fig.7.4: Bedrock depression at present. Values are relative to the interglacial reference run and indicate the bedrock rise needed to achieve isostatic equilibrium under steady conditions.

Local ice thickness imbalance [m/y]

ABOVE 0.005
0.000 - 0.005
-0.010 - 0.000
-0.050 - -0.010
-0.100 - -0.050
-0.500 - -0.100
BELOW -0.500

fig.7.5: Geographical distribution of the present-day ice thickness imbalance following the last glacial-interglacial cycle. Plotted values have undergone light smoothing.

that the above assumption of stationarity would significantly influence the modelled imbalance *relative* to a reference topography, once such a reference bedrock has been defined.

The geographical distribution of the local ice thickness imbalance, i.e. the present-day rate of change in ice depth, is shown in fig. 7.5. Since grounding line migration is included, the result differs substantially from fig. 5.13, where only thermomechanical effects were taken 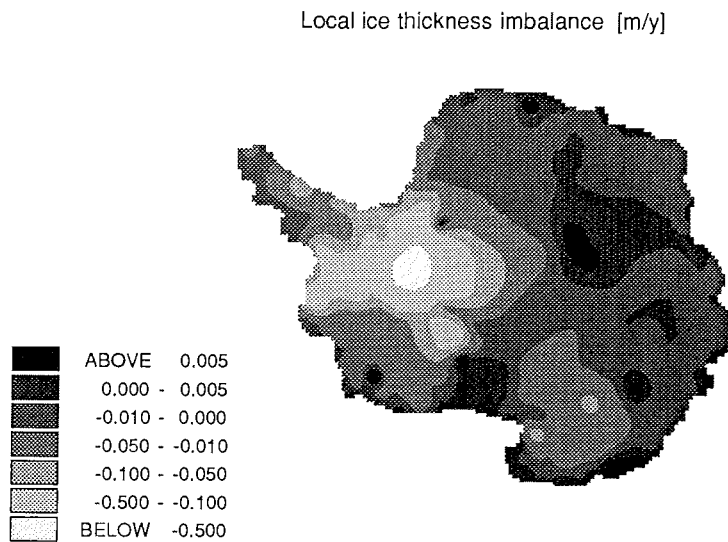into account. The difference is particularly pronounced over the West Antarctic ice sheet, which in the present experiment is still thinning at rates of typically between 10 and 50 cm/y. More in agreement with the previous result, however, is the ongoing slow thickening in interior areas of East Antarctica, although that postglacial grounding-line retreat leads also here to falling elevations inland of the large ice shelves. The mean imbalance, spread out over the entire ice sheet, is -1.6 cm/y. This is less than 10% of the mean annual mass balance and corresponds to a contribution to global sea level of less than 0.5 mm/y. According to the model, this slow thinning trend goes on for another 10000 years at a mean rate of 0.15 mm/y sea-level equivalent, before reversing to a slight growth towards the final equilibrium. Although this result should be interpreted with the necessary caution for the reasons discussed before, one could nevertheless state that the ice sheet as a whole is probably not too far from balance.

7.2.4. Impact of sea level forcing

Fluctuations in the Antarctic ice sheet appear to be primarily driven by changes in eustatic sea level. This implies that the question of how far the ice sheet is out of steady state at maximum extent should essentially depend on the magnitude and duration of the sea level depression during the final stages of a glacial period. Unfortunately, the reconstruction of a reliable record for world-wide sea level during the last glacial cycle proves to be a difficult matter. For various reasons discussed in § 4.8.3, different proxy data were shown to yield different results, which was why the sawtooth function was finally used. Nevertheless, in order to assess the impact of this specific choice, an additional experiment was conducted, in which the sea level record derived from New Guinea terraces was used as model forcing. This sea level curve

should be regarded as a minimum scenario, that is, it indicates a significantly higher sea level, in particular between 30 and 16 ky BP.

The results of this experiment are compared with the standard model run in fig. 7.6. As expected, the difference is largest towards the end of the Wisconsin, and the Antarctic contribution to global sea level at 16 ky BP reduces to 7.8 m. Further inspection of the ice sheet geometry revealed that this lower ice volume is largely caused by the reduced ice sheet extent in the Ross Sea, which now reaches only halfway between its positions in the interglacial reference run and in the steady state glacial model experiment. On the other hand, the positions of the grounding line in the Weddell Sea, along the East Antarctic coast and in the Antarctic Peninsula, are not affected much by this alternative sea level function, nor is the timing of Holocene retreat. In this experiment the ice sheet extent does not expand any further after 15 ky BP, however the actual volume maximum is only reached around 9 ky BP. At that time, corresponding sea-level falls are 12.6 m for the 'New Guinea' experiment and 16.1 m for the 'standard' model run. As discussed before, this is because of the dominant effect of increased snowfall rates during early stages of a glacial-interglacial transition.

7.3. COMPARISON WITH FIELD OBSERVATIONS

There are basically two types of field observations against which the model can be tested. First, the predicted past behaviour of the Antarctic ice sheet can be compared with reconstructions based on geomorphological and glacial-geological evidence. Characteristics available for comparison are the flow pattern, ice thickness distribution and ice sheet extent during the LGM as well as the timing, duration and order of Holocene retreat. Second, present-day model output can be compared with glaciological and geophysical observations of the present ice sheet and its evolution with time.

7.3.1. Geomorphological tests

Available geomorphological evidence, the CLIMAP (model) reconstruction (fig. 3.5) and a more recent sketch by Denton et al. (1986) (fig. 3.7), have been extensively reviewed in § 3.3.2 and § 3.3.3. In general, the flow pattern

GLACIAL CYCLE
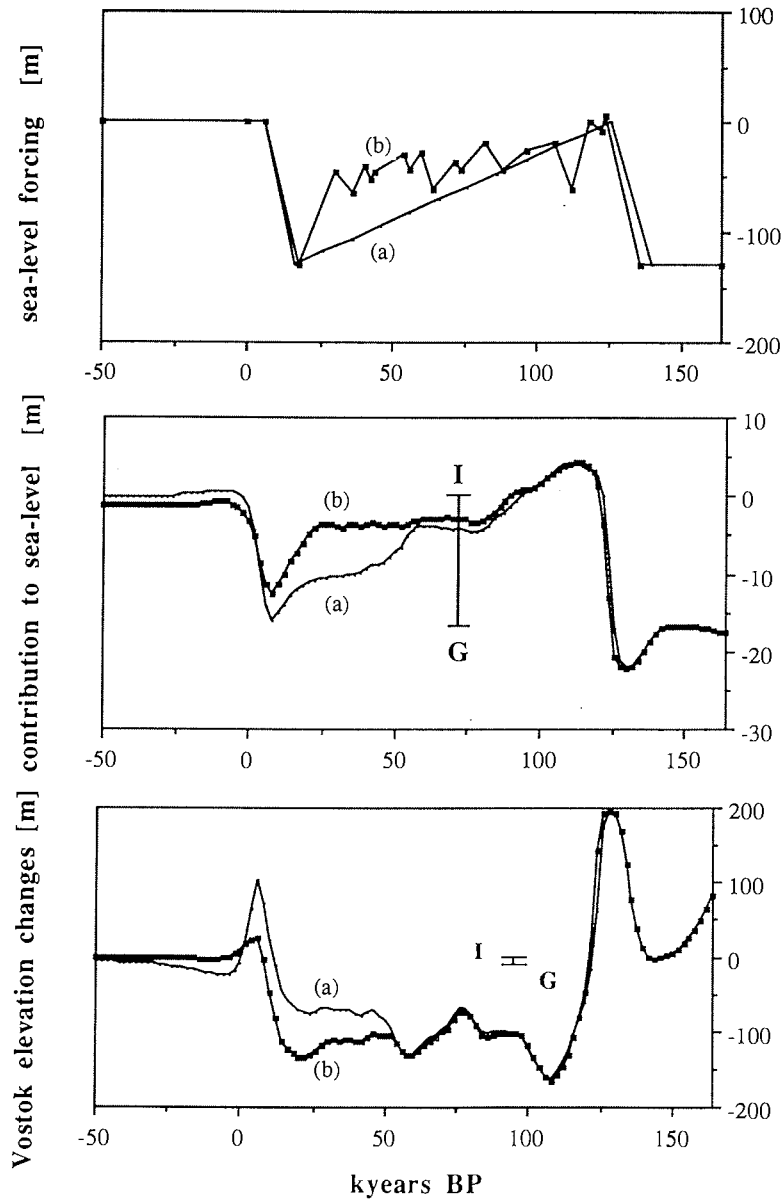
fig.7.6: Sensitivity of the results to the type of sea-level forcing. Shown are the impacts on both the Antarctic contribution to the global sea-level fall and elevation changes at Vostok station (relative to present). Vertical bars refer to the glacial (G) and interglacial (I) steady states as discussed in the previous chapter. a: 'sawtooth' sea level forcing; b: sea level record derived from New Guinea terraces.

predicted by the model agrees most closely with fig. 3.7. Both surface morphologies demonstrate that the respective domes are well preserved throughout the glacial cycle. Also the positions of ice divides, saddles and local maxima do not change much in either reconstruction. This is in contradiction with the CLIMAP-reconstruction, which predicted only one central dome located over East Antarctica. There is however some disagreement between the model (fig. 7.1) and the Denton et al. (1986) sketch with respect to certain features of the elevation distribution. The model predicts lower elevations for the ice domes centred over the Executive Committee Range and Palmer Land and to a lesser extent in parts of East Antarctica. In the latter area, the model suggests a lower LGM surface than at present, especially in interior regions above 3000 m. Also the existence of peripheral domes is not supported by the model results presented here. A similar remark applies to the lower LGM surface elevation in parts of West Antarctica as inferred from the total gas content in the Byrd ice core (Raynaud and Whillans, 1982). Actually, the latter feature is not found in any of the reconstructions and may point to limitations in the method of relating total gas content to surface elevation.

Both the model and glacial-geological reconstructions call for a late Wisconsin expansion close to the edge of the continental platform. Except in the Ross Sea, the agreement between the modelled extent and fig. 3.5 / fig. 3.7 is generally good. However, the Ross Sea is also the area where the interpretation of the field data is subject to the largest degree of uncertainty. Here, the model predicts a maximum extent intermediate to the minimum and maximum reconstructions of Denton et al. (1989), shown in fig. 3.6. In this case the model may be more realistic than e.g. CLIMAP, because the experiments discussed in this thesis have clearly demonstrated that the ice sheet in the Ross Sea is unlikely to have attained equilibrium. The model is however unable to discriminate in the Ross basin between a series of low-lying ice lobes or a convex surface morphology, though the latter possibility is preferred. This is because the model does not include a special treatment for individual ice streams.

The calculated ice sheet geometries shown in fig. 7.1 (lower row of pictures) give a chronological pattern of deglaciation which can be compared with the retreat history derived from field work (cf. § 3.3.3). This yields elements of both

agreement and disagreement. The model results agree well with the environmental record in that there is a time-lag between the onset of the sea-level rise and the ensuing ice-sheet retreat. The model's prediction of both the approximate stability during the glacial-interglacial transition (no catastrophic collapse) and the retreat duration of 6000 years are reasonably well supported by the field data. By contrast, the predicted grounding-line retreat in the Ross Sea occurs 3000 to 5000 years too late, depending on which chronology for Holocene retreat is accepted. This probably represents the weakest point of the modelled cycle. It may well indicate that the model misses the subtleties of the grounding-line mechanics responsible for recession early in the retreat. The model supports evidence for retreat histories which are out of phase with the Ross ice shelf (e.g. along George VI coast), however there are no dates available to support the late deglaciation produced in the Weddell Sea region. Clearly the latter area constitutes a high priority for further field investigations.

7.3.2. Glaciological tests

Another test of the model is to compare the present ice-sheet geometry (cf. fig. 6.1) with that predicted by the model (last panel of fig. 7.1). The agreement is acceptable and in both cases grounded ice has withdrawn from the offshore shelves in the Weddell and Ross Seas. However, since the predicted present-day ice sheet is already close to the interglacial reference run, discrepancies with respect to the observations are likely to have the same origin as those discussed in § 5.2.1 and § 6.2.1. In this respect, incomplete retreat in the vicinity of the Antarctic Peninsula is the result of an inadequate representation of the bedrock topography, whereas thicker ice in the Thwaites/ Pine Island Glaciers area may point to a type of irregular behaviour that is not produced by the model.

Finally, it is of interest to examine how the scattered observations of the ice sheet's present evolution (cf. § 3.3.4) may fit into the picture provided by fig. 7.5. Even though the model result is likely to be biased by a late deglaciation, both approaches indicate a complex and non-uniform response pattern. Also the calculated overall imbalance of less than 10% falls within the range of uncertainty provided by the observations. A few features deserve additional comment. In the Ross basin, geophysical observations suggest a positive

mass balance and a tendency for grounding-line advance. The model, on the other hand, predicts a general thinning at a rate of over 10 cm/y in places. Moreover, this trend is found to continue for another 10000 years, before it reverses to a growth phase. A possible explanation is that the modelled bedrock adjusts too slowly to changes in the loading history, and consequently, that the diffusivity model for the asthenosphere may not be well adapted to the situation in Antarctica. The model does not reproduce such small-scale features as the thinning of the Shirase catchment area and the assumed oscillatory behaviour of the Ross ice streams. However, closer inspection of the local imbalance field (fig. 7.5) also reveals that thinning rates of up to 0.5- 1 m/y may not be unreasonable.

7.4. SUMMARY

In this chapter, an attempt was made to simulate the Antarctic ice sheet during the last glacial-interglacial cycle. Apart from validating the model, this allowed us to investigate the transient behaviour of the ice sheet. Output of this experiment has, among other things, revealed that:

(i) the model is able to reproduce the gross features of a complete cycle of advance and retreat. Not only does the model simulate a glacial buildup, but when boundary conditions are reset, the subsequent interglacial retreat as well. This suggests that the model incorporates the relevant physical mechanisms of the coupled ice sheet- ice shelf system in an essentially correct way.

(ii) the eustatic threshold for grounding appears to be larger for the Ross ice shelf than for the Ronne-Filchner ice shelf. Consequently, the latter grounds more readily and ungrounds less easily. Furthermore, because of specific topographic conditions, grounding-line migration is more gradual in the Ross Sea than in the Weddell Sea.

(iii) the Antarctic ice sheet does not reach its full glacial extent until 16 ky BP, particularly not in the Ross Sea. Depending on the type of sea-level forcing, the calculated LGM contribution to the world-wide sea level drop is between 8 and 12 m. This is substantially less than the equilibrium value of 16 m.

(iv) in times postdating the Eemian, changes of surface elevation over interior portions of the East Antarctic plateau are generally within 100- 150 m. Maxima occur during the early stages of an *interglacial* period; mimima coincide with cold intervals during the first half of a *glacial* period. In central West Antarctica, the corresponding range is around 500 m, but maxima occur towards the end of a glacial period when the sea-level stand is lowest. At Vostok station, the postglacial (16-6 ky BP) rise of the surface is 155 m. It is currently falling because of a delayed response to grounding-line retreat.

(v) according to the model, the ice sheet is still in the retreat phase and is slowly thinning at a mean rate of about 0.5 mm/y sea-level equivalent. At present, only the central parts of the East Antarctic plateau are thickening, by a few cm/y. The overall thinning trend reverses to a growth phase after 10000 AP. In addition, present bedrock elevations in the Weddell sector of West Antarctica may be out of steady state by 100-200 m. This is more than the free-water depth below large parts of the Ronne-Filchner ice shelf, and has possible consequences for renewed grounding.

(vi) the most important discrepancy between the model predictions and available field evidence is that the model produces an interglacial retreat which comes a few thousand years too late. However, the field evidence is still poor and present data do not yet seem to permit conclusive testing.

8. RESPONSE TO FUTURE GREENHOUSE WARMING

8.1. EXPERIMENTAL SETUP

In this chapter, we address the question of how the Antarctic ice sheet may respond to the anticipated greenhouse warming of the earth's atmosphere and present results of a tentative calculation of its contribution to world-wide sea levels. To do this, temperature scenario's are prescribed based on GCM studies, and output from a comprehensive mass balance model serves to drive the ice sheet model. The Antarctic ice sheet is of large interest as it contains over 90% of global ice volume and because of the possibility of a surge of its marine component (cf. § 2.4.1). In addition, since the inland ice covers an area of about one-thirtieth of the world oceans, any small imbalance between the total mass accumulated over its surface and the total rate of discharge across the grounding line should have a marked influence. So far, few studies have been conducted on the effect of such a change in surface mass balance.

A climatic warming will affect components of the surface mass balance in different ways. At present, there is virtually no surface melting. This is because of the very low air temperatures, which remain largely below freezing even during summer. These low air temperatures also limit the amount of water vapour that can be held by the atmosphere. Since warmer air can carry more moisture, an increase in the temperature of snow formation will lead to higher precipitation rates. As a result, more water is extracted from the oceans and accumulates on the ice sheet. Since this additional ice mass will not be returned back to the ocean immediately, this should lead to a fall in global sea level. When the warming becomes larger than a few °C, however, melting in

the coastal zone could also become important, in particular on the Antarctic Peninsula. This point has received much less attention.

The net effect on sea level should thus depend on which process is dominant for which rise of temperature. However, surface melting will not necessarily result in runoff and, depending on the thermal properties of the upper ice layers, it may well completely refreeze in situ to form superimposed ice. The effect of meltwater transport in the snowpack may also be an important process, but is not so easy to quantify.

With regard to the response of the Antarctic ice sheet to a climatic warming, a distinction has to be made between the direct or static effect of a changing surface mass balance and the subsequent effect of changing ice sheet dynamics. On a short time scale (say, less than 100 years), it may be assumed that flow changes are too slow to significantly affect the amount of ice that is transported across the flotation line. Consequences for sea level can then be investigated by integrating mass-balance changes forward in time. When a somewhat longer time integration is envisaged or bottom melting on ice shelves becomes important, the assumption of stationarity is probably no longer justified. In this case, grounding line retreat may occur and ice dynamics have to be considered too.

A further complication is introduced by the state of balance of the Antarctic ice sheet. As discussed previously (cf. § 3.3.4), it is not really known whether the total mass of the ice sheet is at present increasing, decreasing or unchanging. Data reviewed by Warrick and Oerlemans (1990) suggest that the total imbalance is not known to an accuracy better than 20%. This would correspond to a change in sea level of 1.2 mm/y. Modelling experiments discussed in previous chapters also indicate that the ice sheet must still be responding to the last glacial-interglacial transition, but the associated rate of sea level change falls within the above range of uncertainty. In the model experiments discussed in this chapter, however, this complication is neglected and a stationary ice sheet (the 'interglacial reference run') is taken as initial condition.

An early model study on the possible contribution of the Antarctic ice sheet to future sea levels was conducted by Oerlemans (1982a). He used results from

197

GCM experiments, which indicated a 3 K temperature rise and an increase in precipitation by 12 % for a doubling of the CO_2 content. These data served to force the mass balance, that was subsequently used to drive a 2-D Antarctic ice sheet model. This would lead to a sea level drop of about 30 cm in the next 200 years. The present approach follows a similar philosophy, but with a more detailed treatment of the mass balance components, updated scenario's for the greenhouse warming and a much more refined model for ice dynamics. § 8.2 presents the temperature scenario's needed to force the mass balance. The mass balance model is described in § 8.3 and model results discussed in § 8.4. Much of this material draws on a paper by Huybrechts and Oerlemans (1990).

8.2. THE ENHANCED GREENHOUSE WARMING EFFECT

Comprehensive reviews of the current knowledge of the potential effects of rising concentrations of greenhouse gases have been published as the SCOPE29-report (Bolin et al., 1986) and the IPCC Scientific Assessment report (Houghton et al., 1990). These studies indicate that the concentration of greenhouse gases (CO_2, methane, etc...) is likely to exceed a level equivalent to a carbon dioxide doubling somewhere during the second half of the next century. Based on theoretical considerations as well as on model studies, it is generally believed that this will result in an increase of the global mean temperature. This is because these gases are transparent to the incoming short wave radiation from the Sun, but absorb the outgoing longwave radiation, which is subsequently re-emitted in all directions. This leads to an increase of the downward flux of infrared radiation. The partial trapping of the outgoing thermal radiation by radiatively active gases helps to increase the surface temperature of the earth by several tens of degrees compared to what it would be without the atmosphere. This process, usually referred to as the 'greenhouse effect', occurs largely in the first 10-15 km of the atmosphere, that is, the troposphere.

Actually, by far the most important greenhouse gas is water vapour, but water vapour distributions are internal to the climatic system, that is, they are controlled by the hydrological cycle, rather than being perturbed by anthropogenic sources. The general feeling, however, is that in a warmer

climate vapour levels will also increase and thus enhance the greenhouse effect, although much also seems to depend on the nature of the clouds (high clouds/ low clouds), e.g. Cess et al. (1989). Of the man-influenced radiatively active gasses, carbon dioxide is the most important. Measurements taken at Mauna Loa, Hawaii, show that its concentration has been steadily rising from about 315 ppmv in 1958 to 353 ppmv in 1990 (fig. 8.1). Most of this increase can be attributed to the ever increasing combustion of fossil fuels, with minor contributions from deforestation and land-exploitation. The pre-industrial concentration during the period 1750-1800, as obtained from the analysis of air trapped in glacier ice, was around 275 ppmv (Neftel et al., 1985).

In addition to this, other less-abundant trace gases are also increasing. These include methane (CH_4), tropospheric ozone (O_3), nitrous oxide (N_2O) and the chlorofluorocarbons (CFC's) CCl_3F and CCl_2F_2. Although their sources and sinks are not yet well known, it is estimated that their change may in total have an effect on climate which is about half of that of carbon dioxide (Dickinson and Cicerone, 1986). In model studies, their effects are usually incorporated in terms of an equivalent amount of CO_2.
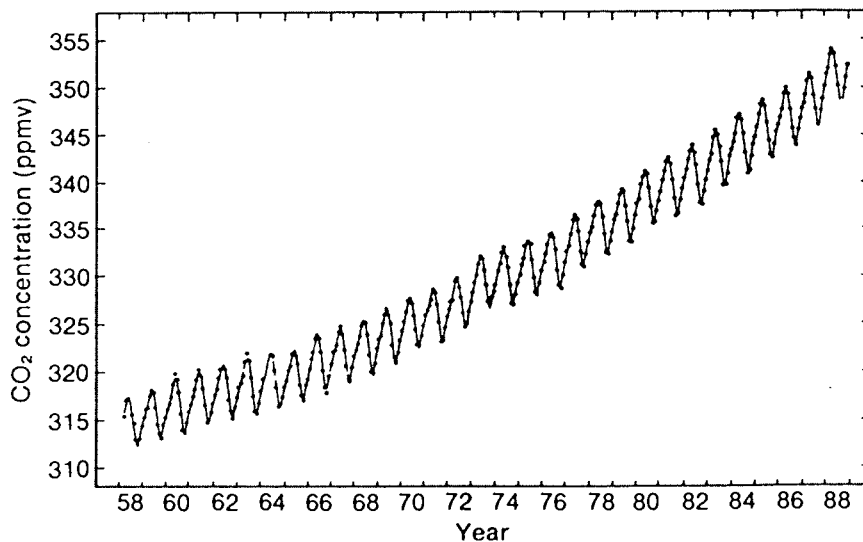

fig. 8.1: Monthly average CO_2 concentration in parts per million of dry air, observed continuously since 1958 at Mauna Loa, Hawaii. From Houghton et al., 1990.

199

GREENHOUSE WARMING EXPERIMENT

In the past decade, various computer simulations have been made of the response of the climatic system to an equivalent doubling of the CO_2 concentration, with models ranging from zero-dimensional simple energy balance models (EBM's) to complex 3-D general circulation models of the atmosphere-land-ocean system (GCM's). The latter studies give a value for the warming of 1.9°C to 5.2°C in the global mean surface temperature (Houghton et al., 1990). Most results are close to 4°C. The largest sources of uncertainty appear to be levels of feedback from clouds, ice-albedo and possibly, lapse-rate and water vapour changes.

Storage of heat in the oceans delays the warming expected for an equilibrium response and may also significantly modify the geographical distribution of climatic change (e.g. Schlesinger, 1986; Tricot and Berger, 1987). A typical value for the 'e-folding time' of the transient effect induced by the transport of the surface heating in the interior of the oceans is estimated at 50 years. At present (1990 A.D.) model results suggest that the atmospheric warming should be in the range of 0.6°C to 1.3°C relative to pre-industrial times (taken to be 1765). Although one cannot yet state that the enhanced greenhouse warming effect has been 'detected' in an unequivocal and statistically convincing way, the model estimates are certainly compatible with the observed global-scale warming over the past century of ≈0.5°C (Jones et al., 1986), see fig. 8.2. Some of the factors hindering an 'early detection' include the noise of natural climatic variability and the time lag between cause and effect introduced by the transient response of the oceans, as mentioned above.

Only GCM's are capable of providing adequate information on details regarding regional climatic change. Fig. 8.3 shows calculated seasonal and geographical changes in the surface air temperature for a CO_2-doubling during december-january-february (DJF), i.e. during the austral summer. As can be seen from this figure, all three models give qualitatively quite similar responses, although there are quantitative differences. Of interest for the experiments discussed in this chapter is the fact that the largest temperature increase occurs in the high latitudes, in particular during the fall and winter seasons. This is because of the albedo-temperature effect and a stable vertical stratification in the lower troposphere, which prevents large-scale mixing of the air. During summer months when melting may occur, the polar
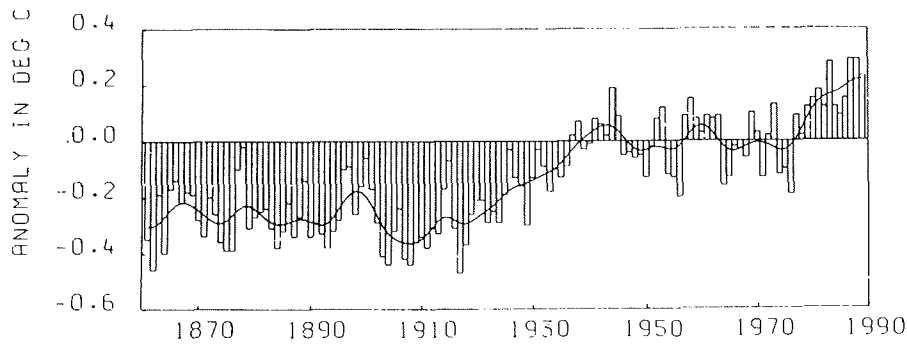
fig. 8.2: Combined land air and sea surface temperatures for the Globe from 1861 to 1989. Smooth curves show 10-year Gaussian filtered values. Values are relative to the 1951-1980 mean. From IPCC Working Group I Report (Houghton et al., 1990) after land air temperatures from Jones and co-workers and sea surface temperatures (SST) from UK Meteorological Office.

amplification over Antarctica appears to be smaller, but the warming in coastal zones may still reach values of between 4 and 6°C, i.e. close to the global mean.

Based on these GCM simulations and calculations of time-dependent climatic change, two temperature scenario's are derived to force the mass balance model. They are shown in fig. 8.4. The low scenario is simply a fit to the 'business-as-usual' temperature scenario proposed by the IPCC Working Group I Report (Houghton et al., 1990). It does not differ much from the earlier 'Bellagio' temperature scenario that came out of the Villach II discussions in 1987 (see e.g. Oerlemans, 1989). It predicts that temperature rises by 4.2°C by the year 2100, starting from 1850, which is considered as an undisturbed reference state. This figure applies to the global mean surface temperature, however. In order to take into account the larger temperature rise predicted for polar latitudes, an alternative forcing function will be used in which temperature rises by twice as much (the 'high scenario'). The disagreement produced by the various GCM-simulations does not really allow us to differentiate the greenhouse warming over Antarctica according to location and season. Consequently, in the model experiments temperature perturbations are assumed to be uniform through the year and independent of latitude. Since it is not known what will happen after 2100 AD (given that such
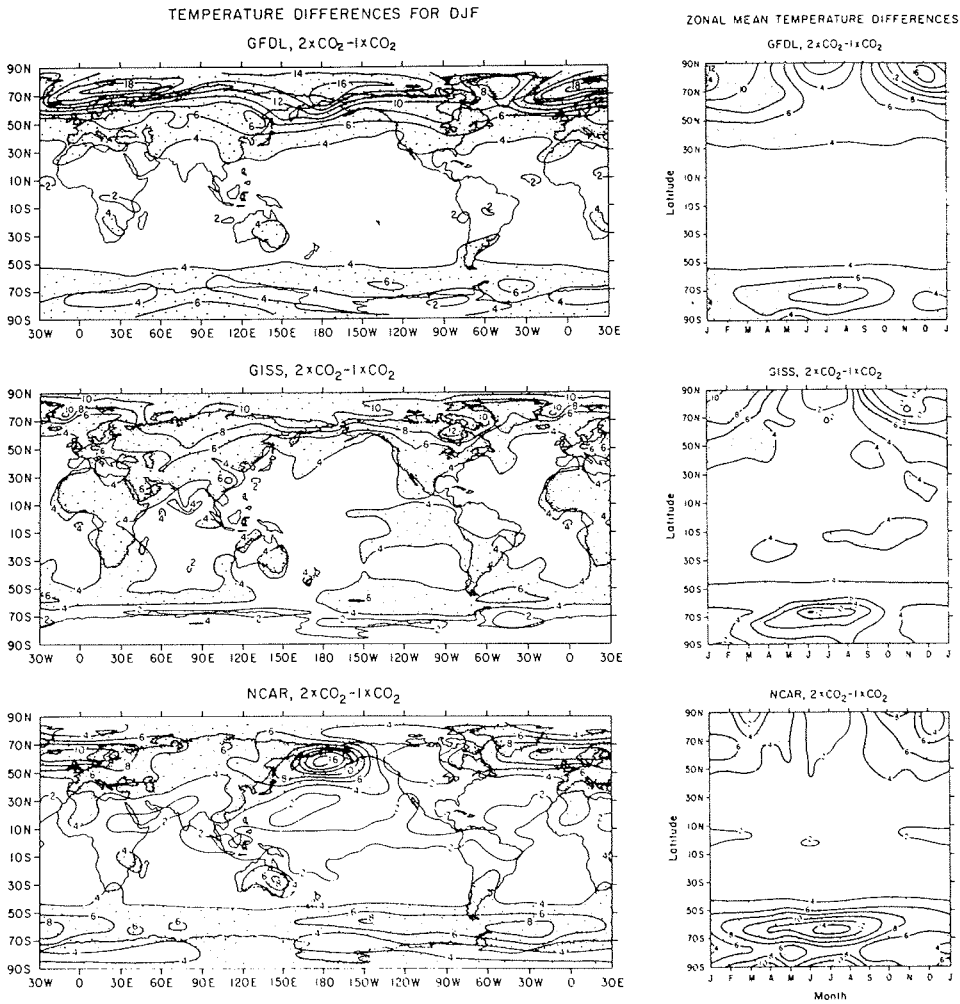
fig. 8.3: The geographical distribution of surface air temperature for DJF (left panels) and the seasonal variation of the zonal mean surface air temperature (right panels) for an increase of CO_2 and other greenhouse gases equivalent to a doubling of the CO_2 concentration. Simulations are by the GCM's of the Geophysical Fluid Dynamics Laboratory (GFDL), the Goddard Institute of Space Sciences (GISS) and the National Center for Atmospheric Research (NCAR). From Schlesinger (1986).
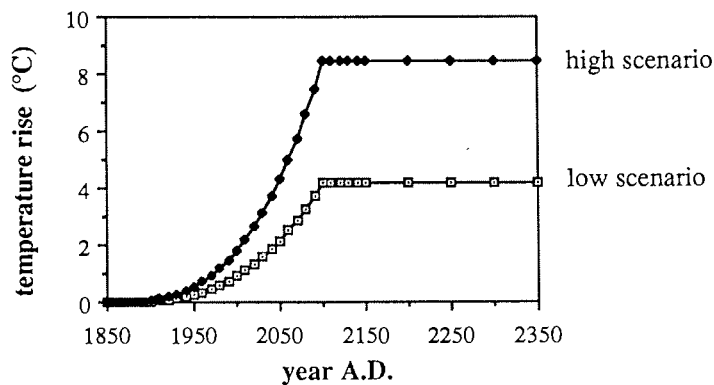
fig. 8.4: The temperature scenario's ('high' and 'low') used to force the mass balance and ice dynamics model. The lower curve is a fit to the 'business-as-usual' scenario of IPCC, the upper curve corresponds to a temperature rise by twice as much.

a warming occurs in the first place!), temperature forcing is held constant after this date.

As discussed in Schlesinger and Mitchell (1985), corresponding $2xCO_2$ minus $1xCO_2$ patterns of precipitation rate change, on the other hand, do not show much resemblance, not even in a qualitative sense. Consequently, these GCM simulations are of little use in the present study and it is more appropriate to model changes in the Antarctic mass balance in an independent way, involving the local physics.

8.3. MODELLING THE SURFACE MASS BALANCE

In the present approach, the components of the mass balance and its perturbations are parameterized in terms of temperature, which is the principal forcing parameter. Although accumulation and runoff result from quite complex processes, involving the circulation pattern in the atmosphere and the energy balance at the ice sheet surface, such an approach is preferable in the light of the large uncertainties in GCM results. Also, the thermodynamic models for the melting processes in the upper snow/firn/ice layers currently

available are not sufficiently universal to justify application to the type of sensitivity tests described here.

8.3.1 Accumulation

As described before, the spatial distribution of accumulation rate on the Antarctic ice sheet appears to be strongly related to air temperature, which controls the amount of vapour that can be advected inland. Such a relationship seems to be particularly strong over the inland plateau, where year-round temperatures are far below freezing, and snow deposition results from an almost continuous fallout of ice crystals and also some surface sublimation. In the present climatic warming experiments we will treat changes in the accumulation rate in exactly the same way as in the previous chapters on glacial-interglacial variations, i.e. changes in accumulation are set proportional to the saturation vapour pressure of the air above the inversion layer (cf. § 4.8.2). Support for the idea that higher temperatures will lead to significantly higher accumulation rates comes from observations on the Antarctic Peninsula. Over the past 30 years temperature has gone up by almost 2°C, and accumulation increased by as much as 25% in parallel with this (Peel and Mulvaney, 1988). This is in line with the $\approx 20\%$ estimated on the basis of eq. 4.83.

Our approach neglects possible changes in cyclonic activity and the general air circulation, which could be important for the precipitation regime in the lower parts of the ice sheet, especially along the ice sheet edge and over the ice shelves. However, very little is known in this respect. In addition, net accumulation depends on such factors such as snowdrift and evaporation, and changes in these factors could differ from the change in precipitation alone. Also here, a more sophisticated treatment would be far beyond the scope of the present study and is probably not justified in the light of the other approximations used.

8.3.2. Runoff

At present, there is little or no surface melting in Antarctica. If temperatures go up, however, summer melting may occur in the lower regions of the continent, and ultimately runoff towards the ocean may result. To estimate the

importance of these effects, we have to rely on measurements taken in the ablation zone of the Greenland ice sheet. In the event of a substantial warming, conditions on the Antarctic ice sheet are then likely to resemble those of present-day Greenland.

The annual melt rate will be calculated by means of a degree-day model. As shown by Braithwaite and Olesen (1989), there is a high correlation between positive degree-days and melt rates at the ice margin in West Greenland. The annual number of positive degree-days is parameterized in several steps. Data from 16 Antarctic coastal stations (Orvig, 1970) were used to relate summer temperature (mean of December and January) and annual temperature amplitude (both in °C) to geographical latitude f (in °S):

$$T_{sum} = 25.11 - 0.39 \, \phi + \delta T \qquad (r = 0.84) \qquad (8.1)$$

$$A_{ann} = -30.74 + 0.59 \, \phi \qquad (r = 0.91) \qquad (8.2)$$

The correlation coefficients appear to be sufficiently large to justify this approach. The temperature change δT occurring at the grid points consists of two parts: one associated with the imposed climatic warming $\Theta(t)$ and one with the change in surface elevation (δH):

$$\delta T = \gamma \, \delta H + \Theta(t) \, , \text{ where}$$
$$\gamma = 5.1 \, °C / km \quad \text{if} \quad H \leq 1500 \, m$$
$$\gamma = 14.3 \, °C / km \quad \text{if} \quad H > 1500 \, m \qquad (8.3)$$

Lapse rates are suggested by a linear multiple regression study by Fortuin and Oerlemans (1990).

In the calculations the daily cycle during the summer months (NDJF) was set to 3.02 °C (mean value of the 16 coastal stations with a standard deviation of 0.16 °C) and temperature during the summer season was fitted by a sinusoidal function with a half-period of 5 months and peaking on January 1st. This is necessary because the yearly temperature march has a rather flat profile in winter, because insolation is zero. The procedure is illustrated in fig.
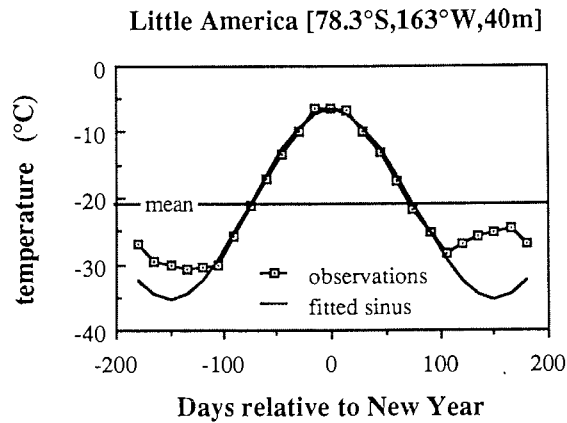
205

Little America [78.3°S,163°W,40m]

fig. 8.5: Fitting the temperature in the summer half year to a sine function. This example is for station Little America.

8.5. By integrating the parameterized annual and daily temperature cycle through the year (with a 30 min. time step), the number of positive degree-days (PDD) is easily obtained. The result can be approximated quite accurately by a fourth-order polynomial:

$$
\begin{aligned}
\text{PDD [°C day]} = \ & (58.259 - 2.201\,A_{ann} + 0.038\,A^2_{ann}) \\
+ \ & (50.263 - 2.265\,A_{ann} + 0.045\,A^2_{ann})\ T_{sum} \\
+ \ & (12.326 - 0.788\,A_{ann} + 0.019\,A^2_{ann})\ T^2_{sum} \qquad (8.4)
\end{aligned}
$$

This is subject to the conditions that the summer temperature is between -3 and +10°C, and that the annual amplitude is between 7 and 22°C

PDD represents the potential energy for melting. Fig. 8.6 shows this potential for some selected stations. The potential energy is used for melting snow and/or ice according to the following two-step scheme:

Step 1. Snow is melted with a degree-day factor of 0.003 m ice equivalent per unit of PDD, and the meltwater percolates into the snowcover and refreezes. The amount of refrozen meltwater depends on the cold content of the

Positive degree-days
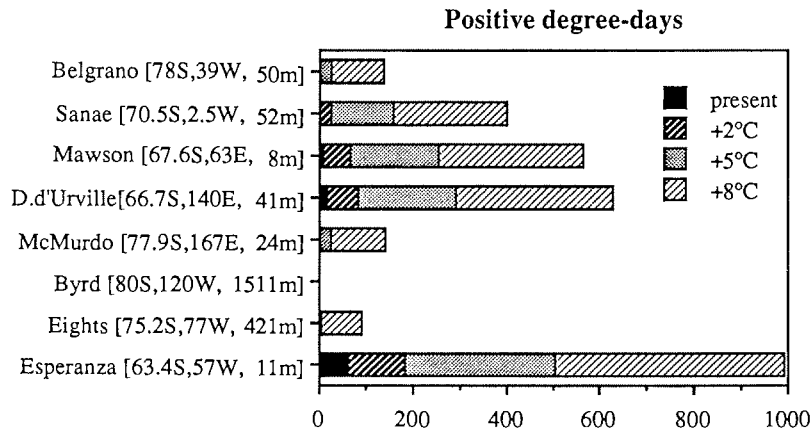
fig. 8.6: Calculated number of positive degree-days (PDD) for various Antarctic stations.

snowpack. Runoff occurs when enough latent heat is released by the refreezing process to raise the uppermost 2 m from the mean annual temperature to the melting point:

$$RM = \frac{\Delta T \times 2m \times c_p}{L} \approx 0.012 \times \Delta T \qquad (8.5)$$

where RM is the maximum amount of refrozen meltwater [m/y], ΔT the temperature difference between the mean annual temperature and the melting point, L the latent heat of fusion [3.35×10^5 Jkg^{-1}] and c_p specific heat capacity [2009 Jkg^{-1}°C^{-1}].

Step 2. Refrozen melt water ('superimposed ice') and in a later stage glacier ice are melted with a higher degree-day factor of 0.008 m ice equivalent per unit of PDD. This higher value is essentially related to a lower albedo for bare ice as compared to snow. Degree-day factors are from Braithwaite and Olesen (1989).

This process may stop at either of the stages 1 or 2, depending on the magnitude of PDD.

On the ice shelf, all melting is assumed to refreeze into superimposed ice and no runoff takes place. In view of the very small surface slope, this is to be expected for a long time to come. Also, at this stage we do not consider melting beneath the ice shelves.

The treatment of the refreezing process sketched above is admittedly rather crude. However, an alternative technique seems difficult to construct with our present knowledge. Some theoretical model studies on wetting-front propagation into cold snow exist (Pfeffer et al., 1990), but these results are not readily transferable to the present problem. Also field studies of the energy transfers involved in the formation of ice lenses and superimposed ice have been very limited. Useful data were obtained from field campaigns on the Laika ice cap in arctic Canada (Blatter and Kappenberger, 1988) and on the Greenland ice sheet (Ambach, 1963, 1968). Analysis of Ambach's results suggests that taking a 2 m thick (ice equivalent) layer to heat up annually by refreezing gives the correct order of magnitude.

8.3.3 Sensitivity of the surface mass balance

With the mass-balance model described above it is possible to study how the total ice budget gained (or lost) at the surface depends on temperature. Fig. 8.7 displays the surface mass balance and its components integrated over the entire ice sheet. Only grounded ice has been considered as ice mass changes in the floating shelves do not affect global sea level. The surface elevation of the ice sheet, which is a necessary input parameter for the mass-balance model, was taken from the 'interglacial steady-state reference run' (cf. § 6.2.1). For present conditions, it is found that an amount of 24.06×10^{11} m^3 of ice equivalent is deposited on the ice sheet surface every year. This amount of ice would lower global sea level by 6 mm/y, were it not that each year a same amount is discharged across the grounding line to form an ice shelf and, ultimately, ice-bergs (assuming a stationary state).

For a 1°C temperature rise with respect to present conditions, the mass balance increases by an amount of 1.43×10^{11} m^3 of ice, i.e. by 5.9%. This corresponds to an additional mean accumulation rate spread out over the entire grounded ice sheet of 10.3 mm/y water equivalent. Since the area of the world oceans is about 29 times larger than the area of the Antarctic ice sheet,

Antarctic mass balance

d/dT(runoff) > d/dT(accumulation)

accumulation

present

runoff starts

mass balance

runoff

10**13 m**3 of ice

temperature perturbation (°C)
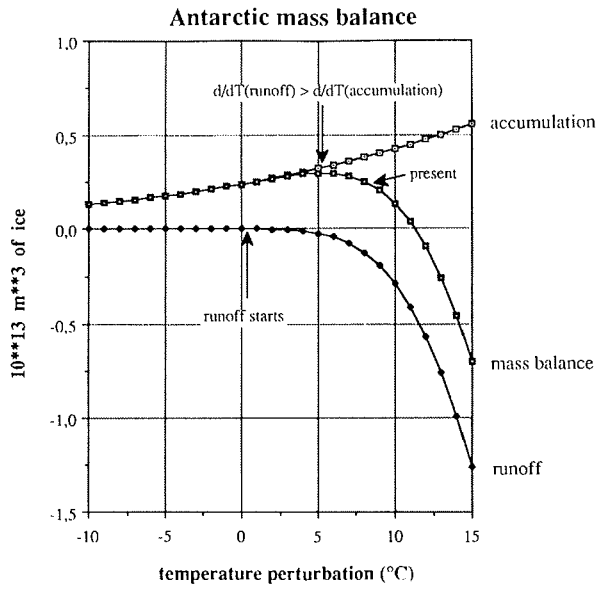
fig. 8.7: Dependence of Antarctic mass balance components on temperature relative to present. For a temperature increase below 8.3°C, the mass balance would be larger than today.

Antarctic runoff

model

no superimposed ice formation

excluding
Antarctic Peninsula

10**13 m**3 of ice

temperature perturbation (°C)

fig. 8.8: The effect of superimposed ice formation on the predicted runoff. The lower curve shows the relative importance of the Antarctic Peninsula.

this would imply a rate of sea-level lowering of 0.36 mm/y.

Runoff is negligible for the present climate, but it is found to increase progressively with temperature. This higher-order dependence occurs because a warming climate will not only increase melting rates, but also the length of the ablation season. In the calculation, the refreezing process does not make a too large difference (fig. 8.8). Typically, excluding superimposed ice formation leads to a horizontal shift in the runoff curve by 0.9°C for present conditions and to as little as 0.4°C for a temperature rise of 8°C.

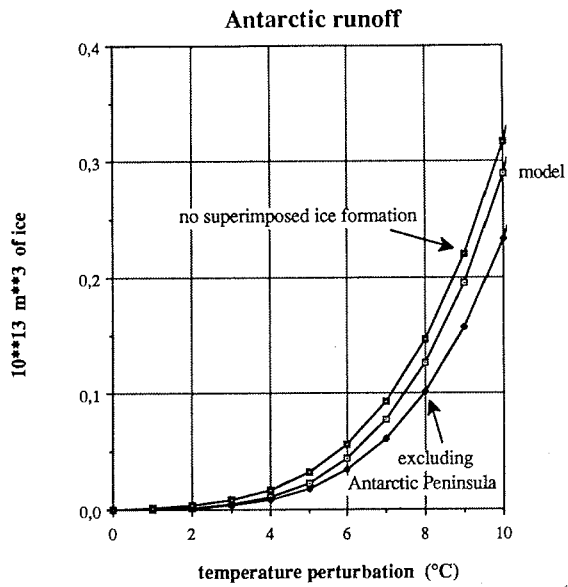While the temperature increase is below 5.3 °C, the mass balance increases, because the increase in accumulation outweighs the increase in runoff. At this stage, the total accumulation amounts to 32.75 x 10^{11} m^3, of which 8.7 % runs off in summer. This would extract an annual amount of 1.46 mm from the world's oceans, if ice sheet dynamics were to
remain unchanged. This applies to the total surface balance, but the spatial pattern of change of course depends on altitude.

Temperature has to rise by 8.3 °C to match the present mass balance, and an increase of 11.4 °C leads to a negative total surface balance. If this situation were to last over a long time (say thousand of years) ice shelves could not be
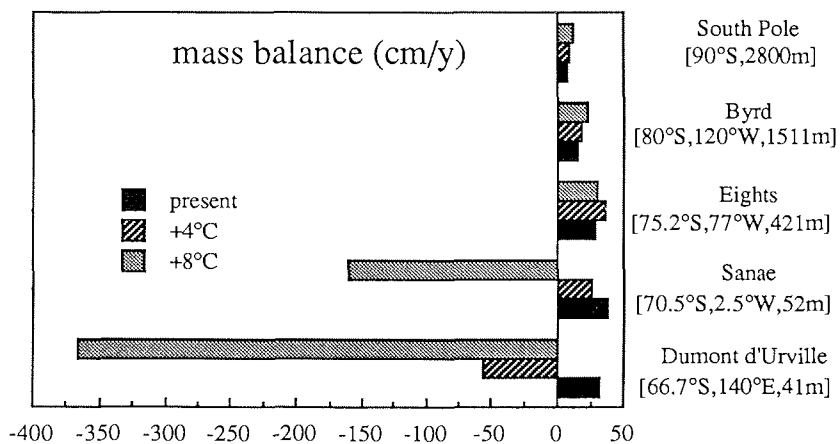

fig. 8.9: Surface mass balance (in cm/y ice equivalent) for present conditions and a warmer climate at some selected Antarctic stations.

sustained and a large ice-free strip would develop on the Antarctic continent.

Fig. 8.9 demonstrates how the surface mass balance changes for various values of the imposed climatic warming. Near the coast, the mass balance will quickly decrease and even become negative, while the mass balance on the plateau increases. As a consequence, the balance gradient steepens in a warmer climate, which has significant consequences for the ice-flow regime. This point is taken up in the next section.

8.4. RESPONSE OF THE ICE SHEET

In order to estimate implications for global sea level for the next few centuries, a number of time-dependent runs are conducted in which the temperature scenario's displayed in fig. 8.4 are used as model forcing. In the interpretation of these results, a distinction is made between the 'static effect', which can be studied with the mass balance model solely, and the 'dynamic effect', in which also ice dynamics come into play.

8.4.1. Static response

In view of the long response time scales, in particular in the interior of the East Antarctic ice sheet, initially a 'static experiment' is considered, i.e. the present ice-sheet geometry is assumed to be in equilibrium with the velocity field, and changes with respect to the present mass balance are accumulated forward in time. So the velocity field remains unchanged, in effect keeping the amount of ice transported across the grounding line constant. In this calculation, changing surface elevations have been taken into account as a contribution to local temperature changes (although this contribution is very small) and the maximum amount of ice that can melt away is equal to the present ice thickness. The results in terms of equivalent sea-level rise are shown in fig. 8.10. Since the imposed temperature perturbations are lower or equal to the 8.3 K mark (implying that the mass balance is always larger than at present), the expected increase in ice volume occurs. This is particularly apparent for the low scenario, where the volume increase lowers global sea level by 1.2 cm by the year 2000, 9.1 cm by the year 2100 and up to 41 cm by the year 2350, i.e. 500 years after the onset of the warming. However, a somewhat

high scenario
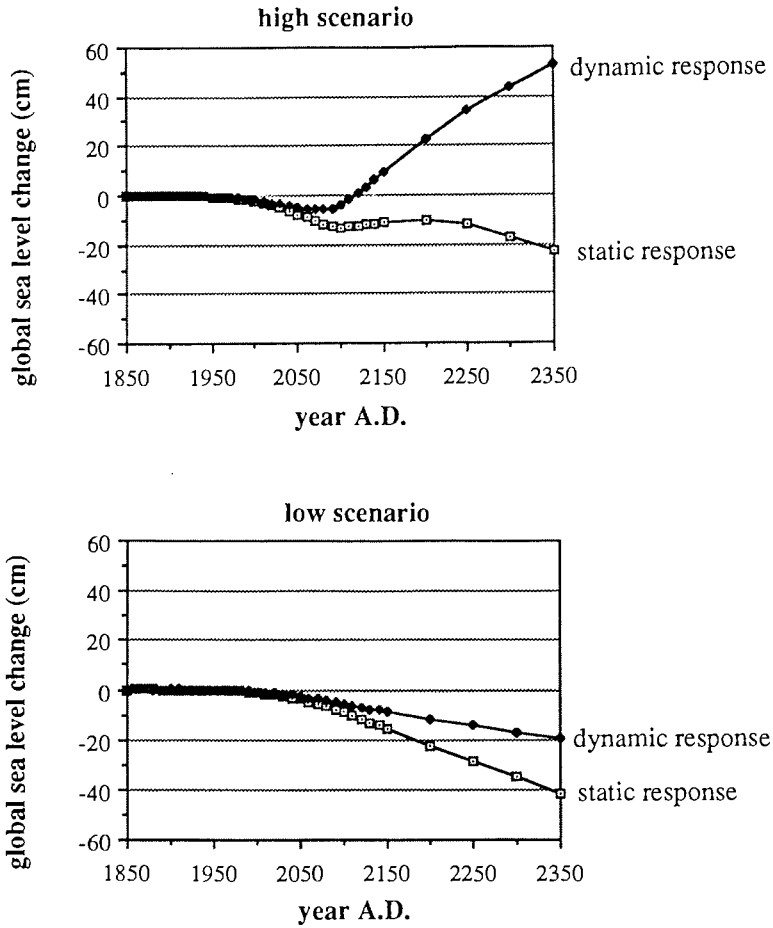
low scenario

fig. 8.10: Response of the ice sheet expressed in global sea-level changes for the high scenario (upper graph) and the low scenario (lower graph).

more complicated response shows up in the high scenario, where the ice volume decreases somewhat around 2100, because the 8.4 °C temperature perturbation just exceeds the 8.3 °C mark a little bit. This effect disappears later because at the edge, where melting rates have gone up to a few meters per year, the total ice thickness has melted away. Obviously, at this stage the assumptions made in this static experiment break down.

212

8.4.2. Dynamic response

Considering the substantial changes in ice thickness, in particular for the high scenario, the ice sheet is expected to show a dynamical response too. On the plateau this is not the case, and the increased accumulation rates lead to increased ice thicknesses of a few tens of meters at most, without a significant change in the velocity field at all. On the other hand, nearer to the coast and the grounding line the situation becomes quite different, because response times are much shorter here.

Several dynamic processes can be distinguished that result in lower grounded ice volumes compared to the corresponding static run. For the 'low' warming case, the mass balance at first increases everywhere and ice thickening is largest at low elevations. After a while, however, velocities in the lower reaches start to react to this and increase, and ice transport towards the ocean is enhanced. This leads to a thinning, which partly counteracts the thickening caused by increased accumulation. This sucking effect is mainly caused by increased ice-mass discharge on the ice shelves and is apparent along a few gridpoints inland. For a somewhat larger warming the mass balance at lower elevations decreases and eventually surface melting and runoff occur in the most northerly locations. However, the resulting change in ice thickness near the grounding line is not large enough to produce significant grounding-line retreat. In summary, initially there is some seaward migration (if there is no melting), followed by a slight recession in some places, but overall the grounded domain does not change its dimensions much.

This is essentially the picture that applies to the low scenario. By 2350 some seaward migration of the grounding line occurs in the most poleward locations (the Ronne-Filchner and Ross ice shelf) and a slight retreat is apparent in the Antarctic Peninsula and along parts of the East-Antarctic coast, in particular between 110 and 150°E. Basically, the net static effect is partially counteracted by an increased ice-mass discharge across the grounding line, and this leads to reduced rates of global sea-level lowering. Compared to the static effect, this reduction amounts to 18% by 2000, 36% by 2100 and 53% by 2350 (see fig. 8.10). This increasing fraction reflects the response time scale near and beyond the grounding line. So, from this low greenhouse warming

213

experiment it can be concluded that, as long as the warming is below some 5°C, the Antarctic ice sheet will probably lower global sea level by some tens of centimeters after a few centuries.

As can also be seen from the results shown in fig. 8.10, the situation becomes quite different for a larger warming. In particular, when this warming exceeds 5-6°C, i.e. after 2060-2070 in the high scenario, thinning at the grounding line becomes larger and significant grounding-line retreat sets in. Viscous spreading of the newly-formed ice shelves then enhances ice-mass discharge from the grounded ice sheet. This has immediate consequences for global sea level and the dynamic effect now becomes dominant, leading to a global sea level *rise* of as much as 0.5 m after 500 years of simulated time. Nevertheless, grounding-line recession is still insignificant along the major ice shelves (Ronne-Filchner and Ross), because, even with a warming of 8.4°C,
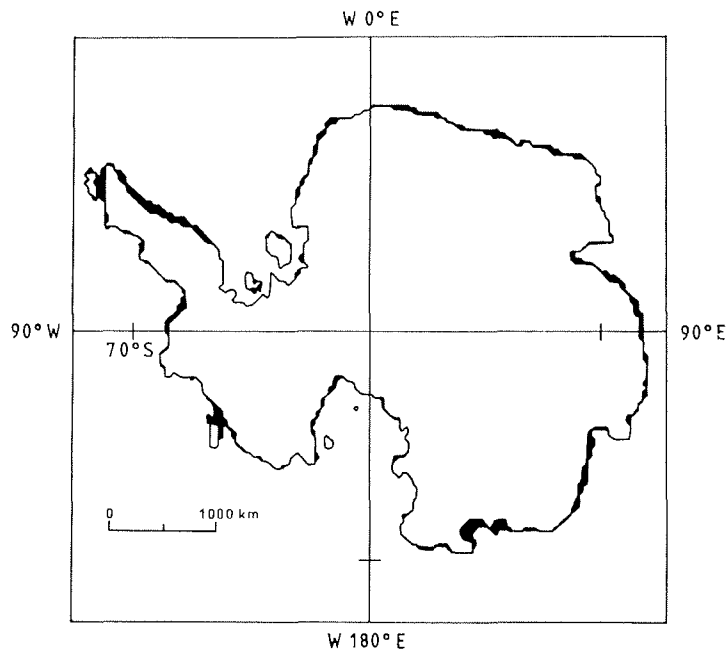

fig. 8.11: Grounding-line retreat for the 'high scenario' experiment. The black areas indicate where grounded ice has been replaced by ice shelf by the year 2500 (when the integration stops).

the number of positive degree-days at these locations is still below 50 and no runoff takes place. The areas where grounding line retreat has taken place by 2500 (when calculations end) are shown in black in fig. 8.11.

8.4.3. Effect of melting beneath ice shelves

In the experiments discussed above, basal melting beneath ice shelves was not considered. This is simply because it is not known how the oceanic circulation and the heat exchange with the ice shelves will react to higher ocean temperatures following a climatic warming. In the parameterization of the surface mass balance, no surface runoff occurs in the catchment areas feeding the Filchner-Ronne and Ross ice shelves, not even in the rather extreme +8.4°C warming. Thus, it is clear that no significant grounding line retreat occurred there, let alone a catastrophic collapse of the West Antarctic ice sheet (WAIS). Nevertheless, it has been suggested by several authors that increased melting could weaken the ice shelves and reduce their buttressing effect, ultimately inducing a collapse of the entire WAIS. To investigate this point somewhat further, a final schematic experiment was performed, in which the mass balance of the ice shelf was reduced stepwise by 1m/y at time zero, while keeping the surface climate fixed. From qualitative reasoning, such an estimate appears to be of a realistic order of magnitude (cf. Bentley, 1984). In this experiment, we were mainly interested in the effect of ice shelf thinning on the grounded ice sheet, and did not consider the possibility of the ice shelf completely breaking up, so that calving could take place at the grounding line.

Results for 500 years of simulated time are summarized in fig. 8.12. The number of gridpoints with grounded ice and sea-level change are shown. As can be judged from this figure, ice shelf thinning does lead to grounding-line retreat, but the total effect is smaller than the direct surface mass-balance response in the high scenario. For instance, the areas denoted in black on fig. 8.11 correspond to a decrease of the ice sheet domain of 240 gridpoints (compared to 70 in the bottom melting experiment). On the basis of these model results, it can be concluded that a West Antarctic ice sheet collapse on a time scale of half a millenium or so is unlikely to happen. It is also realized, however, that the fast ice streams presently flowing through the ice sheet are not explicitly modelled here, and that they could possibly speed up the response under particular circumstances.

215
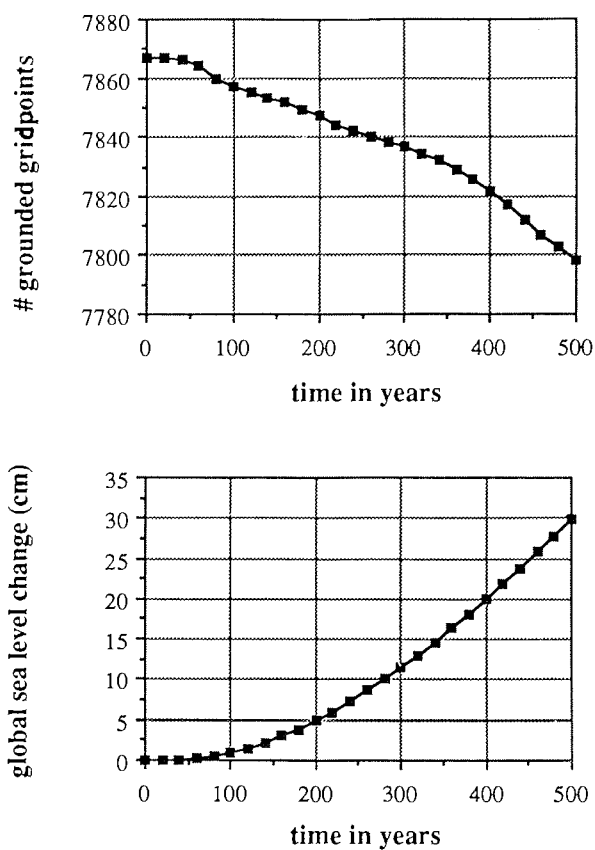
fig. 8.12: Response of the Antarctic ice sheet to an instantaneously imposed melting rate beneath ice shelves of 1 m/y. According to the model, the area of grounded ice would decrease by less than 1% in 500 years.

8.5. SUMMARY

In this chapter, we have discussed the sensitivity of Antarctica's mass balance and the response of the ice sheet in terms of future greenhouse warming. To do this, a model was developed for the mass balance, that was in a subsequent stage coupled with the ice-flow model. The results of the numerical experiments can be summarized as follows:

216

GREENHOUSE WARMING EXPERIMENT

(i) For present conditions, an amount of 21.89 x 10^{11} m^3 water equivalent is deposited on the ice sheet's surface every year and no runoff takes place.
(ii) A 1°C uniform temperature rise increases the overall surface mass balance by 5.9%. This corresponds to a world-wide sea-level drop of 0.36 mm/y.

(iii) For a rise in annual mean temperature of less than 5.3 °C, the increase in accumulation outweighs the increase in runoff and a larger-than-present surface budget results. For a temperature increase of more than 8.3 K, the mass balance drops below the present value. To make the surface balance negative, a 11.4 K temperature rise is needed.

(iv) Imposing the IPCC 'business-as-usual' scenario, the model predicts a 6 cm sea-level lowering by 2100 AD caused by changes on the Antarctic ice sheet and up to 20 cm after 500 years from the onset of the warming (assuming that increased melting beneath ice shelves is not important). Corresponding values for the experiment in which ice dynamics are not considered ('static response') are 9 cm and 41 cm.

(v) If the warming exceeds 5-6°C, grounding line retreat becomes apparent along the East Antarctic coast and in the Antarctic Peninsula. Imposing a temperature rise of twice as much as the IPCC 'business-as-usual' scenario would then result in a positive contribution to global sea level after the year 2100.

(vi) A stepwise 1 m/y increase in the melting rate beneath ice shelves, all other things being equal, would cause a sea-level rise of only 5 cm in 200 years, and 30 cm in 500 years. This does not produce a catastrophic collapse of the West Antarctic ice sheet.

It should be noted, however, that these figures depend strongly on the respective temperature and melting scenario's employed. Consequently, experimental results should primarily be regarded as a response to the specified mass balance forcing, and not necessarily as a firm prediction.

217

9. CONCLUSION

In this thesis, a rather detailed model for the entire Antarctic ice sheet was developed, designed for climatic change experiments. In my opinion, this model represents a well-balanced reflection of our current knowledge of the dynamics of ice sheets and ice shelves, supplemented with mass-balance treatments which are reasonable. The reasons for stating this are that the ice sheet model accounts for the most essential features of ice-dynamics and thermodynamics, i.e. the non-linear rheology of glacier ice, the varying temperatures within the ice sheet caused by changes in ice-sheet surface temperature, the temperature dependence of the ice-flow properties and the thermal inertia of the ice-sheet sub-stratum. Moreover, the model includes basal sliding, ice shelf flow, a dynamic treatment of the grounding line and glacial isostasy. Also snow accumulation depends on temperature in the way that cooler climates cause decreasing accumulation rates. When the model is submitted to a varying climatic input, it is able to satisfactorily account for major characteristics of the Antarctic ice sheet, in present as well as past environments. As such, the model can certainly be considered a useful tool for simulating the ice sheet under a wide range of environmental conditions, and therefore, can aid in our understanding of its fundamental behaviour.

Most of the experimental results discussed in this thesis were devoted to the behaviour of the ice sheet during a glacial-interglacial cycle. This is the period that is best documented in the environmental record and where most field data are available against which to test the model. In a first series of numerical experiments, in which changes in the horizontal extent were excluded, I investigated the effects of thermomechanical coupling on the ice thickness distribution. These calculations revealed how the interaction between ice temperature and deformation rates may have a neutralizing influence on the steady state configuration of, in particular, the East Antarctic ice sheet. Ice

CONCLUSION

thickness, and consequently bed topography, were found to exert a main control on the basal temperature field and its general sensitivity to climatic change. Moreover, thermodynamics, also in the underlying bed, appeared to introduce long response time scales. A consequence was that during a glacial cycle the amplitude of the transient ice thickness change is significantly larger than the amplitude of the corresponding steady states. This means that ice temperature may in effect be considered to constitute a 'memory' for the ice sheet. The implication is that any attempt to reconstruct the ice sheet history must involve a fully time-dependent calculation over a sufficiently long period of time (>100 ky).

In a subsequent stage, the model was used to examine the ice sheet extent. In good agreement with glacial-geological observations, the model called for a maximum Wisconsin ice sheet grounded at the edge of the continental shelf. Only in the Outer Ross Embayment did the model not produce widespread grounding, but this is also the area where the interpretation of the field evidence is subject to the largest degree of uncertainty. The Ronne-Filchner ice shelf appeared to be more sensitive to grounding than the Ross ice shelf. This is suggestive of topographic thresholds for stability, which are different for each drainage system. The implication is that a successful model should operate at a sufficiently high spatial resolution to represent the main topographic features, in particular in those areas where grounding-line migration takes place.

During the glacial-interglacial contrast, I found the model to be most sensitive to changes in sea level, which was the most decisive factor in controlling changes of the ice sheet extent. Changes in accumulation rate and ice temperature were also of some importance, but on the longer time scales (>10 ky), their effects appeared to approximately counteract each other. The role of sea level is particularly interesting given the difficulties in reconciling the approximate simultaneity of glacial expansion in both hemispheres with the Milankovitch forcing. Consequently, these results support the hypothesis that the Antarctic ice sheet is linked to glacial events on the northern hemisphere continents through changes in eustatic sea level. On the East Antarctic plateau, changes in surface elevation were found to be generally around 100-150 m. This is also of wider significance, as it indicates that the palaeoclimatic information derived from deep ice cores (Vostok, Dome C) has probably not

CONCLUSION

been biased too much by level fluctuations and, hence, is likely to be essentially of climatic origin.

However, the long response time for grounding-line advance mean that the Antarctic ice sheet did not reach its full glacial extent until 16 ky BP. At this stage, its contribution to the global sea level lowering was some 12 m. Although not changing the response in an essential way, prescribing a sea level record derived from New Guinea terraces, reduced this number to 7.8 m. These figures are significantly less than the equilibrium value of 16 m and certainly less than the 25-35 m reported in previous studies. In particular, our ice thicknesses did not support the CLIMAP reconstruction of Stuiver et al. (1981). These discrepancies may have implications for global ice volume during the Last Glacial Maximum. They may indicate that the northern hemisphere ice sheets contained substantially more ice than currently believed, or, alternatively, that sea level was depressed by less than the often quoted value of 130 m.

The satisfactorily simulation of the major features of the Antarctic ice sheet during the last glacial-interglacial cycle may be considered to validate the model. In a final series of experiments, an attempt was therefore made to investigate the possible response of the ice sheet to future greenhouse warming. On the basis of prescribed changes in surface temperature and a simple model for meltwater runoff, these calculations indicate that when the temperature rise is below some 5°C, the Antarctic ice sheet is likely to grow. Moreover, the hypothesis of a catastrophic collapse of the West Antarctic ice sheet, which may lead to a 5 m sea level rise in a few centuries time, is not supported by the model results presented here, even when basal melting beneath ice shelves was taken into account. A similar lack of unstable behaviour was found during a glacial-interglacial transition. Although on the basis of model results in the initializing phase, an interglacial transition of larger amplitude than the last one (16-6 ky) could not be excluded, if the bed under the West Antarctic ice sheet is depressed deeply enough. These results confirm a recent trend in model studies on the stability of West Antarctica, in which the ice sheet-ice shelf system is investigated in an integrated way and in which rapid disintegration is progressively considered unlikely, at least on such a short time-scale.

CONCLUSION

Nevertheless, in the present study a considerable number of uncertainties remain and the results could still be refined in several ways. The late Holocene deglaciation produced by the model may indicate shortcomings in the description of the ice mechanics. A more detailed treatment of basal sliding and explicit modelling of ice streams could be such 'missing factors' which could potentially speed up the response during a warming climate. Extensive field studies are currently being carried out to study the dynamics of ice streams, and one may hope that improved understanding and modelling will result. In a future development of the model, advantage could then also be taken of numerical nesting techniques in which a denser grid is used in those areas where this is required. These improvements should then enable the model to treat the flow near the grounding line and in the ice shelves in a more accurate way.

Alternatively, also shortcomings in the isostasy model could be responsible for enhancing the delayed deglaciation. Incorporation of a discontinuous, variable rigidity plate and a more accurate treatment of asthenospheric viscous flow may lead to small changes in bed elevation. Future runs could then clarify to what extent the timing and speed of the last deglaciation are a function of the phase lag between the response to sea-level and air temperature (accumulation rate).

However, much of the uncertainty concerning the numerical results probably arises from imperfections in the environmental forcing. For instance, a better quality record for global sea level depression, especially during the final stages of the Wisconsin, may yield a somewhat different maximum glacier stand, especially in the Ross Sea. Also, the model may be used in an iterative fashion to date the Vostok temperature record more precisely and correct for shifts in surface elevation. In this respect, particle trajectories and ice age-depth profiles could easily be constructed, even in a transient situation.

With respect to a significant warming, the formulation of the melting/run-off process can certainly be improved, and here much information can be taken from energy balance/ mass balance studies in other parts of the world (Greenland in particular). Also the effects of a warming on the oceanic circulation and melting rates beneath ice shelves are not really known. A similar remark applies to changes in the accumulation distribution resulting

CONCLUSION

from potential changes in the atmospheric circulation pattern and possibly, from changes in snow drift and surface sublimation. Nevertheless, in spite of the fact that our knowledge appears still inadequate in many respects, I have no firm reasons to believe that these refinements would influence the basic model outcome in the sense that the results would become entirely different.

Finally an indication on future studies. The Antarctic ice sheet simulations performed in this thesis may be viewed as pilot tests of a combined thermo-dynamic model for ice sheets and ice shelves. A natural extension of this work would then also be to apply the ice sheet model to other large ice masses. At present, calculations are in progress in which the continental ice sheet model (i.e. without the ice shelves) is used to examine the Greenland ice sheet. Eventually, however, I would also like to apply the model to the Quaternary ice sheets of the northern hemisphere (Fennoscandian and Laurentide). In such a model, ice shelves should be retained in order to allow for ice sheet expansion onto shallow parts of the Arctic Ocean and to be able to study the dynamics of ice sheet decay. In addition, in such a model ways should be investigated of including a more refined treatment of basal hydraulics, in order to address the possibility of enhanced sliding on soft sediments. The goal of such a study would be to find out how these ice sheets form and disintegrate, how extensive the glacial coverage is during the glacial cycle and how these ice sheets would contribute to global sea levels. In first instance, the mass balance could then be dealt with in a way similar to the greenhouse experiments reported here. In the long term, however, I believe that such experiments should be driven by output from circulation models of other components of the climate system, in particular of the atmosphere. With future developments in supercomputer technology and an improved understanding of ice and climate interactions, one may expect that such combined studies will become feasible during the coming decade.

REFERENCES

Abramowitz, M. and I.A. Stegun (1970): Handbook of mathematical functions, Dover Publications (New York).

Adamson, D. and J.Pickard (1983): Late Quaternary ice movement across the Vestvold Hills, East Antarctica, in: R.L. Oliver, P.R. James and J.B. Jago (eds): Antarctic Earth Science, Cambridge University Press, 465-469.

Alley, R.B. and I.M. Whillans (1984): Response of the East Antarctic ice sheet to sea-level rise, J.Geophys.Res. 89 (C4), 6487-6493.

Alley, R.B; D.D. Blankenship; C.R. Bentley and S.T. Rooney (1986): Deformation of till beneath ice stream B, West Antarctica, Nature 322, 57-59.

Ambach, W. (1963): Untersuchungen zum Energieumsatz in der Ablationszone des Grönlandischen Inlandeises, Meddelelser om Grønland 174(4),311p.

Ambach, W. (1968): Ein Beitrag zur Kenntnis des Wärmehaushaltes des Grönlandischen Inlandeises. Vorlaufige Ergebnisse, EGIG 1967, Polarforschung VI, 18-23.

Anderson, J.B.; D. Kurtz; F. Weaver and M. Weaver (1982): Sedimentation on the West Antarctic continental margin, in: C. Craddock (ed): Antarctic Geoscience (IUGS Ser.B,no.4), University of Wisconsin Press (Madison), 1003-1012.

Axelrod, D.I. (1984): An interpretation of Cretaceous and Tertiary biota in polar regions, Palaeogeog. Palaeoclim. Palaeoecol. 45, 105-147.

Barnola, J.M.; D. Raynaud; Y.S. Korotkevich and C. Lorius (1987): Vostok ice core provides 160,000-year record of atmospheric CO_2, Nature 329, 408-414.

Bentley, C.R. (1984): Some aspects of the cryosphere and its role in climatic change, in: J.E. Hansen (ed.): Climate processes and climate sensitivity, Geophys.Monogr. 29, AGU (Washington D.C.), 207-220.

Bentley, C.R. (1987): Antarctic ice streams: a review, J.Geophys.Res. 92(B9), 8843-8858.

Bentley, C.R.; J.D. Robertson and L.L. Greishar (1982): Isostatic gravity anomalies on the Ross ice shelf, in: C. Craddock (ed): Antarctic Geoscience (IUGS Ser.B,no.4), University of Wisconsin Press (Madison), 1077-1082.

REFERENCES

Berggren, W.A. and many others (1980): Towards a Quaternary time scale, Quat.Res. 13, 277-302.

Bindschadler, R. (1983): The importance of pressurized subglacial water in separation and sliding at the glacier bed, J.Glaciol. 29 (101), 3-19.

Blankenship, D.D., C.R. Bentley, S.T. Rooney and R.B. Alley (1986): Seismic measurements reveal a saturated porous layer beneath an active Antarctic ice stream, Nature 322, 54-57.

Blatter, H. and G. Kappenberger (1988): Mass balance and thermal regime of Laika ice cap, Coburg Island, N.W.T., Canada, J. Glaciol. 34, 102-110.

Bolin, B.; B. Döös; J. Jäger and R.A. Warrick (eds) (1986): The greenhouse effect, climate change and ecosystems, SCOPE 29, John Wiley (Chichester).

Bolzan, J.F. (1985): Ice flow at the Dome C ice divide based on a deep temperature profile, J.Geophys.Res. 90 (D5), 8111-8124.

Bockheim, J.G.; S.C. Wilson; G.H. Denton; B.G. Anderson and M. Stuiver (1989): Late Quaternary ice-surface fluctuations of the Hatherton Glacier, Transantarctic Mountains, Quat.Res. 31, 229-254.

Böhmer, W.J. and K. Herterich (1990): A simplified 3-D ice sheet model including ice shelves, Ann.Glaciol. 14, 17-19.

Boyer, S.J. (1979): Glacial geologic observations in the Dufek Massif and Forrestal Range, 1978-79, Ant.Journal U.S. 14 (5), 46-48.

Brady,H.T. (1982): Late Cenozoic history of Taylor and Wright Valley and Mc Murdo Sound inferred from diatoms in Dry Valley Drilling Project cores, in: C. Craddock (ed): Antarctic geoscience (IUGS Ser. B, no.4), University of Wisconsin Press (Madison), 1123-1131.

Braithwaite, R. and O.B. Olesen (1989): Calculation of glacier ablation from air temperature, West Greenland, in: J. Oerlemans (ed.), Glacier fluctuations and climatic change, Kluwer Academic Publishers, 219-233.

Broccolli, A.J. and S. Manabe (1987): The influence of continental ice, atmospheric CO_2, and land albedo on the climate of the last glacial maximum, Clim.Dyn. 1, 87-99.

Broecker, W.S. (1984): Carbon dioxide circulation through ocean and atmosphere, Nature 308, 602.

Broecker, W.S.; D.M. Peteet and D. Rind (1985): Does the ocean-atmosphere system have more than one stable mode of operation, Nature 315, 21-26.

REFERENCES

Broecker, W. and G.H. Denton (1989): The role of ocean-atmosphere reorganizations in glacial cycles, Geochimica et Cosmochimica Acta 53, 2465-2501.

Brotchie, J.F. and R. Silvester (1969): On crustal flexure, J.Geophys.Res. 74 (22), 5240-5252.

Budd, W.F. (1970): Ice flow over bedrock perturbations, J.Glaciol.9 (55), 29-48.

Budd, W.F. (1982): The role of Antarctica in southern hemisphere weather and climate, Australian Meteorological Magazine 30, 256-272.

Budd, W.F.; D. Jenssen and U. Radok (1971): Derived physical characteristics of the Antarctic ice sheet, ANARE Interim Report, Series A (IV), Glaciology Publ. 120, 178 p. + maps.

Budd, W.F. and D. Jenssen (1975): Numerical modelling of glacier systems, IAHS Publ. 104, 257-291.

Budd, W.F. and B.J. Mc Innes (1979): Periodic surging of the Antarctic ice sheet - an assessment by modelling, Hydrol.Sci.Bull. 24 (1), 95-104.

Budd, W.F.; P.L. Keage and N.A. Blundy (1979): Empirical studies of ice sliding, J.Glaciol. 23 (89), 157-170.

Budd, W.F.; M.J. Corry and T.H. Jacka (1982): Results from the Amery ice shelf project, Ann.Glaciol. 3, 36-41.

Budd, W.F. and I.N. Smith (1982): Large-scale numerical modelling of the Antarctic ice sheet, Ann.Glaciol. 3, 42-49.

Budd, W.F.; D. Jenssen and I.N. Smith (1984): A three-dimensional time-dependent model of the West Antarctic ice sheet, Ann.Glaciol. 5, 29-36.

Budd, W.F. and I.N. Smith (1985): The state of balance of the Antarctic ice sheet, an updated assessment 1984, in: Glaciers, ice sheets and sea level: effects of a CO_2-induced climatic change, DOE/ER/60235-1, National Academy Press (Washington), 172-177.

Budd, W.F. and D. Jenssen (1989): The dynamics of the Antarctic ice sheet, Ann.Glaciol. 12, 16-22.

Budd, W.F. and T.H. Jacka (1989): A review of ice rheology for ice sheet modelling, Cold Regions Science and Technology 16, 107-144.

Carrara, P. (1981): Evidence for a former large ice sheet in the Orville Coast - Ronne ice shelf area, Antarctica, J.Glaciol. 27 (97), 487-491.

Cess, R.D and many others (1989): Interpretation of cloud-climate feedback as produced by 14 atmospheric general circulation models, Science 245, 513-516.

225

REFERENCES

Chapell, J. and N.J. Shackleton (1986): Oxygen isotopes and sea level, Nature 324, 137-140.

Clapperton, C.M. and D.E. Sugden (1982): Late Quaternary glacial history of George VI Sound Area, West Antarctica, Quat.Res. 18, 243-267.

Clark, J.A. and C.S. Lingle (1979): Predicted relative sea level changes (18000 years B.P. to present) caused by late-glacial retreat of the Antarctic ice sheet, Quat.Res. 11, 279-298.

Clarke, G.K.C., U. Nitsan and W.S.B. Paterson (1977): Strain heating and creep instability in glaciers and ice sheets, Reviews of Geophysics and Space Physics 15 (2), 235-247.

Cooke, D.W. and J.D. Hays (1982): Estimates of Antarctic ocean seasonal sea-ice cover during glacial intervals, in: C. Craddock (ed): Antarctic Geoscience (IUGS Ser.B no 4), University of Wisconsin Press (Madison), 1017-1025.

Cooper, A.P.R.; N.F. McIntyre and G. de Q. Robin (1982): Driving stresses in the Antarctic ice sheet, Ann. Glaciol. 3, 59-64.

Craddock, C. (1982): Antarctica and Gondwanaland, in: C. Craddock (ed.): Antarctic Geoscience (IUGS Ser.B, no 4), University of Wisconsin Press (Madison), 3-13.

Creber, G.T. and W.G. Chaloner (1985): Tree growth in the Mesozoic and early Tertiary and the reconstruction of palaeoclimates, Palaeogeog. Palaeoclim. Palaeoecol. 52, 35-60.

Dahl-Jensen, D. (1989): Steady thermomechanical flow along two-dimensional flow lines in large grounded ice sheets, J.Geophys.Res 94 (B8), 10355-10362.

Denton, G.H.; R.L. Armstrong and M. Stuiver (1971): Late Cenozoic glacial history of Antarctica, in: Turekian, K.K. (ed.), Late Cenozoic Glaciological Ages, Yale Univ. Press (New Haven & London), 267-306.

Denton, G.H. and T.J. Hughes (eds) (1981): The last great ice sheets, John Wiley (New York), 485 p.

Denton, G.H. et al. (1983): Ice sheet overriding of the Transantarctic Mountains, Ant.Journal U.S. 18 (5), 93-95.

Denton, G.H.; B.G. Anderson and H.W. Conway (1986): Late Quaternary surface fluctuations of Beardmore Glacier, Antarctica, Ant.Journal U.S. 21 (5), 90-92.

REFERENCES

Denton, G.H.; J.G. Bockheim; S.C. Wilson; J.E. Leide and B.G. Anderson
(1989a): Late Quaternary ice-surface fluctuations of Beardmore Glacier,
Transantarctic Mountains, Quat.Res. 31, 183-209.

Denton, G.H.; J.G. Bockheim; S.C. Wilson and M. Stuiver (1989b): Late
Wisconsin and early Holocene glacial history, Inner Ross Embayment,
Antarctica, Quat.Res. 31, 151-182.

Dickinson, R.E. and R.J. Cicerone (1986): Future global warming from
atmospheric trace gases, Nature 319, 109-115.

Doake, C.S.M. (1982): State of balance of the ice sheet in the Antarctic
Peninsula, Ann.Glaciol. 3, 77-83.

Doake, C.S.M. and E.W. Wolff (1985): Flow law for ice in polar ice sheets,
Nature 314, 255-257.

DOE (1985): Glaciers, ice sheets and sea level: effect of a CO_2-induced
climatic change, U.S. Department of Energy report DOE/EV/60235-1
(Washington D.C.), 320p.

Domack, E.W.; A.J.T. Jull; J.B. Anderson; T.W. Linick and C.R. Williams (1989):
Application of tandem accelerator mass-spectrometer dating to Late-
Pleistocene- Holocene sediments of the East Antarctic Continental
Shelf, Quat.Res. 31, 277-287.

Drewry, D.J. (1975): Initiation and growth of the East Antarctic ice sheet,
J.Geol.Soc. 131, 255-273.

Drewry, D.J. (1978): Aspects of the early evolution of West Antarctic ice, in:
Van Zinderen Bakker, E.M.(ed.), Antarctic glacial history and world
paleoenvironments, A.A. Balkema (Rotterdam), 25-32.

Drewry, D.J. (1979): Late Wisconsin reconstruction for the Ross Sea Region,
Antarctica, J.Glaciol. 24 (90), 231-244.

Drewry, D.J. (1980): Pleistocene bimodal response of Antarctic ice, Nature
287, 214-216.

Drewry, D.J. (ed.) (1983): Antarctic glaciological and geophysical folio, Scott
Polar Research Institute (Cambridge).

Drewry, D.J. (1983): Antarctic ice sheet: aspects of current configuration and
flow, in: R. Gardner and H. Scoging (eds): Megageomorphology,
Clarendon Press (Oxford), 18-38.

Drewry, D.J.; S.R. Jordan and E. Jankowski (1982): Measured properties of
the Antarctic ice sheet: surface configuration, ice thickness, volume and
bedrock characteristics, Ann.Glaciol. 3, 83-91.

227

REFERENCES

Elverhøi, A. (1981): Evidence for a late Wisconsin glaciation of the Weddell Sea, Nature 293, 641-642.

Engelhardt, H. and J. Determann (1987): Borehole evidence for a thick layer of basal ice in the central Ronne Ice Shelf, Nature 327, 318-319.

Engelhardt, H.; N. Humphrey; B. Kamb and M. Fahnestock (1990): Physical conditions at the base of a fast moving Antarctic ice stream, Science 248, 57-59.

Fastook, J.L. and J.E. Chapman (1989): A map-plane finite-element model: three modeling experiments, J.Glaciol.35(119), 48-52.

Fitzgerald, P.G.; M. Sandiford; P.J. Barrett and A.J.W. Gleadow (1987): Asymmetric extension associated with uplift and subsidence in the Transantarctic Mountains and Ross Embayment, Earth and Planetary Science Letters 81, 67-78.

Flohn, H. (1974): Background of a geophysical model of the initiation of the next glaciation, Quat.Res. 4, 385-404.

Fortuin, J.P.F. and J.Oerlemans (1990): Parameterization of the annual surface temperature and mass balance of Antarctica, Ann. Glaciol. 14, 78-84.

Frakes, L.A. (1978): Cenozoic climates: Antarctica and the southern ocean, in: A.B. Pittock et al. (eds): Climatic change and variability, a southern perspective, Cambridge University Press, 53-69.

Frakes, L.A. and J.E. Francis (1988): A guide to Phanerozoic cold polar climates from high-latitude ice-rafting in the Cretaceous, Nature 333, 547-549.

Giovinetto, M.B. and C.R. Bentley (1985): Surface balance in ice drainage systems of Antarctica, Ant.Journal U.S. 20 (4), 6-13.

Gladwell, I. and R. Wait (1979): A survey of numerical methods for partial differential equations, Clarendon Press (Oxford), 425 p.

Greishar, L. and C.R. Bentley (1980): Isostatic equilibrium grounding line between the West Antarctic inland ice sheet and the Ross ice shelf, Nature 283, 651-654.

Grikurov, G.E. (1982): Structure of Antarctica and outline of its evolution, in: C. Craddock (ed.): Antarctic Geoscience (IUGS Ser.B no.4), University of Wisconsin Press (Madison), 791-807.

REFERENCES

Haltiner, G.J. (1971): Numerical weather prediction, John Wiley (New York), 317 p.

Hansen, J.E. (1985): Global sea level trends, Nature 313, 349-350.

Harmon, R.S., L.S. Land, R.M. Mitterer, P.Garrett, H.P. Schwarcz and G.J. Larson (1981): Bermuda sea level during the last interglacial, Nature 289, 481-483.

Harwood, D.M. (1983): Diatoms from the Sirius formation, Transantarctic Mountains, Ant. Journal U.S. 18(5), 98-100.

Hendy, C.H.; T.R. Healy; E.M. Rayner; J. Shaw and A.T. Wilson (1979): Late Pleistocene glacial chronology of the Taylor Valley, Antarctica, and the global climate, Quat.Res. 11, 172-184.

Herrod, L.D.B. (1986): Sea-bottom topography beneath Ronne ice shelf, Antarctica, Filchner Ronne Ice Shelf Program Report no. 3, Alfred Wegener Institut (Bremerhaven), 72-80.

Herterich, K. (1987): On the flow within the transition zone between ice sheet and ice shelf, in: Van der Veen, C.J. and J. Oerlemans (eds): Dynamics of the West Antarctic ice sheet, D. Reidel (Dordrecht), 185-202.

Herterich, K. (1988): A three-dimensional model of the Antarctic ice sheet, Ann.Glaciol. 11, 32-35.

Hindmarsch, R.C.A. and K. Hutter (1988): Numerical fixed domain mapping solution of free-surface flows coupled with an evolving interior field, Int.J.Num.Anal.Meth. Geomech. 12, 437-459.

Hindmarsh, R.C.A.; G.S. Boulton and K. Hutter (1989): Modes of operation of thermo-mechanically coupled ice sheets, Ann.Glaciol. 12, 57-69.

Hirakawa, K.; N. Matsuoka and K. Moriwaki (1988): Reconstruction of maximum glacial extent in the central Sør Rondane Mountains, East Antarctica, Proc. NIPR Symp. Antarct. Geoscience 2, 146-161.

Hodge, S.M. (1985): Two-dimensional, time dependent modeling of an arbitrarily shaped ice mass with the finite-element technique, J.Glaciol. 31 (109), 350-359.

Hollin, J.T. (1962): On the glacial history of Antarctica, J.Glaciol. 4 (32), 173-195.

Hollin, J.T. (1972): Interglacial climates and Antarctic ice surges, Quat.Res. 2, 401-408.

Hollin, J.T. (1980): Climate and sea level in isotope stage 5: an East Antarctic ice surge at
+- 95.000 BP ?, Nature 293, 629-633.

REFERENCES

Hooke, R. LeB. et al. (1979): Calculations of velocity and temperature in a polar glacier using the finite-element method, J.Glaciol. 24 (90), 131-146.

Houghton, J.T.; G.J. Jenkins and J.J. Ephraums (1990): Climate change: The IPCC scientific assessment, Cambridge University Press, 365p.

Hughes, T.J. (1973): Is the West Antarctic ice sheet disintegrating?, J.Geophys.Res.78(33), 7884-7910.

Hughes, T. (1975): The West Antarctic ice sheet: instability, desintegration and initiation of ice ages, Reviews of Geophysics and Space Physics 13 (4), 502-526.

Hughes, T.J. (1981): The weak underbelly of the West Antarctic ice sheet, J.Glaciol.27(97), 518-525.

Hughes, T.J. (1982): Did the West Antarctic ice sheet create the East Antarctic ice sheet ?, Ann.Glaciol. 3, 138-145.

Hunt, B.G. (1984): Polar glaciation and the genesis of ice ages, Nature 308, 48-51.

Hutter, K. (1983): Theoretical glaciology, D. Reidel (Dordrecht), 510 p.

Hutter, K.; S. Yakowitz and F. Szidarovszky (1986): A numerical study of plane ice-sheet flow, J.Glaciol. 32(111),139-160.

Huybrechts, Ph. (1986): A three-dimensional time-dependent numerical model for polar ice sheets: some basic testing with a stable and efficient finite difference scheme, Geografisch Instituut VUB Report 86-1, 39 p.

Huybrechts, Ph. (1987): Dynamics of the Antarctic ice cap Part II: Sensitivity experiments with a numerical ice sheet model with full thermo-mechanical coupling, Proceedings of the Belgian National Colloquium on Antarctic Research, 226-239.

Huybrechts, Ph. and J. Oerlemans (1988): Evolution of the East-Antarctic ice sheet: a numerical study on thermo-mechanical response patterns with changing climate, Ann. Glaciol. 11, 52-59.

Huybrechts, Ph. (1990a): The Antarctic ice sheet during the last glacial-interglacial cycle: a three-dimensional experiment, Ann. Glaciol. 14, 115-119.

Huybrechts, Ph. (1990b): A 3-D model for the Antarctic ice sheet: a sensitivity study on the glacial-interglacial contrast, Clim. Dyn.5, 79-92.

Huybrechts, Ph. and J. Oerlemans (1990): Response of the Antarctic ice sheet to future greenhouse warming, Clim. Dyn.5, 93-102.

REFERENCES

Huybrechts, Ph.; A. Letreguilly and N. Reeh (1991): The Greenland ice sheet and greenhouse warming, Palaeogeog. Palaeoclim. Palaeoecol.(Global and Planetary Change Section) 89, 399-412.

Jenssen, D. (1977): A three-dimensional polar ice sheet model, J.Glaciol. 18 (80), 373-389.

Johnson, R.G. and J.T. Andrews (1986): Glacial terminations in the oxygen isotope record of deep sea cores: hypothesis of massive Antarctic ice-shelf destruction, Palaeogeog. Palaeoclim. Palaeoecol. 53, 107-138.

Jones, P.D.; T.M.L. Wigley and P.B. Wright (1986): Global temperature variations between 1861 and 1984, Nature 322, 430-434.

Jouzel, J. and L. Merlivat (1984): Deuterium and oxygen 18 in precipitation: modelling of the isotopic effects during snow formation, J.Geophys.Res. 89 (D7), 11749-11757.

Jouzel, J.; C. Lorius, J.R. Petit; C. Genthon; N.I. Barkov; V.M. Kotlyakov and V.M. Petrov (1987): Vostok ice core: a continuous isotope temperature record over the last climatic cycle (160.000 years), Nature 329, 403-408.

Jouzel, J.; G. Raisbeck; J.P. Benoist; F. Yiou; C. Lorius; D. Raynaud; J.R. Petit; N.I. Barkov; Y.S. Korotkevich and V.M. Kotlyakov (1989): A comparison of deep Antarctic ice cores and their implication for climate between 65,000 and 15,000 years ago, Quat.Res. 31, 135-150.

Kadmina, I.N.; R.G. Kurinin; V.N. Masolov and G.E. Grikurov (1983): Antarctic crustal structure from geophysical evidence: a review, in: R.L. Oliver, P.R. James and J.B. Jago (eds): Antarctic Earth Science, Cambridge University Press, 498-502.

Kameda, T.: M. Nakawo, S. Mae; O. Watanabe and R. Naruse (1990): Thinning of the ice sheet estimated from total gas content of ice cores in Mizuho Plateau, East Antarctica, Ann.Glaciol.14, 131-135.

Kellogg, T.B. and D.E. Kellogg (1981): Pleistocene sediments beneath the Ross Ice Shelf, Nature 293, 130-133.

Kellogg, T.B. and D.E. Kellogg (1987a): Recent glacial history and rapid retreat in the Amundsen Sea, J.Geophys.Res. 92 (B9), 8859-8864.

Kellogg, T.B. and D.E. Kellogg (1987b): Late Quaternary deglaciation of the Amundsen Sea: implications for ice sheet modelling, IAHS Publ. 170, 349-357.

REFERENCES

Kennedy, D.S. and J.B. Anderson (1989): Glacial-marine sedimentation and
Quaternary glacial history of Marguerite Bay, Antarctic Peninsula,
Quat.Res.31, 255-276.

Kennett, J.P. (1977): Cenozoic evolution of Antarctic glaciation, the circum-
Antarctic ocean and their impact on global palaeoceanography,
J.Geophys.Res.82(27), 3843-3860.

Kennett, J.P, R.E. Burns, J.E. Andrews, M. Churkin jun., T.A. Davies, P.
Dumitrica, A.R. Edwards, J.S. Galehouse, G.H. Packham and G.J. van
der Lingen (1972): Australian-Antarctic Continental Drift,
Palaeocirculation Changes and Oligocene Deep-Sea Erosion, Nature
239, 51-55.

Koerner, R.M. (1989): Ice core evidence for extensive melting of the
Greenland ice sheet in the last interglacial, Science 244, 964-968.

Kvasov, D.D. and M.Y. Verbitsky (1981): Causes of Antarctic glaciation in the
Cenozoic, Quat.Res. 15, 1-17.

Le Masurier, W.E. and D.C. Rex (1983): Rates of uplift and the scale of ice
level instabilities recorded by volcanic rocks in Marie Byrd Land, West
Antarctica, in: R.L. Oliver, P.R. James and J.B. Jago (eds): Antarctic Earth
Science, Cambridge University Press, 663-670.

Letreguilly, A., Ph. Huybrechts and N. Reeh (1991a): Steady state
characteristics of the Greenland ice sheet under different climates,
J.Glaciol., 149-157.

Letreguilly, A.; N. Reeh and Ph. Huybrechts (1991b): The Greenland ice sheet
through the last glacial-interglacial cycle, Paleogeog., Palaeoclim.,
Palaeoecol. (Global and Planetary Change section), in press.

Lian, M.S. and R.D. Cess (1977): Energy balance climate models: a
reappraisal of ice-albedo feedback, J.Atmosph.Science 34 (7), 1058-
1062.

Lindstrom, D.R. (1988): Formation of the West Antarctic ice sheet,
Ann.Glac.11, 71-76.

Lindstrom, D. and T.J. Hughes (1984): Downdraw of Pine Island Bay drainage
basins of the West Antarctic ice sheet, Ant.Journal U.S. 19 (5), 56-58.

Lingle, C.S. (1984): A numerical model of interactions between a polar ice
stream and the ocean: application to ice stream E, West Antarctica,
J.Geophys.Res (C89), 3523-3549.

REFERENCES

Lingle, C.S. (1985): A model of a polar ice stream, and future sea-level rise
    due to possible drastic retreat of the West Antarctic ice sheet, in:
    Glaciers, ice sheets and sea level: effect of a CO2 induced climatic
    change, U.S. Dept. of Energy Report DOE/EU/60235-1, 317-330.
Lingle, C.S. and J.A. Clark (1985): A numerical model of interactions between
    a marine ice sheet and the solid earth: application to a West Antarctic ice
    stream, J.Geophys.Res. 90 (C1), 1100-1114.
Lliboutry, L.A. (1968): General theory of subglacial cavitation and sliding of
    temperate glaciers, J.Glaciol. 7(49), 21-58.
Lliboutry, L.A. (1987): Very slow flows of solids, Martinus Nijhoff Publishers
    (Dordrecht), 510 p.
Loewe, F. (1970): Screen temperatures and 10 m temperatures, J.Glaciol.
    9(56), 263-268.
Lorius, C.; J. Jouzel; C. Ritz, L. Merlivat; N.I. Barkov; Y.S. Korotkevich and V.M.
    Kotlyakov (1985), A 150.000-year climatic record from Antarctic ice,
    Nature 316, 591-596.
Lorius, C.; J. Jouzel; D. Raynaud; J. Hansen and H. Letreut (1990): The ice-
    core record: climate sensitivity and future greenhouse warming, Nature
    347, 139-145.

MacAyeal, D.R. (1989): Large-scale ice flow over a viscous basal sediment:
    theory and application to ice stream B, Antarctica, J.Geophys.Res.
    94(B4), 4071-4087.
MacAyeal, D.R. and R.H. Thomas (1986): The effects of basal melting on the
    present flow of the Ross Ice Shelf, Antarctica, J.Glaciol. 32 (110), 72-86.
Mahaffy, M.W. (1976): A three-dimensional numerical model of ice sheets:
    tests on the Barnes Ice Cap, Northwest Territories, J.Geophys.Res. 81
    (6), 1059-1066.
Manabe, S. and A.J. Broccoli (1985): The influence of continental ice sheets
    on the climate of an ice age, J.Geophys.Res. 90, 2167-2190.
Margolis, S.V. and J.P. Kennett (1971): Cenozoic palaeoglacial history of
    Antarctica recorded in sub-Antarctic deep sea cores, Am.J.Science 271,
    1-36.
Mayewski, P.A. and R.P. Goldthwait (1985): Glacial events in the
    Transantarctic Mountains: a record of the East Antarctic ice sheet, in:
    Geology of the Central Transantarctic Mountains, Antarctic Research
    Studies 36, 275-324.

233

REFERENCES

McIntyre, N.F. (1985): A re-assessment of the mass balance of the Lambert glacier drainage basin, Antarctica, J.Glaciol. 31 (107), 34-38.

McKelvey, B.C.; J.H Mercer; D.M. Harwood and L.D Stott (1984): The Sirius Formation: further considerations, Ant.Journal U.S. 19 (5), 42-43.

McMeeking, R.M. and R.E. Johnson (1985): On the analysis of longitudinal stress in glaciers, J.Glaciol 31 (109), 293-302.

Mercer, J.H. (1978a): West Antarctic ice sheet and CO_2 greenhouse effect: a threat of disaster, Nature 271, 321-325.

Mercer, J.H. (1978b): Glacial development and temperature trends in the Antarctic and in South America, in: van Zinderen Bakker, E.M. (ed), Antarctic glacial history and world Paleoenvironments, A.A. Balkema (Rotterdam), 73-93.

Mercer, J.H. (1979): West Antarctic ice volume: the interplay of sea level and temperature, and a strandline test for absence of the ice sheet during the last interglacial, IAHS Publ. 131, 323-330.

Mikolajewicz, U.; B.D. Santer and E. Maier-Reimer (1990): Ocean response to greenhouse warming, Nature 345, 589-593.

Mitchell, A.R. and D.F. Griffiths (1980): The finite difference method in partial differential equations, John Wiley (Chichester), 272 p.

Mix, A.C. and W.F. Ruddiman (1984): Oxygen-isotope analyses and Pleistocene ice volumes, Quat.Res. 21, 1-20.

Morland, L.W. (1984): Thermomechanical balances of ice sheet flows, Geophys. Astrophys. Fluid Dynamics 29, 237-266.

Mörner, N.-A. (ed.) (1980): Earth rheology, isostasy and eustasy, John Wiley (Chichester),

Muszynski, I. and G.E. Birchfield (1985): The dependance of Antarctic accumulation rates on surface temperature and elevation, Tellus 37A, 204-208.

Muszynski, I. and G.E. Birchfield (1987): A coupled marine ice stream - ice shelf model, J.Glaciol. 33 (113), 3-15.

Nakada, M. and K. Lambeck (1988): The melting history of the late Pleistocene Antarctic ice sheet, Nature 333, 36-40.

Naruse, R. (1979): Thinning of the ice sheet in Mizuho Plateau, East Antarctica, J.Glaciol.24(90), 45-52.

REFERENCES

Neftel, A.; E. Moor; H. Oeschger and B. Stauffer (1985): The increase of atmospheric CO_2 in the last two centuries. Evidence from polar ice cores, Nature 315, 45-47.

Nixon, W.A. et al. (1985): Applications and limitations of finite element modeling to glaciers: a case study, J.Geophys.Res.90 (B13), 11303-11311.

North, G.R. and J.A. Coakley (1979): Differences between seasonal and mean annual energy balance model calculations of climate and clamate sensitivity, J.Atmosph.Sci.36, 1189-1204.

Ocean Drilling Program (1987): Glacial history of Antarctica, Nature 328, 115-116.

Ocean Drilling Program (1988): Early glaciation of Antarctica, Nature 333, 303-304.

Oerlemans, J. (1980): Some model studies on the ice-age problem, Ph.D. thesis, KNMI Publ. 158, 88p.

Oerlemans, J. (1981a): Some basic experiments with a vertically-integrated ice sheet model, Tellus 33A, 1-11.

Oerlemans, J. (1981b): Effect of irregular fluctuation in Antarctic precipitation on global sea level, Nature 290, 770-772.

Oerlemans, J. (1982a): Response of the Antarctic ice sheet to a climatic warming: a model study, J.Climat. 2, 1-11.

Oerlemans, J. (1982b): A model of the Antarctic ice sheet, Nature 297, 550-553.

Oerlemans, J. (1984): Numerical experiments on large-scale glacial erosion, Z. Gletscherkd. Glazialgeol. 20, 107-126.

Oerlemans, J. (1989): A projection of future sea level, Clim.Change 15, 151-174.

Oerlemans, J. and C.J. Van der Veen (1984): Ice sheets and climate, D.Reidel (Dordrecht), 217 p.

Officer, C.B.; W.S. Newman; J.M. Sullivan and D.R. Lynch (1988): Glacial isostatic adjustment and mantle viscosity, J.Geophys.Res. 93 (B6), 6397-6409.

Oglesby, R.J. (1989): A GCM study of Antarctic glaciation, Clim.Dyn. 3, 135-156.

Orvig, S. (ed.) (1970): Climates of the polar regions, World Survey of Climatology 14, Elsevier (Amsterdam), 370 p.

REFERENCES

Oswald, G.K.A. and G.de Q. Robin (1973): Lakes beneath the Antarctic ice sheet, <u>Nature 245</u>, 251-254.

Parish, T.R. and D.H. Bromwich (1987): The surface windfield over the Antarctic ice sheet, <u>Nature 328</u>, 51-54.

Paterson, W.S.B. (1981): <u>The physics of glaciers 2nd edition</u>, Pergamon Press (Oxford), 380 p.

Paterson, W.S.B. and W.F. Budd (1982): Flow parameters for ice sheet modelling, <u>Cold Regions Science and Technology 6</u>, 175-177.

Payne, A.J.; D.E. Sugden and C.M. Clapperton (1989): Modelling the growth and decay of the Antarctic Peninsula ice sheet, <u>Quat.Res. 31</u>, 119-134.

Peel, D.A. and R. Mulvaney (1988): Air temperature and snow accumulation in the Antarctic Peninsula during the past 50 years, <u>Ann. Glaciol. 11</u>, 206-207.

Peltier, W.R. (1985): New constraints on transient lower mantle rheology and internal mantle buoyancy from glacial rebound data, <u>Nature 318</u>, 614-617.

Peltier, W.R. (1988): Lithospheric thickness, Antarctic deglaciation history, and ocean basin discretization effects in a global model of postglacial sea level change: a summary of some sources of nonuniqueness, <u>Quat.Res. 29</u>, 93-112.

Pfeffer, W.T.; T.H. Illangasekare and M.F. Meier (1990): Analysis and modelling of meltwater refreezing in dry snow, <u>J. Glaciol. 36 (123)</u>, 238-246.

Philberth, K. and B. Federer (1971): On the temperature profile and age profile in the central part of old ice sheets, <u>J.Glaciol. 10</u>, 3-14.

Pounder, E.R. (1965): <u>Physics of ice</u>, Pergamon Press (Oxford), 151 p.

Prentice, M.L.; S.C. Wilson; J.G. Bockheim and G.H. Denton (1985): Geological evidence for pre-late Quaternary East Antarctic glaciation of central and eastern Wright valley, <u>Ant.Journal U.S. 19(20). 5</u>, 61-62.

Prentice, M.L.; G.H. Denton; T.V. Lowell; H.C. Conway and L.E. Heusser (1986): Pre-late Quaternary glaciation of the Beardmore Glaciar region, Antarctica, <u>Ant.Journal U.S. 21 (5)</u>, 95-98.

Radok, U.; B.J. McInnes; D. Jenssen and W.F. Budd (1989): Model studies on ice-stream surging, <u>Ann. Glaciol. 12</u>, 132-137.

236

REFERENCES

Raper, S.C.B.; T.M.L. Wigley; P.D. Jones; P.M. Kelly; P.R. Mayes and D.W.S. Limbert (1983): Recent temperature changes in the Arctic and Antarctic, Nature 306, 458-459.

Rasmussen, L.A. and W.J. Campbell (1973): Comparison of three contemporary flow laws in a three-dimensional time-dependent glacier model, J. Glaciol. 12, 361-373.

Raynaud, D. and I.M. Whillans (1982): Air content of the Byrd core and past changes in the West Antarctic ice sheet, Ann. Glaciol. 3, 269-273.

Ritz, C. (1987): Time dependent boundary conditions for calculation of temperature fields in ice sheets, IAHS Publ. 170, 207-216.

Ritz, C. (1989): Interpretation of the temperature profile measured at Vostok, East Antarctica, Ann.Glaciol. 12, 138-144.

Robin, G. de Q. (1955): Ice movement and temperature distribution in glaciers and ice sheets, J.Glaciol. 2, 523-532.

Robin, G. de Q. (1977): Ice cores and climatic change, Phil.Trans.R.Soc.London Ser.B 280, 143-168.

Robin, G. de Q. (ed.) (1983): The climatic record in polar ice sheets, Cambridge University Press, 212 p.

Robin, G. de Q.; C.S.M. Doake; H. Kohnen; R.D. Crabtree; S.J. Jordan and D. Möller (1983): Regime of the Filchner-Ronne ice shelves, Antarctica, Nature 302, 582-586.

Rose, K.E. (1982): Radio-echo studies of bedrock in southern Marie Byrd Land, West Antarctica, in: C. Craddock (ed.): Antarctic Geoscience (IUGS Ser.B no. 4), University of Wisconsin Press (Madison), 985-992.

Rutford, R.H.; G.H. Denton and B.G. Andersen (1980): Glacial history of the Ellsworth Mountains, Ant.Journal U.S. 15 (5), 56-57.

Saari, M.R.; D.A. Yuen and G. Schubert (1987): Climatic warming and basal melting of large ice sheets: possible implications for East Antarctica, Geophys.Research Letters 14(1), 33-36.

Savage, M.L. and P.F. Ciesielski (1983): A revised history of glacial sedimentation in the Ross Sea region, in: Oliver, R.L.; P.R. James and J.B. Jago (eds): Antarctic Earth Science, Cambridge University Press, 555-559.

Schlesinger, M.E. (1986): Equilibrium and transient climatic warming induced by increased atmospheric CO_2, Clim.Dyn. 1, 35-51.

REFERENCES

Schlesinger, M.E. and J.F.B. Mitchell (1985): Model projections of the equilibrium climatic response to increased carbon dioxide, in: M.C. MacCracken and F.M. Luther (eds): Projecting the climatic effects of increasing carbon dioxide, DOE/ER-0237, US Department of Energy (Washington DC), 81-147.

Schubert, G. and D.A. Yuen (1982): Initiation of ice ages by creep instability and surging of the East Antarctic ice sheet, Nature 296, 127-130.

Schwerdtfeger, W. (1970): The climate of the Antarctic, in: S. Orvig (ed.): World survey of climatology 14, Elsevier (Amsterdam), 253-355.

Schwerdtfeger, W. (1984): Weather and climate of the Antarctic, Developments in atmospheric science 15, Elsevier (Amsterdam), 261 p.

Sclater, J.G.; C. Jaupart and D. Galson (1980): The heat flow through oceanic and continental crust and the heat loss of the earth, Rev.Geophys. Space Phys. 18, 289-311.

Shabtaie, S. and C.R. Bentley (1987): West Antarctic ice streams draining into the Ross ice shelf: configuration and mass balance, J.Geophys.Res. 92 (B2), 1311-1336.

Shabtaie, S.; C.R. Bentley; R.A. Bindschadler and D.R. Macayeal (1988): Mass-balance studies of ice streams A, B and C, West Antarctica, and possible surging behaviour of ice stream B, Ann. Glaciol. 11, 137-149.

Shackleton, N.J. (1987): Oxygen isotopes, ice volume and sea level, Quat.Science Rev. 6, 183-190.

Smith, A.D. and D.J. Drewry (1984): Delayed phase change due to hot asthenosphere causes Transantarctic uplift, Nature 309, 536-538.

Smith, G.D. (1969): Numerical solution of partial differential equations, Oxford University Press (London), 173 p.

Snyder, J.P. (1982): Map projections used by the U.S. Geological Survey, Geological Survey Bulletin 1532, U.S. Government Printing Office (Washington D.C.), 313 p.

Stephenson, S.N. and R.A. Bindschadler (1988): Observed velocity fluctuations on a major Antarctic ice stream, Nature 334, 695-697.

Stern, T.A. and U.S. ten Brink (1989): Flexural uplift of the Transantarctic Mountains, J. Geophys. Res. 94 (B8), 10315-10330.

Stuiver, M.; G.H. Denton; T.J. Hughes and J.L. Fastook (1981): History of the marine ice sheet in West Antarctica during the last glaciation: a working hypothesis, in: Denton, G.H. and T.J. Hughes (eds): The last great ice sheets, John Wiley (New York), 319-436.

REFERENCES

Sugden, D.E. and C.M. Clapperton (1980): West Antarctica ice sheet fluctuations in the Antarctic Peninsula area, Nature 286, 378-381.

Takahashi, S.; R. Naruse; M. Nakawo and S. Mae (1988): A bare ice field in East Queen Maud Land, Antarctica, caused by horizontal divergence of drifting snow, Ann. Glaciol. 11, 156-160.

Thomas, R.H. (1973): The creep of ice shelves, J.Glaciol. 12 (64), 45-53.

Thomas, R.H. (1976): Thickening of the Ross ice shelf and equiibrium state of the West Antarctic ice sheet, Nature 259, 180-183.

Thomas, R.H. (1977): Calving bay dynamics and ice sheet retreat up the St Laurence valley system, Geographie Physique et Quaternaire 31 (3-4), 167-177.

Thomas, R.H. (1979a): Ice shelves: a review, J. Glaciol. 24(90), 273-286.

Thomas, R.H. (1979b): The dynamics of marine ice sheets, J.Glaciol. 24 (90), 167-177.

Thomas, R.H. and C.R. Bentley (1978): A model for Holocene retreat of the West Antarctic ice sheet, Quat.Res. 10, 150-170.

Thomas, R.H.; T.J.O. Sanderson and K.E. Rose (1979): Effect of climatic warming on the West Antarctic ice sheet, Nature 277, 355-358.

Thomas, R.H. and D.R. MacAyeal (1982): Derived characteristics of the Ross ice shelf, Antarctica, J.Glaciol. 28 (100), 397-413.

Thomas, R.H.; D.R. MacAyeal; D.H. Eilers and D.R. Gaylord (1984): Glaciological studies on the Ross ice shelf, Antarctica, 1973-1978, in: Bentley, C.R. and D.E. Hayes (eds): The Ross ice shelf: Glaciology and geophysics, Antarctic Research Series 42, 21-53.

Thomas, R.H.; S.N. Stephenson; R.A. Bindschadler; S. Shabtaie ans C.R. Bentley (1988): Thinning and grounding line retreat on Ross ice shelf, Antarctica, Ann. Glaciol. 11, 165-172.

Tricot, C. and A. Berger (1987): Modelling the equilibrium and transient responses of global temperature to past and future trace gas concentrations, Clim.Dyn. 2, 39-61.

Turcotte, D.L. and G. Schubert (1982): Geodynamics. John Wiley (New York) 440 p.

Van der Veen, C.J. (1985): Response of a marine ice sheet to changes at the grounding line, Quat.Res. 24, 257-267.

REFERENCES

Van der Veen, C.J. (1986): Ice sheets, atmospheric CO_2 and sea level, Ph.D. thesis, University of Utrecht, 184 p.

Van der Veen, C.J. (1987): Longitudinal stresses and basal sliding: a comparative study, in: C.J. Van der Veen and J. Oerlemans (eds): Dynamics of the West Antarctic ice sheet, D. Reidel (Dordrecht), 223-248.

Walcott, R.I. (1973): Structure of the earth from glacio-isostatic rebound, Ann.Rev. Earth Plan.Sci. 1, 15-37.

Waitt, R.B.Jr. (1983): Thicker West Antarctic ice sheet and Peninsula ice cap in late-Wisconsin time - sparse evidence from northern Lassiter Coast, Ant.Journal U.S. 18(5), 91-93.

Warrick, R and J. Oerlemans (1990): Sea level rise, in: Houghton J.T., G.J. Jenkins and J.E. Ephraums (eds.): Climate Change, the IPCC Scientific Assessment, Cambridge University Press, 257-282.

Watts, A.B. (1982): Tectonic subsidence, flexure and global changes of sea level, Nature 297, 469-474.

Webb, P.-N. (1990): The Cenozoic history of Antarctica and its global impact, Ant. Science 2, 3-21.

Webb, P.-N.; D.M. Harwood; B.C. McKelvey; J.H. Mercer; L.D. Stott (1983): Late Neogene and older Cenozoic microfossils in high elevation deposits of the Transantarctic Mountains: evidence for marine sedimentation and ice volume variation on the East Antarctic craton, Ant.Journal U.S. 18 (5), 96-97.

Webb, P.-N.; D.M. Harwood; B.C. McKelvey; M.C.G. Mabin and J.H. Mercer (1986): Late Cenozoic tectonic and glacial history of the Transantarctic Mountains, Ant.Journal U.S. 21 (5), 99-100.

Weertman, J. (1957): Deformation of floating ice shelves, J. Glaciol. 3, 38-42.

Weertman, J. (1961): Stability of ice-age ice sheets, J.Geophys.Res. 66 (11), 3783-3792.

Weertman, J. (1964): The theory of glacier sliding, J.Glaciol. 5(39), 287-303.

Weertman, J. (1968): Comparison between measured and theoretical temperature profiles of the Camp century, Greenland, borehole, J.Geophys.Res. 73, 2691-2700.

Weertman, J. (1972): General theory of water flow at the base of a glacier or ice sheet, Rev.Geoph.Space Phys. 10(1), 287-333.

REFERENCES

Weller, G.; C.R. Bentley, D.H. Elliot; L.J. Lanzerotti and P.J. Webber (1987): Laboratory Antarctica: research contributions to global problems, Science 238, 1361-1368.

Wellman, P. and R.J. Tingley (1981): Glaciation, erosion and uplift over part of East Antarctica, Nature 291, 142-144.

Whillans, I.M. (1976): Radio-echo layers and the recent stability of the West Antarctic ice sheet, Nature 264, 152-155.

Whillans, I.M. (1977): The equation of continuity and its application to the ice sheet near Byrd station, Antarctica, J. Glaciol. 18 (80), 359-371.

Whillans, I.M.; J. Bolzan and S. Shabtaie (1987): Velocity of ice streams B and C, Antarctica, J.Geophys.Res. 92 (B9), 8895-8902.

Whillans, I.M.; Y.H. Chen; C.J. Van der Veen and T.J. Hughes (1989): Force budget: III. Application to three-dimensional flow of Byrd Glacier, Antarctica, J.Glaciol. 35 (119), 68-80.

Wilson, A.T. (1964): Origin of ice ages: an ice shelf theory for Pleistocene glaciation, Nature 201, 147-149.

Yiou, F.; G.M. Raisbeck, D. Bowles, C. Lorius and N.I. Barkov (1985): [10]Be in ice at Vostok Antarctica during the last climatic cycle, Nature 316, 616-617.

Yoshida, Y. (1985): A note on the ice sheet fluctuations and problems of Cenozoic studies in Antarctica, in: Proceedings of the fifth symposium on Antarctic geosciences 1984, 187-199.

Yuen, D.A.; M. Saari and G. Schubert (1986): Explosive growth of shear-heating instabilities in the down-slope creep of ice sheets, J.Glaciol. 32 (112), 314-320.